

**MODELING AND OPTIMIZATION OF
SYSTEMS FOR NUTRIENT RECOVERY FROM
LIVESTOCK WASTE**

EDGAR MARTÍN HERNÁNDEZ

A dissertation submitted for the degree of
DOCTOR IN CHEMICAL SCIENCE AND TECHNOLOGY

at the
UNIVERSIDAD DE SALAMANCA



**VNiVERSiDAD
D SALAMANCA**

CAMPUS OF INTERNATIONAL EXCELLENCE

Academic advisor: Mariano Martín Martín

Programa de Doctorado en Ciencia y Teconología Química

Departamento de Ingeniería Química y Textil

Universidad de Salamanca

February 2022



El Dr. D. Mariano Martín Martín, Profesor Titular de Universidad del Departamento de Ingeniería Química y Textil de la Universidad de Salamanca

Informa:

Que la memoria titulada: “Modeling and optimization of systems for nutrient recovery from livestock waste”, que para optar al Grado de Doctor en Ciencia y Tecnología Química con Mención Internacional presenta **D. Edgar Martín Hernández**, ha sido realizada bajo nuestra dirección dentro del Programa de Doctorado Ciencia y Tecnología Químicas (RD 99/2011) de la Universidad de Salamanca, y que considerando que constituye un trabajo de tesis.

Autoriza:

Su presentación ante la Escuela de Doctorado de la Universidad de Salamanca, mediante el formato de compendio de publicaciones.

Y para que conste a los efectos oportunos, firmo la presente en Salamanca, a 01 de diciembre de 2021.

Fdo: Mariano Martín Martín

A mi familia, y a todos los que por mi vida pasaron.

*Non exiguum temporis habemus, sed multum perdimus.
Satis longa vita et in maximarum rerum consummationem
large data est, si tota bene collocaretur;
sed ubi per luxum ac neglegentiam difflit,
ubi nulli bonae rei impenditur,
ultima demum necessitate cogente quam ire non
intelleximus transisse sentimus.*

— Lucius Annaeus Seneca, De brevitate vitae.

*No tenemos un tiempo escaso, sino que perdemos mucho.
La vida es lo bastante larga para realizar las mayores empresas,
pero si se desparrama en la ostentación y la dejadez,
donde no se gasta en nada bueno, cuando al final
nos acosa el inevitable trance final, nos damos cuenta
de que ha pasado una vida que no supimos que estaba pasando.*

— Lucius Annaeus Seneca, De la brevedad de la vida.

ACKNOWLEDGMENTS

Complete

ABSTRACT

To be completed.

RESUMEN

Completar.

PUBLICATIONS

This thesis is presented as a compendium of publications, where each of the chapters corresponds to a formal manuscript published in a scientific journal, or currently under review, and book chapters. The relation of manuscripts published or under review, and book chapters that comprise this dissertation is detailed below:

- Martín-Hernández, E., Guerras, L., & Martín, M. (2020). Optimal technology selection for the biogas upgrading to biomethane. *Journal of Cleaner Production*, 122032.
- Martín-Hernández, E., Hu, Y., Zavala, V., Martín, M., & Ruiz-Mercado, G. (Under Review). Analysis of incentive policies for phosphorus recovery at livestock facilities in the Great Lakes area. *Resources, Conservation & Recycling*.
- Martín-Hernández, E., Martín, M., & Ruiz-Mercado, G. (2021). A geospatial environmental and techno-economic framework for sustainable phosphorus management at livestock facilities. *Resources, Conservation & Recycling*, 175, 105843.
- Martín-Hernández, E., Ruiz-Mercado, G., & Martín, M. (2020). Model-driven spatial evaluation of nutrient recovery from livestock leachate for struvite production. *Journal of Environmental Management*, 271, 110967.
- Martín-Hernández, E., Sampat, A., Martin, M., Zavala, V., & Ruiz-Mercado, G. (2021). A Logistics Analysis for Advancing Carbon and Nutrient Recovery from Organic Waste. In *Advances in Carbon Management Technologies* (pp. 186–207). CRC Press.
- Martín-Hernández, E., Sampat, A., Zavala, V., & Martín, M. (2018). Optimal integrated facility for waste processing. *Chemical Engineering Research and Design*, 131, 160–182.

CONTENTS

1	INTRODUCTION	1
1.1	Rationale: Overview of the nutrient pollution challenge	1
1.2	Approaches for processes modeling	6
1.2.1	Short-cut methods	7
1.2.2	Rules of thumb	8
1.2.3	Dimensionless analysis	8
1.2.4	Mechanistic models	8
1.2.5	Surrogate models	8
1.2.6	Experimental correlations	9
1.3	Approaches for decision-support systems	9
1.3.1	Multi-Attribute Decision Analysis (MADA)	11
1.4	Approaches for geospatial environmental assessment	16
1.5	Thesis outline	17
1.5.1	Part I - Phosphorus management and recovery	17
1.5.2	Part II - Nitrogen management and recovery	18
1.5.3	Part III - Nitrogen management and recovery	18
	Bibliography	19
2	OBJECTIVE	21
2.1	Scope and objectives of the thesis	21
2.2	Main objective	21
2.3	Specific objectives	21
I	PHOSPHORUS MANAGEMENT AND RECOVERY	
3	TECHNOLOGIES FOR PHOSPHORUS RECOVERY	25
3.1	Introduction	25
3.2	Process description	26
3.3	Modelling issues	28
3.3.1	Biogas production	28
3.3.2	Biogas purification	29
3.3.3	Electricity generation	29
3.3.4	Digestate conditioning	30
3.3.5	Solution procedure	49
3.4	Results	52
3.4.1	Mass and energy balances	53
3.4.2	Economic evaluation	54
3.4.3	Effect on the power, operating conditions and digestate treatment	56

3.5 Conclusions	57
Nomenclature	57
Acknowledgments	61
Bibliography	61
4 ASSESSMENT OF PHOSPHORUS RECOVERY THROUGH THE DEPLOYMENT OF STRUVITE PRECIPITATION SYSTEMS	69
4.1 Introduction	69
4.2 Methods	71
4.2.1 Spatial resolution	71
4.2.2 Assessment of anthropogenic phosphorus from agricultural activities	72
4.2.3 Thermodynamic model for precipitates formation	74
4.3 Results and discussion	80
4.3.1 Surrogate models to estimate the formation of precipitates from livestock organic waste	80
4.3.2 Phosphorus releases from cattle leachate potentially avoided via struvite formation	84
4.4 Conclusions	87
Nomenclature	88
Acknowledgments	89
Bibliography	90
5 GEOSPATIAL ENVIRONMENTAL AND TECHNO-ECONOMIC FRAMEWORK FOR SUSTAINABLE PHOSPHORUS MANAGEMENT AT LIVESTOCK FACILITIES	95
5.1 Introduction	95
5.2 Methods	97
5.2.1 Environmental geographic information model	98
5.2.2 Techno-economic model	101
5.2.3 Multi-criteria decision model	107
5.2.4 Framework limitations	111
5.2.5 Case study	111
5.3 Results	113
5.3.1 Implementation of phosphorus recovery systems in the Great Lakes area	113
5.3.2 Economic results	115
5.4 Discussion	118
5.4.1 Economic implications	118
5.4.2 Phosphorus use efficiency	119
5.5 Conclusion	121
Acknowledgments	122
Bibliography	122

6 ANALYSIS OF INCENTIVE POLICIES FOR PHOSPHORUS RECOVERY	123
6.1 Introduction	123
6.2 Incentive policy assessment framework	124
6.2.1 Assessment of nutrient management systems	125
6.2.2 Environmental vulnerability to nutrient pollution . .	126
6.2.3 Multi-criteria decision analysis model for the assess- ment of nutrient management systems	128
6.2.4 Types of incentives considered	129
6.2.5 Scenarios description	130
6.2.6 Study Region - The Great Lakes area	130
6.3 Results and discussion	131
6.3.1 Single incentives	131
6.3.2 Combined effect of incentives for phosphorus and renewable electricity recovery	133
6.3.3 Environmental cost-benefit analysis	135
6.3.4 Fair distribution of incentives	136
6.4 Conclusions	139
Acknowledgments	140
Bibliography	140

II NITROGEN MANAGEMENT AND RECOVERY

III INTEGRATION OF ANAEROBIC DIGESTION AND NUTRIENT MANAGEMENT SYSTEMS

7 OPTIMAL TECHNOLOGY SELECTION FOR THE BIOGAS UP- GRADING TO BIOMETHANE	149
7.1 Introduction	149
7.2 Methodology for process design	151
7.3 Process design	152
7.3.1 Technology screening	152
7.3.2 Mathematical modelling	154
7.3.3 Selection of optimal configurations	157
7.3.4 Superstructure configuration	159
7.3.5 Economic evaluation	160
7.4 Results	160
7.4.1 Biogas composition	160
7.4.2 Selection of technology	161
7.4.3 Estimation of production and investment costs . .	162
7.4.4 Comparison with renewable-based hydrogenation processes	164
7.4.5 Plant scale-up study	166
7.5 Conclusions	169

Nomenclature	171
Acknowledgments	173
Bibliography	173
IV APPENDIX	
A APPENDIX A: SUPPLEMENTARY INFORMATION OF CHAPTER 2	177
A.1 Biogas production	178
A.2 H ₂ S removal	181
A.3 CO ₂ , NH ₃ and H ₂ O removal (PSA)	181
A.4 Brayton cycle	181
A.5 Rankine cycle	182
Bibliography	185
B APPENDIX B: SUPPLEMENTARY INFORMATION OF CHAPTER 3	187
B.1 Cattle organic waste composition	187
B.2 Distribution functions of elements from cattle waste	187
B.3 Thermodynamic modeling of the carbonates system	191
B.4 Surrogate models to estimate precipitates formation from livestock waste	194
B.4.1 Influence of magnesium	194
Bibliography	197
C APPENDIX C: SUPPLEMENTARY INFORMATION OF CHAPTER 4	199
C.1 Environmental geographic information model	199
C.1.1 Trophic State Index	199
C.1.2 Balance of anthropogenic phosphorus releases	200
C.1.3 Phosphorus in soils	201
C.2 Framework development	203
C.2.1 Data entry	203
C.2.2 Techno-economic model	203
C.3 Multi-criteria decision model	214
C.4 Description of the Great Lakes area	214
Bibliography	214
D APPENDIX D: SUPPLEMENTARY INFORMATION OF CHAPTER 6	217
D.1 Biogas production	217
E APPENDIX E: SUPPLEMENTARY INFORMATION OF CHAPTER 7	219
E.1 Literature review	219
E.2 Modelling approach	220
E.2.1 Amines	220
E.2.2 PSA	224
E.2.3 Membranes	226
E.3 Economic evaluation	228
E.4 Scaling-up study	229

Bibliography	230
------------------------	-----

LIST OF FIGURES

Figure 1.1	Main flows of nutrients released by anthropogenic activities.	2
Figure 1.2	Main topics covered in this work.	7
Figure 1.3	Classification of MCDA methods.	10
Figure 3.1	Flowsheet for the production of power and fertilizers.	62
Figure 3.2	Scheme of the filter.	63
Figure 3.3	Scheme of the coagulation process.	63
Figure 3.4	Scheme for the centrifugation treatment.	63
Figure 3.5	Scheme for the FBR system.	64
Figure 3.6	Scheme for the CSTR based struvite production system.	64
Figure 3.7	Units cost distributions for cattle, pig, poultry and sheep manure treatment (ST: steam turbine, GT: gas turbine, HX: heat exchangers, FBR: fluidized bed reactor).	67
Figure 3.8	Operation cost distribution for cattle, pig, poultry and sheep manure treatment.	67
Figure 4.1	Flowchart of the proposed algorithm to solve the thermodynamic model for the formation of precipitates in cattle organic waste.	91
Figure 4.2	A solution procedure to evaluate the influence of the cattle waste composition variability in the formation of struvite.	92
Figure 4.3	Comparison between experimental results reported by Zeng and Li (2006) and the results provided by the model developed in this work.	92
Figure 4.4	Influence of magnesium and calcium in struvite precipitation.	92
Figure 4.5	Techno-ecological synergy (TES) metric values for HUC8 watersheds. Red indicates watersheds with unbalanced agricultural phosphorus releases, and blue indicates watersheds with balanced agricultural phosphorus releases. White indicates watersheds with not available data.	93
Figure 4.6	Phosphorus releases avoided through struvite production for the different scenarios considered. Darker colors represent larger phosphorus recovery	94

Figure 5.1	Structure of the COW2NUTRIENT decision support framework for the assessment and selection of phosphorus recovery systems.	98
Figure 5.2	Process flowsheet for manure management and phosphorus recovery stages included in COW2NUTRIENT.	102
Figure 5.3	Flowsheet for the MCDA model.	109
Figure 5.4	Distribution of the phosphorus recovery systems selected for the CAFOs in the Great Lakes area. The boxplots represent the distribution of CAFO sizes in each studied state.	114
Figure 5.5	Capital expenses for deploying phosphorus recovery systems in the studied CAFOs. The dots represent the P recovery technologies installed in the studied CAFOs.	117
Figure 5.6	Operating expenses for deploying phosphorus recovery processes in the studied CAFOs. The dots represent the P recovery technologies installed in the studied CAFOs.	118
Figure 5.7	Net revenue from the phosphorus recovery processes selected in the studied CAFOs. The dots represent the P recovery technologies installed in the studied CAFOs.	119
Figure 6.1	Flowchart of the models for selection, sizing, and evaluation of nutrient recovery systems at livestock facilities.	126
Figure 6.2	Flowchart of the processes evaluated for livestock waste management.	127
Figure 6.3	States of the Great Lakes region studied in this work.	131
Figure 6.4	Distribution of profitable phosphorus recovery processes in the Great Lakes area for the scenarios considering phosphorus credits and renewable energy credits. The box-plots represent the distribution of CAFOs size in each state.	133
Figure 6.5	Economic evaluation of P recovery processes for the different incentives scenarios studied	141

Figure 6.6	Comparison of the total cost of phosphorus recovery for each scenario assessed and the environmental remediation cost due to phosphorus releases. REC denotes the electricity incentive values considered in USD/MWh, and PC denotes the value of phosphorus credits in USD/kg _P recovered. The red dotted line represents the economic losses due to phosphorus releases to the environment.	142
Figure 6.7	Allocation of incentives for achieving the economic neutrality of nutrient recovery systems minimizing the total cost of incentives.	142
Figure 6.8	Distribution of incentives considering the Nash allocation scheme. Scenarios assuming available incentives equal to the 10%, 30%, 50%, 70%, and 100% of the incentives needed to cover the economic losses of unprofitable P recovery systems in the Great Lakes area are illustrated.	143
Figure 7.1	Scheme of the methodology followed to determine the optimal biogas upgrading technology.	153
Figure 7.2	Scheme of the proposed superstructure for biogas upgrading into biomethane.	160
Figure 7.3	Breakdown of biomethane production costs for each residue analyzed.	163
Figure 7.4	Relation between population and food waste produced in Spain.	168
Figure 7.5	Scale-up in the investment costs for municipal food waste.	169
Figure 7.6	Scale-up in the investment costs for cattle manure. .	170
Figure B.1	Kernel density estimation (red dashed line) and probability density distribution (blue solid line) for the evaluated components in cattle organic waste. .	190
Figure B.2	Evolution phosphorus as phosphate fraction recovered as struvite and calcium fraction recovered as precipitates along Mg ²⁺ /PO ₄ ³⁻ molar ratio values considering 50 different composition data sets. . .	194
Figure B.3	Evolution of phosphorus as phosphate fraction recovered as struvite and calcium fraction recovered as precipitates along Ca ²⁺ /PO ₄ ³⁻ molar ratio values considering 50 different composition data sets. . .	195

Figure B.4	Evolution of phosphorus as phosphate fraction recovered as struvite and calcium fraction recovered as precipitates among alkalinity values considering 50 different composition data sets.	196
Figure C.1	Trophic State Index in the contiguous US HUC8 watersheds	200
Figure C.2	Balance of anthropogenic phosphorus releases in the contiguous US at a HUC8 spatial resolution	201
Figure C.3	Soil Fertility Level in the contiguous US at a HUC8 spatial resolution	203
Figure C.4	Adequate manure properties for anaerobic digestion. Adapted from U.S. Environmental Protection Agency (2004).	204
Figure C.5	Correlations between AD capital and O&M costs, and the number of cattle in the livestock facility.	206
Figure C.6	Estimated screw press investment costs (USD) as a function of the size.	207
Figure C.7	Estimated capital and operating costs for screw press units.	208
Figure C.8	Flowsheets of the nutrient recovery systems considered in the proposed framework. a: Multiform, b: Crystalactor, c: Ostara Pearl, d: Nuresys, e: P-RoC, f: MAPHEX.	209
Figure C.9	Estimated investment costs for a non-jacketed vessel, based on data from CAPCOST (Turton, 2010).	212
Figure C.10	Estimated investment costs for conveyor dryer unit.	213
Figure C.11	Example of feasible weights space for a three criteria problem considering ranking of criteria. Figure adapted from Tervonen and Lahdelma (2007)	215
Figure E.1	Scheme of the proposed superstructure for biogas upgrading into biomethane.	221

INTRODUCTION

1.1 RATIONALE: OVERVIEW OF THE NUTRIENT POLLUTION CHALLENGE

Human population is experiencing a continuous growth since the end of the Black Death in the XIV century (Biraben, 1980), which is at 7.8 billion as of 2020, and it is estimated to be at 9.7 billion and 10.9 billion by 2050 and 2100 respectively (United Nations, Department of Economic and Social Affairs, 2019). Population growth demands increasing amounts of food, which in turn requires an efficient food production system to ensure global food security. In this context, the development of different technical advancements has been a key factor to increase the productivity of the food production system. Notably, crucial developments were achieved in the late modern period¹, including the commercial production of phosphate in 1847 (Samreen & Kausar, 2019), the development of the Haber-Bosch process for the production of synthetic nitrogen-based fertilizers in 1913 (Smil, 1999), and the mechanization of agriculture and the development of the modern intensive farming in the XX century (Constable & Somerville, 2003; Nierenberg & Mastny, 2005).

Despite these advancements have increased the productivity of agriculture and farming industries, multiple environmental impacts associated with them emerges, including water scarcity, greenhouse gases emissions, nutrient pollution of waterbodies, and soil degradation, among others. These threats must be carefully addressed in order to avoid the depletion of natural resources and reach a sustainable food production system.

Focusing on the impacts derived from agriculture and farming on the nutrient cycles, it can be observed that the natural cycles of phosphorus and nitrogen have been altered by these activities (Bouwman et al., 2009). Large amounts of nutrients are released into the environment in the form of synthetic fertilizers and livestock manure. Nitrogen and phosphorus are accumulated in soils, creating a nutrient legacy that is further transported to waterbodies by runoff. This process results in the eutrophication of waterbodies, which can lead algal bloom episodes. Algal blooms are events

¹ The terminology used in this dissertation for the periodization of human history follows the English-language historiographical approach. It should be noted that the late modern period is referred to as the contemporary period in the European historiographical approaches.

resulting from the rapid increase of algae in a water system which can be promoted by an excess of nutrients in water. These episodes alter the normal functioning of aquatic ecosystems, since they cause hypoxia as a consequence of the aerobic degradation of algal biomass by bacteria. Moreover, some species of algae that cause algal blooms can release toxins into the water systems. The main flows of nutrient releases into the environment by anthropogenic activities is shown in Figure 1.1.

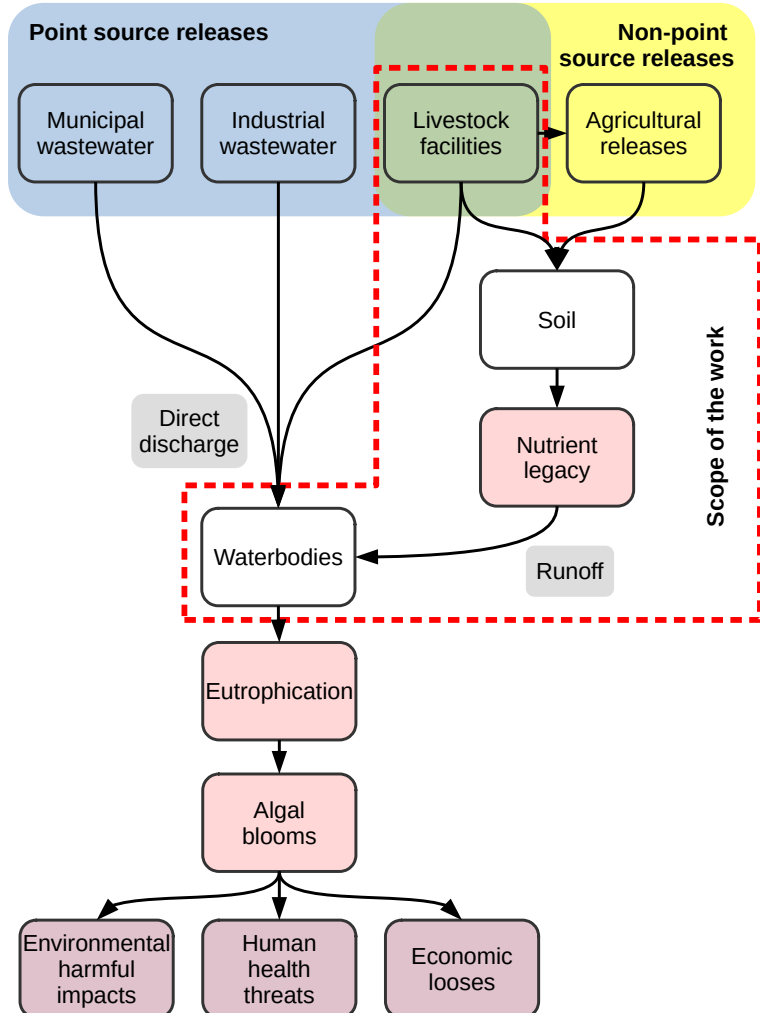


Figure 1.1: Main flows of nutrients released by anthropogenic activities.

In addition to the environmental problems, the use of nutrients for food production also raises geopolitical concerns since phosphorus is one of the most sensitive elements to depletion. Phosphorus is a non-renewable material whose reserves are expected to be depleted in the next 50 to 100 years. Moreover, no substitute material is currently known

(Cordell et al., 2009). Conversely, synthetic nitrogen can be produced using the atmospheric N₂ as raw material through the Haber-Bosh process. However, nowadays this process relies on non-renewable energy sources, and therefore the production of synthetic nitrogen-based fertilizers is dependent on non-renewable resources as well.

Considering the two challenges described, i.e., nutrient pollution of waterbodies as a consequence of agricultural and farming activities, and the current dependency on non-renewable resources for the production of synthetic fertilizers, nutrient recovery and recycling is not only a desirable but also a necessary approach to develop a sustainable agricultural paradigm and ensure the global food security.

Attending to the nutrient releases from intensive livestock farming facilities, known as concentrated animal feeding operations (CAFOs)², several manure management techniques are currently used. The land application of manure is a common technique that allows the recycling of nutrients as fertilizers for crops (Kellogg et al., 2000). However, the increase of intensive livestock farming generates vast amounts of waste generated by CAFOs, e.g., each adult cow generates between 28 and 39 kg of manure per day, and each adult pig generates around 11.5 kg of manure per day (USDA, 2009). Manure processing is commonly based on the separation of liquid and solid phases. The liquid phase can be treated in anaerobic and/or aerobic lagoons for organic matter and pathogens removal, as well as odor control (Tilley et al., 2014). The obtained liquid effluent can be used for irrigation and nutrient supplementation of crops. The solid phase can be composted for the degradation of organic matter and pathogens removal, resulting in a solid material called compost with a larger amount of nitrogen and phosphorus available for plants, which is result of the mineralization of nutrients previously contained in organic compounds. Since compost is also a good source of organic matter for crops, it is a valuable material suitable for sale (Tilley et al., 2014). However, both materials, the liquid effluent obtained from the lagoons and compost, are too bulky to be economically transported to nutrient deficient locations (Burns & Moody, 2002). As a result, livestock waste is usually spread in the surroundings of livestock facilities, at a detrimental cost of environment. This result in the gradual build-up of nutrients in soils, which might lead the harmful environmental impacts previously described.

A promising alternative for abating nutrient releases and reducing the environmental footprint of livestock industry is the implementation of processes for the recovery of phosphorus and nitrogen at CAFOs. At the

² CAFO is a regulatory term defined by the U.S. Environmental Protection Agency for large facilities where animals are kept and raised in confined situations (USDA, 2011). This term is used in this dissertation to denote the intensive livestock farming facilities studied.

time, that valuable nutrient-rich materials are obtained for the redistribution of phosphorus and nitrogen to nutrient-deficient areas. There exist a number of processes for nutrient recovery from livestock waste, which can be differentiated into those technologies oriented to phosphorus recovery, including struvite precipitation, calcium-based precipitates production, coagulation-flocculation, electrochemical processes, and systems based on solid-liquid separation; and processes focused on nitrogen recovery, such as stripping, membrane separation, waste drying coupled with ammonia scrubbing, and solid-liquid separation processes. We note that anaerobic digestion is an additional process that can be integrated for manure treatment if the generation of biomethane is pursued, and for increasing the amount of recoverable nutrients through the partial mineralization of nutrients contained in organic compounds. It must be noted that only phosphorus and nitrogen in inorganic compounds can be taken by plants, and therefore the recovery of inorganic nutrients will be the target of the processes studied in this thesis.

The multiple processes for the recovery of phosphorus and nitrogen from livestock waste differ in aspects such as recovery efficiency, processing capacity, capital and operating costs, and products obtained. Therefore, a detailed analysis of each CAFO must be performed in order to select the optimal nutrient recovery system attending to type factors such as the type and amount of waste to be processed, the environmental vulnerability to eutrophication of each region, the current or potential installation of anaerobic digestion systems, etc. Additionally, in the decision-making process these factors have to be prioritized, i.e., sorted by relevance, to select the most suitable nutrient recovery system for each particular facility. As example, more economical processes for nutrient recovery, whose recovery efficiencies are typically lower, could be installed in regions with a low risk of eutrophication. Conversely, regions at severe eutrophication risk require highly efficient nutrient recovery systems that may incur in larger investment and operating expenses. In order to perform a systematic evaluation of CAFOs and their context, we introduce a multi-criteria decision analysis (MCDA) framework integrating geospatial environmental data on eutrophication risk at the subbasin level and techno-economic information of the studied processes.

Attending to the regulatory aspect, nowadays most of the efforts for abating of nutrient releases into the environment and mitigating the eutrophication of waterbodies are focused on the limitation of fertilizer application in croplands. The application of fertilizer and manure for nitrogen supplementation in the European Union (EU) is currently regulated by the Nitrates Directive (91/676/EEC) (Grizzetti et al., 2021). Regarding the limitations for phosphorus application, these are defined at national level. Several

European countries have implemented phosphorus application standards based on the different crops and materials used as fertilizers, being generally more restrictive in Northwestern Europe (Amery & Schoumans, 2014).

In sum, it can be observed that nutrient application is limited either in the form of synthetic fertilizers or manure application. However, at present there is a lack of regulation regarding livestock waste treatment (Piot-Lepetit, 2011). In this regard, new efforts to promote the production and adoption of bio-fertilizers obtained from organic waste are being performed through the development of the "Integrated Nutrient Management Plan" (INMAP), which is part of the EU Farm-to-Fork strategy and part of the Circular Economy Action Plan. INMAP should propose actions to promote the recovery and recycling of nutrients, as well as the development of markets for recovered nutrients (Comission, 2020; ESSP, 2021). In this regard, a new regulation for fertilizer products has been released in 2019 (EU 2019/1009), moving struvite and other biofertilizers from the category of waste to fertilizers, establishing a regulatory framework for their use and trade.

In the United States, CAFOs are regulated under the Clean Water Act as point source waste discharges. This regulation sets the need of permits for discharging pollutants to water, which are called National Pollutant Discharge Elimination System (NPDES) permits, including nitrogen and phosphorus releases. These permits must include the necessary provisions for avoiding the harmful effects of the discharges on water and human health (US EPA, 2020b). The development and implementation of a Nutrient Management Plan (NMP) is a required element to obtain an NPDES permit. This document must identify the management practices to be implemented at each CAFO to protect natural resources from nutrient pollution. Land spreading of manure can also be regulated by the NPDES permits, establishing soil nutrient concentration limits and the yearly schedule for manure application. However, no specific methods or processes for waste treatment are defined under federal regulation (US EPA, 2020a). Regarding the use of the recovered nutrients, products obtained from nutrient recovery processes could be classified as waste by the Clean Water Act, preventing the application of these materials on croplands (NACWA, 2014). However, the U.S. Environmental Protection Agency (US EPA) determined that, although these products could not be directly applied to land under the current regulation, they can be sold as a commodity to be outside of the Clean Water Act restrictions coverage (CNP, 2021). Moreover, US EPA acknowledges that highly refined and primarily inorganic products (such as struvite) could be outside of the scope of these restrictions (CNP, 2021). Nevertheless, further regulation is needed for defining the products ob-

tained from nutrient recovery processes and to clearly state the conditions for their use as fertilizers on croplands.

Considering the previously described aspects, we note that the regulation of the products obtained from nutrient recovery systems is not totally developed yet either in the European Union and the United States, although important efforts are being performed in order to set a comprehensive regulatory framework for the recycling of phosphorus and nitrogen. Furthermore, no regulation regarding the implementation of nutrient recovery processes has been developed. However, both regions have developed previous programs to study and promote the implementation of other technologies for the treatment of livestock and other organic waste. Particularly, the deployment of anaerobic digestion systems have received a considerable support from governmental agencies, resulting in programs such as AgSTAR in the US (US EPA, 2021), and BiogasAction (European Comission, 2021) and BIOGAS³ (BIOGAS₃ PROJECT, 2021) in Europe, among many others. These programs could be a guideline for the development of nutrient recovery plans at CAFOs. In this regard, we have studied the impact of the implementation of nutrient recovery systems in the economy of CAFOs, either considering the deployment of standalone nutrient recovery processes, or integrated systems combining nutrient recovery with anaerobic digestion for the production of electricity and biomethane. Moreover, incentive policies have been analyzed to minimize the negative impact of nutrient recovery on CAFOs economy using the Great Lakes area as case study. In addition, the fair distribution of monetary resources when limited budget is available has been studied using the Nash allocation scheme.

An overview of the main topics studied in this thesis can be observed in Figure 1.2. This work pretends to analyze strategies for promoting effective nutrient recycling addressing studies on the technical, environmental and economic dimensions involved, pursuing the development of sustainable food production paradigm.

1.2 APPROACHES FOR PROCESSES MODELING

Process modeling, defined as the mathematical modeling and simulation of systems, falls under the scope of the Process System Engineering (PSE) discipline. These systems include physical, chemical, and/or biological operations. Process modeling forms the foundation for other activities involved in the scope of PSE, including process design, optimal scheduling

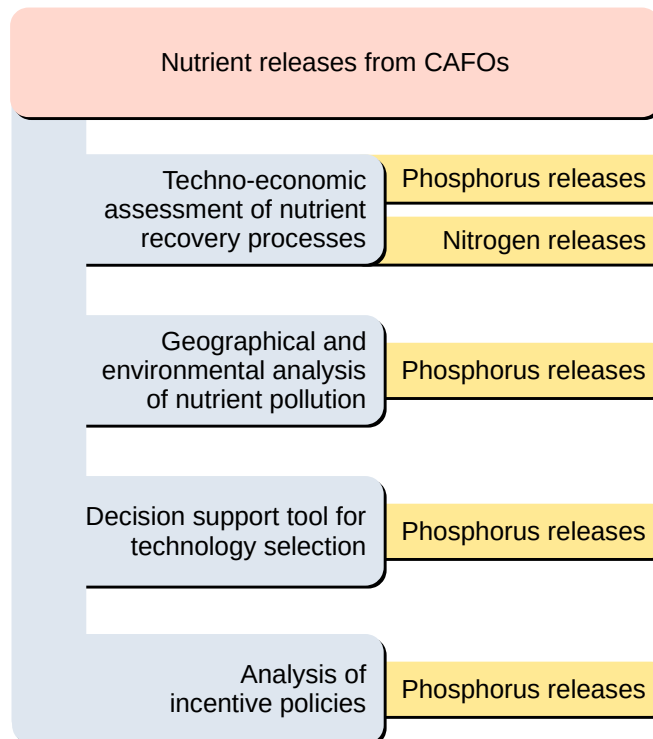


Figure 1.2: Main topics covered in this work.

and planning of the systems operations, and process control (Stephanopoulos & Reklaitis, 2011).

Different modeling techniques have been developed to mathematically describe and represent systems from different domains, including but not limited to the chemical, biochemical, agrochemical, food, and pharmaceutical domains of engineering (Pistikopoulos et al., 2021). An overview of the main modeling techniques is shown in the next sections based on the classification proposed by Martín and Grossmann (2012).

1.2.1 Short-cut methods

These type models are the most basic approach to process modeling. They are based on mass, energy, and momentum balances, and can be embedded in other models, such as supply chain models.

1.2.2 *Rules of thumb*

This approach is based on industrial operational data. It provides typical ranges for operating and design values, reflecting the actual parameters of the systems modeled. However, the use of these models is constrained by the availability of data. Compendiums of rules of thumb for different systems can be found in Couper et al. (2005), Hall (2012), Sadhukhan et al. (2014).

1.2.3 *Dimensionless analysis*

This methodology is based on dimensionless groups that describe the performance of a particular system. These models are able to capture the physical meaning of the modeled processes, and they are specially useful to capture scale-up and scale-down issues (Szirtes, 2007).

1.2.4 *Mechanistic models*

This approach relies on first principles for systems modeling, as short-cut models. However, mechanistic models rely in more detailed first principles such as the underlying chemistry, physics or biology that governs the behavior of a particular system. Chemical (Loeppert et al., 1995) and phase (Brignole & Pereda, 2013) equilibrium models, kinetic models (Buzzi-Ferraris & Manenti, 2009), population balances (Ramkrishna, 2000), and computer fluid dynamics (CFD) (Anderson & Wendt, 1995) fall under this category.

1.2.5 *Surrogate models*

These models aim at developed simplified models from data obtained from rigorous mechanistic models. This approach is widely used for embedding system models into other applications such as process control or supply chain design. Surrogate models building has been systematized into four steps, i.e., design of experiments (DOE), running the rigorous models at the sampling points designated by the DOE, construction of the surrogate model, and validation of the model obtained (Queipo et al., 2005).

Polynomial regression models, in which the relationship between the variables is expressed using a polynomial function, are one of the most basic types of surrogate models. In the case of polynomial regression models involving multiple variables, the optimal variables to be addressed

within the pool of variables considered can be determined by using machine learning-based tools such as ALAMO (Wilson & Sahinidis, 2017), ensuring an optimal trade-off between model accuracy and complexity. Other types of surrogate models are Kriging models, which estimate the relationship between variables as a sum of a linear model and a stochastic Gaussian function representing the fluctuations of data (Quirante et al., 2015), and artificial neural networks (ANN), which are based on generating an input signal as the summation of all the weighted inputs, which is through nodes containing a transfer function. Nodes are connected by edges with assigned weights that adjust the signals transmitted between nodes. Nodes are structured in layers, in a way that nodes receive signals from nodes of the preceding layer, and if the output of the node is above a threshold value defined by the transfer function, sends the output signal to the next layer (Himmelblau, 2000).

1.2.6 *Experimental correlations*

As the surrogate models, experimental correlations are models built using data of the systems represented, but conversely to those one, experimental correlations are built using data from experimental results. Similarly to the rules of thumb, the accuracy of these models is limited by the availability of data, and they are only applicable to the range of operating conditions of the data used for constructing the model.

1.3 APPROACHES FOR DECISION-SUPPORT SYSTEMS

Decision-making activities require to analyze multiple relevant criteria for each course of action. Since criteria often conflict each other, each decision-making process requires the balancing of criteria, prioritizing some criteria over other through the use of some criteria weighting scheme. This procedure requires managing a vast amount of information of conflicting nature, leading to a complex decision-making process. Therefore, different approaches generally called multiple-criteria decision analysis (MCDA) have been developed to explicitly structure and solve decision problems. MDCA aim is to integrate criteria assessment with value judgment to analyze and compare the different available alternatives, identifying the best solution for the specific decision-making context studied. However, it must be highlighted that a certain grade of subjectivity might exist in several steps of MCDA, such as the choice of the set of criteria considered relevant for a particular problem. Therefore, the solution proposed by any MCDA approach must be analyzed considering the assumptions made

for building the problem. In sum, MCDA seeks to structure problems with multiple conflicting criteria, and providing justifiable and explainable solutions to guide decision-makers facing such problems. The solution of a multiple-criteria decision-making problem can be defined as a unique solution representing the most suitable alternative from the set of potential alternatives, or as a subset of satisfactory alternatives (Belton & Stewart, 2002).

An MCDA problem can be articulated in different stages, starting with the problem definition and structuring. At this stage, the goals, constraints, and stakeholders comprising the problem are defined, as well as the different solution alternatives. Based on this information, a model can be built for the assessment and comparison of alternatives. This stage includes the definition of the relevant criteria used for alternatives comparison, their relative priority, and the system for criteria evaluation. Finally, the information retrieved by the model can be used for making informed decisions.

Multi-criteria decision-making problems can be classified into Multi-Attribute Decision Analysis (MADA), which are discrete choice problems where the number of alternatives is finite, and Multi-Objective Decision Analysis (MODA), that are mathematical programming problems that consider infinite number of alternatives, as shown in Figure 1.3. However, we note that mathematical programming techniques are not limited to formulating and solving problems with infinite alternatives, but they can also be used for dealing with discrete decision-making problems (Giove et al., 2009).

1.3.1 Multi-Attribute Decision Analysis (MADA)

In the case of problems consisting of a finite number of alternatives, the suitability of each alternative to the problem given can be measured through its performance according to the multiple criteria considered. A large number of MCDA approaches have been (and are currently being) developed for discrete choice problems, including methods based on value functions (Multi-Attribute Value Theory methods, MAVT) and outranking methods.

1.3.1.1 Multi-Attribute Value Theory (MAVT)

INDICATOR-BASED METHODS Multi-Attribute Value Theory (MAVT) approaches are based on an indicator-based methodology for alternatives comparison. The relevant criteria considered in the decision-making process are normalized to a common scale to allow criteria comparison using

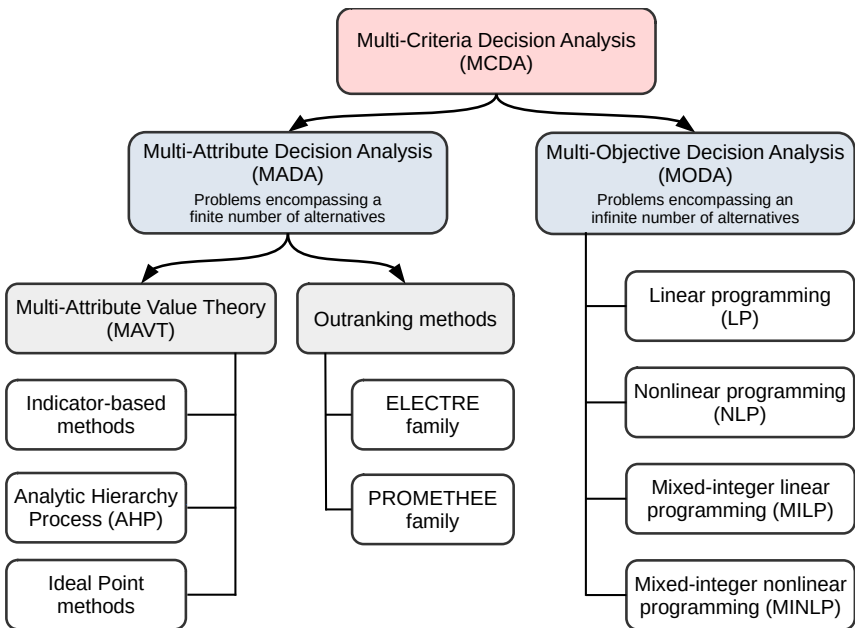


Figure 1.3: Classification of MCDA methods.

an utility or value function. A number of utility functions have been proposed in the literature, including standardization, min-max, and target utility functions (OECD and European Commission, 2008). The normalized criteria are weighted and aggregated to build a composite index, prioritizing some criteria over others. Different aggregation schemes have been proposed, providing different degrees of compensability between indicators, i.e. a deficit in one criteria can be fully, partially, or not compensated by a surplus in other criteria (Gasser et al., 2020). Additive weighting aggregation is a full compensatory method, while geometric and harmonic aggregation methods are partial compensation schemes. Other aggregation schemes include geometric averaging, which is a non-compensatory method, and the Choquet integral (Marichal & Roubens, 2000). The composite index obtained is a single numerical value that can be used to score and rank the proposed alternatives based on their suitability to the criteria considered.

A major source of uncertainty in indicator-based methods is the value of criteria weights. This issue can be addressed using the stochastic multi-criteria acceptability analysis (SMAA) method. SMAA is a sensitivity analysis method that address the uncertainty of criteria weights value exploring the feasible space of weights through the Monte Carlo method. Further, details about the SMAA approach can be found in Tervonen and Lahdelma (2007).

In this thesis, an indicator-based methodology has been used to assess and select phosphorus recovery technologies based on technical, environmental, and economic criteria combined in a composite index, as it is shown in Chapter .

ANALYTIC HIERARCHY PROCESS (AHP) Analytic Hierarchy Process (AHP) decomposes the decision problem into multiple simpler sub-problems. These sub-problems are hierarchized and independently analyzed. The sub-problems are solved through the pairwise comparison of alternatives, obtaining numerical indexes that can be used to compare their performance. Finally a numerical weight (priority) is assigned to each element of the hierarchy, and they are used for aggregating the indexes obtained by each alternative at each element of the hierarchy in a final numerical value that can be used to score the overall performance of each alternative accordingly to the set of criteria considered (Saaty, 2000).

IDEAL POINT METHODS Ideal Point methods set an optimal solution, that represent a utopia point where all criteria values are optimal. The performance of each alternative is evaluated through a composite index, that can be constructed using the MAVT approach. The alternatives are ranked based on their relative distance relative to the optimal solution. One of the most common Ideal Point methods is TOPSIS (Hwang & Yoon, 1995).

1.3.1.2 *Outranking methods*

Outranking methods are based on the pairwise comparison of the alternatives for each criterion considered, determining the preferred alternative for each of the criteria. Preference information about all criteria is aggregated to establish evidence for selecting one alternative over another. These methods indicate the dominance of one alternative over another, but they do not quantify the performance gap between the alternatives compared (Giove et al., 2009). Some of the most popular outranking methods are ELECTRE I (Roy, 1968), II (Roy & Bertier, 1973), and III (Roy et al., 1978), and PROMETHEE (Vincke & Brans, 1985).

1.3.1.3 *Multi-Objective Decision Analysis (MODA)*

Problems consisting of an infinite number of solutions require multi-objective mathematical programming (optimization) techniques to be solved. These problems are subjected to a number of equality and/or inequality constraints restricting the solutions that are feasible. The multiple conflict-

ing criteria are combined in an objective function. This objective function represents the improving level of the criteria, and it will be minimized or maximized for selecting the best solution that represents the optimal trade-off between the different conflicting criteria (Giove et al., 2009). In this thesis, this technique has been employed for determining the operating conditions of processes for the recovery of nutrient, energy and biomethane from livestock waste, as it is shown in Chapters 3 and 7. Other approach for solving multi-objective mathematical programming problems is to set a priori targets for different criteria, or combinations of criteria, that are considered satisfactory, obtaining the problem solution by minimizing the deviations from these goals. Mathematical programming problems can be also classified according to the use of linear or nonlinear equations, and continuous and/or discrete variables (Giove et al., 2009).

LINEAR PROGRAMMING (LP) Linear programming (LP) refers to those mathematical programming problems based on linear equations and continuous variables. A linear programming problem can be expressed as shown in Eq. 1.1, where x is a vector of dimension n , A is a mxn matrix, c is the n dimension vector of cost coefficients, and the right-hand side b is a vector of dimension m (Grossmann, 2021).

$$\begin{aligned} \min \quad & Z = c^T x \\ \text{s.t.} \quad & Ax \leq b \\ & x \geq 0 \end{aligned} \tag{1.1}$$

The two most widely used methods to solve LP problems are the Simplex algorithm (Murty, 1983) and interior-point methods (Potra & Wright, 2000). The Simplex method is more efficient for solving problems with thousands of variables and constraints, while interior-point is more efficient on very large scale and sparse problems (Grossmann, 2021). These methods are implemented in solvers such as CPLEX (IBM, 2009), Gurobi (Gurobi Optimization, LLC, 2021), or XPRESS (FICO, 2021).

NONLINEAR PROGRAMMING (NLP) Nonlinear programming (NLP) refers to those mathematical programming problems containing nonlinear equations, either in the constraints or in the objective function, and continuous variables. A nonlinear programming problem can be expressed as shown in Eq. 1.2, where x is an n dimension vector, $f(x)$ is the objective function of the problem, $h(x)$ is the set of equality constraints and $g(x)$ is the set of inequality constraints (Floudas, 1995).

$$\begin{aligned}
 \min \quad & f(x) \\
 \text{s.t.} \quad & h(x) = 0 \\
 & g(x) \leq 0 \\
 & x \in X \subseteq \Re^n
 \end{aligned} \tag{1.2}$$

Some of the most common algorithms to solve NLP problems are successive quadratic programming (SQP), reduced gradient algorithms, and interior point methods.

SQP algorithms are based on the solution of quadratic programming subproblems. Each subproblem optimizes a quadratic model of the objective function subject to linearized constraints. In each of the iterations a search direction is determined reducing some merit function to ensure problem convergence (Gill et al., 2005). SNOPT is a solver based on this method (Gill et al., 2005).

Reduced gradient methods consider a linear approximation of the constraints and eliminate variables to reduce the dimension of the problem. The resulting problem is solved by applying the Newton's method. In each of the iterations, the reduced gradient is calculated, the search direction is determined, and finally a line search is performed minimizing the objective function. MINOS (Murtagh & Saunders, 1983) or CONOPT (Drud, 1985) are solvers based on this algorithm.

Interior point methods reformulate the original NLP problem by means of slack variables to replace the inequalities by equalities and the log-barrier function to handle the non-negativity of the x variables. The new problem is solved applying the Newton's method. IPOPT Wächter and Biegler, 2006 and KNITRO (Waltz & Nocedal, 2004) are solvers based on this approach

MIXED-INTEGER LINEAR PROGRAMMING (MILP) Mixed-integer linear programming (MILP) refers to those mathematical programming problems based on linear equations and containing discrete variables. A mixed-integer linear programming problem can be expressed as shown in Eq. 1.3, where x are continuous variables and y are discrete variables. Typically, discrete variables are binary variables (Grossmann, 2021).

$$\begin{aligned}
 \min \quad & Z = a^T x + b^T y \\
 \text{s.t.} \quad & Ax + By \leq d
 \end{aligned} \tag{1.3}$$

$$\begin{aligned}
 & x \geq 0 \\
 & y \in \{0, 1\}^m
 \end{aligned} \tag{1.4}$$

A number of methods have been proposed to solve MILP problems, including cutting planes, Benders decomposition, branch and bound search, and branch and cut methods.

Cutting planes consist of a sequence of LP problems in which different cutting planes are generated to cut-off the solution of the relaxed LP. They reduce the feasible region of the linear relaxation of the original problem excluding those solutions that are feasible in the linear relaxation but not in the original MILP problem.

Benders decomposition is based on the generation of a lower and an upper bound of the solution of the MILP problem in each iteration. The upper bound is calculated from the primal problem, which correspond with the original problem where the binary variables have been fixed. Conversely, the lower bound is determined through a master problem, which is a LP problem derived from the original problem by means of the duality theory. Branch and bound method structure the problem in form of a binary tree that includes all possible combinations of binary variables. The tree is explored by solving the relaxed versions of the original problem. If the relaxation does not result in an integer solution (0 or 1), it is necessary to go deeper into the solution tree to explore further combinations of the binary variables. If the result obtained is an integer, the next step is to return to the previous subproblem to explore the alternative branch. However, diverse procedures have been developed to discard certain branches, avoiding the need of exploring the whole tree and reducing the problem (Floudas, 1995).

Branch and cut methods combine branch and bound methods with cutting planes targeting a tighter lower bound. In the different nodes, the relaxed problem is solved. If the solution is not integer, the relaxing problem is solved by adding cutting planes in order to strengthen the lower bound (Grossmann, 2021). Gurobi (Gurobi Optimization, LLC, 2021) and CPLEX (IBM, 2009) are solvers based on this approach.

MIXED-INTEGER NONLINEAR PROGRAMMING (MINLP) Mixed-integer nonlinear programming (MINLP) refers to those mathematical programming problems containing nonlinear equations and discrete variables, typically, binary variables. A mixed-integer nonlinear programming problem can be expressed as shown in Eq 1.5, where x represents a vector of continuous variables, y is the vector of binary variables, $h(x, y)$ and $g(x, y)$ denote the equality and inequality constraints respectively. $f(x)$ represents the objective function (Grossmann, 2021).

$$\begin{aligned}
 \min \quad & f(x, y) \\
 \text{s.t.} \quad & h(x, y) = 0 \\
 & g(x, y) \leq 0 \\
 & x \in X \subseteq \mathbb{R}^n \\
 & y \in \{0, 1\}^m
 \end{aligned} \tag{1.5}$$

Some algorithms for solving MINLP problems are the generalized Benders decomposition, outer approximation, and generalized cross decomposition.

Generalized Benders decomposition (GBD) is based on the generation of a lower and an upper bound of the solution of the MINLP problem in each iteration. Similarly to the Benders decomposition, the upper bound is calculated from the primal problem, which correspond with the original problem where the binary variables have been fixed. The lower bound is determined through a master problem, which is a LP problem derived from the original problem by means of the duality theory. In addition, the master problem provides information about the binary variables to be fixed in the next iteration (Floudas, 1995).

Outer approximation (OA) provides a lower and an upper bound in each iteration. As the previous case, the upper bound is calculated from the primal problem. The lower bound is calculate from a master problem obtained based on an outer approximation, i.e., the nonlinear objective function and the constraints are linearized around the primal solution. Additionally, the master problem provides information about the binary variables to be fixed in the next iteration.

Generalized cross decomposition (GCD) is based on the generation of a primal problem that provides an upper bound of the solution and also the Lagrange multipliers for the dual subproblem. The dual problem is used to determine the lower bound of the problem, and provides a vector of binary variables to be fixed in the primal problem. The solution of the primal and dual problems go through convergence tests. If any of these test fails, a master problem is solved. This approach seeks to minimize the number of master problems to be solved since the computational requirements of the this problem are higher. This procedure is repeated at each iteration of the algorithm (Floudas, 1995).

1.4 APPROACHES FOR GEOSPATIAL ENVIRONMENTAL ASSESSMENT

The development of mitigation measures to reduce the environmental footprint of anthropogenic activities requires the previous understanding

and quantification of the environmental impacts associated to each sector. This process, called environmental impact assessment (EIA), involves the analysis of multi-disciplinary information, including environmental, physical, geological, ecological, economic, and social data (Gharehbaghi & Scott-Young, 2018). Since EIA aims to evaluate the environmental impact of an activity on a particular geographical location, all these data have a common geographic component, becoming geospatial data.

Geospatial data can be managed and analyzed through specific systems denoted as geographic information system (GIS). GIS is a key tool for EIA that uses the geographic component of geospatial data as an integrative framework that provides the ability to analyze and map the descriptive information of the locations studied. The geographic component of data is the key element of GIS systems, since the spatial (or spatio-temporal) location is used as a key to relate other descriptive information. From the perspective of EIA, this information can be analyzed, interpreted, and mapped in order to determine the vulnerability level to a particular environmental threat at each location, find relationships between human activities and environmental damages, measure the performance of mitigation and remediation processes, etc.

As a result, the combination of GIS, EIA, and methods for the analysis of multi-dimensional information, such as MCDA, provides tools for the development of strategies to promote the transition to a sustainable paradigm for human growth. In this regard, the development of a sustainable, reliable, and resilient water, energy and food nexus is a major issue for food security and environmental protection.

1.5 THESIS OUTLINE

This dissertation is structured in three parts. Part I is devoted to the study of phosphorus management and recovery, Part II addresses a techno-economic assessment of the technologies for nitrogen recovery, and Part III conducts a techno-economic analysis for determining the optimal biomethane production process in order to integrate biogas production and nutrient recovery processes.

1.5.1 *Part I - Phosphorus management and recovery*

CHAPTER 3 - TECHNOLOGIES FOR PHOSPHORUS RECOVERY. This chapter performs a review of the main processes for phosphorus recovery from livestock waste, identifying the most promising processes to be deployed at CAFOs using a mixed-integer nonlinear programming model.

CHAPTER 4 - ASSESSMENT OF PHOSPHORUS RECOVERY THROUGH STRUVITE PRECIPITATION. This chapter studies the mitigation of phosphorus releases through the deployment of struvite precipitation systems in the watersheds of the contiguous United States. Specific surrogate models to predict the production of struvite and calcium precipitates from cattle leachate were developed based on a detailed thermodynamic model. In addition, the variability in the organic waste composition is captured through a probability framework based on the Monte Carlo method.

CHAPTER 5 - GEOSPATIAL ENVIRONMENTAL AND TECHNO-ECONOMIC FRAMEWORK FOR SUSTAINABLE PHOSPHORUS MANAGEMENT AT LIVESTOCK FACILITIES. This chapter presents a decision support framework, COW2NUTRIENT (Cattle Organic Waste to NUTRIent and ENergy Technologies), for the assessment and selection of phosphorus recovery technologies at CAFOs based on environmental information on nutrient pollution and techno-economic criteria. This framework combines eutrophication risk data at subbasin level and the techno-economic assessment of six state-of-the-art phosphorus recovery processes in a multi-criteria decision analysis (MCDA) model. We aimed to provide a useful framework for the selection of the most suitable P recovery system for each particular CAFO, and for designing and evaluating effective GIS-based incentives and regulatory policies to control and mitigate nutrient pollution of waterbodies.

CHAPTER 6 - ANALYSIS OF INCENTIVE POLICIES FOR PHOSPHORUS RECOVERY. This chapter conduct a research on the design and analysis of incentive policies using the COW2NUTRIENT framework for the implementation of phosphorus recovery technologies at CAFOs minimizing the negative impact in the economic performance of CAFOs. Moreover, the fair allocation of monetary resources when the available budget is limited is studied using the Nash allocation scheme.

1.5.2 *Part II - Nitrogen management and recovery*

CHAPTER ?? - MULTI-SCALE TECHNO-ECONOMIC ASSESSMENT OF NITROGEN RECOVERY SYSTEMS FOR SWINE OPERATIONS. This chapter evaluates the main processes for nitrogen recovery at intensive swine operations. A multi-scale techno-economic analysis is performed to estimate the capital and operating costs for different treatment capacities, identifying the most promising processes.

1.5.3 Part III - Nitrogen management and recovery

CHAPTER 7 - OPTIMAL TECHNOLOGY SELECTION FOR THE BIOGAS UPGRADING TO BIOMETHANE. This chapter performs a systematic study of different biogas upgrading to biomethane processes in order to identify the optimal process attending to the particular characteristics of the biogas produced from livestock manure. Food waste and wastewater sludge are also included for comparison. We aimed to determine the optimal biomethane production processes for the potential combination of biomethane production and nutrient recovery processes into an integrated resources recovery facility.

BIBLIOGRAPHY

- Amery, F., & Schoumans, O. F. (2014). *Agricultural phosphorus legislation in Europe*. Institute for Agricultural; Fisheries Research (ILVO); Alterra Wageningen UR.
- Anderson, J. D., & Wendt, J. (1995). *Computational fluid dynamics* (Vol. 206). Springer.
- Belton, V., & Stewart, T. (2002). *Multiple criteria decision analysis: an integrated approach*. Springer Science & Business Media.
- BIOGAS₃ PROJECT. (2021). BIOGAS₃ PROJECT - Sustainable small-scale biogas from agri-food waste for energy self-sufficiency [[Online; accessed 28-September-2021]].
- Biraben, J. N. (1980). An essay concerning mankind's demographic evolution. *Journal of Human Evolution*, 9(8), 655–663.
- Bouwman, A. F., Beusen, A. H. W., & Billen, G. (2009). Human alteration of the global nitrogen and phosphorus soil balances for the period 1970–2050. *Global Biogeochemical Cycles*, 23(4). <https://doi.org/doi.org/10.1029/2009GB003576>
- Brignole, E. A., & Pereda, S. (2013). *Phase equilibrium engineering*. Newnes.
- Burns, R. T., & Moody, L. B. (2002). Phosphorus recovery from animal manures using optimized struvite precipitation. *Proceedings of Coagulants and Flocculants: Global market and technical opportunities for water treatment chemicals*, 1–4.
- Buzzi-Ferraris, G., & Manenti, F. (2009). Kinetic models analysis. *Chemical Engineering Science*, 64(5), 1061–1074.
- CNP. (2021). *Review of Applicability of EPA's Part 503 Biosolids Rule on Phosphorus Minerals recovered at Water Resource Recovery Facilities* (tech. rep.). CNP.

- Comission, E. (2020). *A new Circular Economy Action for a cleaner and more competitive Europe* (tech. rep.). European Comission.
- Constable, G., & Somerville, B. (2003). *A century of innovation: Twenty engineering achievements that transformed our lives. Chapter 7, Agricultural mechanization*. Joseph Henry Press.
- Cordell, D., Drangert, J.-O., & White, S. (2009). The story of phosphorus: global food security and food for thought. *Global environmental change*, 19(2), 292–305.
- Couper, J. R., Penney, W. R., Fair, J. R., & Walas, S. M. (2005). *Chemical process equipment: selection and design*. Gulf professional publishing.
- Drud, A. (1985). CONOPT: A GRG code for large sparse dynamic nonlinear optimization problems. *Mathematical programming*, 31(2), 153–191.
- ESSP. (2021). *ESPP input for the EU's "Integrated Nutrient Management Action Plan"* (INMAP) (tech. rep.). European Sustainable Phosphorus Platform.
- European Comission. (2021). BiogasAction [[Online; accessed 28-September-2021]].
- FICO. (2021). Xpress-Optimizer Reference manual, 20.0 edition. <http://www.fico.com/xpress>
- Floudas, C. A. (1995). *Nonlinear and mixed-integer optimization: fundamentals and applications*. Oxford University Press.
- Gasser, P., Suter, J., Cinelli, M., Spada, M., Burgherr, P., Hirschberg, S., Kadziński, M., & Stojadinović, B. (2020). Comprehensive resilience assessment of electricity supply security for 140 countries. *Ecological Indicators*, 109. <https://doi.org/10.1016/j.ecolind.2019.105731>
- Gharehbaghi, K., & Scott-Young, C. (2018). GIS as a vital tool for Environmental Impact Assessment and Mitigation, In *IOP Conference Series: Earth and Environmental Science*. IOP Publishing.
- Gill, P. E., Murray, W., & Saunders, M. A. (2005). SNOPT: An SQP algorithm for large-scale constrained optimization. *SIAM review*, 47(1), 99–131.
- Giove, S., Brancia, A., Satterstrom, F. K., & Linkov, I. (2009). Decision support systems and environment: Role of MCDA. In *Decision support systems for risk-based management of contaminated sites* (pp. 1–21). Springer.
- Grizzetti, B., Vigiak, O., Udiás, A., Aloe, A., Zanri, M., Bouraoui, F., Pistocchi, A., Dorati, C., Friedland, R., De Roo, A., Benitez Sanz, C., Leip, A., & Bielza, M. (2021). How EU policies could reduce nutrient pollution in European inland and coastal waters. *Global Environmental Change*, 69, 102281.
- Grossmann, I. E. (2021). *Advanced Optimization for Process Systems Engineering*. Cambridge University Press.

- Gurobi Optimization, LLC. (2021). Gurobi Optimizer Reference Manual.
<https://www.gurobi.com>
- Hall, S. M. (2012). *Rules of thumb for chemical engineers*. Butterworth-Heinemann.
- Himmelblau, D. M. (2000). Applications of artificial neural networks in chemical engineering. *Korean journal of chemical engineering*, 17(4), 373–392.
- Hwang, C., & Yoon, K. (1995). Multi attribute decision making—an introduction. Sage University Papers.
- IBM. (2009). *V12.1: User's Manual for CPLEX* (tech. rep.).
- Kellogg, R. L., Lander, C. H., Moffitt, D. C., & Gollehon, N. (2000). *Manure Nutrients Relative to the Capacity of Cropland and Pastureland to Assimilate Nutrients: Spatial and Temporal Trends for the United States* (tech. rep.). U.S. Department of Agriculture.
- Loeppert, R. H., Schwab, A. P., & Goldberg, S. (1995). *Chemical equilibrium and reaction models*. Soil Science Society of America.
- Marichal, J.-L., & Roubens, M. (2000). Determination of weights of interacting criteria from a reference set. *European journal of operational Research*, 124(3), 641–650.
- Martín, M., & Grossmann, I. E. (2012). BIOpt: A library of models for optimization of biofuel production processes. In I. D. L. Bogle & M. Fairweather (Eds.), *22nd European Symposium on Computer Aided Process Engineering* (pp. 16–20). Elsevier.
- Murtagh, B. A., & Saunders, M. A. (1983). *MINOS 5.0 User's Guide*. (tech. rep.). Stanford Univ CA Systems Optimization Lab.
- Murty, K. G. (1983). *Linear programming*. Springer.
- NACWA. (2014). *Issue Outline on Resource Recovery from Wastewater and Coverage of 40 C.F.R. Part 503* (tech. rep.). National Association of Clean Water Agencies.
- Nierenberg, D., & Mastny, L. (2005). *Happier meals: Rethinking the global meat industry* (Vol. 171). Worldwatch Institute.
- OECD and European Commission. (2008). *Handbook on Constructing Composite Indicators. Methodology and User Guide*. OECD.
- Piot-Lepetit, I. (2011). *Agricultural externalities and environmental regulation: The case od manure management and spreading land allocation*. Bentham Science Publishers.
- Pistikopoulos, E. N., Barbosa-Povoa, A., Lee, J. H., Misener, R., Mitsos, A., Reklaitis, G. V., Venkatasubramanian, V., You, F., & Gani, R. (2021). Process systems engineering – The generation next? *Computers & Chemical Engineering*, 147, 107252.
- Potra, F. A., & Wright, S. J. (2000). Interior-point methods. *Journal of Computational and Applied Mathematics*, 124(1), 281–302.

- Queipo, N. V., Haftka, R. T., Shyy, W., Goel, T., Vaidyanathan, R., & Tucker, P. K. (2005). Surrogate-based analysis and optimization. *Progress in aerospace sciences*, 41(1), 1–28.
- Quirante, N., Javaloyes, J., & Caballero, J. A. (2015). Rigorous design of distillation columns using surrogate models based on Kriging interpolation. *AIChE Journal*, 61(7), 2169–2187.
- Ramkrishna, D. (2000). *Population balances: Theory and applications to particulate systems in engineering*. Elsevier.
- Roy, B. (1968). Classement et choix en présence de points de vue multiples. *Revue française d'informatique et de recherche opérationnelle*, 2(8), 57–75.
- Roy, B. Et al. (1978). ELECTRE III: Un algorithme de classements fondé sur une représentation floue des préférences en présence de critères multiples. *Cahiers Centre d'Etudes de Recherche Opérationnelle*.
- Roy, B., & Bertier, P. (1973). La Méthode ELECTRE II: Une application au média-planning.
- Saaty, T. L. (2000). *Fundamentals of decision making and priority theory with the analytic hierarchy process* (Vol. 6). RWS publications.
- Sadhukhan, J., Ng, K. S., & Hernandez, E. M. (2014). *Biorefineries and chemical processes: design, integration and sustainability analysis*. John Wiley & Sons.
- Samreen, S., & Kausar, S. (2019). Phosphorus Fertilizer: The Original and Commercial Sources. IntechOpen. <https://doi.org/10.5772/intechopen.82240>
- Smil, V. (1999). Detonator of the population explosion. *Nature*, 400(6743), 415–415.
- Stephanopoulos, G., & Reklaitis, G. V. (2011). Process systems engineering: From Solvay to modern bio- and nanotechnology.: A history of development, successes and prospects for the future. *Chemical Engineering Science*, 66(19), 4272–4306.
- Szirtes, T. (2007). *Applied dimensional analysis and modeling*. Butterworth-Heinemann.
- Tervonen, T., & Lahdelma, R. (2007). Implementing stochastic multicriteria acceptability analysis. *European Journal of Operational Research*, 178(2), 500–513. <https://doi.org/10.1016/j.ejor.2005.12.037>
- Tilley, E., Ulrich, L., Lüthi, C., Reymond, P., & Zurbrügg, C. (2014). *Compendium of sanitation systems and technologies*. Eawag.
- United Nations, Department of Economic and Social Affairs. (2019). World Population Prospects 2019 [[Online; accessed 22-August-2021]].
- US EPA. (2020a). *Elements of an NPDES Permit for a CAFO*. NPDES Permit Writers' Manual for CAFOs (tech. rep.). U.S. Environmental Protection Agency.
- US EPA. (2020b). NPDES Permit Basics [[Online; accessed 24-August-2021]].

- US EPA. (2021). AgSTAR: Biogas Recovery in the Agriculture Sector [[On-line; accessed 28-September-2021]].
- USDA. (2009). *Agricultural Water Management Field Handbook* (tech. rep.). U.S. Department of Agriculture.
- USDA. (2011). Animal Feeding Operations (AFO) and Concentrated Animal Feeding Operations (CAFO) [[Online; accessed 10-August-2021]].
- Vincke, J. P., & Brans, P. (1985). A preference ranking organization method. The PROMETHEE method for MCDM. *Management Science*, 31(6), 647–656.
- Wächter, A., & Biegler, L. T. (2006). On the implementation of an interior-point filter line-search algorithm for large-scale nonlinear programming. *Mathematical programming*, 106(1), 25–57.
- Waltz, R. A., & Nocedal, J. (2004). KNITRO 2.0 User's Manual. Ziena Optimization, Inc.[en ligne] disponible sur <http://www.ziena.com> (September, 2010), 7, 33–34.
- Wilson, Z. T., & Sahinidis, N. V. (2017). The ALAMO approach to machine learning. *Computers & Chemical Engineering*, 106, 785–795.

2

OBJECTIVE

2.1 SCOPE AND OBJECTIVES OF THE THESIS

2.2 MAIN OBJECTIVE

This thesis seeks to promote the recovery and recycling of nutrients contained in livestock waste by identifying the most appropriate technologies for phosphorus and nitrogen recovery at cattle and swine CAFOs, assessing the potential nutrient releases abatement that could be achieved by the deployment of these systems and analyzing incentive policies for their effective implementation at livestock facilities. Moreover, we introduce a systematic framework for evaluating and selecting the most suitable nutrient recovery system at CAFOs considering geospatial environmental vulnerability to nutrient pollution.

2.3 SPECIFIC OBJECTIVES

OBJECTIVE I: To identify the role of intensive farming activities on nutrient pollution, including the main sources of nutrient releases, as well as potential processes and systems for nutrient recovery.

OBJECTIVE II: To identify environmental indicators for nutrient pollution, and use them to assess the potential for the abatement of phosphorus releases by deploying the processes previously selected at livestock facilities at subbasin spatial resolution.

OBJECTIVE III: To develop a decision-support system for the evaluation and selection of nutrient recovery systems at livestock facilities integrating techno-economic data of the nutrient recovery technologies and environmental vulnerability to nutrient pollution information determined through a tailored geographic information system (GIS) in order to select the most suitable system for each particular livestock facility.

OBJECTIVE IV: To design and analyze potential incentive policies for the deployment of phosphorus recovery technologies at livestock facilities, as well as to study the fair allocation of limited monetary resources.

Part I

PHOSPHORUS MANAGEMENT AND RECOVERY

3

TECHNOLOGIES FOR PHOSPHORUS RECOVERY

3.1 INTRODUCTION

Countries across the globe generate large amounts of organic waste that include urban residues and sludge and manure from livestock activities. While many of these waste streams can be used as a source for power and chemical products, identifying suitable cost-effective technologies is challenging. Anaerobic digestion (AD) is a promising technology to treat these residues to produce biogas, which can be used as a source for thermal energy and electrical power (León & Martín, 2016) or chemicals (Hernández & Martín, 2016). However, AD technologies also generate a nutrient-rich residual stream called digestate, that must be further processed to prevent waste and soil contamination. In particular, nutrient management is needed to prevent losses of phosphorous and nitrogen to surface and underground water bodies which leads to eutrophication processes (García-Serrano et al., 2009; Sampat et al., 2017). There are a number of technologies that can be used to process the digestate that range from simple mechanical separations such as filters (Gustafsson et al., 2008) and centrifugation units (Meixner et al., 2015) to chemical processing such as struvite precipitation (Bhuiyan et al., 2008). Recent studies have analyzed the production of highly concentrated nutrient products such as struvite (Lin et al., 2015). The variability in the recovered product quality, selling price, and production cost presents complex trade-offs for the optimal use of the digestate. Existing studies have only addressed the performance of various treatment mechanisms and lack a systematic design perspective that evaluates the performance of coupled biogas and nutrient recovery technologies (Drosg et al., 2015). This is necessary, for instance, to assess economic performance of nutrient recovery in the face of strong variations in the digestate content obtained from AD (Al Seadi et al., 2008).

In this work we propose a systematic design framework to optimize the simultaneous production of energy from the biogas obtained by anaerobic digestion of cattle, sheep, poultry and pig manure, along with the recovery of nitrogen and phosphorous from the digestate. The proposed framework determines the optimal technology configuration, equipment sizing, and operational conditions for various compositions of manure and digestate and revenues for biogas, electricity, and fertilizer.

The section is organized as follows. In Section 3.2 we present a brief description of the process and the flowsheet. In Section 3.3 we focus on the modelling of the digestate processing technologies and costing. Section 3.4 presents the results for various feedstocks, and Section 3.5 draws conclusions.

3.2 PROCESS DESCRIPTION

The proposed process consists of four sections: biogas production, biogas purification (biogas generation), electrical power generation, and nutrient recovery from digestate. This is illustrated in Figure 3.1.

The biomass together with water and nutrients (manure slurry) are fed to a bioreactor through stream 1, where the mixture is anaerobically digested to produce biogas and a decomposed substrate (digestate). The biogas, composed of methane, carbon dioxide, nitrogen, hydrogen sulfide, ammonia and moisture leaves the bioreactor through stream 2, and it is then sent to the purification section to remove H₂S in a fixed-bed reactor and to eliminate CO₂ and traces of NH₃ in a second step by using a pressure swing adsorption (PSA) system. The purified biogas (stream 3) is used in a Brayton cycle, modelled as a furnace and an expansion, producing power. Air is fed via stream 4 and the exhaust gases (stream 7) are fed to a regenerative Rankine cycle, where it produces high pressure overheated steam extracted in stream 8. This overheated steam is fed to a steam turbine, where it is expanded to produce power. The exhaust steam from the turbine is recovered in stream 9 and reused in the Rankine cycle through stream 10. Between streams 9 and 10 hot flue gases from the gas turbine reheat and produced overheated steam from the recycled water (León & Martín, 2016).

The digestate is released from the digester through stream 12, and it can be processed through a number of technologies to remove nitrogen and phosphorous. We consider filtration, centrifugation, coagulation, and struvite production using either a fluidized bed reactor (FBR) or a continuous stirred tank reactor (CSTR). These technologies are described in detail in Section 3.3.4.

Four manure types have been considered as raw material for the process: cattle, pig, poultry and sheep manure. Table 6.1 shows the composition and properties of each type of manure.

Table 3.1: Manure composition and properties (Al Seadi et al., 2008; Kowalski et al., 2013; Lorimor et al., 2004; Martins das Neves et al., 2009).

Manure/ element	Dry matter (% wt)		N (% dry mass)		P (% dry mass)		K (% dry mass)		VS (% dry mass)		V _{biogas} (m ³ _{gas} kg _{vs})	Density (kg/m ³)	
	Max	Min	Max	Min	Max	Min	Max	Min	Max	Min	Max	Min	
Cattle	10	2	8	4.7	1.3	0.8	10	3.3	0.8	0.8	0.3	0.2	1041.2
Pig	6	2	15	13	2.2	1.9	8.3	3.9	0.8	0.7	0.5	0.25	1000.0
Poultry	60	30	5.4	5.4	1.7	1.7	1.2	2.3	0.8	0.8	0.6	0.35	1009.2
Sheep	28	28	2.9	2.9	0.78	0.78	2.9	2.9	0.8	0.8	0.61	0.37	1009.2

Table 3.2: Set of components.

Number of component	Component	Number of component	Component	Number of component	Component	Number of component	Component
1	Wa	12	O	23	K ₂ O	34	Cl
2	CO ₂	13	N	24	CaCO ₃	35	Struvite
3	CO	14	Norg	25	FeCl ₃	36	K-Struvite
4	O ₂	15	P	26	Antifoam	37	MgCl ₂ (CSTR)
5	N ₂	16	K	27	Fe ₂ (SO ₄) ₃	38	NaOH (CSTR)
6	H ₂ S	17	S	28	Al ₂ (SO ₄) ₃	39	Mg (CSTR)
7	NH ₃	18	Rest	29	AlCl ₃	40	Cl (CSTR)
8	CH ₄	19	Cattle slurry	30	MgCl ₂	41	Struvite (CSTR)
9	SO ₂	20	Pig slurry	31	NaOH	42	K-Struvite (CSTR)
10	C	21	Poultry slurry	32	Struvite seeds	43	FeCl ₃ Coag
11	H	22	P ₂ O ₅	33	Mg		

3.3 MODELLING ISSUES

We evaluate the performance of the different unit operations in the process by using detailed models that comprise mass and energy balances, thermodynamics, chemical and vapor–liquid equilibria, and product yield calculations. The global process model comprises total mass flows, component mass flows, component mass fractions, temperatures and pressures of the streams in the process network. The components that are considered in our calculations belong to the set shown in Table 3.2.

In the following subsections, we briefly present the main equations used to characterize the operation of the different units. For the sake of brevity, simpler balances based on removal efficiency or stoichiometry and equations connecting units are omitted. The power production system is described in detail in previous work (León & Martín, 2016) and we thus only provide a brief description.

The cost estimation for the alternatives and for the entire process is based on the estimation of the unit costs from different sources using the factorial method. From the units cost, the facility cost is estimated using the coefficients in Sinnott (1999a), so that the total physical plant cost involving equipment erection, piping instrumentation, electrical, buildings, utilities, storage, site development, and ancillary buildings is 3.15 times the total equipment cost for processes which use fluids and solids. On the other hand, the fixed cost, which includes design and engineering, contractor's fees, and contingency items is determined as 1.4 times the total physical plant cost for the fluid and solid processes. In the subsequent cost estimation procedures these parameters are denoted as f_i for the total physical plant parameter and f_j for the fixed cost parameter.

3.3.1 Biogas production

AD is a complex microbiological process that decomposes organic matter in the absence of oxygen. It produces a gas mixture following hydrolysis, acidogenesis, acetogenesis, and methanogenesis steps, consisting mainly of methane and carbon dioxide (biogas), and decomposed substrate (digestate). The anaerobic reactor is modeled using mass balances of the species involved in the production of biogas and digestate. Inorganic nitrogen, organic nitrogen, sulfur, carbon, and phosphorus balances are formulated by using the composition of volatile solids in manure, see Table 6.1 (Al Seadi et al., 2008; Kowalski et al., 2013; Lorimor et al., 2004; Martins das Neves et al., 2009). Typical bounds for the biogas composition are provided. The reactor operates at 55 °C. We refer the reader to the Supplementary

Material and León and Martín (2016) for details on the modelling of the digester.

3.3.2 Biogas purification

This system consists of a number of stages to remove H₂S, CO₂ and NH₃. Here we highlight some basics about the operation of these stages. For further details we refer the reader to previous work (León & Martín, 2016).

The removal of H₂S is carried out in a bed of Fe₂O₃, that operates at 25–50 °C producing Fe₂S₃. The regeneration of the bed uses oxygen to produce elemental sulfur and Fe₂O₃.

CO₂ is adsorbed using a packed bed of zeolite 5A. The typical operating conditions for PSA systems are low temperature (25 °C) and moderate pressure (4.5 bar). The recovery of the PSA system is assumed to be 100% for NH₃ and H₂O (because of their low total quantities in the biogas, in general), 95% for CO₂, and 0% for all other gas of the mixture.

In both cases the system is modelled as two beds in parallel so that one bed is in adsorption mode while the second one is in regeneration mode, to allow for continuous operation of the plant. Further details can be found in the Supplementary Material.

3.3.3 Electricity generation

We consider two stages for the generation of power. The initial one consists of the use of a gas turbine, a common alternative for using any gas fuel. However, the flue gas that exits the gas turbine is at high temperature. We can either produce steam as a utility or use that steam within a regenerative Rankine cycle to enhance the production of power. The details for the process appear in León and Martín (2016) or in the Supplementary Material.

3.3.3.1 Brayton cycle

We model the Brayton cycle as a double-stage compression system (one for the air and one for the fuel) with intercooling with variable operating pressure for the gas turbine. The compression is assumed to be polytropic with a coefficient equal to 1.4 and an efficiency of 85% (Moran & Shapiro, 2003).

The combustion of methane from the biogas is assumed to be adiabatic, heating up the mixture. We consider the combustion chamber as an

adiabatic furnace. We use an excess of 20% of air with respect to the stoichiometry and 100% conversion of the reaction:



The hot flue gas is expanded in the gas turbine to generate power and the expansion is assumed polytropic. In this case, a value of 1.3 is used based on an offline simulation using CHEMCAD®, with an efficiency of 85% (Moran & Shapiro, 2003). Finally, the exhaust gas is cooled down and used to generate high-pressure steam to be fed to the Rankine cycle.

3.3.3.2 *Rankine cycle*

We use the hot flue gas from the turbine to generate steam following a scheme that consists of using the hot gas in the order that follows. First, the hot flue gas is used for the superheating stage of the steam that is to be fed to the turbine. Next, the hot gas is used in the regenerative stage of the Rankine cycle, reheating the steam from the expansion of the high pressure turbine. Subsequently, the flue gas is used in the evaporation and preheating of the condensed water, see Figure 3.1. The details of the modelling of the Rankine cycle can be seen in Martín and Martín (2013). We assume an isentropic efficiency of 0.9 for each expansion.

3.3.4 *Digestate conditioning*

Four different alternatives are considered to process the digestate including filtration, centrifugation, coagulation, and struvite production. For struvite production, the performance of fluidized bed reactors (FBR) and stirred tanks reactors (CSTR) systems is compared. For filtration, centrifugation, and coagulation technologies, nutrients output is a cake composed of different solids and nutrients, with a complex composition. The credit that we can get from the cake has been estimated based on the amount of nutrients contained. The prices for the nutrients (N, P and K) are assumed as follows: 0.45 €/kg for N, 0.24 €/kg for K and 0.32 €/kg for P (Hernandez et al., 2017).

3.3.4.1 *Filtration*

Filtration is a low-cost technology that is appropriate for small installations where the amount of P to be removed is moderate. This technology consists of a filter that contains a reactive medium to help remove phosphorus. P removal using reactive filtration takes place through various mechanisms depending on the characteristics of the filter media. For

instance, filter media made of compounds rich in cations under basic environments (usually containing calcium silicates at pH values above 9) form orthophosphate precipitates in the form of calcium phosphates, principally as hydroxyapatite (Pratt et al., 2012). Metallurgical slag captures P by adsorption over metal at pH close to 7 (Pratt et al., 2012). In this work we consider the use of five different types of filter media. Among them, we have studied wollastonite as a filter media rich in alkaline calcium silicates, dolomite Polonite® as calcium carbonate based components, and Filtra P as calcium hydroxide based product (Österberg, 2012; Vohla et al., 2011). For the metallurgical slag, we have considered the blast furnace slag described by Cucarella et al. (2008). These filters are used in wastewater treatment facilities (Gustafsson et al., 2008) and further analysis can be found in Shilton et al. (2006). Details on Ca-rich filters can be found in Kõiv et al. (2010). The removal yield of P and N for the different filter media is shown in Table 3. It is possible to combine this filter medium with nitrogen-philic filters to simultaneously remove nitrogen and phosphorous. An advantage of this technology is that the cake produced can be used as soil fertilizer (Hylander et al., 2006). The removal yield of nitrogen for Filtra P® has been considered similar to the limestone nitrogen removal yield, as Filtra P® is a limestone derived product.

The model for the filtration is based on the removal efficiency per filter media, see Fig. 3.2. It has been considered that materials such as total solids, carbon and potassium are forming solid compounds, so they will be retained by the filter media, Eqs. 3.4–3.7.

$$\begin{aligned} F_i^{cake} &\geq F_i^{in} \cdot \eta_i^j - M \cdot (1 - y^j) \\ i &\in \{\text{P, N}\} \\ j &\in \{\text{filter media}\} \end{aligned} \quad (3.2)$$

$$\sum y^j = 1 \quad (3.3)$$

$$F_i^{liquid effluent} = F_i^{in} - F_i^{cake} \quad (3.4)$$

$$F_k^{cake} = F_k^{in}; k \in \{\text{TS, C, K}\} \quad (3.5)$$

$$F_{Wa}^{cake} = \left(F_{TS}^{cake} + \sum_i F_i^{cake} \right) \cdot \frac{C_{Wa}^{cake}}{1 - C_{Wa}^{cake}} \quad (3.6)$$

Table 3.3: Recovered P and N yield for different filter media..

Media/nutrient	P (% recovered)	N (% recovered)
Polonite	96.7 ^a	18.0 ^c
Filtra P	98.2 ^a	50.0 ^e
Wollastonite	51.1 ^a	70.0 ^d
Dolomite	44.0 ^b	50.0 ^e
Metal slag	85.6 ^a	67.0 ^f

a: Gustafsson et al. (2008)

b: Pant et al. (2001)

c: Kietlińska and Renman (2005)

d: Lind et al. (2000)

e: Aziz et al. (2004)

f: Yang et al. (2009)

$$F_{Wa}^{liquid\ effluent} = F_{Wa}^{in} - F_{Wa}^{cake} \quad (3.7)$$

To select among the five filter media, we use a Big M formulation to select one of them assigning a binary variable $y_{filter\ media}$ for each filter media, Eqs. 3.2 and 3.3. This variable takes a value of 1 for the selected filter media and 0 for the rest, so that we are able to evaluate one filter media per time.

It is assumed that the cake obtained contains moisture with a value of 55% in weight basis (C_{Wa}^{cake}). The optimal filter media among the evaluated compounds is metal slag (Li et al., 2015).

The cost of each alternative has been estimated according to the number of filters, which depends on the maximum flow they can process. The maximum flow per filter unit, F_{max}^{filter} , is 1,300 ft³/min (Loh et al., 2002). To design the filter units we have taken the minimum value between the flow provided by mass balances and the maximum flow allowed per filter, Eqs. 3.8–3.10.

$$F \left(\frac{\text{ft}^3}{\text{min}} \right) = \frac{F_{in}}{\rho_{digestate}} \quad (3.8)$$

$$n_{filters} \geq \frac{F_{total}^{filter}}{F_{max}^{filter}} \quad (3.9)$$

$$F_{design}^{filter} \left(\frac{\text{ft}^3}{\text{min}} \right) = \min \left(F_{max}^{filter}, F_{total}^{filter} \right) \quad (3.10)$$

In fact, since the maximum flow for a cartridge filter is 1,300 ft³/min, for this facility the number of filters considered in this work will always be one and the design flow is equal to the flow provided by mass balances.

The correlation used to calculate the filter cost, Eq. 3.11, is obtained from data reported in Loh et al. (2002). This correlation provides the price in 1998 dollars, so we use the Chemical Engineering Index to update it.

$$FC_{filtration} (\text{USD}) = 4.7436 \cdot F_{design}^{filter} + 807.6923 \quad (3.11)$$

The operating cost is estimated using a simple correlation, Eq. 3.14, where we assume that the utilities contribute 20% of the total (Vian Ortuño, 1991). The other economical contributions considered are chemicals, estimated as in Eq. 3.12, labour, as per Eq. 3.13, and the contribution of the investment cost of the units given by Eqs. 3.10 and 3.11. The filter media are considered as chemicals that will be replaced annually.

$$ChemC_{filtration} \left(\frac{\text{EUR}}{\text{year}} \right) = \frac{F_P^{in} \cdot 3600 \cdot h \cdot d}{\frac{kg_P}{kg_{filter\ media}}} \cdot Price_{filter\ media} \quad (3.12)$$

In Eq. 3.12, $kg_{filter\ media}$ are calculated as the P content in the inlet stream divided by the filter media P adsorption capacity.

$$\begin{aligned} Labour\ cost \left(\frac{\text{EUR}}{\text{year}} \right) &= \\ &\left(61.33 \cdot F_P^{recovered} \cdot 3.6 \cdot h^{-0.82} \right) \cdot \left(F_P^{recovered} \cdot 3.6 \cdot h \cdot d \right) \cdot \left(\frac{Salary}{h \cdot d} \right) \cdot n_{OP} \end{aligned} \quad (3.13)$$

The number of operations considered, n_{OP} , is equal to 1.

$$\begin{aligned} Operating\ cost \left(\frac{\text{EUR}}{\text{year}} \right) &= \\ &\frac{ChemC + 1.5 \cdot Labour\ cost + 0.3 \cdot Fixed\ Cost \cdot f_i \cdot f_j}{(1 - Utilities)} \end{aligned} \quad (3.14)$$

Finally the credit obtained from the cake is computed as the weighted sum of each nutrient value, Eq. 3.15, (Hernandez et al., 2017), and the

benefits (or losses) are computed as the difference between the credit obtained from the cake and the operating costs of the facility, Eq. 3.16.

$$\begin{aligned} Cost_{cake} \left(\frac{\text{EUR}}{\text{year}} \right) = & \\ & \left(F_P^{recovered} \cdot Price_P + F_N^{recovered} \cdot Price_N + F_K^{recovered} \cdot Price_K \right) \\ & \cdot 3600 \cdot h \cdot d \end{aligned} \quad (3.15)$$

$$Benefits_{Filtration} \left(\frac{\text{EUR}}{\text{year}} \right) = Cost_{cake} - Operating\ cost \quad (3.16)$$

3.3.4.2 Coagulation

Coagulation is a chemical treatment to process the digestate. The goal of this process is to destabilize colloidal suspensions by reducing the attractive forces, followed by a flocculation process to form flocs from the previously destabilized colloids and to subsequently precipitate them. The nutrients are then recovered with other sedimented solids by clarification. Both N and P can be removed from the influent through coagulation–flocculation, where phosphorus is removed primarily in the form of metal hydroxides, which is the dominant process at typical plant pH values (Szabó et al., 2008). Nitrogen elimination is related to the removal of the colloidal matter (Aguilar et al., 2002). Different coagulation agents are considered aiming at selecting the optimal one: FeCl_3 , $\text{Fe}_2(\text{SO}_4)_3$, $\text{Al}_2(\text{SO}_4)_3$, and AlCl_3 . The flowsheet for the process of coagulation is presented in Fig. 3.3.

The removal efficiency achieved is similar for the different coagulant agents, with values up to 99% for phosphorus and 57% for nitrogen (Aguilar et al., 2002). The main variables which influence the coagulation–flocculation process are the initial ratio of metal to phosphorus, pH, and chemical oxygen demand (COD). The initial metal-phosphorus molar ratio must be between 1.5 and 2.0, and the recommended pH range is from 5.5 to 7. COD has a negative impact on the removal efficiency when its value is increased (Szabó et al., 2008).

To determine the amount of coagulant agent to be added to the system, it has been considered that a metal/phosphorus molar ratio of 1.75 must be achieved (Szabó et al., 2008). Given the relationship between the P in the raw material stream, the metal added, and the metal concentration in the commercial presentation of the coagulant agent, we are able to compute the coagulant agent amount that should be added. In the coagulation and flocculation tanks the flocs are formed and nutrients are recovered in the

sediment together with coagulation agents and organic solids contained in the raw material. In the decanter, it has been considered that the stream with solids has a water content of 50% ($C_{Wa}^{sedimentator}$) (Williams & Esteves, 2011) and the water content of the centrifuge outlet solids stream is 60% ($C_{Wa}^{centrifuge}$) (Wakeman, 2007).

Other elements present in the digestate, such as total solids, carbon, and potassium are assumed to be present in the solid forming compounds that sediment. Thus, they are among species that constitute the cake. Taking into account the elements mentioned above mass balances have been formulated with the corresponding removal ratios. To select and evaluate the different coagulant agents, the problem has been modelled using a mixed-integer nonlinear programming (MINLP) formulation with Big-M constraints, Eqs. 3.17 and 3.18.

$$F_j^{coag\ tank} \geq \frac{F_P^{in}}{MW_P} \cdot MeP_{ratio} \cdot \frac{MW_j}{C_{Me}} - M \cdot (1 - y^j) \quad (3.17)$$

$$j \in \{\text{coagulant agents}\}$$

$$\sum y^j = 1 \quad (3.18)$$

where MeP is the metal/phosphorus ratio and M is a large value to formulate the Big-M constraint to select and evaluate the different coagulant agents. Mass balances are computed using Eqs. 3.19–3.28.

$$F_j^{coag\ tank} = F_j^{floc\ tank} = F_j^{sedimentator} = F_j^{centrifuge} = F_j^{cake} \quad (3.19)$$

$$j \in \{\text{coagulants}\}$$

$$F_i^{in} = F_i^{coag\ tank} = F_i^{floc\ tank} = F_i^{sedimentator} \quad (3.20)$$

$$i \in \{\text{P, N}\}$$

$$F_i^{cake} = F_i^{centrifuge} = F_i^{sedimentator} \cdot \eta_i^j \quad (3.21)$$

$$F_i^{sink1} = F_i^{sedimentator} - F_i^{centrifuge} \quad (3.22)$$

$$F_k^{in} = F_k^{coag\ tank} = F_k^{floc\ tank} = F_k^{sedimentator} = F_k^{centrifuge} = F_k^{cake} \quad (3.23)$$

$k \in \{\text{TS}, \text{C}, \text{K}\}$

$$F_{Wa}^{in} = F_{Wa}^{coag\ tank} = F_{Wa}^{floc\ tank} = F_{Wa}^{sedimentator} \quad (3.24)$$

$$F_{Wa}^{centrifuge} = \left(F_{TS}^{centrifuge} + \sum_i F_i^{centrifuge} + \sum_j F_j^{centrifuge} \right) \cdot \frac{C_{Wa}^{sedimentator}}{1 - C_{Wa}^{centrifuge}} \quad (3.25)$$

$$F_{Wa}^{sink1} = F_{Wa}^{sedimentator} - F_{Wa}^{centrifuge} \quad (3.26)$$

$$F_{Wa}^{cake} = \left(F_{TS}^{cake} + \sum_i F_i^{cake} + \sum_j F_j^{cake} \right) \cdot \frac{C_{Wa}^{centrifuge}}{1 - C_{Wa}^{centrifuge}} \quad (3.27)$$

$$F_{Wa}^{sink2} = F_{Wa}^{centrifuge} - F_{Wa}^{cake} \quad (3.28)$$

The estimation of the size and cost of both the coagulation and flocculation tanks has been carried out using a correlation developed by Almena and Martín (2016) as a function of the weight of the vessels. To simplify the mass balances it is considered that the volume provided by the coagulant agents is negligible with respect to the processed stream of the digestate. The vessel size is computed from the residence time. The hydraulic retention time considered in the coagulation tank is 4 min (Zhou et al., 2008). The vessel size is computed from the residence time, Eq. 3.29. Using these data, the diameter and length are computed using rules of thumb, Eqs. 3.30 and 3.31. Finally, a correlation for the thickness as a function of the diameters allows determining the mass of metal required for the vessel and its weight, Eqs. 3.32 and 3.33. Vessel cost estimation is provided by Eq. 3.34.

$$V_{Coagtank} (\text{m}^3) = HRT_{Coag\ tank} \cdot \frac{F_{digestate}^{in}}{\rho_{digestate}} \quad (3.29)$$

$$D_{Coag\ tank} (m) = \left(\frac{6 \cdot V_{Coag\ tank}}{7 \cdot \pi} \right)^{1/3} \quad (3.30)$$

$$L_{Coag\ tank} (m) = 4 \cdot D_{Coag\ tank} \quad (3.31)$$

$$e_{Coag\ tank} (m) = 0.0023 + 0.003 \cdot D_{Coag\ tank} \quad (3.32)$$

$$W_{Coag\ tank} (\text{kg}) = \rho_{SS316} \cdot \quad (3.33)$$

$$\left[\pi \cdot \left(\left(\frac{D_{Coag\ tank}}{2} + e_{Coag\ tank} \right)^2 - \left(\frac{D_{Prec\ tank}}{2} \right)^2 \right) \cdot L_{Coag\ tank} + \frac{4}{3} \cdot \pi \cdot \left(\left(\frac{D_{Coag\ tank}}{2} + e_{Coag\ tank} \right)^3 - \left(\frac{D_{Coag\ tank}}{2} \right)^3 \right) \right]$$

$$Cost_{Vessel} (\text{USD}) = 6839.8 \cdot V_{Coag\ tank} (\text{m}^3)^{0.65} \quad (3.34)$$

To estimate the power consumed by the agitator, Eq. 3.35, rules of thumb have been used; where the specific power consumed, $\kappa_{agitator}$, is tabulated in Walas et al. (1990). For our slurries a value of $\kappa_{agitator}$ equal to 10 HP per 1000 US gallons is the most appropriate.

$$P_{Agitator} (\text{HP}) = V_{Coag\ tank} (\text{US gallon}) \cdot \frac{\kappa_{agitator}}{1000} \quad (3.35)$$

The agitator cost is also estimated using a correlation from Walas et al. (1990), Eq. (36). For cost estimation purposes we have considered stainless steel 316 as construction material and a dual impeller operating at speed between 56 and 100 rpm depending on the tanks size. With these considerations the values for a , b and c are 8.8200, 0.1235 and 0.0818 respectively (Walas et al., 1990). This correlation provides the cost in 1985 dollars, so it is necessary to update the result using the Chemical Engineering Index as before.

$$Cost_{Agitator} (\text{USD}_{1985}) = e^{a+b \cdot \ln(P_{agitator}(\text{HP})) + c \cdot [\ln(P_{agitator}(\text{HP}))]^2} \quad (3.36)$$

The total cost of the coagulation tank is equal to the sum of the vessel cost and the agitator cost, Eq. 3.37.

$$Cost_{Coag\ tank} = Cost_{Vessel} + Cost_{Agitator} \quad (3.37)$$

The flocculation tank is designed similarly to that of the coagulation, using Eqs. 3.29–3.37. For this step the hydraulic retention time is 25 min (Zhou et al., 2008).

The decanter is assumed to be circular because of its lower operating and maintenance costs. The area, Eq. 3.38, is computed using the parameter $A_{specific}$, which is the specific clarifier area in m^2 per ton of inlet flow per day (WEF, 2005). The typical value, $10 \text{ m}^2/(\text{t/day})$, is taken from Green and Southard (2008). The diameter of the clarifier, $D_{clarifier}$, is computed from the area value, Eq. 3.39.

$$A_{clarifier} (\text{m}^2) = \frac{A_{specific} \cdot F_{digestate}^{in} \left(\frac{\text{m}^3}{\text{day}} \right)}{1000} \quad (3.38)$$

$$D_{clarifier} (\text{m}) = \left(\frac{4 \cdot A_{clarifier}}{\pi} \right)^{1/2} \quad (3.39)$$

The number of clarifiers is an integer value that is computed as the minimum integer from the ratio between the clarifier diameter calculated before and the maximum clarifier diameter, $D_{max}^{clarifier}$, Eq. 3.40. The maximum clarifier diameter value considered is 40 m (Green & Southard, 2008).

$$n_{clarifiers} \geq \frac{D_{clarifier}}{D_{max}^{clarifier}} \quad (3.40)$$

The diameter used in the final design will be the smallest between $D_{clarifier}$ and $D_{max}^{clarifier}$, Eq. 3.41.

$$D_{design}^{clarifier} (\text{m}) = \min(D_{max}^{clarifier}, D_{clarifier}) \quad (3.41)$$

To model the minimization function and compute $D_{design}^{clarifier}$, the following smooth function approximation, given by Eq. 3.42, is used based on previous work (de la Cruz & Martín, 2016) to avoid discontinuities within the problem formulation.

$$D_{design}^{clarifier} (\text{m}) = \frac{D_{max}^{clarifier}}{1 + e^{(-F_{digestate}^{in} + 0.342) \cdot 2.718}} \quad (3.42)$$

The cost estimation correlation has been developed from the data in WEF (2005), Eq. 3.43. It includes all the items involved in the operation of such an unit. The correlation must be updated to current prices using the Chemical Engineering Index.

$$Cost_{clarifier} (\text{USD}_{1979}) = (13060 \cdot D_{design}^{clarifier} - 58763) \cdot n_{clarifiers} \quad (3.43)$$

Centrifuge sizing and costing is based on the data by Green and Southard (2008). We assume pusher type with a maximum diameter of 1250 mm. The modelling equation for sizing is given in Eq. 3.44.

$$D_{Centrifuge} (\text{in}) = 0.3308 \cdot \frac{F_{digestate}^{in}}{1000} \cdot 3600 + 9.5092 \quad (3.44)$$

The number of centrifuges is calculated taking into account the maximum centrifuge diameter, Eq. 3.45, and the diameter used in the final design will be the minimum value between D Centrifuge and D Centrifuge max , Eq. 3.46.

$$n_{centrifuges} \geq \frac{D_{centrifuge}}{D_{max}^{centrifuge}} \quad (3.45)$$

$$D_{design}^{centrifuge} = \min(D_{max}^{centrifuge}, D_{max}^{centrifuge}) \quad (3.46)$$

As in the clarifier, we develop a smooth approximation, Eq. 3.47, to compute the design diameter avoiding discontinuities as follows:

$$D_{design}^{centrifuge} = \frac{D_{max}^{centrifuge}}{1 + e^{(-F_{digestate}^{in} + 35.369) \cdot 0.0395}} \quad (3.47)$$

The cost for the centrifuge is estimated based on the data by Green and Southard (2008) as a function of its diameter, Eq. 3.48. Since the cost correlation is based on 2004 values, the Chemical Engineering Index it used to update the equipment cost.

$$Cost_{centrifuge} (\text{USD}_{2004}) = \left(10272 \cdot D_{design}^{centrifuge} - 24512 \right) \cdot n_{centrifuges} \quad (3.48)$$

We estimate the operating cost of this system by accounting for the annualized equipment cost (fixed cost), chemicals and labor cost. A similar procedure as before is followed (Vian Ortuño, 1991) but for the clarifier fixed costs as the correlation to estimate its costs already includes the operating cost, Eq. 3.49.

$$FC_{coagulation} \left(\frac{\text{EUR}}{\text{year}} \right) = (Cost_{Coag\ tank} + Cost_{Floc\ tank} + Cost_{centrifuge}) \cdot f_i \cdot f_j + Cost_{clarifier} \quad (3.49)$$

The chemicals costs are estimated as Eq. 3.50.

$$ChemC_{coagulation} \left(\frac{\text{EUR}}{\text{year}} \right) = (F_{Fe_2(SO_4)_3}^{in} \cdot Price_{Fe_2(SO_4)_3} + F_{Al_2(SO_4)_3}^{in} \cdot Price_{Al_2(SO_4)_3} + F_{FeCl_3}^{in} \cdot Price_{FeCl_3} + F_{AlCl_3}^{in} \cdot Price_{AlCl_3}) \cdot 3600 \cdot h \cdot d \quad (3.50)$$

To estimate the price for the cake, as in the previous case, we assume the price of each of the nutrients contained (N, P, and K). The price for each nutrient is taken same as before. Thus, the cake price is computed as the weighted sum of each nutrient, as in Eq. 3.15 (Hernandez et al., 2017).

Finally, the economic benefits or losses of operating this system are calculated as the difference between the credit obtained from the cake and the operating costs of section of the facility, as in Eq. 3.16.

3.3.4.3 Centrifugation

Centrifugation is a pretreatment that separates solid and liquid phases and that can be used to recover nutrients from the digestate. The advantage of this system is the simple equipment used. Precipitant agents can be added to improve the removal efficiency significantly. Previous studies show that an appropriate mixture of CaCO_3 and FeCl_3 promotes nutrients recovery. In particular, a ratio of 0.61 kg CaCO_3 per kilogram of total solids in the raw material inlet stream, and 0.44 kg of FeCl_3 per kilogram of total solids in the raw material inlet stream, achieves a removal efficiency up to 95% and 47% for P and N respectively (Meixner et al., 2015). Fig. 3.4 presents a scheme of the process.

Centrifugation process consists of two units, a precipitation tank where CaCO_3 and FeCl_3 are added, and the centrifuge. These equipment have been modeled using mass balances and removal ratios for the precipitating species. Note that the total solids, carbon, and potassium are assumed to be present in the form of solid compounds, so they will be removed as part of the cake. Moreover, the water content of the centrifuge outlet solids stream is assumed to be 60% ($C_{Wa}^{\text{centrifuge}}$) (Wakeman, 2007). Mass balances for the process have been evaluated in Eqs. 3.51-3.59:

$$F_j^{in} = F_{TS}^{in} \cdot \frac{\varphi_j}{C_j} \quad (3.51)$$

$j \in \{\text{precipitation agents}\}$

$$F_j^{in} = F_j^{\text{prec tank}} = F_j^{\text{centrifuge}} = F_j^{\text{cake}} \quad (3.52)$$

$$F_i^{in} = F_i^{\text{prec tank}} = F_i^{\text{centrifuge}} \quad (3.53)$$

$i \in \{\text{P, N}\}$

$$F_i^{\text{cake}} = F_i^{\text{centrifuge}} \cdot \eta_i \quad (3.54)$$

$$F_i^{\text{liquid effluent}} = F_i^{\text{centrifuge}} - F_i^{\text{cake}} \quad (3.55)$$

$$F_k^{in} = F_k^{\text{prec tank}} = F_k^{\text{centrifuge}} = F_k^{\text{cake}} \quad (3.56)$$

$k \in \{\text{TS, C, K}\}$

$$F_{Wa}^{in} = F_{Wa}^{\text{prec tank}} = F_{Wa}^{\text{centrifuge}} \quad (3.57)$$

$$F_{Wa}^{\text{cake}} = \left(F_{TS}^{\text{cake}} + \sum_i F_i^{\text{cake}} + \sum_j F_j^{\text{cake}} \right) \cdot \frac{C_{Wa}^{\text{centrifuge}}}{1 - C_{Wa}^{\text{centrifuge}}} \quad (3.58)$$

$$F_{Wa}^{liquid\ effluent} = F_{Wa}^{centrifuge} - F_{Wa}^{cake} \quad (3.59)$$

where φ_j is the precipitation agent per total solids mass ratio (0.61 kg CaCO₃/kg TS and 0.44 kg FeCl₃ /kg TS).

These units have been designed using correlations as a function of the flow processed. For the design of the precipitation tank (volume, diameter, length, thickness, weight, and cost calculations) the equations provided by Almena and Martín (2016) have been used as before, Eqs. 3.29-3.37, considering a hydraulic retention time of 2.5 min (Szabó et al., 2008).

$$V_{Prec\ tank}\ (\text{m}^3) = HRT_{Prec\ tank} \cdot \left(\frac{F_{digestate}^{in}}{\rho_{digestate}} + \frac{F_{FeCl_3}^{in}}{\rho_{FeCl_3}} \right) \quad (3.60)$$

The volume of CaCO₃ added is assumed negligible compared to the volume of the liquid because it is added as a solid. Thus, the diameter of the tanks is computed using Eqs. 3.60 and 3.30 as in the previous unit. The cost of the vessel is given by the weight of the metal, using the correlations provided by (Almena & Martín, 2016), Eqs. 3.31-3.34. The power required is computed, as in previous cases, using the rules of thumb in (Walas et al., 1990), Eq. 3.35, where the value of $\kappa_{agitator}$ agitator is equal to 10 HP per 1000 gal, in accordance with the data collected in the literature Walas et al. (1990). The cost correlation is given by Eq. 3.36 and updated to 2016 prices. The total cost of the precipitation tank included the vessel and the agitator costs, Eq. 3.37.

The centrifuge size is characterized by its diameter. We model it as in the previous technologies using Eqs. 3.44-3.48. The operating costs involve fixed, chemicals and labour costs. Fixed costs are estimated using Eq. 3.61. The labor cost is estimated in Eq. 3.13, where n_{OP} is equal to 1 (Vian Ortuño, 1991). Total operating cost is given by Eq. 3.14. The chemicals costs involve the consumption of CaCO₃ and FeCl₃, and it is estimated using Eq. 3.62:

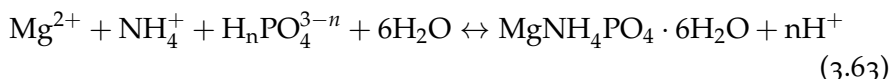
$$FC_{centrifugation} \left(\frac{\text{EUR}}{\text{year}} \right) = (Cost_{centrifuge} + Cost_{Prec\ tank}) \cdot f_i \cdot f_j \quad (3.61)$$

$$\begin{aligned} ChemC_{centrifugation} \left(\frac{\text{EUR}}{\text{year}} \right) = \\ \left(F_{CaCO_3}^{in} \cdot Price_{CaCO_3} + F_{FeCl_3}^{in} \cdot Price_{FeCl_3} \right) \cdot 3600 \cdot h \cdot d \end{aligned} \quad (3.62)$$

The cake recovered is the main asset of the process. Its price is estimated as the weighted sum of each nutrient, Eq. 3.15, (Hernandez et al., 2017). Finally, the benefits or losses of operating this system are calculated as the difference between the revenue obtained from the cake and the operating costs of the facility, Eq. 3.16.

3.3.4.4 Struvite production

P and N can be recovered from digestate through the formation of struvite, which is a phosphate mineral with a chemical formula of $\text{MgNH}_4\text{PO}_4 \cdot 6\text{H}_2\text{O}$. The advantage of this technology is that struvite is a solid with a high nutrients density, it is easy to transport, and it can be used as slow-release fertilizer without any post-processing (Doyle & Parsons, 2002). The removal of nutrients via struvite production follows the reaction below, requiring the addition of MgCl_2 , resulting in the production of struvite crystals that can be recovered as solid:



Due to the presence of potassium in the digestate, together with struvite, another product called potassium struvite or K-Struvite, is also produced. In this case the ammonia cation is substituted by the potassium cation (Wilsenach et al., 2007).



Since the formation of struvite is favored over the formation of K-Struvite, it is considered that only 15% of the potassium contained in the digestate will react to form K-Struvite (Zeng & Li, 2006). The mass balance for the reactors is given by the stoichiometry of the reactions above.

Two different types of reactors can be used to obtain struvite, either a stirred tank (CSTR) or a fluidized bed reactor (FBR). Figs. 3.5 and 3.6 provide detailed flowsheets of each case. In case of the FBR, struvite is recovered from the bottoms and the liquid must be processed in a hydrocyclone to avoid discharging fines. In the case of CSTR tanks, we need to use a centrifuge to recover the struvite. We can help the crystal growth by seeding (Doyle & Parsons, 2002; Kumashiro et al., 2001). Due to the substantial increase in the struvite formation yield, we consider the addition of struvite seeds in both cases. The reaction takes place at about 27 °C, with the addition of MgCl_2 at a concentration of 57.5 mg/dm³ (Zhang et al., 2014). A Mg:P molar ratio of 2 (Bhuiyan et al., 2008) is used.

The FBR system is composed of three elements: a mixer tank, a FBR reactor, and a hydrocyclone. The system operation consists of a digestate flow which is mixed with a stream of MgCl₂ in the mixing tank. The addition of MgCl₂ helps precipitate the struvite by increasing the concentration of the species inside the reactor. As the concentration of NH₄⁺ is high due to the pH, and the inorganic N and P are the elements we want to recover, the only element which is necessary to be added is Mg in form of MgCl₂.

In the tank there is a suspension of struvite seeds with a size of 0.8 mm which promote the precipitation of struvite. The solid struvite is evacuated from the reactor at the bottom and its moisture is low enough to avoid the use of a dryer. The other stream which leaves the reactor contains liquid water in a high proportion with the excess of Mg, the total solids from the digestate, and low amounts of nutrients and other components. This stream is introduced in a hydrocyclone to recover fines of struvite which can be removed by this stream. 100% of fines removal is assumed but no fines production is considered in the model.

To estimate the cost of this system we evaluate the effect of the following variables, whose operating values are shown between parenthesis:

- Digestate input mass and volume flow (between 1 and 100 kg/s)
- Recovered struvite humidity (5% in mass)
- Amount of phosphorus recovered (90%)
- Mg:P molar ratio with a value of 2

In an FBR there are some variables which influence in the design and hence the cost. The variables considered in this work are showed below with the typical values used in the present study between parenthesis:

- d_p : bed particle diameter, assumed to be 0.8 mm (Jordaan, 2011)
- Sphericity: 0.6 is a standard sphericity for particles used in fluidized bed reactors (Fogler, 2005)

Furthermore, the reaction kinetics and equilibrium are considered to estimate the residence time in the reactor. A first order kinetics, developed by (Nelson et al., 2003), has been used, Eqs. 3.65 and 3.66. The kinetic constant is $3.42 \cdot 10^{-3} \text{ s}^{-1}$ for a pH of 9.

$$\frac{-dC}{dt} = k(C - C_{eq}) \quad (3.65)$$

$$\ln(C - C_{eq}) = -kt + \ln(C_0 - C_{eq}) \quad (3.66)$$

Struvite formation is an equilibrium reaction. We use the equilibrium ion activity product (IAP_{eq}) value of $7.08 \cdot 10^{-14}$ (Nelson et al., 2003) to calculate the equilibrium concentrations in the kinetic model, Eq. 3.67. We assumed that the values of ions concentration are equal to ions activity.

$$IAP_{eq} = (Mg^{2+})(NH_4^+)(PO_4^{3-}) = 7.08 \cdot 10^{-14} \quad (3.67)$$

Minimum fluidization velocity is calculated in the first step by considering that the fluid stream is a liquid (Mangin & Klein, 2004). This consideration is motivated because the liquid digestate works as fluidization agent (Le Corre, 2006). The digestate density is 950 kg/m^3 (Rigby & Smith, 2011). The expression used to calculate u_{mf} through Reynolds and Archimedes numbers is given by Eq. 3.68, (Tisa et al., 2014).

$$u_{mf} = \frac{Re_l \cdot \mu_{digestate}}{\rho_{digestate} - d_p} \quad (3.68)$$

Eq. 3.68 parameters are determined by Eqs. 3.69 and 3.70.

$$Re_l = \sqrt{33.72 + 0.0404 Ar_l (1 - \alpha_{mf})^3} - 33.7 \quad (3.69)$$

$$Ar_l = \rho_{digestate} (\rho_{struvite} - \rho_{digestate}) g \frac{d_p^3}{\mu_{digestate}^2} \quad (3.70)$$

If the flow has no gas phase, α_{mf} is equal to zero. The terminal velocity is computed using Eq. 3.71 (Tisa et al., 2014).

$$u_t = \left(\frac{1.78 \cdot 10^{-2} \cdot \eta^2}{\rho_{digestate} \cdot \mu_{digestate}} \right)^{1/3} d_p \quad (3.71)$$

where the parameter η is given by Eq. 3.72:

$$\eta = g (\rho_{struvite} - \rho_{digestate}) \quad (3.72)$$

Finally, the fluid velocity u_0 must be between u_{mf} and u_t . A superficial velocity equal to five times the minimum fluidization velocity is selected (Tejero-Ezpeleta et al., 2004), Eqs. 3.73 and 3.74.

$$u_{mf} < u_0 < u_t \quad (3.73)$$

$$u_0 = 5 \cdot u_{mf} \quad (3.74)$$

Once the superficial velocity is computed, the area and diameter can be calculated from the mass flow Eqs. 3.75 and 3.76.

$$A_{FBR} = \frac{F_{digestate}^{in}}{u_0} \quad (3.75)$$

$$D_{FBR} = \sqrt{\frac{4A_{FBR}}{\pi}} \quad (3.76)$$

The length of the bed is determined by the residence time through the kinetics and the equilibrium ion activity product presented above. Consequently, the magnesium and ammonium concentrations can be calculated from the digestate mass balance and the external magnesium added. Using the IAP_{eq} value, the phosphate concentration in equilibrium at the operational conditions can be determined. This equilibrium value will be used in kinetics, Eq. 3.77.

$$t = \frac{\ln(C_0 - C_{eq}) - \ln(C - C_{eq})}{k} \quad (3.77)$$

Thus, the bed length is computed as per Eq. 3.78. Typically, the length of the reactor must be 15% larger than the bed, Eq. 3.79.

$$L_{bed} = \frac{u_0}{t} \quad (3.78)$$

$$L_{FBR} = 1.15 \cdot L_{bed} \quad (3.79)$$

The estimation of the reactor cost is carried out assuming that it is a vessel as presented in the processes above, Eqs. 3.30-3.34 (Almena & Martín, 2016). The cost of the mixer tank is also estimated as that of a vessel, using

Eqs. 3.29-3.34, with a volume given by that to provide a hydraulic retention time of 150 s (Szabó et al., 2008). The impeller is also designed using the same procedure as before, Eqs. 3.35 and 3.36 (Walas et al., 1990).

Finally, to estimate the cost of the hydrocyclone, a surrogate model using data from Matche website has been developed (Matche, 2014) (www.matche.com). There is a maximum diameter, therefore, if a unit larger than the standard is required, we actually need to duplicate the equipment, Eq. 3.81. To estimate the diameter, we considered that there is a linear relationship between the diameter and the flow based on rules of thumb in design literature. A typical unit size of a 20 in diameter hydrocyclone can process 1,000 US gallons per min, Eq. 3.80 (Walas et al., 1990).

$$D_{\text{hydrocyclone}} \text{ (in)} = F_{\text{digestate}}^{\text{in}} \left(\frac{\text{US gallon}}{\text{min}} \right) \cdot \frac{20}{1000} \quad (3.80)$$

$$n_{\text{hydrocyclone}} \geq \frac{D_{\text{hydrocyclone}}}{D_{\text{max}}^{\text{hydrocyclone}}} \quad (3.81)$$

where $n_{\text{hydrocyclone}}$ is an integer. The maximum diameter for a hydrocyclone, $D_{\text{max}}^{\text{hydrocyclone}}$, is 30 inch based on standard sizes (www.matche.com). Thus, the design diameter is the lower diameter between $D_{\text{hydrocyclone}}$ and $D_{\text{max}}^{\text{hydrocyclone}}$, 3.82.

$$D_{\text{design}}^{\text{hydrocyclone}} = \min(D_{\text{total}}^{\text{hydrocyclone}}, D_{\text{max}}^{\text{hydrocyclone}}) \quad (3.82)$$

The estimation of the cost for the fines recovery equipment is computed using Eq. 3.83 and updated as explained above.

$$\text{Cost}_{\text{hydrocyclone}} \text{ (USD}_{2014}) = \quad (3.83)$$

$$n_{\text{hydrocyclone}} \cdot \left(2953.2 \cdot D_{\text{design}}^{\text{hydrocyclone}} - 34,131 \right)$$

The CSTR process consists of four elements: the CSTR reactor, a centrifuge, and a dryer with its corresponding heat exchanger. As the residence time in the CSTR is large enough, it is not necessary to use a mixing tank and MgCl² is added directly in the reactor. Thus, struvite is formed in one step in the CSTR. Since the digestate already contains NH₄⁺ and P, we need to add MgCl². As a result, struvite precipitates, and it is recovered from the bottoms of the reactor and dried in a two step process. The first step consists of a centrifuge that recovers struvite with 5% (on weight basis)

water (Baasal, 1977). Next, a drum dryer is implemented to remove the residual moisture to reach commercial standards and reduce transportation costs. Fig. 3.6 shows the details of the flowsheet.

The design of the units involved in this process and their cost estimation is based on the following variables:

- Digestate input mass and volume flow (between 1 and 100 kg/s)
- Recovered struvite humidity (5% in mass)
- Amount of phosphorus recovered (90%)
- Mg:P molar ratio with a value of 2

The CSTR is assumed to be a stirred vessel; consequently, it is designed as in the previous cases, Eqs. 3.29-3.37, with a residence of 471.05 s. The residence time is calculated from mass balances and the kinetics described in the FBR process, Eqs. 3.65 and 3.66.

The centrifuge size is characterized by its diameter. Both, the size and cost are computed using the data in Green and Southard (2008). We assume a pusher type for the centrifuge with a maximum diameter of 1250 mm as before, Eqs. 3.44-3.48.

The cost estimation for the dryer relies on the amount of water to evaporate, and the evaporation capacity. The evaporation capacity ($e_{capacity}$) is reported in the literature to be equal to 0.01897 (kg/(s · m²)) (Walas et al., 1990). Consequently, the dryer cost is computed using a correlation provided by Martín and Grossmann (2011), Eq. 3.84, updating the cost to current prices using the Chemical Engineering Index.

$$Cost_{dryer} (\text{USD}_{2007}) = 1.15 \cdot \left(6477.1 \cdot \frac{F_{water}^{in}}{e_{capacity}} + 102394 \right) \quad (3.84)$$

The operating cost of the CSTR and the FBR based processes is computed considering three items, fixed, chemicals and labor, and assuming that utilities account for 20% of the operating costs. The correlations for computing each of them are taken from Vian Ortuño (1991) and Sinnott (1999b), Eq. 3.13 for labour and Eq. 3.14 for total operating cost. Fixed cost for struvite processes is calculated using Eq. 3.85. We assume that the seeds required for the FBR process are internally produced in the startup of the facility.

$$FC_{struvite} \left(\frac{\text{EUR}}{\text{year}} \right) = \left(\sum Cost_{equipment} \right) \cdot f_i \cdot f_j \quad (3.85)$$

The revenue obtained from the struvite is determined assuming a selling price of 0.763D EUR/kg, Eq. 3.86, (Molinos-Senante et al., 2011).

$$Cost_{struvite} \left(\frac{\text{EUR}}{\text{year}} \right) = \left(F_{struvite}^{\text{recovered}} \cdot Price_{struvite} \right) \cdot 3600 \cdot h \cdot d \quad (3.86)$$

Finally, the benefits or losses for CSTR and FBR are calculated as the difference between the credit obtained from the struvite and the operating costs of the facility, Eq. 3.16.

3.3.5 Solution procedure

The detailed models for each of the alternatives such as the five filter media or the number of different coagulants result in a large and complex MINLP when cost estimation is involved. We use a two-stage procedure to select the best technology. In the first stage we develop MINLP subproblems to select the appropriate filter media or coagulant. Next, using the detailed models for the best option, surrogate cost models are developed for the five alternative technologies used to process the digestate. However, there are still binary decisions to account for the cost of the active alternative in the superstructure. Thus, the surrogate models are in the form of linear equations. For instance, the surrogate model for the filter to be implemented in the superstructure is given by a linear function as given by Eq. 3.87.

$$Operating\ cost \left(\frac{\text{EUR}}{\text{year}} \right) = 20,521 \cdot F_{design} \left(\frac{\text{ft}^3}{\text{min}} \right) - 33,488 \cdot a_{Filter} \quad (3.87)$$

We avoid the use of binary variables within the formulation (due to highly non linear model of the entire superstructure) by using smooth approximations. We define a_{Filter} as a parameter that takes a value of 0 when F_{design}^{Filter} is 0 and 1 if F_{design}^{Filter} is not equal to 0. The smooth approximation for a_{Filter} is defined as follows, Eq. 3.88:

$$a_{Filter} = \frac{1}{1 + e^{(-F_{design} + 0.049) \cdot 361}} \quad (3.88)$$

Metal slag is selected as the best filter for the filtration process. For the case of the coagulants, the solution of the subproblem, Eqs. 3.17-3.50 selects the use of AlCl₃. As in the previous case, a surrogate model is

developed to be included in the superstructure so that we avoid including binary variables and allow for zero operating costs in case this technology is not selected, Eq. 3.89.

$$\begin{aligned} \text{Operating cost} \left(\frac{\text{EUR}}{\text{year}} \right) = \\ 1,019,589.91 \cdot F_{\text{digestate}}^{\text{in}} \left(\frac{\text{kg}}{\text{s}} \right) - 368,838.56 \cdot a_{\text{Coag}} \end{aligned} \quad (3.89)$$

where the smooth approximation for the term a_{Coag} is given by Eq. 3.90.

$$a_{\text{Coag}} = \frac{1}{1 + e^{\left(-F_{\text{digestate}}^{\text{in}} + 0.068\right) \cdot 863}} \quad (3.90)$$

Similar to previous cases we develop a surrogate model to estimate the operating cost for the centrifugation as a function of the flowrate of digestate, Eq. 3.91:

$$\text{Operating cost} \left(\frac{\text{EUR}}{\text{year}} \right) = 458,498.29 \cdot F_{\text{digestate}}^{\text{in}} + 24,924.67 \cdot a_{\text{Centrifugation}} \quad (3.91)$$

As before, $a_{\text{Centrifugation}}$ is approximated as follows, Eq. 3.92:

$$a_{\text{Centrifugation}} = \frac{1}{1 + e^{\left(-F_{\text{digestate}}^{\text{in}} + 0.068\right) \cdot 863}} \quad (3.92)$$

Finally, to include the operating costs for the production of struvite, we again develop surrogate models for the FBR, Eq. 3.93 and for the CSRT Eq. 3.95, where a smooth approximation is proposed for the fixed term, a_{FBR} and a_{CSTR} respectively, Eqs. 3.94 and 3.96.

$$\text{Operating Cost}_{\text{FBR}} \left(\frac{\text{EUR}}{\text{year}} \right) = 245,008 \cdot F_{\text{digestate}}^{\text{in}} + 1 \cdot 10^6 \cdot a_{\text{FBR}} \quad (3.93)$$

$$a_{\text{FBR}} = \frac{1}{1 + e^{\left(-F_{\text{digestate}}^{\text{in}} + 0.06785\right) \cdot 862.9679}} \quad (3.94)$$

$$\text{Operating Cost}_{CSTR} \left(\frac{\text{EUR}}{\text{year}} \right) = 277,051 \cdot F_{digestate}^{in} + 1 \cdot 10^6 \cdot a_{CSTR} \quad (3.95)$$

$$a_{CSTR} = \frac{1}{1 + e^{\left(-F_{digestate}^{in} + 0.06785 \right)} \cdot 862.9679} \quad (3.96)$$

The benefits/losses in the superstructure for any of the technologies to process the digestate is computed as the difference between the revenue obtained from the nutrients and generated power, and the operating costs of the facility.

Finally, the whole superstructure is built (see Fig. 3.1). This superstructure contains models of the fermenter, biogas purification, gas cycle, steam cycle, and digestate treatment processes. The aim of this superstructure is to determine the optimal operating conditions and to select the best digestate treatment technology. Thus, digestate treatment processes have been implemented in the superstructure through detailed mass balances including the solution to the kinetics of the fluidized bed reactors as well as the surrogate models developed in the previous stage to estimate the operating costs. It should be noted that in filtration, centrifugation, and coagulation processes we have included a benefits penalty, $F_{total}^{recovered}$, due to the fact that the product recovered is a mixture of nutrients and organic matter with a nutrients concentration lower than struvite. This penalty represents the concentration of nutrients in the recovered product given by the ratio between the nutrients recovered and the total recovered mass flow, Eq. 3.97.

$$\begin{aligned} \text{Price} \left(\frac{\text{EUR}}{\text{year}} \right) = & \\ & \left(F_P^{recovered} \cdot Price_P + F_N^{recovered} \cdot Price_N + F_K^{recovered} \cdot Price_K \right) \\ & \cdot \frac{1}{F_{total}^{recovered}} \cdot 3600 \cdot h \cdot d \end{aligned} \quad (3.97)$$

The total energy obtained in the system to be optimized is the sum of the one generated at the three sections of the turbine, high, medium and low pressure and that of the gas turbine. We use part of the energy produced to power the compressors used across the facility. The economic benefits or losses of each digestate treatment process are added to the energy benefits.

$$\begin{aligned}
Z = & \left[\left(\sum_{i \in \text{Turbines}} W_{(\text{Turbine})} + W_{\text{GasTurbine}} - \sum_{j \in \text{Compressors}} W_{\text{Compressors}} \right) \right. \\
& \cdot 3600 \cdot h \cdot d \cdot C_{\text{Electricity}} \Big] + \text{Benefits}_{\text{Filtration}} + \text{Benefits}_{\text{Centrif}} + \\
& \text{Benefits}_{\text{Coagulation}} + \text{Benefits}_{\text{FBR}} + \text{Benefits}_{\text{CSTR}}
\end{aligned} \tag{3.98}$$

Eq. 3.98 is the objective function that we maximize to determine the optimal operational conditions and to select the best digestate treatment process subject to the following constraints:

- Bioreactor and biogas composition model. Described in Section 3.3.1
- Digestate processing. Described in Section 3.3.4
- Biogas purification. Described in Section 3.3.2
- Brayton cycle. Described in Section 3.3.3.1
- Rankine cycle. Described in Section 3.3.3.2

The main decision variables are related to the selection of the digestate processing technology, among filtration, centrifugation, coagulation and struvite production using CSTR or FBR. The decision variables are also associated with the selection of the type of filter and the coagulation agent. Furthermore, the biogas usage to produce steam requires the operating pressures and temperatures at the gas turbine, and the steam turbine as well as the extraction from the steam turbine to reheat the condensate before regenerating steam using the flue gas from the gas turbine. The superstructure consists of an NLP of approximately 4,000 equations and 5,000 variables solved using a multistart procedure with CONOPT 3.0 as the preferred solver. The computational time is around 60 min, although it varies for each problem as a consequence of the different data used in each case.

3.4 RESULTS

Following the optimization procedure presented in Section 3.4 we first decide on the filter media and the coagulant chemical. We solve MINLP subproblems leading to the selection of the filter media and the coagulant

agent. We use the metal slag as the filter media and the AlCl_3 as the coagulant for all raw materials. Next, we developed surrogate models for the five technologies included in the superstructure and solve a reformulated NLP including smooth approximations for the cost functions of the digestate treatment so as to maximize the power produced and the treatment section. The plant size is assumed to be that which processes 10 kg/s of manure based on the typical amount of manure produced in cattle farms (Le ón, 2015). Four manures have been evaluated on the plant: cattle, pig, poultry and sheep, with the aim of determining, for each one, the power generated the composition of the biogas produced, the optimal digestate treatment technology to recover its nutrients and the biogas-manure and digestate-manure ratios. Section 3.4.1 summarizes the main operating conditions of the major units in the process and the selection of digestate processing technology. Section 3.4.2 presents the detail economic evaluation of the four optimal processes, one per manure type. Finally, in Section 3.4.3 an analysis of the effect of the manure composition on the power, operating conditions and digestate treatment is performed.

3.4.1 *Mass and energy balances*

Table 3.4 shows the main operating conditions of major units for the four different manure types. Cattle, pig, and poultry show similar values among them and to previous work (León & Martín, 2016). The gas in the gas turbine reaches a temperature of 2400 °C and a pressure of 8.2 bar before expansion for cattle, pig and poultry manure. However, sheep manure shows different values. While the temperature is similar, the pressure is 15.6 bar, almost twice the value found for the rest of the raw materials. Furthermore the flue gas exits the turbine 300 °C below that when the rest of the manure types are used. Furthermore while the high pressure of the steam turbine is 125 bar for cattle, pig, and poultry manure, in case of sheep manure the steam turbine operates at 95 bar at the high pressure section of the turbine. This is related to the lower gas temperature from the gas turbine since the overheated steam needs to be produced using that stream. Intermediate and low pressures are the same in the steam turbine using any of the manure types, but the exhaust pressure of the steam is higher in case of sheep manure. Table 3.5 shows the products obtained from the various manure types, power, biogas, and digestate. Poultry is the waste that is more efficient towards power production due to its higher concentration. In all cases an FBR reactor for the production of struvite is the selected technology to recover N and P. In the table we also see the effect of the fact that cattle and pig manure are mostly liquids,

since most of the product is digestate, almost 98%, while the use of poultry or sheep manure reduces the production of digestate to 75% and 88% respectively, increasing the production of biogas and power. Finally in Table 3.6 the biogas composition for each manure considered are presented. The main purpose of the facility is the production of power. However, the biogas composition is typically within a range of values per component that have been imposed as bounds. As a result of maximizing the electricity production for all studied cases, the same biogas composition is obtained, 67.5% molar in CH₄ and the rest is mostly CO₂.

3.4.2 Economic evaluation

This section is divided into the estimation of the investment cost, using a factorial method based on the cost of the units, and the estimation of the electricity production cost.

3.4.2.1 Investment cost

We use the factorial method to estimate the investment cost for this facility. This is based on the estimation of the equipment cost and several coefficients to account for pipes, installation, etc. (Sinnott and Towler, 2009). The cost for the different units has been estimated based on (Matche, 2014) website (www.matche.com), (Towler & Sinnott, 2009) and (Peters et al., 2003), updating the cost of the units when required. We assume a plant that processes fluids and solids. Due to the different composition of each manure the specific production of biogas for each one is different, being larger for poultry and sheep than for cattle and pig. The reason for that could be that sheep and poultry manures have less water content while the water content in cattle and pig reaches 98% (<http://adlib.eversite.co.uk>). For cost estimation proposes the digester maximum size considered is 6,000 m³ per unit, since the larger units could face mixing and homogenization problems (Rohstoffe eV, 2010). This result for the facility investment cost will be different for each raw material. Fig. 3.7 shows the equipment cost distribution where digester and gas turbine are the most important contributions:

- **Cattle manure:** a plant that processes 10 kg/s of this type of manure requires an investment of 69.1 M EUR, of which 14.9 M EUR represents the equipment cost. The larger cost is assumed by the digester units, with a 75% of the total units cost, followed by the heat exchanger network with a contribution of 12% while both turbines add up to 12%.

- **Pig manure:** a facility to process 10 kg/s of this manure requires an investment of 69.5 M EUR, with a cost of 14.9 M EUR in equipment. Since the digestate-manure and biogas-manure ratios between cattle and pig manure are very similar, the investment costs are analogous among them. The unit cost distribution is similar to the cattle manure case.
- **Poultry manure:** The investment for a plant that processes 10 kg/s of this manure is 208.0 M EUR. The units investment adds up to 44.7 M EUR. In this case the units cost distribution is more homogeneous among different items: 60% to digester units, 20% to gas turbine, 10% to heat exchanger network and 9% to steam turbine. It should be noted that, as poultry manure has a high content of dry matter (around 60% on a weight basis), it is necessary to add additional water to decrease the dry matter content to reach 25% with the aim of avoid mixing problems in the digester due to an excessive solids concentration inside.
- **Sheep manure:** The facility to treat 10 kg/s of this manure requires an investment of 105.0 M EUR, where 22.5 M EUR represents the equipment cost. For this plant the main units cost distribution is as follows: 50% for the digester, 25% for gas turbine, 17% for heat exchanger network and 7% for steam turbine.

It is clear that the digester shows the largest share in the investment cost and therefore the concentration of the manure highly determines the cost of the facility. Lantz (2012) presented the investment cost of a facility for heat and power production as a function of its scale. Actually, our plant does not produce steam as a final product but only power. Thus, it is interesting to see that the raw material determines the investment per kW from the 4,000 EUR/kW in case of poultry manure or the 7,500 EUR/kW in case of sheep manure, to the more than 25,000 EUR/kW in case of pig and cattle.

3.4.2.2 Production cost

To calculate the production cost, 20 years of plant life is considered, with a capacity factor of 98%. Apart from the equipment amortization, other items are also taken into account such as salaries, administrative fees, chemicals cost, maintenance cost, utilities and contingency costs. Thus, apart from the annualized equipment cost, 1.5 M EUR are spent in salaries, 0.25 M EUR in Administration, 2 M EUR in Maintenance, 0.25 M EUR in other expenses (León & Martín, 2016) while chemicals are computed

as described in Section 3.2. The cost of utilities adds up to 0.08 M EUR, accounting for the cooling water and the steam needed to maintain the operation of the digester and to condition the digestate for its use as a fertilizer. Finally, we assume that the livestock manure is for free. Fig. 3.8 shows the distribution of the production costs for each of the manure types. We see that the figures are very similar. The equipment amortization represents at least 43% of the production costs. This share increases up to 60% for the case of the use of poultry. As the investment is lower, the annual cost for other items is almost constant and their contribution to the electricity cost plays a more important role. Chemicals is the second most important contribution to the cost of electricity with a share of up to 23% for the use of cattle or pig manure and down to 16% in the case of sheep manure. We assume in all cases that waste is for free. Under these considerations the electricity production costs obtained are presented in Table 3.7.

The Net Profit Value has also been calculated as a measure of the project profitability, considering an electricity price of sale of 0.06 EUR/kWh. To compare the profitability of this project a secure investment as the inversion in Spanish national debt has been chosen, considering a discount rate of 3% (Ministerio de Economía, Industria y Competitividad, 2017). The results obtained are presented in Table 3.7, and it should be noted that facilities for poultry and sheep manures obtain positive NPV while those which use cattle and pig manure as raw material show negative NPV, so from the point of view of NPV as an indicator to decide the project viability, those ones would be disregarded.

3.4.3 Effect on the power, operating conditions and digestate treatment

The results obtained from the treatment of different manure streams show the influence of the manure composition in the amount produced and the composition of biogas and digestate obtained. Struvite production using FBR is the best choice for digestate treatment. This can be explained by the advantages in recovering nutrients in solid form since they can be easily transported and stored. Furthermore the material is highly concentrated in nutrients with a relatively high selling price. Biogas production is similar for cattle and pig manures, but is significantly higher in the poultry and sheep cases. The investment cost when processing cattle and pig manure is dominated by the digester, resulting in similar investment and production costs for facilities using either of the two types of manure. However, the higher concentration in organic matter in sheep and poultry manure does not only results in higher power production capacities, but

the fact that the contribution to the cost of the turbines is also larger and so is the investment cost of these facilities. On the other hand, the electricity production cost is lower in the last two cases as result of the economies of scale between the investment cost and the biogas produced and the higher amount of struvite produced, with the extreme case of poultry manure where the struvite selling benefits are capable to cover the electricity production costs. Note that the availability of poultry and or sheep manure should be less than for cattle and pig manure.

3.5 CONCLUSIONS

In this work, we have designed optimal integrated facilities for the production of biogas-based electrical power and fertilizers from manure. Detailed equation based models for the anaerobic digestion, the Brayton and regenerative Rankine cycles and different technologies for digestate treatment have been developed. To solve the model a two-step procedure has been performed. First, the individual detailed models for each digestate treatment technology are used to formulate a MINLP model aiming at selecting the best configuration for that technology: the best precipitation agent, filter media, etc. In the second step, the best configuration of each technology has been implemented in the entire superstructure. Due to the fact that only one digestate processing technology is allowed and the highly non-linear nature of the model, surrogate models for the cost of each alternatives with a smooth approximations have been developed. For the optimal selection a detailed economic evaluation is performed. The results show that FBR technologies are preferred to recovery nutrients. Furthermore, in some cases this process can produce electricity at a competitive price (in case of poultry and sheep manure). The investment cost is highly dependent on the water and organic content of the manure type, ranging from 70 M EUR to 208 M EUR when a large energy production is possible and large gas and steam turbines are to be installed. However, for these cases of higher investment cost, the production cost of power is the most competitive due to the large production capacity. Biogas power plants show a wide range of values of power per kW installed depending on the manure concentration. Competitive values of 4,000 EUR/kW for poultry manure are obtained, due to the highly concentrated manure, while large values of 25,000 EUR/kW installed are reported in case of the diluted cattle or pig manure.

NOMENCLATURE

CHECK IF ALL THESE VARIABLES APPEAR IN THE CHAPTER

Sets

- a $\in \{\text{H}_2\text{O}, \text{CH}_4, \text{CO}_2, \text{NH}_3, \text{H}_2\text{S}, \text{O}_2, \text{N}_2\}$
- a' $\in \{\text{CH}_4, \text{CO}_2, \text{NH}_3, \text{H}_2\text{S}, \text{O}_2, \text{N}_2\}$
- d $\in \{\text{C}, \text{N}_{\text{organic}}, \text{N}_{\text{NH}_3}, \text{P}, \text{K}, \text{H}_2\text{O}, \text{Rest}\}$
- e $\in \{\text{CH}_4, \text{NH}_3, \text{H}_2\text{S}\}$
- h $\in \{\text{CH}_4, \text{CO}_2, \text{O}_2, \text{N}_2\}$
- i $\in \{\text{P}, \text{N}\}$
- j $\in \{\text{filter media}\}$
- k $\in \{\text{TS}, \text{C}, \text{K}\}$

Parameters

- $A(i)$ Antoine A coefficient for vapor pressure of component i
- A_{specific} specific clarifier area ($\text{m}^2 / (\text{ton}\cdot\text{day})$)
- $B(i)$ Antoine B coefficient for vapor pressure of component i
- $C(i)$ Antoine C coefficient for vapor pressure of component i
- HRT_{unit} hydraulic retention time of $unit$ (s)
- IAP_{eq} ion activity product equilibrium
- $MW_{\text{component}}$ molecular weight of $component$ (kg/kmol)
- MeP_{ratio} metal/phosphorus molar ratio in coagulation process
- P_{atm} atmospheric pressure (1 bar)
- $Price_{\text{component}}$ price of $component$ (EUR/kg)
- R ideal gas constant (8.314 J/mol·K)
- T_{atm} room temperature (25 °C)
- η_c compressors efficiency (0.85)
- η_i^j separation yield of component i in inprocess j
- η_s isentropic efficiency (0.9)
- κ_{agitator} agitator specific power consumed (HP/1000 US gallon)
- φ_j precipitation agent j : total solids (mass ratio)
- $c_{p_{\text{H}_2\text{O}}}$ specific heat capacity of water (4.18 kJ/kg °C)
- $c_{p_{sat}}$ specific heat capacity of flue gas
- d working days per year
- d_p particle diameter (m)
- g gravity acceleration (m^2/s)

h	working hours per day
k	kinetic constant (s^{-1})

Variables

A_{unit}	area of unit (m^2)
Ar_l	Arquimedes number for liquid
$Benefits_{technology}$	benefits or losses obtained with <i>technology</i>
$C : N$	carbon to nitrogen molar ratio
C_0	initial concentration (kmol/m^3)
$C_{component}^{unit}$	concentration of <i>component</i> in the <i>unit</i> inlet stream ($\text{kg}_{\text{component}}/\text{kg}_{\text{total}}$)
C_{eq}	equilibrium concentration (kmol/m^3)
$ChemC_{technology}$	cost of chemicals for <i>technology</i>
$Cost_{unit}$	cost of <i>unit</i>
D_{unit}	diameter of <i>unit</i>
$E_{cj}(T)$	equilibrium constant of component j at temperature T
$FC_{technology}$	fixed cost of <i>technology</i>
$F_{unit,unit1}$	mass flow from stream from <i>unit</i> to <i>unit1</i> (kg/s)
$F_{component}^{unit}$	mass flow of <i>component</i> in the <i>unit</i> inlet stream (kg/s)
F_{design}^{unit}	mass inlet flow used in the design of <i>unit</i> (kg/s)
F_{max}^{unit}	maximum mass inlet flow admitted by a single <i>unit</i> (kg/s)
$F_{total}^{recovered}$	recovered matter total mass flow (kg/s)
$H_b^{unit,unit1}$	enthalpy of the stream at state b from <i>unit</i> to <i>unit1</i> (kJ/kg)
$H_{steam(isoentropy)}$	isentropic expansion enthalpy of steam (kJ/kg)
K_{index}	potassium index of fertilizer
L_{unit}	length of <i>unit</i>
N_{NH_3}	nitrogen contained in ammonia
N_{index}	nitrogen index of fertilizer
N_{org}	nitrogen contained in organic matter
$P_j^*(T)$	saturation pressure of pure component j at temperature T (bar)
P_v	vapor pressure (bar)
$P_{in/compressor}$	inlet pressure to compressor (bar)
P_{index}	phosphorous index of fertilizer
$P_{out/compressor}$	outlet pressure of compressor (bar)

P_{unit}	power of unit
$Q_{(unit)}$	heat exchanged in <i>unit</i> (kW)
$R_{C-N/fertilizer}$	carbon to nitrogen ratio in fertilizer
$R_{C-N/k}$	carbon to nitrogen ratio in <i>k</i>
$R_{V-F/i}$	rate of evaporation in equilibrium system <i>i</i>
$Re_{l,mf}$	Reynolds number for liquid in minimum fluidization conditions
<i>Rest</i>	rest of the elements contained in the biomass
$T_{(unit,unit1)}$	temperature of the stream from <i>unit</i> to <i>unit1</i> (°C)
$T_{bubble/i}$	bubble point temperature of equilibrium system <i>i</i> (°C)
$T_{in/compressor}$	inlet temperature to compressor (°C)
$T_{m/i}$	average temperature in equilibrium system <i>i</i> (°C)
$T_{out/compressor}$	outlet temperature of compressor (°C)
$T_{turb,i,min}^*$	saturated temperature at exit of body <i>i</i> (°C)
$V_{biogas,k}$	biogas volume produced per unit of volatile solids (VS) associated to waste <i>k</i> ($\text{m}^3_{\text{biogas}}/\text{kg}_{\text{VS}/k}$)
V_{unit}	volume of <i>unit</i>
W_{unit}	weight of <i>unit</i>
W_{unit}	power produced or consumed in <i>unit</i> (kW)
$Y_{a',biogas-dry}$	molar fraction of component <i>a</i> in the dry biogas
Z	objective function
$\Delta H_{comb,digestate-dry}$	heat of combustion of dry digestate (kW)
$\Delta H_{comb,e}$	heat of combustion of component <i>e</i> (kW)
$\Delta H_{comb,k}$	heat of combustion of component <i>k</i> (kW)
$\Delta H_{f,h}(T)$	heat of formation of component <i>h</i> at temperature <i>T</i> (kW)
$\Delta H_{reaction(bioreactor)}$	reaction heat of anaerobic digestion (kW)
α_{mf}	parameter dependent of the number of phases in the FBR
$\mu_{component}$	viscosity of component (kg/(m·s))
$\rho_{component}$	density of <i>component</i> (kg/m ³)
$a_{technology}$	selection parameter which takes value 0 when $F_{design}^{technology}$ is 0 and 1 if $F_{design}^{technology}$ is not equal to 0
e_{unit}	thickness of <i>unit</i>
$fc_j^{unit,unit1}$	mass flow of component <i>j</i> from <i>unit</i> to <i>unit1</i> (kg/s)
l_{j-i}	molar fraction of component <i>j</i> in the liquid phase of equilibrium system <i>i</i>

$n_{(unit,unit1)}$	total mol flow from stream from <i>unit</i> to <i>unit1</i> (kmol/s)
n_{unit}	number of units used in the process
$p_{turb,i}$	inlet pressure to body <i>i</i> in the turbine (bar)
$s_{b,(unit,unit1)}$	entropy the stream at the state <i>b</i> for the stream from <i>unit</i> to <i>unit1</i> (kJ/kg·K)
t	time (s)
u_0	fluid velocity (m/s)
u_t	terminal velocity (m/s)
u_{mf}	minimum fluidization velocity (m/s)
v_{j-i}	molar fraction of component <i>j</i> in the vapor phase of equilibrium system <i>i</i>
$w'_{C/k}$	dry mass fraction of C in <i>k</i> (kg _{C/k} /kg _{DM/k})
$w'_{DM/k}$	dry mass fraction of <i>k</i> (kg _{DM/k} /kg)
$w'_{K/k}$	dry mass fraction of K in <i>k</i> (kg _{K/k} /kg _{DM/k})
$w'_{NH_3/k}$	dry mass fraction of NH ₃ in <i>k</i> (kg _{NH₃/k} /kg _{DM/k})
$w'_{N_{org}/k}$	dry mass fraction of N _{org} in <i>k</i> (kg _{N_{org}/k} /kg _{DM/k})
$w'_{P/k}$	dry mass fraction of P in <i>k</i> (kg _{P/k} /kg _{DM/k})
$w'_{Rest/k}$	dry mass fraction of the rest of the elements contained in <i>k</i> (kg _{Rest/k} /kg _{DM/k})
$w'_{Rest/k}$	dry mass fraction of the rest of the elements contained in <i>k</i> (kg _{Rest/k} /kg _{DM/k})
$w'_{Rest/k}$	dry mass fraction of the rest of the elements contained in <i>k</i> (kg _{Rest/k} /kg _{DM/k})
$w'_{VS/k}$	dry mass fraction of volatile solids out of the dry mass of <i>k</i> (kg _{VS/k} /kg _{DM/k})
$x_{a/biogas}$	mass fraction of component <i>a</i> in the biogas
y^j	binary variable to evaluate the element <i>j</i>
y_{biogas}	specific saturated moisture of biogas

ACKNOWLEDGMENTS

We acknowledge funding from the National Science Foundation (under grant CBET-1604374) and MINECO (under grant DPI2015-67341-C2-1-R) and E.M. also acknowledges an undergraduate research grant.

BIBLIOGRAPHY

- Aguilar, M., Saez, J., Llorens, M., Soler, A., & Ortuno, J. (2002). Nutrient removal and sludge production in the coagulation–flocculation process. *Water research*, 36(11), 2910–2919.
- Al Seadi, T., Rutz, D., Prassl, H., Köttner, M., Finsterwalder, T., Volk, S., & Janssen, R. (2008). *Biogas handbook* (2008th ed.). Denmark, Syddansk Universitet.
- Almena, A., & Martín, M. (2016). Technoeconomic analysis of the production of epichlorohydrin from glycerol. *Industrial & Engineering Chemistry Research*, 55(12), 3226–3238.
- Aziz, H. A., Adlan, M. N., Zahari, M. S. M., & Alias, S. (2004). Removal of ammoniacal nitrogen (N-NH₃) from municipal solid waste leachate by using activated carbon and limestone. *Waste management & research*, 22(5), 371–375.
- Baasal, W. (1977). *Preliminary chemical engineering plant design*. Springer Science & Business Media.
- Bhuiyan, M., Mavinic, D., & Koch, F. (2008). Phosphorus recovery from wastewater through struvite formation in fluidized bed reactors: a sustainable approach. *Water Science and Technology*, 57(2), 175–181.
- Cucarella, V., Zaleski, T., Mazurek, R., & Renman, G. (2008). Effect of reactive substrates used for the removal of phosphorus from wastewater on the fertility of acid soils. *Bioresource technology*, 99(10), 4308–4314.
- de la Cruz, V., & Martín, M. (2016). Characterization and optimal site matching of wind turbines: Effects on the economics of synthetic methane production. *Journal of Cleaner Production*, 133, 1302–1311.
- Doyle, J. D., & Parsons, S. A. (2002). Struvite formation, control and recovery. *Water research*, 36(16), 3925–3940.
- Drosg, B., Fuchs, W., Al Seadi, T., Madsen, M., & Linke, B. (2015). *Nutrient recovery by biogas digestate processing* (Vol. 2015). IEA Bioenergy Dublin.
- Fogler, H. S. (2005). *Elements of Chemical Reaction Engineering* (4th Edition) (4th ed.). Prentice Hall.
- García-Serrano, P., Ruano, S., Lucena, J., & Nogales, M. (2009). *Guia práctica de la fertilización racional de los cultivos en España* (tech. rep.). Ministerio de Medio Ambiente y Medio Rural y Marino. Spanish Government.
- Green, D. W., & Southard, M. Z. (2008). *Perry's chemical engineers' handbook*. McGraw-Hill Education.
- Gustafsson, J., Renman, A., Renman, G., & Poll, K. (2008). Phosphate removal by mineral-based sorbents used in filters for small-scale wastewater treatment. *Water research*, 42(1-2), 189–197.

- Hernandez, B., Leon, E., & Martin, M. (2017). Bio-waste selection and blending for the optimal production of power and fuels via anaerobic digestion. *Chemical Engineering Research and Design*, 121, 163–172.
- Hernández, B., & Martín, M. (2016). Optimal process operation for biogas reforming to methanol: effects of dry reforming and biogas composition. *Industrial & Engineering Chemistry Research*, 55(23), 6677–6685.
- Hylander, L. D., Kietlińska, A., Renman, G., & Simán, G. (2006). Phosphorus retention in filter materials for wastewater treatment and its subsequent suitability for plant production. *Bioresource technology*, 97(7), 914–921.
- Jordan, E. M. (2011). *Development of an aerated struvite crystallization reactor for phosphorus removal and recovery from swine manure*. University of Manitoba (Canada).
- Kietlińska, A., & Renman, G. (2005). An evaluation of reactive filter media for treating landfill leachate. *Chemosphere*, 61(7), 933–940.
- Kõiv, M., Liira, M., Mander, Ü., Mõtlep, R., Vohla, C., & Kirsimäe, K. (2010). Phosphorus removal using Ca-rich hydrated oil shale ash as filter material—The effect of different phosphorus loadings and wastewater compositions. *Water Research*, 44(18), 5232–5239.
- Kowalski, Z., Makara, A., & Fijorek, K. (2013). Changes in the properties of pig manure slurry. *Acta Biochimica Polonica*, 60(4).
- Kumashiro, K., Ishiwatari, H., & Nawamura, Y. (2001). A pilot plant study on using seawater as a magnesium source for struvite precipitation, In *second international conference on recovery of phosphates from sewage and animal wastes, Noordwijkerhout, Holland*.
- Lantz, M. (2012). The economic performance of combined heat and power from biogas produced from manure in Sweden—A comparison of different CHP technologies. *Applied Energy*, 98, 502–511.
- Le Corre, K. S. (2006). Understanding struvite crystallisation and recovery.
- León, E. (2015). *Design of a Thermoelectric Plant Combined Cycle Using Manure Based Biogas* (Master's thesis). University of Salamanca.
- León, E., & Martín, M. (2016). Optimal production of power in a combined cycle from manure based biogas. *Energy Conv. Manage.*, 114, 89–99.
- Li, L., Gao, J., Zhu, S., Li, Y., & Zhang, R. (2015). Study of bioleaching under different hydraulic retention time for enhancing the dewaterability of digestate. *Applied microbiology and biotechnology*, 99(24), 10735–10743.
- Lin, H., Gan, J., Rajendran, A., Reis, C., & Hu, B. (2015). Phosphorus removal and recovery from digestate after biogas production. In *Biofuels-status and perspective*. IntechOpen.

- Lind, B.-B., Ban, Z., & Bydén, S. (2000). Nutrient recovery from human urine by struvite crystallization with ammonia adsorption on zeolite and wollastonite. *Bioresource technology*, 73(2), 169–174.
- Loh, H., Lyons, J., & White, C. W. (2002). *Process equipment cost estimation, final report* (tech. rep.). National Energy Technology Lab.(NETL), Morgantown, WV (United States).
- Lorimor, J., Powers, W., & Sutton, A. (2004). *Manure Characteristics* (tech. rep.). MidWest Plan Service.
- Mangin, D., & Klein, J. (2004). Fluid dynamic concepts for a phosphate precipitation reactor design. *Phosphorus in environmental technologies: Principles and applications*, 358–401.
- Martín, L., & Martín, M. (2013). Optimal year-round operation of a concentrated solar energy plant in the south of Europe. *Applied Thermal Engineering*, 59(1-2), 627–633.
- Martín, M., & Grossmann, I. E. (2011). Energy optimization of bioethanol production via gasification of switchgrass. *AIChE Journal*, 57(12), 3408–3428.
- Martins das Neves, L., Converti, A., & Vessoni Penna, T. (2009). Biogas production: new trends for alternative energy sources in rural and urban zones. *Chemical Engineering & Technology*, 32(8), 1147–1153.
- Matche. (2014). Index of process equipment [[Last Accessed 16 March 2017]].
- Meixner, K., Fuchs, W., Valkova, T., Svardal, K., Loderer, C., Neureiter, M., Bochmann, G., & Drosig, B. (2015). Effect of precipitating agents on centrifugation and ultrafiltration performance of thin stillage digestate. *Separation and Purification Technology*, 145, 154–160.
- Ministerio de Economía, Industria y Competitividad. (2017). Tesoro Público [[Online; accessed 21-May-2017]].
- Molinos-Senante, M., Hernández-Sancho, F., Sala-Garrido, R., & Garrido-Baserba, M. (2011). Economic feasibility study for phosphorus recovery processes. *Ambio*, 40(4), 408–416.
- Moran, M., & Shapiro, H. (2003). *Fundamentals of Engineering Thermodynamics* (5th ed.). Wiley.
- Nelson, N. O., Mikkelsen, R. L., & Hesterberg, D. L. (2003). Struvite precipitation in anaerobic swine lagoon liquid: effect of pH and Mg:P ratio and determination of rate constant. *Bioresource Technology*, 89(3), 229–236.
- Österberg, A. (2012). Removal and Recycling of Phosphorus from Wastewater Using Reactive Filter Material Polonite®.
- Pant, H., Reddy, K., & Lemon, E. (2001). Phosphorus retention capacity of root bed media of sub-surface flow constructed wetlands. *Ecological engineering*, 17(4), 345–355.

- Peters, M. S., Timmerhaus, K. D., West, R. E., Et al. (2003). *Plant design and economics for chemical engineers* (Vol. 4). McGraw-Hill New York.
- Pratt, C., Parsons, S. A., Soares, A., & Martin, B. D. (2012). Biologically and chemically mediated adsorption and precipitation of phosphorus from wastewater. *Current opinion in Biotechnology*, 23(6), 890–896.
- Rigby, H., & Smith, S. R. (2011). *New markets for digestate from anaerobic digestion* (tech. rep.). WRAP.
- Rohstoffe eV, F. N. (2010). *Guía sobre el biogás desde la producción hasta el uso* (tech. rep.). Ministerio Federal de Alimentación, Agricultura y Protección al Consumidor, Repùblica Federal Alemana.
- Sampat, A., Martín, E., Martín, M., & Zavala, V. (2017). Optimization formulations for multi-product supply chain networks. *Comput. Chem. Eng.*, 104, 296–310.
- Shilton, A. N., Elmetri, I., Drizo, A., Pratt, S., Haverkamp, R. G., & Bilby, S. C. (2006). Phosphorus removal by an 'active'slag filter—a decade of full scale experience. *Water research*, 40(1), 113–118.
- Sinnott, R. (1999a). Coulson and Richardson's Chemical Engineering (2nd ed.). *Chemical engineering design*.
- Sinnott, R. (1999b). *Chemical engineering design* (Vol. 6). Elsevier.
- Szabó, A., Takács, I., Murthy, S., Daigger, G., Licskó, I., & Smith, S. (2008). Significance of design and operational variables in chemical phosphorus removal. *Water Environment Research*, 80(5), 407–416.
- Tejero-Ezpeleta, M. P., Buchholz, S., & Mleczko, L. (2004). Optimization of reaction conditions in a fluidized-bed for silane pyrolysis. *The Canadian Journal of Chemical Engineering*, 82(3), 520–529.
- Tisa, F., Raman, A. A. A., & Daud, W. (2014). Basic design of a fluidized bed reactor for wastewater treatment using fenton oxidation. *International Journal of Innovation, Management and Technology*, 5(2), 93–98.
- Towler, G., & Sinnott, R. (2009). *Chemical engineering design* (5th ed.). Elsevier.
- Vian Ortuño, A. (1991). *El pronóstico económico en química industrial*.
- Vohla, C., Köiv, M., Bavor, H. J., Chazarenc, F., & Mander, Ü. (2011). Filter materials for phosphorus removal from wastewater in treatment wetlands—A review. *Ecological Engineering*, 37(1), 70–89.
- Wakeman, R. J. (2007). Separation technologies for sludge dewatering. *Journal of hazardous materials*, 144(3), 614–619.
- Walas, S. M. Et al. (1990). *Chemical process equipment: selection and design* (Vol. 1). Butterworths Boston.
- WEF. (2005). *Clarifier Design: WEF Manual of Practice No. FD-8* (tech. rep.). McGraw-Hill Professional.

- Williams, J., & Esteves, S. (2011). *Digestates: Characteristics. Processing and Utilisation* (tech. rep.). University of Glamorgan, South Wales.
- Wilsenach, J., Schuurbiers, C., & Van Loosdrecht, M. (2007). Phosphate and potassium recovery from source separated urine through struvite precipitation. *Water research*, 41(2), 458–466.
- Yang, J., Wang, S., Lu, Z., & Lou, S. (2009). Converter slag-coal cinder columns for the removal of phosphorous and other pollutants. *Journal of Hazardous Materials*, 168(1), 331–337.
- Zeng, L., & Li, X. (2006). Nutrient removal from anaerobically digested cattle manure by struvite precipitation. *Journal of Environmental Engineering and Science*, 5(4), 285–294.
- Zhang, T., Li, P., Fang, C., & Jiang, R. (2014). Phosphate recovery from animal manure wastewater by struvite crystallization and CO₂ degasification reactor. *Ecological Chemistry and Engineering*, 21(1), 89.
- Zhou, Y., Xing, X.-H., Liu, Z., Cui, L., Yu, A., Feng, Q., & Yang, H. (2008). Enhanced coagulation of ferric chloride aided by tannic acid for phosphorus removal from wastewater. *Chemosphere*, 72(2), 290–298.

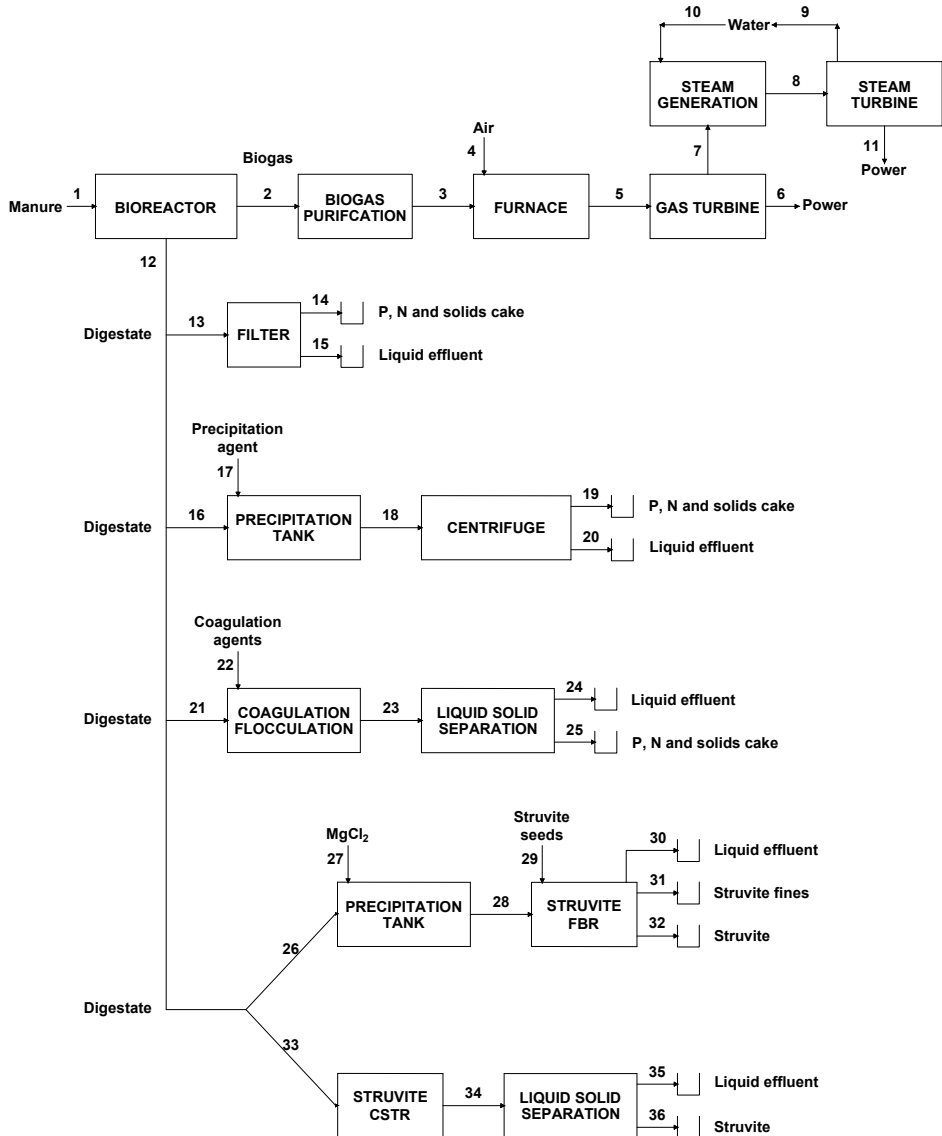


Figure 3.1: Flowsheet for the production of power and fertilizers.

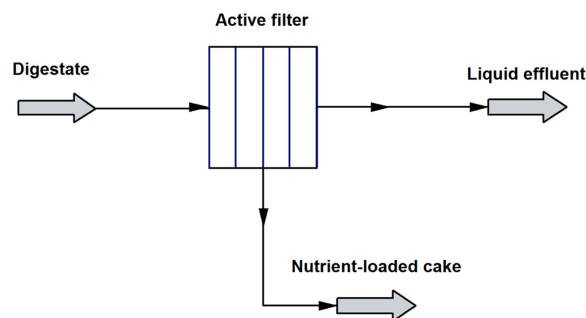


Figure 3.2: Scheme of the filter.

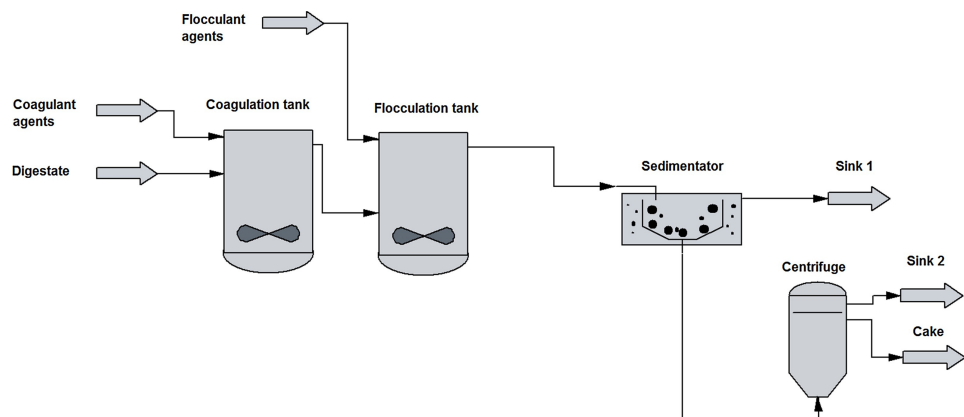


Figure 3.3: Scheme of the coagulation process.

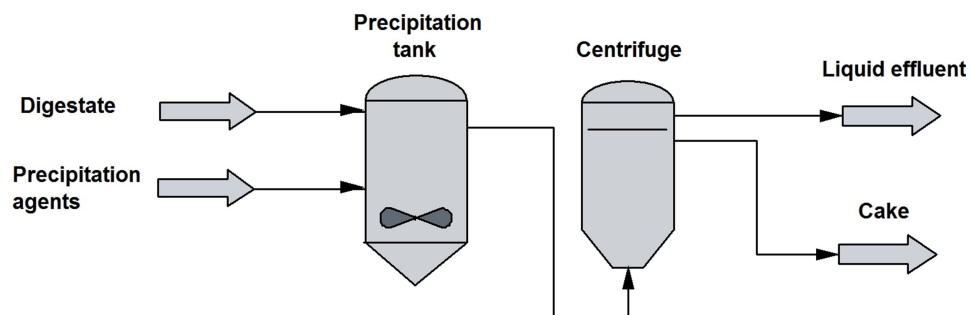


Figure 3.4: Scheme for the centrifugation treatment.

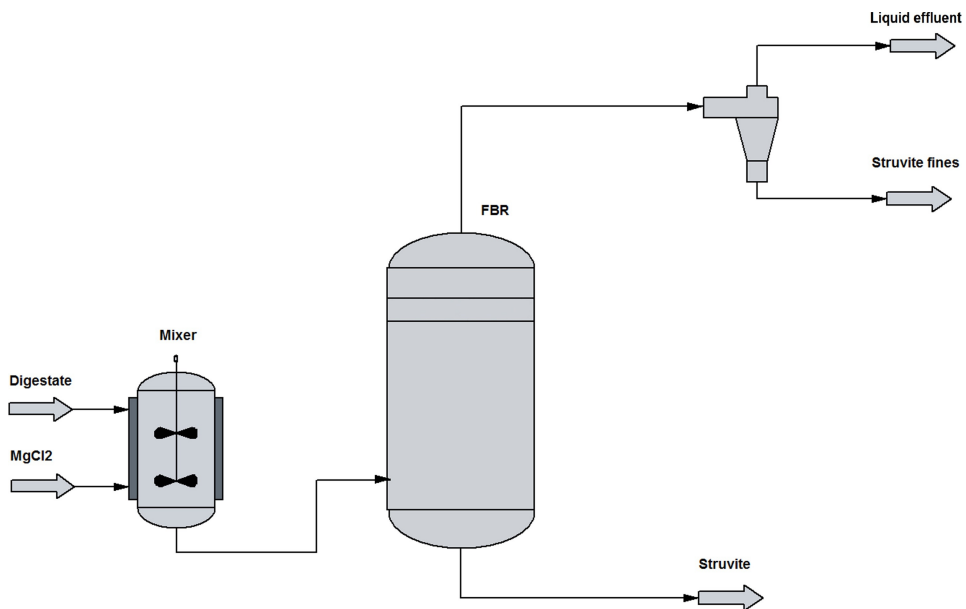


Figure 3.5: Scheme for the FBR system.

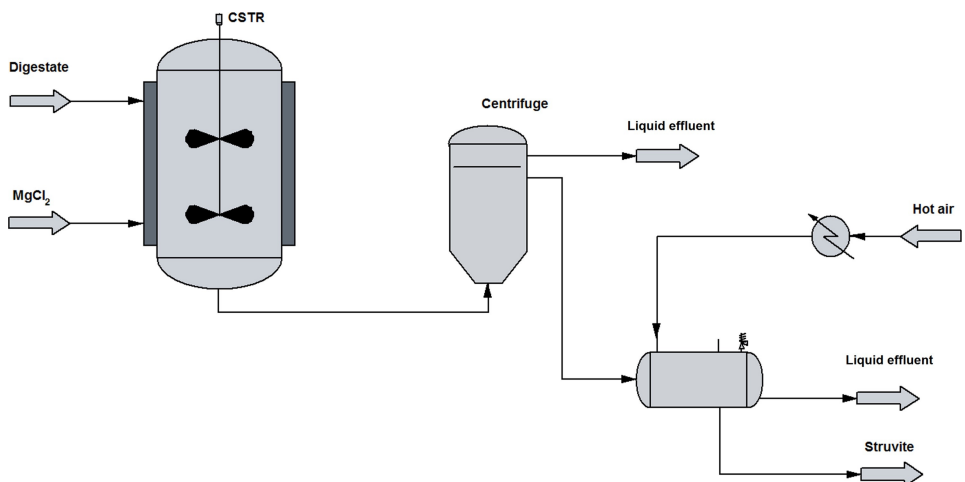


Figure 3.6: Scheme for the CSTR based struvite production system.

Table 3.4: Operating data of the optimal configuration for each raw material.

		T (°C)	P (bar)	Extractions
Cattle	Bioreactor	55	1	–
	Gas turbine	2430 (in)	8.2 (in)	–
		1205 (out)	1 (out)	–
	Steam turbine	1000 (T ₁)	125 (P ₁)	6.7% to HX7
		568 (T ₂)	11 (P ₂)	–
		442 (T ₃)	5 (P ₃)	–
		41.8 (T ₄)	0.08 (P ₄)	–
Pig	FBR	25	1	–
	Bioreactor	55	1	–
	Gas turbine	2430 (in)	8.2 (in)	–
		1205 (out)	1 (out)	–
	Steam turbine	1000 (T ₁)	125 (P ₁)	6.7% to HX7
		568 (T ₂)	11 (P ₂)	–
		442 (T ₃)	5 (P ₃)	–
Poultry	FBR	25	1	–
	Bioreactor	55	1	–
	Gas turbine	2430 (in)	8.2 (in)	–
		1205 (out)	1 (out)	–
	Steam turbine	1000 (T ₁)	125 (P ₁)	6.7% to HX7
		568 (T ₂)	11 (P ₂)	–
		442 (T ₃)	5 (P ₃)	–
Sheep	FBR	25	1	–
	Bioreactor	55	1	–
	Gas turbine	2337 (in)	15.6 (in)	–
		896 (out)	1 (out)	–
	Steam turbine	769.6 (T ₁)	95 (P ₁)	2.9% to HX7
		439.1 (T ₂)	11 (P ₂)	–
		329.6 (T ₃)	5 (P ₃)	–
		73.0 (T ₄)	0.35 (P ₄)	–
	FBR	25	1	–

Table 3.5: Process optimization results for considered manures.

Manure	Power (kW)	Comp. biogas (CH ₄ /CO ₂ ratio)	Digestate treatment technology	Product recovered	Biogas/manure ratio	Digestate/manure ratio
Cattle	2,612	0.816	FBR struvite	Struvite	0.0208	0.9794
Pig	2,612	0.816	FBR struvite	Struvite	0.0208	0.9794
Poultry	31,349	0.818	FBR struvite	Struvite	0.2499	0.7526
Sheep	14,106	0.818 3.4	FBR struvite	Struvite	0.1217	0.8795

Table 3.6: Process optimization results for considered manures.

Manure	CH ₄ (%wt)	CO ₂ (%wt)	Water (%wt)	O ₂ (%wt)	N ₂ (%wt)
Cattle	0.385	0.470 3.4	0.120	0.006	0.020
Pig	0.385	0.470	0.120	0.006	0.020
Poultry	0.385	0.470	0.120	0.006	0.020
Sheep	0.385	0.470	0.120	0.006	0.020

Table 3.7: Electricity production cost and NPV for the facility considering different raw materials.

Raw material	Annual production costs (M EUR /year)	Electricity production cost (EUR/kWh)	NPV (EUR /year)
Cattle manure	12.04	0.45	-1.93 · 10 ⁷
Pig manure	12.07	0.45	-1.96 · 10 ⁷
Poultry manure	25.51	0.03	2.85 · 10 ⁸
Sheep manure	15.53	0.10	5.40 · 10 ⁷

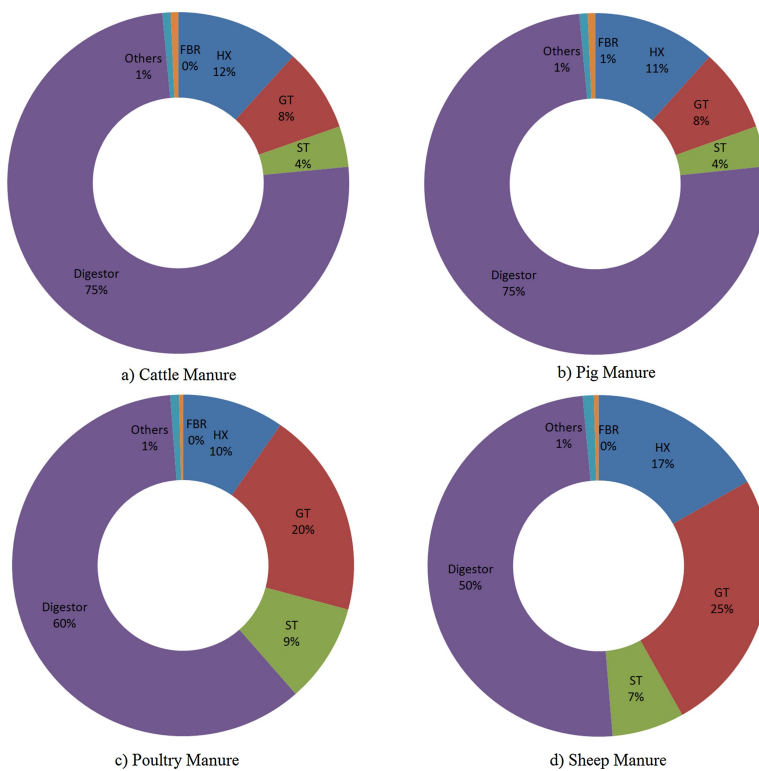


Figure 3.7: Units cost distributions for cattle, pig, poultry and sheep manure treatment (ST: steam turbine, GT: gas turbine, HX: heat exchangers, FBR: fluidized bed reactor).

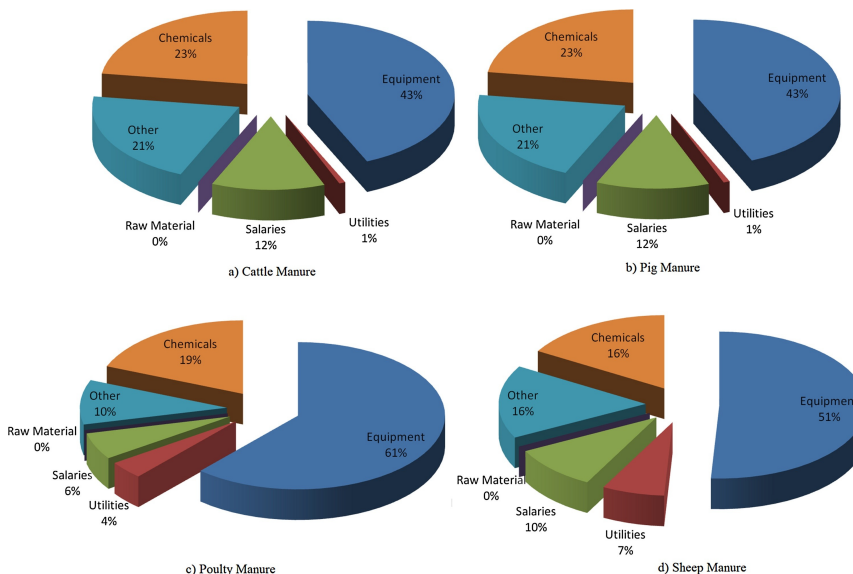


Figure 3.8: Operation cost distribution for cattle, pig, poultry and sheep manure treatment.

4

ASSESSMENT OF PHOSPHORUS RECOVERY THROUGH THE DEPLOYMENT OF STRUVITE PRECIPITATION SYSTEMS

4.1 INTRODUCTION

Livestock farming and other agricultural activities have altered the natural nutrient cycles. Phosphorus, one of the three plant-grow macronutrients, enters to the global cycle as phosphate rock, which through erosion and chemical weathering is transferred to soils and waterbodies. Also, phosphorus deposited in soils will reach fresh and marine waterbodies by runoff. Phosphorus in rivers is transported to stagnant waterbodies (such as lakes) and oceans, reaching the bottom of lakes and oceans as sediments. The cycle is closed when the buried phosphorus is uplifted again by tectonic processes. Along the cycle, phosphorus can be taken by plants and algae, but after the death of living organisms it returns to the cycle (Ruttenberg, 2001). This global natural cycle is largely altered by human activities through the mining and shipping of phosphate rock, mainly for fertilizer production, resulting in unbalanced phosphorus releases to the environment.

Nutrient pollution from anthropogenic sources has become as a critical worldwide water quality problems. Nutrient contamination results in environmental and public health issues as a result of the exponential growth of algae, cyanobacteria, and the occurrence of harmful algal blooms (HABs), which turns into dead zones and hypoxia due to the aerobic degradation of the algal biomass by bacteria; shifting the distribution of aquatic species and releasing toxins in drinking water (Sampat et al., 2018). In addition, the development of HABs and eutrophication processes contributes to climate change through the emission of large amounts of strong greenhouse gases such as CH₄ and N₂O (Beaulieu et al., 2019).

However, phosphorus is a limited non-renewable resource, essential nutrient to support life, and widely used as fertilizer to increase crop yields. Actually, phosphorus is one of the most sensitive elements to depletion, as it is a key agricultural fertilizer that has no known substitute. Current global reserves of phosphate rock could be depleted in the next 50 to 100 years (Cordell et al., 2009). Therefore, the development of a circular economy around phosphorus capable of recovering the nutrient and reintegrating it into the productive cycle is not only desirable but

also a necessary measure to reach sustainable development. Agricultural activities are the main source of nutrients in waterbodies (Dzombak, 2011), and among them, livestock industry is one of the largest economic sectors. Additionally, the increasing income-spending potential of the middle class in developing countries has increased the demand for dairy and beef products, resulting in the generation of large amounts of livestock organic waste. Considering that an average dairy cow generates 51.19 kg of raw manure per day (United States Department of Agriculture (USDA), 2009), the total phosphorus excreted is 11.02 kg per year per animal, equivalent to 5.96 kg of phosphorus as phosphate per year per animal. In the U.S. as of January 2020, a total of 94.4 million head has been reported (United States Department of Agriculture (USDA), National Agricultural Statistics Service, 2020). Thus, this shows potential phosphate U.S. releases of $562.6 \cdot 10^6$ kg/yr. Sampat et al. (2017) presented the link between the presence of livestock facilities and larger concentrations of phosphorus in soil, which potentially can be lost as runoff reaching waterbodies. For animals on pasture, organic waste should not be a resource of concern if stocking rates are not excessive. However, for concentrate animal feeding operations (CAFOs), manure should be correctly managed due to the high rates and spatial concentration of the organic waste generated, representing potential environmental issues. Usually, manure is collected in the animal living zones, and stored as liquid or slurry to be further spread in croplands as nutrient supplementation; or as solid in dry stacking or composting facilities to be sold as compost. Liquid fraction of manure can be also treated in aerobic or anaerobic ponds. However, these approaches do not allow a correct nutrient management since nutrients concentration is variable and not well defined, and nitrogen and phosphorus are unbalanced regarding the nutrient necessities of plants, i.e., if nitrogen demand is covered, there is a surplus in the phosphorus supply which can runoff to waterbodies, and if phosphorus demand is covered, there is a deficit in the nitrogen supply, being necessary to apply additional fertilizers. In addition, during rainy periods the applied manure can runoff, dragging the nutrients contained in it. Nonetheless, phosphorus from liquid cattle waste, either processed in an anaerobic digestion stage or raw waste, can be potentially recovered through different processes (Muhmood et al., 2019), reducing the nutrient inputs to waterbodies and its consequential environmental, economic, and social impacts. Among these, it is found that struvite production is one of the most promising cost-effective choices for the recovery of nutrients from cattle waste (Martín-Hernández et al., 2018). Struvite is a phosphate-based mineral, which can be applied as a slow release fertilizer (Richards & Johnston, 2001), allowing the redistribution of phosphorus from livestock facilities to nutrient-deficient locations.

Previous studies report struvite formation from different sources of waste, such as municipal wastewater treatment plants (Battistoni et al., 2001), mineral fertilizer industry (Matynia et al., 2013), or agricultural industry (Shashvatt et al., 2018). Thermodynamic models representing the formation of struvite and other precipitates have been also developed for various wastes including liquid swine manure (Celen et al., 2007), human urine (Harada et al., 2006; Ronteltap et al., 2007), and municipal wastewater (Rahaman et al., 2014). Additionally, some complex approaches considering the hydrodynamic and kinetic effects in the formation of struvite have been studied but limited to wastewater treatment (Mangin & Klein, 2004; Rahaman et al., 2014). However, the results obtained from those studies cannot be extrapolated to struvite formation from cattle organic waste, since these residues have some characteristics that hinder struvite formation, including high ionic strength, which reduces the effective concentration of ions; the presence of calcium ions competing for phosphate ions (Yan & Shih, 2016), which inhibits a selective recovery by nutrient precipitation techniques; and the high variability in the manure composition, as a function of the geographical area, the animal feed, etc. (Tao et al., 2016). Other controlling factors are the pH level, the magnesium-phosphorus ratio, and the alkalinity of the leachate. Therefore, for an accurate prediction of struvite formation from this waste, it is necessary to include within the thermodynamic model structure for precipitates formation the specific features of cattle waste described above.

In this work, specific surrogate models to predict the production of struvite and calcium precipitates from cattle leachate are developed based on a detailed and robust thermodynamic model. In addition, the variability in the organic waste composition is captured through a probability framework based on Monte Carlo method. The reduced models obtained are used to evaluate the potential of struvite production from cattle waste to mitigate phosphorus releases in watersheds of the United States. Future applications of the developed surrogate models include the development of applications for environmental assessment and the design of policies to prevent nutrient releases, among others.

4.2 METHODS

4.2.1 Spatial resolution

A watershed is an area of land which drains all the streams and rainfall to a common drainage, defining the spatial boundaries for the collection of lost elements as runoff. The surface water drainages of the U.S. are

identified by the U.S. Geological Survey through the Hydrologic Unit Code system (HUC). The HUC system is a hierarchical system indicated by the number of digits in groups of two, with six levels identified by codes from 2 to 12 digits (i.e., HUC₂ to HUC₁₂). These levels refer to regions, subregions, basins, subbasins, watersheds, and subwatersheds. The spatial resolution of this study is the continental United States at watershed scale, considering the boundaries defined by the Hydrologic Unit Code system at 8 digits (HUC8), representing the subbasin level (U.S. Geological Survey, 2013).

4.2.2 Assessment of anthropogenic phosphorus from agricultural activities

4.2.2.1 Phosphorus releases

Agricultural emissions are one of the main sources of anthropogenic P releases due to the excessive use of commercial fertilizers and livestock manure for cropland nutrients needs and the uncontrolled nutrient runoff to waterbodies, although for some areas urban source releases can contribute significantly to the total P releases to the environment. However, this analysis is limited to the evaluation of phosphorus releases from agricultural activities (Alexander et al., 2008; Dzombak, 2011; Smith & Alexander, 1999).

Watershed phosphorus releases (E_x) are computed as the sum of the phosphorus releases from fertilizer applications to croplands and from the manure generated by livestock facilities. The releases of phosphorus to each watershed by manure emissions, accounting cattle, swine and poultry, and by fertilizers application, is reported by the IPNI NuGIS project. This is consistent with the most recent data available (year 2014) for fertilizers sales provided by the Association of American Plant Food Control Officials (AAPFCO), fitting the data to HUC8 watershed boundaries. More information about the methodology used for the estimation of agricultural phosphorus releases can be found in (International Plant Nutrition Institute (IPNI), 2012). Phosphorus content for several commercial phosphate fertilizers and different manure types can be found in Ohio State University Extension (2017) and Ohio State University Extension (2005) respectively.

4.2.2.2 Phosphorus uptakes

The elements considered for phosphorus uptake are the crops sown and managed by humans in each watershed. Additionally, the phosphorus retained by wetlands has been considered in the phosphorus balance. The phosphorus uptake by each type of vegetation at watershed level is computed as the product of the land area occupied, the grow yields per

area unit and the phosphorus uptake per plant mass unit. Therefore, the total watershed phosphorus uptake (U_x) is computed as the sum of the phosphorus uptake by each type of plant, Eq. 4.1.

$$U_x = \sum^i \text{Area}_i \cdot \text{Yield}_i \cdot P_{\text{uptake}\ i} \quad \forall i \in \text{Plant varieties} \quad (4.1)$$

Since different crops have different phosphorus uptakes and yield rates, the amount of each type of crop is estimated for each watershed. To determine the land cover uses, accounting croplands, pasturelands, wetlands and developed areas (urban areas), information available for the most recent year (2011) from the U.S. Environmental Protection Agency's (U.S. EPA) EnviroAtlas database is used (Pickard et al., 2015). Data from EnviroAtlas is provided with higher spatial resolution, at HUC12 level. To ensure spatial consistency, the data is reconciled at HUC8 level. Once the land uses of each watershed are known, data from the 2017 U.S. Census of Agriculture is used to determine the distribution of crops on croplands, considering corn, soybeans, small grains, cotton, rice, vegetables, orchards, greenhouse and other crops (namely oil crops, sugar crops, and fruits) (United States Department of Agriculture (USDA), 2019). The data provided by the U.S. Census of Agriculture have a spatial resolution of HUC6. Therefore, it is reconciled at HUC8 level scaling by the area fraction represented by each HUC8 watershed over the total HUC6 hydrologic unit. If two or more crops were harvested from the same land during the year (double cropping), the area was counted for each crop. To determine the nutrients uptake of each type of crop, data from the U.S. Department of Agriculture (USDA) Waste Management field Handbook is considered (United States Department of Agriculture (USDA), 2009). For croplands, the specific nutrient uptake values are used for corn, soybeans, cotton, rice and orchards, while average values including the most representative species are used for small grains, vegetables, greenhouse crops, pasture crops, and forest. For pasture lands the average nutrient uptake and crop yield including the main pasture crops: alfalfa, switchgrass and wheatgrass; for forests lands the nutrient uptake and crop yield of Northern hardwoods is considered, and for developed areas null nutrient uptake is considered. The wetlands phosphorus uptake value considered is $0.77 \text{ gP m}^{-2} \text{ year}^{-1}$, based in the data reported by Kadlec (2016).

4.2.2.3 Phosphorus balance

To reach environmental sustainability of a productive activity, the releases of phosphorus should be balanced with the phosphorus uptakes

from that activity, reducing the impact over the original ecosystems as much as possible. To evaluate the balance of phosphorus releases involved in agricultural activities throughout the U.S. watersheds, the technoelectological synergy (TES) sustainability metric proposed by Bakshi et al. (2015) has been considered, Eq. 5.1. A negative value of V_x indicates that the emissions, (E_x), are larger than the uptake capacity of the agricultural activities, (U_x), impacting the ecosystems, while positive values reflect that the releases are lower than the uptake capacity.

$$V_x = \frac{(U_x - E_x)}{E_x} \quad (4.2)$$

4.2.3 *Thermodynamic model for precipitates formation*

The behavior of cattle leachate system has been evaluated through a thermodynamic model, evaluating the formation of different precipitates through chemical equilibrium and material balances, capturing the mutual dependencies based on the competition for the same ions. Four aqueous chemical systems have been considered, water, ammonium, phosphoric acid, and carbonates systems. Moreover, the formation of seven possible precipitates is evaluated: struvite, K-struvite, magnesium hydroxide, calcium hydroxide, calcium carbonate, hydroxyapatite, dicalcium phosphate, and tricalcium phosphate.

4.2.3.1 *Uncertainty in livestock organic waste composition*

The variability in the composition of raw material creates operational difficulties that any material recovery process must deal with. The composition of cattle organic waste depends on multiple factors, among which are livestock feed, geographical area, climate, and other local factors of the livestock operation (Tao et al., 2016). Several elements of cattle manure composition play an active role in the formation of struvite and other precipitates. These include the high ionic strength, which reduces the effective concentration of ions; and the distribution ratios between calcium, ammonia and phosphate; and the leachate alkalinity, affecting the chemical equilibrium. To capture the uncertainty generated by the variability in the composition of cattle leachate, 37 data sets of 20 literature references containing the mass fraction of different elements comprising organic livestock waste are evaluated. To estimate feasible cattle leachate compositions, the probability density distribution of each element is calculated by fitting it to the kernel density estimate (KDEs). The selected probability density distributions are normal distribution, as shown in Eq. 4.3, for the distribution

of nitrogen, nitrogen as ammonia/total nitrogen ratio, and phosphorus; and lognormal distribution, as defined by Eq. 4.4, for phosphorus as phosphate/total phosphorus ratio, calcium, and potassium. The probability density distribution parameters for each evaluated compound are collected in Table 4.1, where σ is the standard deviation, σ^2 is the variance, μ is the mean of the distribution, M is equal to e^μ , and γ is a displacement parameter. Kernel density estimations and probability density distributions for each element evaluated can be found in the Supplementary Material.

The uncertainty in the composition of cattle waste is addressed through the evaluation of the thermodynamic model described in the following sections for multiple cattle waste compositions generated including the probability density distribution of each elements in a Monte Carlo model (Thomopoulos, 2012).

$$f(x) = \frac{1}{\sqrt{2\pi}\sigma} e^{-\frac{(x-\mu)^2}{2\sigma^2}} \quad (4.3)$$

$$f(x) = \frac{\frac{1}{\frac{x-\gamma}{M}\sigma\sqrt{2\pi}} e^{-\frac{\ln(\frac{x-\gamma}{M})^2}{2\sigma^2}}}{M} \quad (4.4)$$

Table 4.1: Probability density distributions parameters for cattle organic waste elements.

Param.	Normal distribution			Param.	Lognormal distribution		
	N	N-NH ₄ ⁺ : N _{total}	P		P-PO ₄ ³⁻ : P _{total}	Ca	K
μ	0.3841	0.6200	0.04000	M	42.15	0.08000	0.2600
σ	0.1309	0.1250	0.03684	σ	0.0040	0.4500	0.8000
				γ	-41.53	0.04044	0.03389

4.2.3.2 Initial conditions

A set of initial conditions must be defined to establish the physico-chemical characteristics of the livestock organic material (Tao et al., 2016), see Table 4.2. Please note that pH refers the adjusted pH for optimal struvite precipitation (Tao et al., 2016; Zeng & Li, 2006).

4.2.3.3 Activities

Since the cattle waste is a highly non-ideal media due to the high concentrations of dissolved ions, activities instead of molar concentrations are

Table 4.2: Initial conditions of the livestock organic material system

Variable	Value	Unit
Temperature	298	K
pH	9	-
Electrical conductivity (EC)	18,800	$\frac{\mu\text{S}}{\text{cm}}$
Alkalinity	3000-14500	mg of CaCO_3
$[\text{Ca}^{2+}]$	0.075-0.175 (determined by Monte Carlo model)	% wt wet
$[\text{K}^+]$	0.10-0.65 (determined by Monte Carlo model)	% wt wet
$[\text{P-PO}_4^{3-}]$	0.001-0.024 (determined by Monte Carlo model)	% wt wet
$[\text{N-NH}_4^+]$	0.015-0.64 (determined by Monte Carlo model)	% wt wet
$[\text{Mg}^{2+}]$	0-10	$\text{Mg}^{2+}/\text{PO}_4^{3-}$ molar ratio

used in the model. Activity coefficients (γ_x) for an element x are calculated using the Debye-Hückel relationship, Eq. 4.6, which relates activity coefficient, temperature, and ionic strength, calculated using Eq. 4.5. Eq. 4.7 is employed to estimate the parameter A (Metcalf & Eddy, 2014; Tao et al., 2016). Finally, activities for each compound are calculated using Eq. 4.8

$$I = 1.6 \cdot 10^{-5} \cdot EC, \quad I(M), \quad EC \left(\frac{\mu\text{S}}{\text{cm}} \right) \quad (4.5)$$

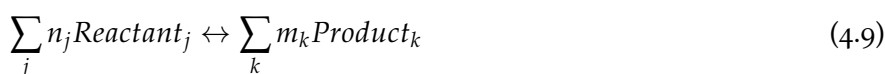
$$\log_{10}(\gamma_x) = -A \cdot z_x^2 \cdot \left(\frac{\sqrt{I}}{1 + \sqrt{I}} \right) - 0.3 \cdot I \quad (4.6)$$

$$A = 0.486 - 6.07 \cdot 10^{-4} \cdot T + 6.43 \cdot 10^{-6} \cdot T^2, \quad T(K) \quad (4.7)$$

$$\{x\} = [x] \cdot \gamma_x \quad (4.8)$$

4.2.3.4 Distribution of species in aqueous phase

The distribution of species for ammonia, water, phosphoric acid, and carbonate systems in cattle leachate is determined by chemical equilibria:



where n_j and m_k are the stoichiometric coefficients of the reactants and products respectively, and defining J as the set of chemical systems described in Table 4.3 for water, ammonia, and phosphoric acid systems,

the thermodynamic equilibrium is defined for all the elements of the set as shown in Eq. 4.10. In combination with the material balances, Eq. 4.11, these define the chemical equilibrium for all the elements of the set. The description of the model for carbonate system is detailed in the Supplementary Material, and pK values are collected in Table 4.3.

$$K_J = \frac{(\prod_k \{Products\}_k^{m_k})_J}{(\prod_j \{Reactants\}_j^{n_j})_J} \quad (4.10)$$

$$[i]_J^{initial} = \sum_J [Compounds]_J \quad (4.11)$$

$$i \in \{\text{NH}_4^+, \text{Ca}^{2+}, \text{Mg}^{2+}, \text{PO}_4^{3-}, \text{CO}_3^{2-}\}$$

Table 4.3: pK_{sp} values for the considered aqueous phase chemical systems.

Name	Chemical system	pK	Source
Ammonia	$\text{NH}_4^+ \leftrightarrow \text{NH}_3 + \text{H}^+$	9.2	(Bates & Pinching, 1949)
Water	$\text{H}_2\text{O} \leftrightarrow \text{OH}^- + \text{H}^+$	14	(Skoog et al., 2014)
	$\text{H}_3\text{PO}_4 \leftrightarrow \text{H}_2\text{PO}_4^- + \text{H}^+$	2.1	(Ohlinger et al., 1998)
Phosphoric acid	$\text{H}_2\text{PO}_4^- \leftrightarrow \text{HPO}_4^{2-} + \text{H}^+$	7.2	(Ohlinger et al., 1998)
	$\text{HPO}_4^{2-} \leftrightarrow \text{PO}_4^{3-} + \text{H}^+$	12.35	(Ohlinger et al., 1998)
Carbonic acid	$\text{H}_2\text{CO}_3 \leftrightarrow \text{HCO}_3^- + \text{H}^+$	6.35	(Skoog et al., 2014)
	$\text{HCO}_3^- \leftrightarrow \text{CO}_3^{2-} + \text{H}^+$	10.33	(Skoog et al., 2014)

4.2.3.5 Precipitates formation

The precipitates that can be potentially formed from cattle waste have been selected based on the precipitates reported by previous studies (Gadekar & Pullammanappallil, 2010; Harada et al., 2006; Tao et al., 2016). A general solubility equilibrium, where n_a and m_b are the stoichiometric coefficients of the reactants and solid products respectively, can be written as:

$$\sum_b m_b \text{Precipitate}_b \downarrow \leftrightarrow \sum_a n_a \text{Reactant}_a \quad (4.12)$$

The solid species considered in this study and their corresponding pK_{sp} values are shown in Table 4.4. These are the main precipitates that can

Table 4.4: Solids species considered in this work.

Name	Chemical system	pK_{sp}	Source
Struvite	$\text{MgNH}_4\text{PO}_4 \cdot 6\text{H}_2\text{O} \leftrightarrow \text{Mg}^{2+} + \text{NH}_4^+ + \text{PO}_4^{3-}$	13.26	(Ohlinger et al., 1998)
K-struvite	$\text{MgKPO}_4 \cdot 6\text{H}_2\text{O} \leftrightarrow \text{Mg}^{2+} + \text{K}^+ + \text{PO}_4^{3-}$	10.6	(Taylor et al., 1963)
Hydroxyapatite	$\text{Ca}_5(\text{PO}_4)_3\text{OH} \leftrightarrow 5\text{Ca}^{2+} + 3\text{PO}_4^{3-} + \text{OH}^-$	44.33	(Brezonik & Arnold, 2011)
Calcium carbonate	$\text{CaCO}_3 \leftrightarrow \text{Ca}^{2+} + \text{CO}_3^{2-}$	8.48	(Morse et al., 2007)
Tricalcium phosphate	$\text{Ca}_3(\text{PO}_4)_2 \leftrightarrow 3\text{Ca}^{2+} + 2\text{PO}_4^{3-}$	25.50	(Fowler & Kuroda, 1986)
Dicalcium phosphate	$\text{CaHPO}_4 \leftrightarrow \text{Ca}^{2+} + \text{HPO}_4^{2-}$	6.57	(Gregory et al., 1970)
Calcium hydroxide	$\text{Ca}(\text{OH})_2 \leftrightarrow \text{Ca}^{2+} + 2\text{OH}^-$	5.19	(Skoog et al., 2014)
Magnesium hydroxide	$\text{Mg}(\text{OH})_2 \leftrightarrow \text{Mg}^{2+} + 2\text{OH}^-$	11.15	(Skoog et al., 2014)

be formed from the ions found in the cattle leachate. Considering the activity of solid species is equal to 1, and defining L as the set of chemical systems described in Table 4.4, the solubility equilibrium is defined for all the elements of the set as shown in Eq. 4.13.

The supersaturation index (Ω) is defined as the ratio between the ion activity product and the solubility product (K_{sp}), as shown in Eq. 4.14 (Tao et al., 2016). Therefore, the value of Ω determines if a compound precipitates. A saturation index $\Omega > 1$ indicates supersaturated conditions where precipitate may form, $\Omega = 1$ indicates equilibrium between solid and liquid phases, and $\Omega < 1$ indicates unsaturated conditions where no precipitate can form.

The higher value of the supersaturation index, the larger formation potential of a precipitate. Therefore, the sequence for the precipitation of different species can be set by comparing the supersaturation index values. The amount of solid species generated is computed through material balances, Eq. 4.15.

$$K_{spL} = \left(\prod \{\text{Reactants}\}_a^{n_a} \right)_L \quad (4.13)$$

$$\Omega_L = \frac{\left(\prod \{\text{Reactants}\}_a^{n_a} \right)_L}{K_{spL}} \quad (4.14)$$

$$[i]_L^{initial} = \sum_L [\text{Compounds}]_L \quad (4.15)$$

$$i \in \{\text{NH}_4^+, \text{Ca}^{2+}, \text{Mg}^{2+}, \text{PO}_4^{3-}, \text{CO}_3^{2-}\}$$

4.2.3.6 Thermodynamic model algorithm

Figure 4.1 shows a flowchart describing the proposed algorithm to solve the thermodynamic model of solid compound formation in cattle organic waste. In step *a*, the operating conditions and the initial molar concentrations of Ca^{2+} , K^+ , Mg^{2+} , NH_4^+ , and PO_4^{3-} in cattle leachate are defined as described previously. In step *b*, ionic strength and activity coefficients are computed. Next, in steps *c* and *d*, two parallel problems are solved, the equilibrium of the aqueous species, and the alkalinity problem to determine the distribution of carbonates. After determining the concentration of all species in the organic waste, the supersaturation index for all species is computed in step *e*. The compound with the maximum supersaturation index is assumed to precipitate first. The amount of formed precipitate is computed by solving the solubility equilibrium and the material balance. As a result of the precipitate formation, the concentration of some species in aqueous phase is reduced. Therefore, the equilibrium of the aqueous species and the alkalinity problem must be recalculated, to obtain the new concentration values of the different compounds in the waste, and the iterative process, starts again.

The iterative process runs until each component saturation index is equal or less than one, and the formation of the precipitates stops.

4.2.3.7 Integration of waste composition uncertainty and precipitates formation thermodynamic models

The evaluation of livestock waste variability in the formation of struvite and other precipitates, consists of 5 steps, as shown in Fig. 4.2. First, cattle waste composition data are collected from literature. Using these data, probability density distributions for the compounds of cattle leachate are estimated, and they are used in the Monte Carlo model to obtain feasible composition data sets of cattle organic waste. Random points are generated for each chemical compound and species ratios (i.e. N, P, K, Ca, $\text{N-NH}_4^+ : \text{N}_{\text{total}}$, and $\text{P-PO}_4^{3-} : \text{P}_{\text{total}}$). Finally, the thermodynamic model is solved for the composition data sets generated, obtaining the precipitated compounds formed.

The thermodynamic model has been implemented in the algebraic modeling language JuMP, embedded in the programming language Julia (Bezanson et al., 2017; Dunning et al., 2017). The statistical study of cattle waste composition data, the Monte Carlo framework, result analysis, and data visualization were made in Python language (Hunter, 2007, 2010; van der Walt et al., 2011; van Rossum, 1995).

4.2.3.8 Model validation and limitations

The developed model was validated using the data provided by Zeng and Li (2006). Their work was carried out under similar operational conditions to which this work intends to evaluate. In Fig. 4.3 experimental and model results are compared. The values at high Mg^{2+} molar ratio, when the largest supersaturation values are reached and the formation of struvite is close to the maximum allowed by the thermodynamic equilibrium, match the experimental data. However, at lower ratios, differences between results of the thermodynamic model proposed and experimental data can be observed. As the authors of the article indicate, this differences can be due to the presence of many suspended solids which interfere in the struvite formation process. Note that this work is focused on the thermodynamic aspect, without considering other aspects such as chemical kinetics or transport phenomena. The scarcity of data is an impediment to further validate the model.

In addition to the lack of previous studies and data availability to evaluate the effects of kinetics and transport phenomena in the formation precipitates from cattle leachate, another improvement of the proposed model can be achieved by the experimental determination of pK_{sp} values for the potential precipitates formed from cattle leachate. For struvite, the selected pK_{sp} value is taken from the work of Ohlinger et al. (1998), as they determined the pK_{sp} value for struvite formation in digestate, a medium with high organic load and dissolved elements like cattle leachate. Otherwise, when pK_{sp} data for cattle waste is unavailable from previous studies, the reported values for water are used. A limitation in the use of the obtained surrogate models is that the formation of struvite and calcium precipitates can only be determined for cattle waste. Although a general formulation for the thermodynamic model is used, and the methodology proposed to include the effect of the uncertainty is not restricted to the use of a specific waste, only cattle leachate has been considered in this study. However, if data on the composition is available, surrogate models to predict the formation of struvite and calcium precipitates from other waste sources can be easily developed.

4.3 RESULTS AND DISCUSSION

4.3.1 Surrogate models to estimate the formation of precipitates from livestock organic waste

The influence of the main controllable parameters for struvite production at industrial scale operation was evaluated: the presence of magnesium and

calcium, and the alkalinity. Surrogate models were developed to allow the analytical estimation of precipitates formation. pH value for the struvite precipitation process has been considered as a fixed variable, since there is a wide consensus about a pH value of 9, at which struvite solubility is minimum, is optimal, enhancing the phosphorus and nitrogen conversion to struvite and its eventual precipitation (Tao et al., 2016; Zeng & Li, 2006).

4.3.1.1 Influence of magnesium

In phosphorus recovery processes through struvite formation, magnesium is usually added to increase the saturation of struvite, enhancing its precipitation. This is especially important for cattle leachate due to the high presence of calcium ions competing with other cations for phosphate anions, and the high ionic strength of livestock leachate, reducing the effective concentration of ions. If the supplementation of magnesium provides enough magnesium ions, struvite will reach higher supersaturation ratio than calcium precipitates, leading the formation of struvite over calcium compounds. To estimate the performance of struvite precipitation from cattle leachate, the developed thermodynamic model was solved for 50 different composition data sets. The average alkalinity value of the range reported by Tao et al. (2016) is considered, 8770.5 mg of CaCO₃. The plots showing evolution of precipitates formation in function of the Mg²⁺/PO₄³⁻ molar ratio are collected in the Supplementary Material. Analyzing the average fraction of PO₄ recovered in form of struvite as a function of the Mg²⁺/PO₄³⁻ molar ratio, a tentative value for Mg²⁺/PO₄³⁻ molar ratio between 2 and 4 can be set as a compromise effectiveness-cost solution. Higher values result in a considerable consumption of magnesium returning lower improvements in phosphate recovery as struvite. The surrogate model obtained to evaluate performance of struvite precipitation in function of the magnesium supplied is a Monod type equation, as shown in Eq. 4.16, where $x_{\text{Mg}^{2+}:\text{PO}_4^{3-}}$ is referred to the Mg²⁺/PO₄³⁻ molar ratio.

$$x_{\text{struvite}}(\text{PO}_4^{3-}) = \frac{0.957 \cdot x_{\text{Mg}^{2+}:\text{PO}_4^{3-}}}{0.996 + x_{\text{Mg}^{2+}:\text{PO}_4^{3-}}} \quad (4.16)$$

The evolution in the formation of calcium precipitates as a function of the Mg²⁺/PO₄³⁻ molar ratio was also studied. Hydroxyapatite and calcium carbonate are the only calcium precipitates produced. Both hydroxyapatite and CaCO₃ patterns can be related to the increment of struvite formation along the increase of Mg²⁺/PO₄³⁻ molar ratio values, which reduces the presence of phosphate ions, and consequently decreases the supersaturation of hydroxyapatite. Therefore, there are more calcium ions available

to form calcium carbonate. Surrogate models fit to first order polynomial equations for hydroxyapatite, Eq. 4.18, and for calcium carbonate, Eq. 4.17.

$$x_{\text{hydroxyapatite}(\text{Ca}^{2+})} = -1.299 \cdot 10^{-2} \cdot x_{\text{Mg:PO}_4^{3-}} + 0.248 \quad (4.17)$$

$$x_{\text{CaCO}_3(\text{Ca}^{2+})} = 1.296 \cdot 10^{-2} \cdot x_{\text{Mg:PO}_4^{3-}} + 0.749 \quad (4.18)$$

4.3.1.2 Influence of calcium

One of the hindrances of cattle leachate for struvite precipitation is the presence of calcium ions competing with other cations for phosphate to form different precipitates. To study the inhibitory influence of calcium in cattle leachate for struvite precipitation, the thermodynamic model was evaluated for the same 50 different composition data sets used in the previous study along $\text{Ca}^{2+}/\text{PO}_4^{3-}$ molar ratio values from 0 to 5. To exclude the influence of magnesium concentration, the study was carried out fixing the $\text{Mg}^{2+}/\text{PO}_4^{3-}$ molar ratio at 2. The plots showing evolution of precipitates formation in function of the $\text{Ca}^{2+}/\text{PO}_4^{3-}$ molar ratio are collected in the Supplementary Material.

The phosphorus as phosphate fraction recovered as struvite exhibits a steep descent at $\text{Ca}^{2+}/\text{PO}_4^{3-}$ values between 0 and 2, followed by an asymptotic behavior tending to 0. The dispersion of the values has slight variations along with the evaluated $\text{Mg}^{2+}/\text{PO}_4^{3-}$ values. For hydroxyapatite and calcium carbonate, the higher $\text{Ca}^{2+}/\text{PO}_4^{3-}$ value, the greater dispersion for the obtained values. This is due to the increase in the supersaturation values for both calcium precipitates because of the presence of a higher number of calcium ions in the leachate.

The surrogate models obtained for struvite and calcium carbonate fit pseudo-sigmoidal equations, Eqs. C.7 and C.9 respectively; while for hydroxyapatite (HAP) is a second polynomial function, Eq. C.8. In all cases, $x_{\text{Ca}^{2+}:\text{PO}_4^{3-}}$ is referred to $\text{Ca}^{2+}/\text{PO}_4^{3-}$ molar ratio.

$$x_{\text{struvite}(\text{PO}_4^{3-})} = \frac{0.798}{1 + \left(x_{\text{Ca}^{2+}:\text{PO}_4^{3-}} \cdot 0.576 \right)^{2.113}} \quad (4.19)$$

$$\begin{aligned} x_{\text{hydroxyapatite}(\text{Ca}^{2+})} = & -4.321 \cdot 10^{-2} \cdot x_{\text{Ca}^{2+}:\text{PO}_4^{3-}}^2 + 0.313 \cdot x_{\text{Ca}^{2+}:\text{PO}_4^{3-}} \\ & - 3.619 \cdot 10^{-2} \end{aligned} \quad (4.20)$$

$$x_{\text{CaCO}_3(\text{Ca}^{2+})} = \frac{1.020}{1 + \left(x_{\text{Ca}^{2+}:\text{PO}_4^{3-}} \cdot 0.410 \right)^{1.029}} \quad (4.21)$$

4.3.1.3 Influence of alkalinity

Alkalinity is a parameter which can be used to control the production of calcium precipitates. When the presence of carbonates is low, the competition between hydroxyapatite and calcium carbonate tends to benefit the first compound because the limited availability of carbonate ions reduces the supersaturation of calcium carbonate. However, the predominance of hydroxyapatite reduces the formation of struvite since both elements compete for phosphate ions. Therefore, the presence of significant amounts of carbonates (performing at alkaline conditions) reduces the formation of hydroxyapatite and promotes the formation of struvite.

The results for the formation of struvite, hydroxyapatite and calcium carbonate considering the same 50 different composition data sets used in the previous studies in function of the alkalinity are collected in the Supplementary Material. It can be observed that the behavior of struvite formation and calcium carbonate are related, with an abrupt change for both elements at alkalinity values between 3,000 and 4,000 mg of CaCO_3 , reaching plateaus beyond these values. The dispersion of values follow a similar pattern for both struvite and calcium carbonate, being lower at low alkalinity values, and progressively growing until reaching a value of 4,000 mg of CaCO_3 . Beyond this value, the dispersion of values remains constant. Hydroxyapatite formation decrease continuously along the alkalinity values, being complementary with the formation of calcium carbonate.

Therefore, struvite formation from livestock leachate can be enhanced inhibiting hydroxyapatite formation by controlling the alkalinity level, increasing the formation of calcium carbonate and reducing the concentration of calcium ions competing for phosphate. Pseudo-sigmoidal fits are shown in Eq. 4.22 for $x_{\text{struvite}(\text{PO}_4^{3-})}$, Eq. 4.23 for the case of hydrox-

yapatite, and Eq. 4.24 for calcium carbonate, where x_{Alk} is referred to alkalinity (mg |CaCO₃).

$$x_{\text{struvite}(\text{PO}_4^{3-})} = \frac{0.695}{1 + (x_{\text{Alk}} \cdot 4.229 \cdot 10^{-4})^{-2.638}} \quad (4.22)$$

$$x_{\text{hydroxyapatite}(\text{Ca}^{2+})} = \frac{0.260}{1 + (x_{\text{Alk}} \cdot 6.460 \cdot 10^{-5})^{3.390}} \quad (4.23)$$

$$x_{\text{CaCO}_3(\text{Ca}^{2+})} = \frac{0.847}{1 + (x_{\text{Alk}} \cdot 4.646 \cdot 10^{-4})^{-1.870}} \quad (4.24)$$

4.3.1.4 Interactions between calcium and magnesium to phosphate ratios

Interactions between calcium and magnesium to phosphate ratios were evaluated to determine a target operational area for optimal struvite production performance. In Fig. 4.4 the formation of struvite as function of Mg²⁺/PO₄³⁻ and Ca²⁺/PO₄³⁻ molar ratios is shown, where the area with the highest phosphate recovery in form of struvite has been shaded. It can be observed that struvite formation depends strongly on the Ca²⁺/PO₄³⁻ molar ratio. For Ca²⁺/PO₄³⁻ values less than 3 struvite formation reaches the maximum values, even for low Mg²⁺/PO₄³⁻ molar ratio values. For high calcium/phosphate ratios, struvite formation decreases abruptly, obtaining low increases in struvite formation even for large supplies of magnesium.

4.3.2 Phosphorus releases from cattle leachate potentially avoided via struvite formation

Phosphorus pollution of waterbodies, followed by eutrophication and hypoxia scenarios, represents a major environmental problem for the current societies. Considering the United States, the Census of Agriculture reports more than 93 million of cattle heads (United States Department of Agriculture (USDA), 2019), generating an estimated amount of 1,144 million of tons of organic waste per year. The phosphorus contained in the organic waste can be lost as runoff, reaching waterbodies, and polluting the surrounding aquatic ecosystems. Actually, several outstanding cases of eutrophication have taken place in the U.S. in recent times, such as the events occurred in Lake Erie since 1990, and the dead zone in the Gulf of Mexico because of in-excess nutrients discharges collected along the

Mississippi River basin. Therefore, nutrient recovery strategies must be implemented to capture phosphorus (and nitrogen) before reaching the waterbodies. Additionally, phosphorus recovery as struvite allows its redistribution to nutrient deficient areas (Martín-Hernández et al., 2018). The surrogate models developed are used to estimate the potential phosphorus emissions avoided in each watershed through phosphorus recovery from cattle leachate as struvite.

4.3.2.1 Balance of phosphorus involved in agricultural activities throughout the U.S. watersheds

To reach environmental sustainability and reduce the impact over the original ecosystems as much as possible, the releases of phosphorus should be balanced with a coordinated network of phosphorus uptakes. To determine the balance between the releases and uptakes of phosphorus from the agricultural sector, the TES sustainability metric is computed for each watershed in the U.S., showing the watersheds where the phosphorus releases are unbalanced and impacting the environment, Fig. 4.5. For a total of 2,104 HUC8 watersheds, data is unavailable for 6 watersheds, the phosphorus releases and uptakes are balanced in 1,410 watersheds, and 691 exhibit unbalanced phosphorus releases, representing the 33.12% of total watersheds. It can be observed a larger concentration of unbalanced watersheds along the Mississippi River basin and around the Lake Erie, areas currently affected by eutrophication issues.

For studies requiring higher spatial resolution, more accurate values for the TES metric can be estimated through the use of local inventories for phosphorus releases and uptakes. A dataset with the phosphorus releases and uptakes, the phosphorus balance, and the TES metric computed for each watershed are available in the Supplementary Material. A dataset with the phosphorus releases and uptakes, the phosphorus balance, and the TES metric computed for each watershed are available in the Supplementary Material.

4.3.2.2 Phosphorus recovered from cattle leachate through struvite precipitation

Since the scope of the surrogate models developed is limited to the treatment of cattle leachate, only P releases from cattle organic waste will be considered for recovery. Additionally, as it is mentioned in the description of the model, only the phosphate fraction of phosphorus can be recovered through struvite precipitation. Data provided by IPNI NuGIS (International Plant Nutrition Institute (IPNI), 2012) report total manure generated, but do not report the breakdown of manure generated by

different livestock sources. Therefore, the inventory of cattle for each HUC6 watershed reported by the U.S. Census of Agriculture is used (United States Department of Agriculture (USDA), 2019). To keep spatial consistency between data, the inventory of cattle was aggregated from HUC6 to HUC8 watershed level scaling by the fraction of area represented by each HUC8 basin over the total HUC6 area. The breakdown of cattle types in the U.S. Census of Agriculture is not available at watershed level, but it is available at state level. Therefore, the number of cattle heads is weighted by the fraction of milk and beef animals in the corresponding state. Finally, the animals number for each type of cattle is calculated using the normalization values provided by Kellogg et al. (2010) (United States Department of Agriculture, 2000). If the watershed is shared among several states, the average of the represented states is considered.

Since the supply of magnesium is the easiest controllable variable in the struvite precipitation process, the scenarios evaluated to determine the phosphorus emissions avoided through struvite precipitation were defined through the use of different amounts of magnesium using the surrogate model shown in Eq. 4.16. The different supplies of magnesium have a direct influence on the economy of the process, being one of the highest operating costs items. A summary of the scenarios evaluated and the results obtained is presented in Table 4.5. The fraction of phosphorus releases avoided is computed over the total phosphorus releases from agricultural activities, including manure releases and fertilizer application, as described in Section 4.2.2.1.

Table 4.5: Scenarios considered and results for cattle leachate phosphorus recovery

Scenario	1	2	3	4
Mg ²⁺ /PO ₄ ³⁻ molar ratio	1	2	4	6
Total P releases avoided (total watersheds) (tons)	422,104	562,430	674,556	722,573
Average P releases avoided (total watersheds) (%)	22.63	30.16	36.17	38.75
Average P releases avoided (unbalanced watersheds) (%)	18.07	24.08	28.88	30.94
kg Mg/kg P recovered	2.68	4.02	6.71	9.40

The results for each scenario considered at watershed scale are shown in Fig. 6.6, where darker colors represent larger phosphorus releases avoided. It can be observed that struvite production can contribute to reducing phosphorus emissions around Lake Erie and the Great Lakes region, one of the most severely affected areas by eutrophication problems. Additionally, other areas where the phosphorus emissions avoided are especially significant are the upper basin of the Mississippi River, and the basins located in the south-central region of the United States, such as the areas of some tributaries rivers to the Mississippi River basin, the Rio Grande river and the Colorado River basin. At national level, struvite production can contribute to reduce the agricultural phosphorus releases by 22% for most conservative case where the lowest amount of magnesium is added. The phosphorus fraction recovered raises until a 30% and 36% when the amount of magnesium added is multiplied by 2 and by 4 respectively. However, for the scenario 4 the increase in the supply of magnesium only increases the phosphorus recovered in 2 percentual points compared with the previous scenario. Therefore, the implementation of struvite production processes for phosphorus recovering in cattle facilities can contribute significantly to the reduction in the phosphorus emissions from agricultural operations, reducing the runoffs to waterbodies and mitigating the nutrient pollution of the aquatic ecosystems. However, when only unbalance watersheds are considered, the average fraction of phosphorus releases avoided decreases, suggesting that, from a global overview, the phosphorus releases due to fertilizers play a major role in these watersheds than when balance and unbalance watersheds are evaluated altogether. Data at watershed level are collected in the Supplementary Material.

Therefore, the phosphorus recovered from livestock facilities have a significant impact in the reduction of phosphorus releases to the environment. However, to achieve a successful implementation of nutrient management strategies, coordinated network management efforts to mitigate nutrient pollution of aquatic systems including point and non-point sources, should be performed for optimizing nutrient management programs that minimize the capital and operating costs while maximizing the environmental benefits. Proposals for the development of coordinated management systems for organic wastes have been presented by Sharara et al. (2017), Sampat et al. (2019), and Hu et al. (2019).

4.4 CONCLUSIONS

To estimate the potential phosphorus releases avoided through struvite precipitation from cattle waste, a thermodynamic framework has been

developed to evaluate struvite production from cattle organic waste as a technology for nutrient management and recovery. A set of practical numerical correlations is developed to help predict the struvite recovery. Cattle waste treatment and nutrient recovery through struvite formation is a feasible process from a thermodynamic perspective, reaching phosphate recovery efficiencies up to 80% with the addition of considerable amounts of magnesium. Additionally, the results show that alkaline conditions can control the calcium ions when their presence in the medium is high and these can interfere in the formation of struvite by precipitating the calcium ions as calcium carbonate, and enhancing the recovery of phosphate as struvite. However, the variability in the organic waste composition is an important parameter that has a high impact on the efficiency of the process. Therefore, an individual composition analysis of the treated cattle waste should be the ideal procedure to achieve the optimal performance of the process by adjusting the operating conditions, particularly the amount of magnesium added and the alkalinity of the medium. Nevertheless, there are opportunities for improving the proposed model by the experimental determination of pK_{sp} values for all potential precipitates from cattle leachate, and by including the effects from kinetics and transport phenomena.

The techno-ecological synergy sustainability metric (TES) is a useful tool for visualizing the spatial distribution of environmental problems, making it possible to determine what areas are more sensible to nutrient pollution, and allowing an adequate distribution of efforts to mitigate phosphorus releases and achieved better nutrient management practices. In the U.S., struvite production has large potential for reducing the phosphorus losses from livestock facilities, avoiding between the 22% and the 36% of the phosphorus releases from the agricultural sector at national level, reducing the phosphorus runoff and mitigating the nutrient pollution of waterbodies. In addition, it can be observed how struvite production can significantly contribute to reducing phosphorus emissions around Lake Erie and the Great Lakes region, some of the most severely affected areas by eutrophication problems. It should be remarked that the production of struvite from cattle leachate allows the redistribution of phosphorus to nutrient deficient areas reducing the phosphorus runoff to waterbodies and mitigating the nutrient pollution of aquatic ecosystems. However, future research is needed to consider temporal aspects, transportation logistics, and coordinated management strategies for achieving global solutions to global problems.

NOMENCLATURE

Variables

A	parameter of the Debye-Hückel relationship
EC	electrical conductivity ($\frac{\mu S}{cm}$)
E_x	emissions of component x
I	ionic strength (M)
K	thermodynamic equilibrium constant
K_{sp}	solubility product
M	equal to e^μ
T	temperature (K)
U_x	uptakes of component x
V_x	techno-ecological synergy sustainability metric for component x
Ω	supersaturation ratio
γ	displacement parameter
γ_x	activity coefficient for element x
μ	mean of the distribution
σ	standard deviation
σ^2	variance
m	stoichiometric coefficient
n	stoichiometric coefficient
x_{Alk}	alkalinity (mg $CaCO_3$)
x_{CaCO_3}	fraction of calcium recovered as calcium carbonate
$x_{Ca^{2+}:PO_4^{3-}}$	Ca^{2+}/PO_4^{3-} molar ratio
$x_{Mg^{2+}:PO_4^{3-}}$	Mg^{2+}/PO_4^{3-} molar ratio
$x_{hydroxyapatite(Ca^{2+})}$	fraction of calcium recovered as hydroxyapatite
$x_{struvite(PO_4^{3-})}$	fraction of phosphorus as phosphate recovered as struvite
z_x	integer charge of ion x

Abbreviations

AAPFCO	Association of American Plant Food Control Officials
CAFO	Concentrated Animal Feeding Operation
HAB	Harmful Algal Bloom
HUC	Hydrologic Unit Code
KDE	Kernel Density Estimation

USDA United States Department of Agriculture

ACKNOWLEDGMENTS

We acknowledge funding from the Junta de Castilla y León, Spain, under grant SA026G18 and grant EDU/556/2019, and by an appointment for E. Martín-Hernández to the Research Participation Program for the Office of Research and Development, U.S. EPA, administered by the Oak Ridge Institute for Science and Education.

Disclaimer: The views expressed in this article are those of the authors and do not necessarily reflect the views or policies of the U.S. EPA. Mention of trade names, products, or services does not convey, and should not be interpreted as conveying, official U.S. EPA approval, endorsement, or recommendation.

BIBLIOGRAPHY

- Alexander, R. B., Smith, R. A., Schwarz, G. E., Boyer, E. W., Nolan, J. V., & Brakebill, J. W. (2008). Differences in Phosphorus and Nitrogen Delivery to The Gulf of Mexico from the Mississippi River Basin. *Environmental Science & Technology*, 42(3), 822–830. <https://doi.org/10.1021/es0716103>
- Bakshi, B., Ziv, G., & Lepech, M. (2015). Techno-ecological synergy: A framework for sustainable engineering. *Environ. Sci. Technol.*, 49(3), 1752–1760.
- Bates, R. G., & Pinching, G. (1949). Acid dissociation constant of ammonium ion at 0–50 °C, and the base strength of ammonia. *Journal of Research of the National Bureau of Standards*, 42, 419–430.
- Battistoni, P., De Angelis, A., Pavan, P., Prisciandaro, M., & Cecchi, F. (2001). Phosphorus removal from a real anaerobic supernatant by struvite crystallization. *Wat. Res.*, 35, 2167–2178.
- Beaulieu, J., DelSontro, T., & Downing, J. (2019). Eutrophication will increase methane emissions from lakes and impoundments during the 21st century. *Nat. Commun.*, 10, 1375.
- Bezanson, J., Edelman, A., Karpinski, S., & Shah, V. B. (2017). Julia: A fresh approach to numerical computing. *SIAM review*, 59(1), 65–98.
- Brezonik, P., & Arnold, W. (2011). *Water Chemistry An Introduction to the Chemistry of Natural and Engineered Aquatic Systems*. Oxford University Press.
- Celen, I., Buchanan, J. R., Burns, R. T., Robinson, R. B., & Raman, D. R. (2007). Using a chemical equilibrium model to predict amendments

- required to precipitate phosphorus as struvite in liquid swine manure. *Water Research*, 41(8), 1689–1696.
- Cordell, D., Drangert, J.-O., & White, S. (2009). The story of phosphorus: Global food security and food for thought. *Glob. Environ. Change.*, 19(2), 292–305.
- Dunning, I., Huchette, J., & Lubin, M. (2017). JuMP: A Modeling Language for Mathematical Optimization. *SIAM Review*, 59(2), 295–320. <https://doi.org/10.1137/15M1020575>
- Dzombak, D. (2011). Nutrient Control in Large-Scale U.S. Watershed. The Chesapeake Bay and Northern Gulf of Mexico). *The Bridge*, 41(4), 13–22.
- Fowler, B., & Kuroda, S. (1986). Changes in heated and in laser-irradiated human tooth enamel and their probable effects on solubility. *Calcif. Tissue. Int.*, 38, 197–208.
- Gadekar, S., & Pullammanappallil, P. (2010). Validation and applications of a chemical equilibrium model for struvite precipitation. *Environmental modeling & assessment*, 15(3), 201–209.
- Gregory, T., Moreno, E., & Brown, W. (1970). Solubility of $\text{CaHPO}_4 \cdot 2\text{H}_2\text{O}$ in the system $\text{Ca}(\text{OH})_2 - \text{H}_3\text{PO}_4 - \text{H}_2\text{O}$ at 5, 15, 25 and 37.5 °C. *J. Res. Natl. Bur. Stand.*, 74, 461–475.
- Harada, H., Shimizu, Y., Miyagoshi, Y., Matsui, S., Matsuda, T., & Nagasaka, T. (2006). Predicting struvite formation for phosphorus recovery from human urine using an equilibrium model. *Water Science and Technology*, 54(8), 247–255.
- Hu, Y., Sampat, A. M., Ruiz-Mercado, G. J., & Zavala, V. M. (2019). Logistics Network Management of Livestock Waste for Spatiotemporal Control of Nutrient Pollution in Water Bodies. *ACS Sustainable Chem. Eng.*, 7(22), 18359–18374. <https://doi.org/10.1021/acssuschemeng.9b03920>
- Hunter, J. D. (2007). Matplotlib: A 2D Graphics Environment. *Comput Sci Eng*, 9, 90–95.
- Hunter, J. D. (2010). Data Structures for Statistical Computing in Python. *Proceedings of the 9th Python in Science Conference*, 51–56.
- International Plant Nutrition Institute (IPNI). (2012). *A Nutrient Use Information System (NuGIS) for the U.S.* (tech. rep.). International Plant Nutrition Institute (IPNI).
- Kadlec, R. (2016). Large Constructed Wetlands for Phosphorus Control: A Review. *Water*, 8, 243.
- Mangin, D., & Klein, J. (2004). Fluid dynamic concepts for a phosphate precipitation reactor design. In *Phosphorus in environmental technologies: Principles and applications* (pp. 358–401). IWA Publishing London, UK.

- Martín-Hernández, E., Sampat, A., Zavala, V., & Martín, M. (2018). Optimal integrated facility for waste processing. *Chem. Eng. Res. Des.*, *131*, 160–182.
- Matynia, A., Wierzbowska, B., Hutnik, N., Mazienczuk, A., Kozik, A., & Piotrowski, K. (2013). Separation of struvite from mineral fertilizer industry wastewater. *Procedia Environ. Sci.*, *18*, 766–775.
- Metcalf, & Eddy. (2014). *Wastewater Engineering: Treatment and Resource Recovery*. McGraw-Hill, New York.
- Morse, J. W., Arvidson, R. S., & Lütge, A. (2007). Calcium Carbonate Formation and Dissolution. *Chem. Rev.*, *107*, 342–381.
- Muhammad, A., Lu, J., Dong, R., & Wu, S. (2019). Formation of struvite from agricultural wastewaters and its reuse on farmlands: Status and hindrances to closing the nutrient loop. *Journal of environmental management*, *230*, 1–13.
- Ohio State University Extension. (2005). *Ohio Agronomy Guide, 14th Edition* (tech. rep.). Ohio State University Extension.
- Ohio State University Extension. (2017). *Ohio Agronomy Guide, 15th Edition* (tech. rep.). Ohio State University Extension.
- Ohlinger, K. N., Young, T., & Schroeder, E. (1998). Predicting struvite formation in digestion. *Wat. Res.*, *32*(12), 3607–3614.
- Pickard, B. R., Daniel, J., Mehaffey, M., Jackson, L. E., & Neale, A. (2015). EnviroAtlas: A new geospatial tool to foster ecosystem services science and resource management. *Ecosyst. Serv.*, *14*, 45–55.
- Rahaman, M. S., Mavinic, D. S., Meikleham, A., & Ellis, N. (2014). Modeling phosphorus removal and recovery from anaerobic digester supernatant through struvite crystallization in a fluidized bed reactor. *Water Research*, *51*, 1–10.
- Richards, I. R., & Johnston, A. E. (2001). *The effectiveness of different precipitated phosphates as sources of phosphorus for plants* (tech. rep.). CEEP, European Fertiliser Manufacturers Association, Anglian Water UK, Thames Water UK and Berlin Wasser Betriebe.
- Ronteltap, M., Maurer, M., & Gujer, W. (2007). Struvite precipitation thermodynamics in source-separated urine. *Water Research*, *41*(5), 977–984.
- Ruttenberg, K. (2001). Phosphorus Cycle*. In J. H. Steele (Ed.), *Encyclopedia of Ocean Sciences (Second Edition)* (Second Edition, pp. 401–412). Oxford, Academic Press.
- Sampat, A., Hu, Y., Sharara, M., Aguirre-Villegas, H., Ruiz-Mercado, G., Larson, R., & Zavala, V. M. (2019). Coordinated management of organic waste and derived products. *Comput. Chem. Eng.*, *128*, 352–363.

- Sampat, A., Martín, E., Martín, M., & Zavala, V. (2017). Optimization formulations for multi-product supply chain networks. *Comput. Chem. Eng.*, 104, 296–310.
- Sampat, A., Ruiz-Mercado, G. J., & Zavala, V. (2018). Economic and Environmental Analysis for Advancing Sustainable Management of Livestock Waste: A Wisconsin Case Study. *ACS Sustain. Chem. Eng.*, 6(5), 6018–6031.
- Sharara, M., Sampat, A., Good, L. W., Smith, A. S., Porter, P., Zavala, V. M., Larson, R., & Runge, T. (2017). Spatially explicit methodology for coordinated manure management in shared watersheds. *J. Environ. Manage.*, 192, 48–56.
- Shashvatt, U., Benoit, J., Aris, H., & Blaney, L. (2018). CO₂-assisted phosphorus extraction from poultry litter and selective recovery of struvite and potassium struvite. *Wat. Res.*, 143, 19–27.
- Skoog, D., West, D., Holler, F., & Crouch, S. (2014). *Fundamentals of analytical chemistry*. Cengage Learning.
- Smith, R. A., & Alexander, R. B. (1999). *Sources of Nutrients in the Nation's Watersheds* (tech. rep.). U. S. Geological Survey.
- Tao, W., Fattah, K., & Huchzermeier, M. (2016). Struvite recovery from anaerobically digested dairy manure: A review of application potential and hindrances. *J. Environ. Manage.*, 169, 46–57.
- Taylor, A., Frazier, A., & Gurneynium, E. (1963). Solubility products of magnesium ammonium and magnesium potassium phosphates. *Trans. Faraday Soc.*, 59, 1580–1584.
- Thomopoulos, P. (2012). *Essentials of Monte Carlo Simulation*. Springer, New York.
- United States Department of Agriculture. (2000). *Manure Nutrients Relative to the Capacity of Cropland and Pastureland to Assimilate Nutrients* (tech. rep.). United States Department of Agriculture.
- United States Department of Agriculture (USDA). (2009). *Waste Management Field Handbook* (tech. rep.).
- United States Department of Agriculture (USDA). (2019). *2017 Census of Agriculture. United Satates. Summary and State Data* (tech. rep.).
- United States Department of Agriculture (USDA), National Agricultural Statistics Service. (2020). *Cattle (January 2020)* (tech. rep.).
- U.S. Geological Survey. (2013). *Federal Standards and Procedures for the National Watershaed Boundary Dataset (WBD)* (tech. rep.). U.S. Geological Survey.
- van der Walt, S., Colbert, S., & Varoquaux, G. (2011). The NumPy Array: A Structure for Efficient Numerical Computation. *Comput Sci Eng*, 13, 22–30.

- van Rossum, G. (1995). *Python tutorial* (tech. rep. CS-R9526). Centrum voor Wiskunde en Informatica (CWI). Amsterdam.
- Yan, H., & Shih, K. (2016). Effects of calcium and ferric ions on struvite precipitation: A new assessment based on quantitative X-ray diffraction analysis. *Wat. Res.*, 95, 310–318.
- Zeng, L., & Li, X. (2006). Nutrient removal from anaerobically digested cattle manure by struvite precipitation. *J. Environ. Eng. Sci.*, 5, 285–294.

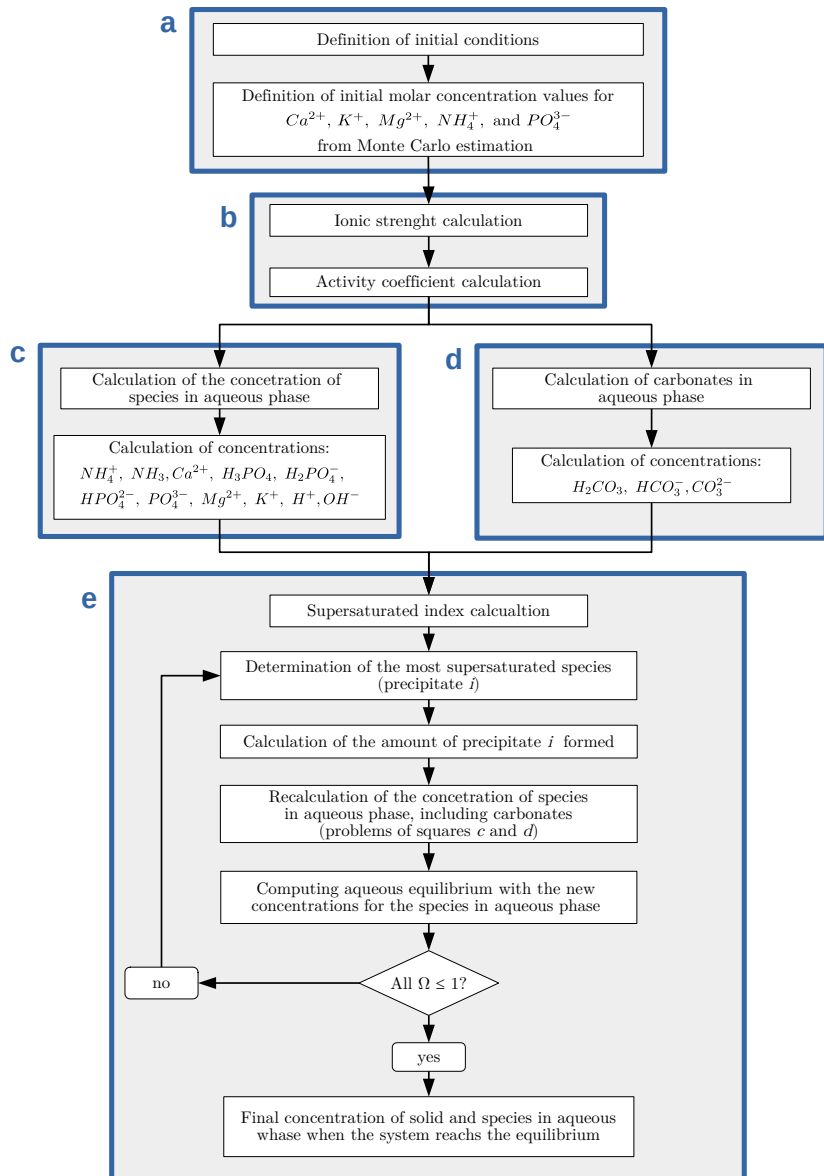


Figure 4.1: Flowchart of the proposed algorithm to solve the thermodynamic model for the formation of precipitates in cattle organic waste.

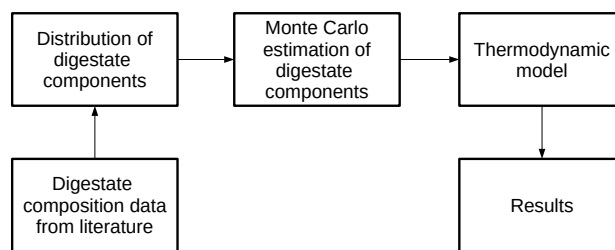


Figure 4.2: A solution procedure to evaluate the influence of the cattle waste composition variability in the formation of struvite.

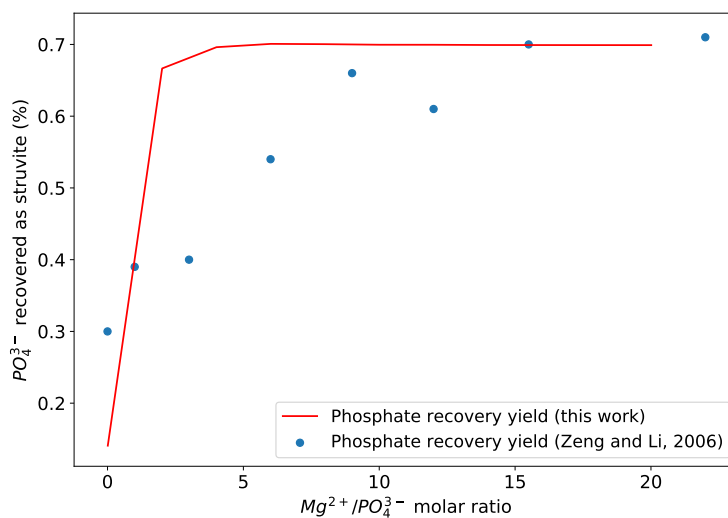


Figure 4.3: Comparison between experimental results reported by Zeng and Li (2006) and the results provided by the model developed in this work.

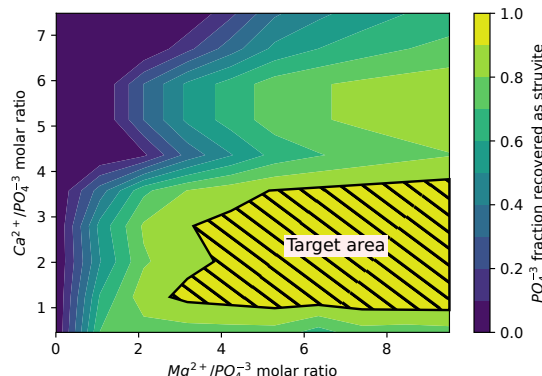


Figure 4.4: Influence of magnesium and calcium in struvite precipitation.

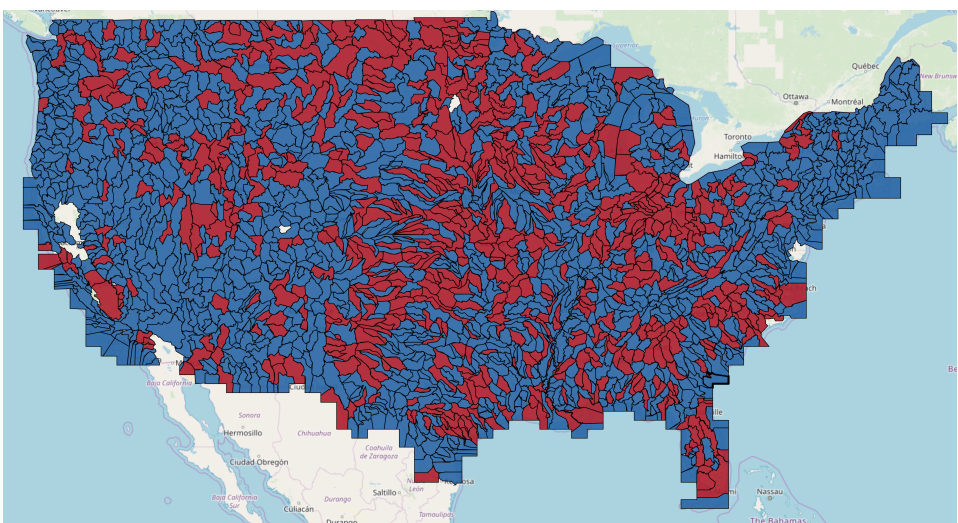
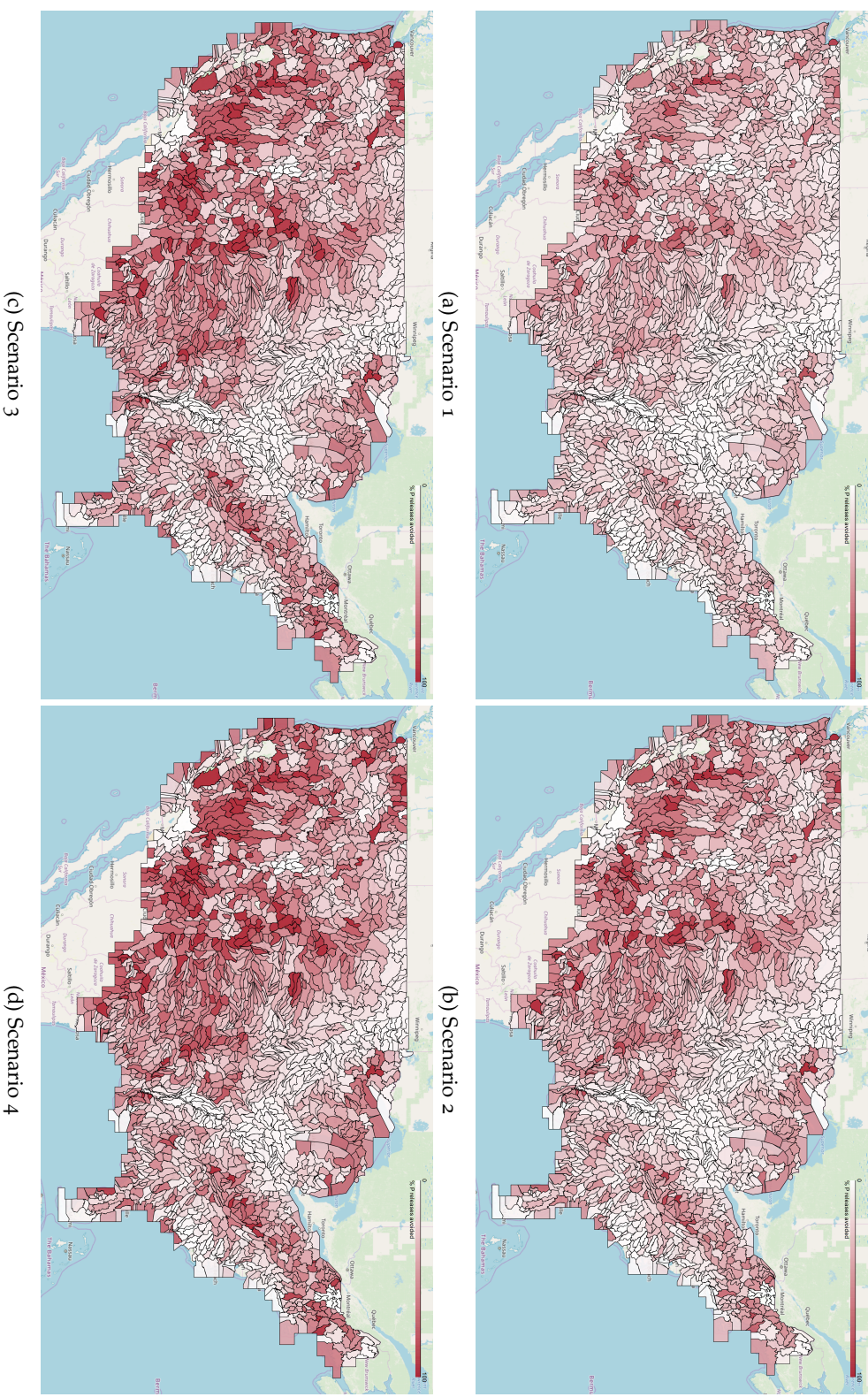


Figure 4.5: Techno-ecological synergy (TES) metric values for HUC8 watersheds. Red indicates watersheds with unbalanced agricultural phosphorus releases, and blue indicates watersheds with balanced agricultural phosphorus releases. White indicates watersheds with not available data.

Figure 4.6: Phosphorus releases avoided through struvite production for the different scenarios considered. Darker colors represent larger phosphorus recovery



GEOSPATIAL ENVIRONMENTAL AND TECHNO-ECONOMIC FRAMEWORK FOR SUSTAINABLE PHOSPHORUS MANAGEMENT AT LIVESTOCK FACILITIES

5.1 INTRODUCTION

Phosphorus is a source of concern for modern societies. On the one hand, nutrient pollution of waterbodies is one of the major water quality problems worldwide, resulting in environmental issues as a consequence of the eutrophication of waterbodies, and the occurrence of cyanobacteria and harmful algal blooms (HABs). Surveys reveal that eutrophication is a global problem, reporting that 54% of lakes in Asia, 53% in Europe, 48% in North America, 41% in South America, and 28% in Africa are eutrophic (Ansari, 2010). In addition to eutrophication, hypoxia of aquatic ecosystems is associated with the aerobic degradation of the algal biomass by bacteria, shifting the distribution of aquatic species and releasing toxins in drinking water sources (A. M. Sampat et al., 2018). Although eutrophication is affected by several factors, such as temperature and the self-purification capacity of waterbodies, the primary limiting factor for eutrophication is often the phosphate concentration (Werner, 2009). Aside from disturbing aquatic ecosystems, eutrophication also contributes to climate change, emitting large amounts of strong greenhouse gases as a consequence of the biomass degradation, such as CH₄ and N₂O (Beaulieu et al., 2019). On the other hand, phosphorus is an essential nutrient for living organisms, and a key element for maintaining agricultural productivity. However, phosphorus is a resource very sensitive to depletion, since extractable deposits of phosphorus rock are limited and there is no known substitute or synthetic replacement. Projections estimate limited availability of phosphate over the next century (Cordell et al., 2009). Therefore, in addition to the environmental perspective, the search for phosphorus recycling processes is a major driving force for the development of nutrient recovery systems (Reijnders, 2014).

Agricultural activities are one of the main contributors to human-based phosphorus releases (Dzombak, 2011), including non-point source releases by over-use of fertilizers in croplands, point source releases originated from the disposal of livestock waste, and nutrient legacy that have accumulated in watersheds due to historical phosphorus releases. Focusing on the

point source releases generated by the cattle industry, these result from the production of large amounts of livestock organic waste, containing substantial amounts of phosphate and ammonia. A. Sampat et al. (2017) presented the link between the presence of livestock facilities and higher concentrations of phosphorus in soil, resulting in increased nutrient runoff to waterbodies. While for animals on pasture, organic waste should not be a source of concern if stocking rates are not excessive, for concentrated animal feeding operations (CAFOs) manure should be properly managed due to the high rates and spatial concentration of the organic waste generated. A common practice to recycle the nutrients contained in the organic waste is the land application of the manure. However, since the high-water content of manure makes its transportation to nutrient deficient locations difficult and expensive, it is usually spread in the surroundings of the CAFOs, leading to surplus of nutrients in soils and phosphorus runoff to waterbodies (United States Department of Agriculture, 2009).

The implementation of nutrient recovery technologies at livestock facilities to recover phosphorus from cattle manure is a promising approach to recycle and leverage nutrients more efficiently, mitigating the nutrient pollution of waterbodies (B. Li et al., 2021). However, the technologies that can be implemented at CAFOs differ widely in aspects such as phosphorus recovery performance, final products obtained, capital expenses, and operational costs. Additionally, different levels of environmental vulnerability to eutrophication may require the use of different P recovery processes, searching for the most effective balance between P recovery efficiency and cost. Previous efforts for the technical evaluation of different phosphorus recovery technology have been performed, resulting in processes with proven technical feasibility for phosphorus recovery. Particularly, there exists a considerable body of literature on the production of struvite (Muhmood et al., 2019). Other mature processes for the recovery of phosphorus are the formation of calcium precipitates (Berg et al., 2006), and systems based on physical separations (Church et al., 2016). Additionally, novel processes are currently under development, such as membrane separation processes (X. Li et al., 2020), microalgae-based processes (Robles et al., 2020), adsorption using biochar (Wang et al., 2020), and electrochemical processes (Belarbi et al., 2020). Moreover, a decision-making framework has been developed for the selection and implementation of phosphorus recovery systems in urban areas (Pearce, 2015). However, to the best of the authors knowledge, there are no specific frameworks to study the implementation of phosphorus recovery systems at livestock facilities considering GIS environmental and techno-economic dimensions.

In this work, we propose a novel framework, COW2NUTRIENT (Cattle Organic Waste to NUTRIent and ENergy Technologies), for the assess-

ment and selection of phosphorus recovery technologies at CAFOs based on environmental and techno-economic criteria. This framework combines eutrophication risk data at subbasin level and the techno-economic assessment of six state-of-the-art phosphorus recovery processes in a multi-criteria decision analysis (MCDA) model. This information is normalized and aggregated for the selection of the most suitable technology for each analyzed CAFO. The goal is to develop a flexible framework able to balance the operating cost of the systems and P recovery efficiency as a function of the environmental vulnerability to eutrophication of each region. The minimization of operating costs is prioritized in regions with low eutrophication risk, while the efficiency of P recovery is the most relevant criteria in regions affected by nutrient pollution. Also, COW2NUTRIENT aims to provide a useful framework for designing and evaluating effective GIS-based incentives and regulatory policies to control and mitigate nutrient pollution of waterbodies. The practicability of the proposed framework is assessed by studying and designing the implementation of P recovery systems at 2,217 current livestock facilities in the Great Lakes area.

5.2 METHODS

COW2NUTRIENT framework is comprised by three models, i.e. environmental geographic information, techno-economic, and multi-criteria decision analysis models, in order to integrate the geographic data on vulnerability to nutrient pollution, and the technical and economic information of the nutrient recovery systems through an MCDA model, as shown in Figure 6.1. First, the geographic location of the individual facilities (longitude and latitude) is supplied to the environmental GIS model to determine the vulnerability level to nutrient pollution of the region where the studied CAFOs are located. Secondly, data regarding the number and type of animals at the facility (i.e., beef and dairy cattle, adult animals, heifers, and calves) are entered into the techno-economic model to capture the characteristics of the livestock facility evaluated. Data reported by the US Department of Agriculture were considered for manure generation ratios (Kellogg et al., 2000) and composition (United States Department of Agriculture, 2009). These values are collected in Table 3S of the Supplementary Material. In addition, economic data are fed into the techno-economic model for economic performance evaluation purposes, including the value of incentives received for phosphorus recovery (in the form of P credits), and for the generation of bio-based methane or electricity (in form of Renewable Energy Certificate (REC) and Renewable Identification Number (RIN) respectively). The output data from the techno-economic and

environmental geographic information models are imported in the MCDA model. In this module, the data is normalized and aggregated, returning a composite index for each technology. This composite index is used to score and rank the nutrient recovery systems based on their performance. All models have been developed using Python (van Rossum, 1995).

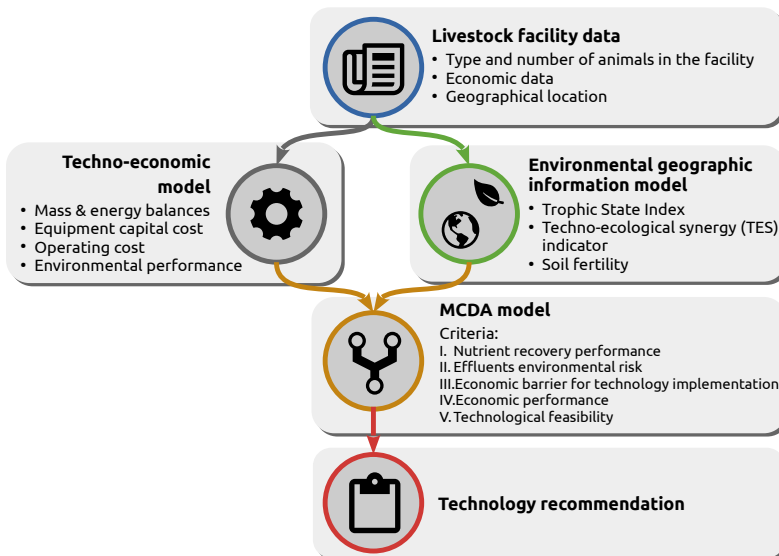


Figure 5.1: Structure of the COW2NUTRIENT decision support framework for the assessment and selection of phosphorus recovery systems.

5.2.1 Environmental geographic information model

The environmental vulnerability to nutrient pollution of the area where the livestock facilities are located determines the preference (i.e., ranks the importance) of each criterion. Three indicators are used to evaluate the eutrophication risk of each region studied at subbasin spatial resolution. The trophic state of waterbodies is evaluated through the Trophic State Index (Carlson, 1977), determining their eutrophication level. The phosphorus saturation of soils, which can result in the transport of phosphorus to waterbodies by run-off, is evaluated through Mehlich 3 phosphorus concentration (Espinoza et al., 2006). Finally, the balance between phosphorus releases and uptakes from anthropogenic activities is assessed through the techno-ecological synergy metric (Bakshi et al., 2015), determining if there is a net accumulation or depletion of phosphorus in a region over time. The use of these three indicators makes it possible to determine if there exist an immediate risk of eutrophication in the region studied (eutrophized waterbodies), a long-term risk (moderate value of TSI, soils saturated by

phosphorus, or phosphorus releases and uptakes from anthropogenic activities unbalanced), or if there is no risk of eutrophication (phosphorus uptakes and releases are balanced). Detailed descriptions of the performed data analysis, and maps for the contiguous US are provided in Section 1 of the Supplementary Material.

5.2.1.1 *Spatial resolution*

A watershed is defined as the region draining all the streams and rainfall to a common waterbody, defining the geographic limits for the collection of runoff elements. US watersheds are designated by the US Geological Survey through the Hydrologic Unit Code (HUC) system. The HUC system divides the US into regions, subregions, basins, subbasins, watersheds, and subwatersheds. Each hydrologic unit of these six levels is identified hierarchically by a unique numeric code from 2 to 12 digits (i.e., HUC₂ to HUC₁₂). The spatial resolution of this study is the contiguous United States at the subbasin level, defined by the HUC system at 8 digits (HUC8) (U.S. Geological Survey, 2013).

5.2.1.2 *Trophic State Index*

The Trophic State Index (TSI) is a metric proposed by Carlson (1977) to determine the trophic status of waterbodies (U.S. Environmental Protection Agency, 2012a). The TSI of a waterbody is scored in a range from 0 to 100 representing its trophic state, as shown in Table 5.1. Oligotrophic and mesotrophic states denote low and intermediate biomass productivities, while eutrophic and hypereutrophic states are referred to waterbodies with high biological productivity and frequent algal blooms. Combined data for chl- α and total phosphorus concentrations retrieved from the National Lakes Assessments conducted by the US EPA in 2007 and 2012 (U.S. Environmental Protection Agency, 2007, 2012b) is used to determine the Trophic State Index of lentic waters in the contiguous US. No TSI values were assigned to the watersheds without reported data. Correlations to estimate the TSI from chlorophyll- α and total phosphorus concentrations are collected in Section 1 of Supplementary Material.

Table 5.1: Relation between TSI value and trophic class.

TSI	<40	40-50	50-70	>70
Trophic Class	Oligotrophic	Mesotrophic	Eutrophic	Hypereutrophic

5.2.1.3 *Techno-ecological synergy sustainability metric*

The techno-ecological synergy sustainability metric (TES) is an indicator proposed by Bakshi et al. (2015) to evaluate the fraction of net anthropogenic phosphorus releases, Eq. 5.1.

$$V_x = \frac{(U_x - E_x)}{E_x} \quad (5.1)$$

A negative value for TES indicator (V_x) indicates that the releases (E_x) are larger than the uptake capacity of the evaluated system, (U_x), and thus impacting in the ecosystems; while positive values reflects that the releases can be absorbed by the system without any harm.

Phosphorus releases from agricultural activities have been estimated from data reported by the Nutrient Use Geographic Information System project. Since this work is limited to the assessment of agricultural phosphorus releases, other possible sources of phosphorus releases are not considered. Further information about the methodology used for the estimation of human-based phosphorus releases can be found in International Plant Nutrition Institute (IPNI) (2012). Anthropogenic phosphorus uptakes are those due to the crops grown in each watershed, including corn, soybeans, small grains, cotton, rice, vegetables, orchards, greenhouse and other crops (i.e., fruits, sugar crops, and oil crops). The estimation of the phosphorus uptakes is performed considering the different phosphorus requirements and yield rates of each crop, as well as the land cover and the crops distribution in each watershed. Data retrieved from United States Department of Agriculture (2019), United States Department of Agriculture (2009), and Pickard et al. (2015) is used for this purpose.

5.2.1.4 *Phosphorus saturation of soils*

Phosphorus concentration in soil is used for the evaluation of the phosphorus legacy that is continuously built up in soils, providing a metric of soil quality. However, only a fraction of phosphorus is available for plants. To measure this phosphorus fraction available for plants, several standardized phosphorus soil tests have been proposed, including Olsen, Bray 1, and Mehlich 3 tests. Among them, Mehlich 3 (M3P) has been selected as a measure of the concentration of P in soils since it is a widely used metric, and it is the P soil test least affected by changes in soil pH. To estimate the fraction of phosphorus available for plants from total phosphorus concentration data, a correlation developed by Allen and Mallarino (2006) has been used, Eq. 5.2. It must be noted that this correlation has been developed for agricultural soils in Iowa, but due to the lack of studies

in this topic, it has been used for soils throughout the contiguous US. Therefore, it must be considered as an exploratory effort to determine the phosphorus saturation in the US soils. Data reported by Smith et al. (2013) is used to evaluate the concentration of total phosphorus along the contiguous US.

$$M_3P (\% \text{ over TP}) = \frac{4.698 \cdot 10^{-1}}{1 + (\text{TotalP (mg/kg)} \cdot 1.336 \cdot 10^{-3})^{-2.148}} \quad (5.2)$$

The relationship between M₃P test value and the quality of soil is shown in Table 5.2. Soil fertility levels below optimum indicate that nutrient supplementation is needed to enhance the yield of crops, optimum values indicates that no nutrient supplementation is needed, and excessive soil fertility level indicate over-saturation of phosphorus in soil that can reach waterbodies by runoff (Espinoza et al., 2006).

Table 5.2: Relationship between Mehlich 3 phosphorus and soil fertility level (Espinoza et al., 2006).

Soil Fertility Level	M ₃ P soil phosphorus concentration (ppm)
Very Low	<16
Low	16-25
Medium	26-35
Optimum	36-50
Excessive	>50

5.2.2 Techno-economic model

COW2NUTRIENT framework evaluates all the stages involved in the processing of manure for P recovery, from organic waste collection to the recovery of nutrients and other by-products such as electricity or biomethane, as represented in Fig 5.2. In addition to the assessment of nutrient recovery systems, the framework is flexible to include anaerobic digestion, and the subsequent biogas valorization, for the production of methane or electricity. The techno-economic model is based on mass balances, thermodynamics, and chemical equilibria for each possible stage of the manure treatment process, i.e. manure conditioning, anaerobic digestion, biogas purification, biogas valorization, and phosphorus recovery. Preliminary design and sizing of equipment is performed to estimate the capital and operating

expenses when no specific costs data are available. A detailed description of equipment design and sizing, as well as the correlations used for costs estimation, can be found in Section 2 of the Supplementary Material.

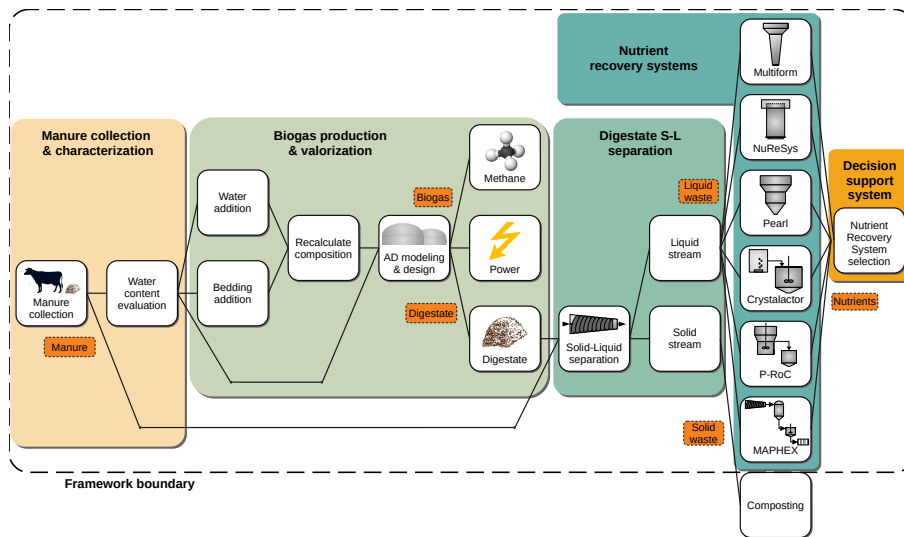


Figure 5.2: Process flowsheet for manure management and phosphorus recovery stages included in COW2NUTRIENT.

5.2.2.1 Manure conditioning

It is considered that the collection of manure does not involve any cost, since CAFOs have manure collection systems already installed. All manure produced is assumed to be collected. If the anaerobic digestion (AD) stage is implemented, a preconditioning stage is considered to adjust the water content of the waste. US EPA determines that the content of total solids in manure should be less than 15% (U.S. Environmental Protection Agency, 2004), as shown in Figure 6S of the Supplementary Material. Therefore, additional water may be added to reduce the solids content in manure before the AD stage.

5.2.2.2 Anaerobic digestion

Anaerobic digestion is a microbiological process that breaks down organic matter in the absence of oxygen. It involves four stages, hydrolysis, acidogenesis, acetogenesis, and methanogenesis; producing a mixture of gases mainly composed of methane and carbon dioxide (biogas), and a decomposed organic substrate (digestate). The model of the anaerobic digester is formulated through the mass balances of the species involved

in the production of biogas and digestate. A detailed description of the digester modeling can be found in León and Martín (2016). As a result of the AD process, a fraction of organic phosphorus and nitrogen are transformed in their inorganic forms. To evaluate the amount of organic nutrients transformed into inorganic phosphorus and nitrogen, data available in literature was considered, resulting in an increase of 24% and 16% over the original inorganic ammonia and phosphate respectively, as shown in Table 5S of the Supplementary Material. Correlations to estimate the capital cost and operating and management costs (O&M) as a function of the animal population of CAFOs were developed using data from the US EPA AgSTAR program (U.S. Environmental Protection Agency, 2003) and the USDA (Beddoes et al., 2007) respectively. We refer the reader to the Supplementary Material for further information.

5.2.2.3 Biogas purification

Before transforming biogas into marketable products, a purification stage has to be carried out to remove H_2S , H_2O , and NH_3 . The removal of H_2S is performed in a bed of ferric oxide through the production of Fe_2S_3 operating at a temperature range of 25–50°C. The bed regeneration is carried out using oxygen to produce elemental sulfur and ferric oxide (Fe_2O_3). Water and ammonia are adsorbed using a pressure swing adsorption system (PSA) with zeolite 5A as adsorbent material, operating at low temperature (25°C) and moderate pressure (4.5 bar). The assumed recovery for NH_3 and H_2O is 100%. For further details about the modeling of the biogas purification stage, we refer the reader to previous works (León & Martín, 2016; Martín-Hernández et al., 2018).

5.2.2.4 Biogas valorization

Two final added value products have been considered, methane and electricity, since they can be obtained through relatively simple processes and there exists developed markets for them.

METHANE PRODUCTION The process considered for methane production is the removal of CO_2 using a PSA system with a bed of zeolite 5A, since this process was demonstrated as the optimal biogas upgrading process by Martín-Hernández, Guerras, et al. (2020), where further details about the modeling of the PSA system can be found.

ELECTRICITY PRODUCTION Electricity is produced from biogas through a gas turbine. A Brayton cycle consisting of double-stage compression

system, one for the air stream and one for the biogas stream, is considered. Polytropic compression is assumed, with a polytropic index of 1.4 and an efficiency of 85% (Moran et al., 2010). The adiabatic combustion of methane contained in the biogas is assumed, with a pre-heating of the biogas-air mixture, considering the combustion chamber as an adiabatic furnace. An air excess of 20% with respect to the stoichiometric needs, and 100% conversion of the reaction are assumed. Further details for electricity production can be found in Martín-Hernández et al. (2018).

5.2.2.5 Solid-liquid separation

Nutrients contained in organic waste (manure or digestate, depending on whether AD is carried out or not) are present in both organic and inorganic forms. Organic nutrients are chemically bonded to carbon, and they have to be converted into their inorganic forms through a mineralization process to be available for the vegetation to grow. Organic nutrients are mainly contained in the solid phase of organic waste. Inorganic nutrients are water soluble, and they are mostly present in the liquid phase, or bounded to soluble minerals. They are immediately available to plants, including algae involved during the occurrence of HABs. To recover the inorganic fraction of nutrients, a solid-liquid separation stage is implemented, keeping the inorganic nutrients in the liquid stage, which will be further processed, and the organic nutrients in the solid phased, which can be composted to mineralize nitrogen and phosphorus and be further used as fertilizers. The study of organic waste composting is out of the scope of this work.

Based on the evaluation reported by Møller et al. (2000), a screw press is the technology selected to carry out the solid-liquid separation stage since it is the most cost-efficient equipment. The partition coefficients for the different components are shown in Table 6S of the Supplementary Material. Assuming the discretization of units due to the commercial sizes available, the investment and operating costs for the screw press equipment are presented in Figure 9S of the Supplementary Material.

5.2.2.6 Phosphorus recovery

The technologies to recover inorganic phosphorus can be classified in three categories: struvite-based phosphorus recovery, calcium precipitates-based phosphorus recovery, and physical separation systems. Table 6.1 shows the classification and characteristics of the evaluated technologies. Regarding struvite-based systems, the formation of struvite has been widely described in the literature, mainly focused on phosphorus recovery from wastewater (Battistoni et al., 2001; Rahaman et al., 2014). However, cat-

tle organic waste shows some characteristics that hinder struvite formation, including high ionic strength, which reduces the effective concentration of ions; and the presence of calcium ions competing for phosphate ions (Yan & Shih, 2016), which inhibits a selective recovery by phosphorus precipitation. The high variability in the manure composition, as a function of the geographic area, the animal feed, etc., represents an additional challenge for nutrient recovery (Tao et al., 2016). Therefore, specific correlations for livestock waste to estimate the molar fraction of PO_4^{3-} and Ca^{2+} recovered as struvite as a function of the amount of calcium contained in the waste were developed in a previous work (Martín-Hernández, Ruiz-Mercado, et al., 2020).

Among the different products obtained by the different processes, only struvite generates income. Calcium precipitates lacks of a well-established market as fertilizer, and therefore no sales of this product are considered. MAPHEX produces an organic solid rich in nutrients, but with a lower nutrient density compared with struvite, hindering transportation of this product and decreasing its market value. Therefore, we have assumed that no income is obtained from this product. Nevertheless, the recovered products allow phosphorus distribution from CAFO releases to phosphorus-deficient areas.

All technologies considered are at or near commercial stage. We note that, for all the technologies evaluated, the installation of several P recovery units in parallel arrangement is considered if the amount of waste to be processed exceeds the treatment capacity of the system. The description of the processes, and the correlations used to estimate the struvite formed, equipment cost, and operating costs are collected in the Section 2.2.4 of the Supplementary Material.

5.2.2.7 Incentives for the installation of nutrient recovery systems

COW2NUTRIENT can evaluate the effect of different kinds of incentives on the economic performance of the nutrient recovery systems. These incentives can be received as a result of the recovery of phosphorus, in the form of P-credits, or for the generation of electricity or biomethane, in form of Renewable Energy Certificates (REC) and Renewable Identification Numbers (RIN) respectively. Renewable Energy Credits are a mechanism implemented in the US which guarantees that energy is generated from renewable sources, providing a system for trading produced renewable electricity. Each produced renewable megawatt-hour generates one REC, that can be sold separately from the electricity commodity itself and can be used to meet regulatory requirements by generators, trades, or end-users. On the other hand, RINs are identification numbers assigned to batches

Table 5.3: Description of phosphorus recovery technologies systems by COW2NUTRIENT framework. $x_{Ca^{2+}:PO_4^{3-}}$ refers to the Ca^{2+}/PO_4^{3-} molar ratio. n_i denotes the number of units of the technology i installed.

Technology	Company	Technology type	Technology readiness level	Phosphorus recovery efficiency (%)	Treatment capacity ($\frac{kg\cdot PO_4}{day\cdot unit}$)	CAPEX ($\frac{MM\ USD}{unit}$)	OPEX ($\frac{USD}{kg\cdot PO_4}$)	Reference
Multiform	Multiform Harvest	Struvite-based	9	$\frac{0.798.100}{1 + \left(x_{Ca^{2+}:PO_4^{3-}} - 0.576 \right)^{2.115}}$	38.5	1.1	1542	1
CrystaLactor	Royal Haskoning DHV	Struvite-based	9	$\frac{0.798.100}{1 + \left(x_{Ca^{2+}:PO_4^{3-}} - 0.576 \right)^{2.115}}$	137.7	$2.3 + 0.71 \cdot n_{CrystaLactor}$	2.12	2
NuReSys	Nutrient Recovery Systems	Struvite-based	9	$\frac{0.798.100}{1 + \left(x_{Ca^{2+}:PO_4^{3-}} - 0.576 \right)^{2.115}}$	204.0	1.38	6.22	1
Pearl 500	Ostara	Struvite-based	9	$\frac{0.798.100}{1 + \left(x_{Ca^{2+}:PO_4^{3-}} - 0.576 \right)^{2.115}}$	65.0	2.3	7.54	3
Pearl 2K	Ostara	Struvite-based	9	$\frac{0.798.100}{1 + \left(x_{Ca^{2+}:PO_4^{3-}} - 0.576 \right)^{2.115}}$	250.0	3.1	7.54	1
Pearl 10K	Ostara	Struvite-based	9	$\frac{0.798.100}{1 + \left(x_{Ca^{2+}:PO_4^{3-}} - 0.576 \right)^{2.115}}$	1250.0	10.0	7.54	4
P-Roc	Karlsruhe Institute of Technology	Calcium precipitates-based	6	60	24.3	See Section 2.2.4.4 of Supplementary Material.	23.22 - 167.8	5
MAPHEX	University of Pennsylvania and USDA	Modular phases separation system	7	90	18.5	0.3	110.8	6.7

1: Australian Meat Processor Corporation (2018)

2: Egle et al. (2016)

3: County of Napa (2013)

4: American Society of Civil Engineers (ASCE) (2013)

5: Ehbrecht et al. (2011)

6: Church et al. (2016)

7: Church et al. (2018)

of biofuel, allowing their tracking through the production, purchase, and final usage. The allocation of RINs is associated with the allocation of incentives for the generation bio-fuels. The considered values for the different incentives are listed in Table 4S of the Supplementary Material.

5.2.3 *Multi-criteria decision model*

The determination of the most suitable nutrient management process is not a trivial procedure since multiple criteria play a critical role at the decision-making stage. COW2NUTRIENT performs the selection of P recovery technologies considering information concerning environmental, economic, and technology readiness dimensions. The integration of these dimensions is justified by the need to find the most suitable system for each CAFO by balancing operating cost and efficiency in the mitigation of nutrient pollution according to the local environmental vulnerability to eutrophication. Finally, the technical maturity of each system is also considered to assess the development level of the different processes. Therefore, a multi-criteria decision analysis (MCDA) model was developed to address the selection of the most suitable phosphorus recovery systems for each studied CAFO. The workflow of the MCDA model is summarized in Figure 5.3.

Five criteria are combined in a composite index for the assessment of the environmental, economic, and technology maturity dimensions of the different technologies. Two environmental criteria are studied to assess the performance of the different technologies to mitigate phosphorus releases from CAFOs, i.e., the fraction of phosphorus recovered, and the potential environmental threat for the local ecosystem of the effluents containing the non-recovered phosphorus evaluated through the eutrophication potential of the effluents. The economic aspect is considered by means of two criteria, the economic barrier for the implementation of P recovery processes, measured in terms of capital cost, and the overall economic performance of the systems, which is evaluated through the net present value (NPV) (Sinnott, 2014). Finally, the technological maturity of the different technologies is considered through the technology readiness level (TRL) index. The construction of a composite index integrating these criteria is composed of three steps: criteria normalization, weighting, and aggregation (Gasser et al., 2020).

5.2.3.1 *Data normalization*

Since each criteria has a different range of potential values, they must be normalized to a common scale to allow each criteria to be compared with

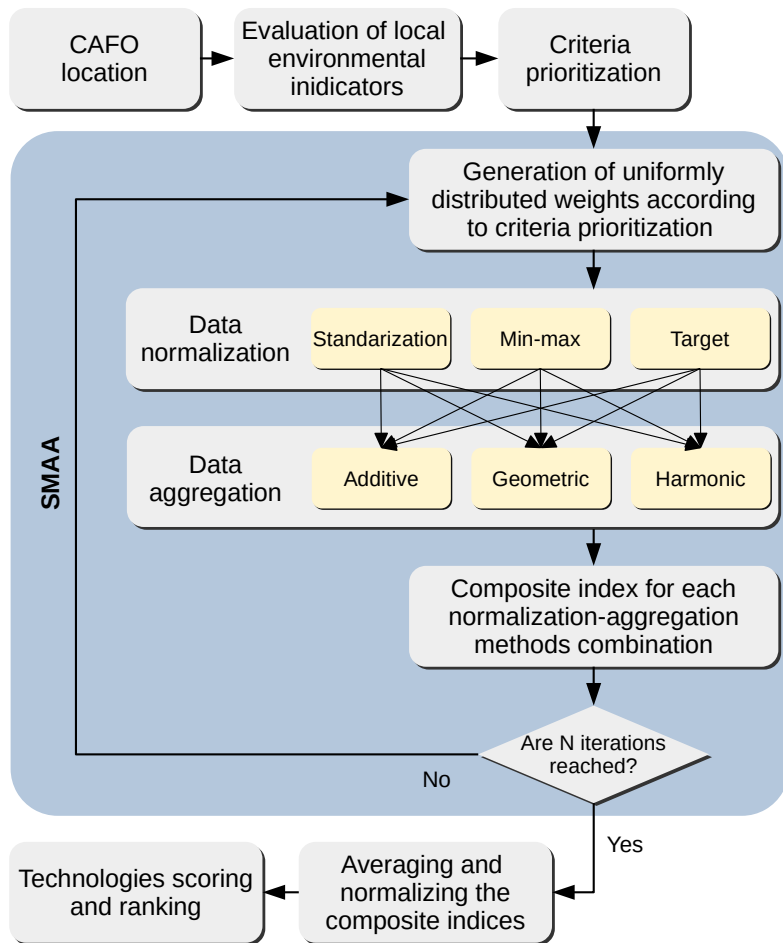


Figure 5.3: Flowsheet for the MCDA model.

the others. However, the composite index can be affected by the normalization technique used. In order to study the robustness of the composite index obtained, and to address the uncertainty originated by data normalization, normalized data using standardization, min-max, and target normalization methods is calculated (OECD and European Commission, 2008).

5.2.3.2 Criteria weighting

The normalized criteria are weighted to set the relative importance of each criterion, prioritizing some criteria over others. This is needed in order to obtain a flexible decision method able to balance the operating cost of the

Table 5.4: Criteria preference as a function of the GIS-based environmental indicators for nutrient pollution.

Local environmental indicators values	Criteria ranking	Description
Condition 1: TES > TSI and TES > Soil fertility Condition 2: TES = Unbalanced	TRL > NPV > Capital cost > TP recovered > Eutrophication potential	Unbalanced phosphorus releases but no immediate threat to soil and water bodies. Prevalence of economic criteria for nutrient recovery system selection.
Condition 1: TSI ≥ TES or TSI ≥ Soil fertility Condition 2: TSI = Eutrophic or Hypereutrophic	TRL > Eutrophication potential > NPV > TP recovered > Capital cost	High Trophic State Index. Immediate environmental risk due to potential algal blooms. Prevalence of environmental criteria for nutrient recovery system selection.
Condition 1: Soil fertility ≥ TES and Soil fertility > TSI Condition 2: Soil fertility = Excessive	TRL > TP recovered > NPV > Eutrophication potential > Capital cost	Excessive P in soil. Immediate environmental risk due to potential P runoff. Prevalence of environmental criteria for nutrient recovery system selection.
Condition: TES ≠ Saturated and TSI ≠ Eutrophic or Hypereutrophic and Soil fertility ≠ Excessive	TRL > NPV > Capital cost > TP recovered > Eutrophication potential	No environmental risk. Prevalence of economic criteria for nutrient recovery system selection.

TRL: Technology Readiness Level

TSI: Trophic State Index

TES: Techno-Ecological Synergy sustainability metric

NPV: Net Present Value

TP: Total Phosphorus

systems and the P recovery efficiency as a function of the environmental vulnerability to eutrophication of each region. The minimization of the operating costs is prioritized in regions with low eutrophication risk, while the efficiency of P recovery is more relevant in regions affected by nutrient pollution. Therefore, the criteria are dynamically weighted according to the values of TSI, TES and Mehlich 3 phosphorus concentration in each region studied. The preference of criteria as a function of the environmental vulnerability to eutrophication is shown in Table 5.4. On the one hand, if there is immediate environmental risk by nutrient pollution (i.e., high values for TSI or soil fertility), phosphorus recovery efficiency is prioritized over economic performance. Conversely, if there is environmental risk in the long run due to the unbalance between anthropogenic phosphorus releases and uptakes (negative value of TES indicator), or there is no potential environmental risk, the economic performance is prioritized over the phosphorus recovery efficiency. Finally, since the objective of this framework is to select P recovery systems that are feasible to install and operate in CAFOs, the TRL index is set as the criteria with highest preference in all cases in order to minimize the risk of selecting non-full-scale processes. As a result, the selection of processes with low TRL will be hampered unless they have good economic or environmental performance.

The procedure described above sets the prioritization of criteria, i.e., they can be sorted in order of importance. However, it does not provide an specific value for the weights, which values are unknown. In order to avoid the risk of biasing the decision-making procedure setting arbitrary values for the weights, a stochastic multi-criteria acceptability analysis (SMAA) is used to explore the weights space (Tervonen & Lahdelma, 2007). Through this approach, the feasible space of each weight (i.e., the space delimited by the previous and the subsequent weights) is explored through the Monte Carlo method, retrieving a set of weights for all criteria according to the assigned order. The SMAA is formulated by defining the set of n weights (ω) as a non-negative set which elements must sum 1, as shown in Eqs. 5.3 and 5.4.

$$\omega_j \geq 0 \quad \forall j \in n \quad (5.3)$$

$$\sum_{j=1}^n \omega_j = 1 \quad (5.4)$$

$$\omega_{j1} \geq \omega_{j2} \geq \dots \geq \omega_{jn} \quad (5.5)$$

The preference information of the criteria, defined through the ranking of the criteria shown in Table 5.4, is expressed as a sequence of inequality constraints, Eq. 5.5. A detailed description of the SMAA method can

be found in Tervonen and Lahdelma (2007). A number of Monte-Carlo simulations (N) of 100 is assumed as a trade-off between computational cost and MCDA model performance.

5.2.3.3 Criteria aggregation

The aggregation stage merges the weighted criteria, resulting in the composite index. Similarly to the normalization stage, different aggregation methods are evaluated to improve the robustness of the solutions retrieved by the framework. Different aggregation schemes denote different degrees of compensability between indicators, i.e. a deficit in one criteria can be fully, partially, or not compensated by a surplus in other criteria (Gasser et al., 2020). Three aggregation functions are evaluated including full compensation (additive aggregation) and partial compensation schemes (geometric and harmonic aggregation methods). Nine composite indexes are obtained for each P recovery technology combining normalization and aggregation techniques, as shown in Figure 5.3. Finally, the composites indexes are normalized in a range from 0 to 1 and ranked to determine the most suitable P recovery process for the CAFO under study.

5.2.4 Framework limitations

The main limitations of the proposed framework lie in the uncertainty of the input data. On the one hand, since the data regarding the animal number, type of animals, and location of CAFOs are reported by the state environmental protection agencies of each state, they are considered reliable. On the other hand, to estimate the local vulnerability to phosphorus pollution throughout the contiguous US, HUC8 spatial resolution has been chosen as a trade-off solution between spatial accuracy and data uncertainty. However, more accurate results can be obtained if reliable data for phosphorus level in soils, fertilizer application rates, etc. are available for higher spatial resolution. Particularly, further studies for developing more accurate correlations to estimate the fraction of phosphorus available to plants based on soil type and climate conditions in each region would improve the accuracy of the assessment of local risk to phosphorus pollution. Additionally, since the proposed framework is focused on phosphorus recovery for freshwater nutrient pollution prevention and control, the recovery of other resources contained in livestock manure (such as organic carbon and nitrogen) is not considered in this study.

5.2.5 Case study

5.2.5.1 Study region

The Great Lakes area, located in North America, is selected in order to demonstrate the implementation of nutrient management systems at CAFOs using the COW2NUTRIENT framework. This region is selected because its high concentration of CAFO facilities, resulting in significant nutrient releases that contribute to frequent HABs and eutrophication episodes, as well as to the nutrient legacy accumulated over time (Han et al., 2012; Sayers et al., 2019). The evaluation and implementation of phosphorus recovery systems at CAFOs already in operation at the US states of Pennsylvania (Pennsylvania Department of Environmental Protection, 2019), Ohio (Ohio Department of Agriculture, 2019), Indiana (Indiana Department of Environmental Management, 2019), Michigan (Michigan Department of Environment, Great Lakes, and Energy, 2019), Wisconsin (Wisconsin Department of Natural Resources, 2019), and Minnesota (Minnesota Center for Environmental Advocacy, 2019) are performed using the criteria prioritization based on the GIS indicators describing the environmental impact of nutrient pollution shown in Table 5.4. The states of Illinois and New York, and the Canadian province of Ontario, which are also part of the Great Lakes area, are not included due to the unavailability of reliable information about their CAFOs. A description of the studied states listing the animal units, annual manure generation, and annual phosphorus releases by the year 2019, disaggregated for dairy and beef cattle, is collected in Table 10S of the Supplementary Material.

It should be noted that, accordingly to the US regulatory definition of CAFOs, only intensive livestock facilities with 300 animal units or more are considered in this study (U.S. Environmental Protection Agency, 2012c), resulting in the evaluation of 2,217 CAFOs. An animal unit is defined as an animal equivalent of 1,000 pounds (453.6 kg) live weight (U.S. Department of Agriculture, 2011). Animal units is used as a unit to measure the size of CAFOs due to the presence of different types of animals in the CAFOs, i.e. beef or dairy cows, and animals of different age, including heifers, calves, and adult animals. Different types of animals result in different manure generation rates and composition. Therefore, the different types of animals within each studied CAFO are normalized using the definition of animal units to estimate the amount and composition of the manure generated.

5.2.5.2 Scenarios description

Two scenarios have been evaluated, the deployment of only phosphorus recovery systems, and the integration of these processes with AD and electricity production processes. Incentives for the recovery of phosphorus based on the work of A. M. Sampat et al. (2018) are considered, assuming a phosphorus credit value of 22 USD/kg_P recovered for both scenarios. We note that this value is significantly lower than the economic impact of P release from livestock waste, valued in 74.5 USD/kg_P released (A. M. Sampat et al., 2021). Additionally, in the scenario considering the production biogas-based electricity, a value of Renewable Energy Certificates (fixed electricity selling price) of 60 USD per MWh generated is assumed. Finally, a discount rate of 7% is considered in both scenarios.

5.3 RESULTS

5.3.1 Implementation of phosphorus recovery systems in the Great Lakes area

Table 5.5 summarizes the results of the phosphorus recovery process selection in the Great Lakes area. It can be observed that only three out of the six commercial processes evaluated are selected to be installed. All selected processes recover P in the form of struvite, which is a valued product that can be sold, generating income. Although the Ostara Pearl process also produces struvite, it results in larger operating costs than the technologies selected. Conversely, P-RoC recovers phosphorus in the form of calcium-based precipitates. This product lacks a well-established market, and therefore it does not generate income. In addition, P-RoC is the technology with the lowest TRL, which hampers the selection of this process. The selection of modular phosphorus recovery systems, such as MAPHEX, which due to economies of scale are especially suitable for small livestock facilities, is largely prevented by the absence of small-scale CAFOs. Therefore, a sub-set of three technologies is obtained. Therefore, it can be concluded that the selection of this pool of three technologies amongst the six systems evaluated is mainly driven by economic factors. Additionally, the low TRL of P-RoC also hampers the selection of this process.

The selection of the most suitable technology for each studied CAFO among the sub-set comprised by Multiform, Nuresys, and Crystalactor systems is based on the CAFO scale and local eutrophication risk, as it is discussed in the following sections.

Table 5.5: Distribution and characteristics studied CAFOs, and phosphorus recovery processes selected. Only selected technologies are included in the table.

State	CAFO average size (animal units)	Number of CAFOs	Manure generated (ton/year)	P recovered (ton/year, (%))	Number of phosphorus recovery systems installed					
					Multiform		NuReSys		Crystalactor	
					S1	S2	S1	S2	S1	S2
Indiana	1,574.41	119	$2.48 \cdot 10^6$	1558.8 (78.7)	116	113	0	0	3	6
Michigan	2,461.52	144	$4.76 \cdot 10^6$	3004.4 (79.0)	127	113	16	30	1	1
Minnesota	634.23	1,487	$1.13 \cdot 10^7$	6938.1 (76.9)	1,477	1,476	0	0	10	11
Ohio	2,415.24	53	$1.68 \cdot 10^6$	1055.8 (78.6)	50	47	1	3	2	3
Pennsylvania	1,495.94	131	$2.59 \cdot 10^6$	1633.2 (78.9)	124	119	6	11	1	1
Wisconsin	2,628.19	283	$1.02 \cdot 10^7$	6510.5 (79.4)	262	255	6	7	15	21

S1: Phosphorus recovery systems only.

S2: Phosphorus recovery systems coupled with AD and electricity production.

5.3.1.1 Effect of CAFOs scale on selecting P recovery systems

A relationship between CAFOs size and the selected technologies can be observed in Table 5.5. This relationship is also observed in Figures 5.4 and 5.5. Multiform is the predominant phosphorus recovery process. Furthermore, we observe that in those states with smaller CAFOs (Minnesota and Indiana) the selection of Multiform is more predominant than in states with larger CAFOs. On the contrary, in the states with large CAFOs or with outliers representing large facilities, (such as Ohio and Wisconsin) Crystalactor is selected for some facilities. Additionally, NuReSys is a technology also selected for medium-size CAFOs.

The integration of biogas production and upgrading affects the selection of P recovery processes as a consequence of the high investment expenditures associated to the installation of AD processes. These large costs blur the capital investment differences between different P recovery processes. As a result, the MDCA model promotes the implementation of technologies with better long-term economic performance (lower operating costs), such as NuReSys and Crystalactor, in spite of the fact that they involve larger investments costs than other technologies like Multiform, as shown in Figure 5.4b.

Based on the data illustrated in Figures 5.5 to 5.7, a preliminary screening of P recovery systems can be performed based on the size of the CAFOs. If the installation of only nutrient recovery systems is considered, Multiform can be selected for CAFOs with sizes up to 5,000 animal units, NuReSys can be selected for CAFOs with a size between 2,000 and 5,000 animal units, and Crystalactor is selected for CAFOs larger than 5,000 animal units. For the scenario integrating anaerobic digestion and phosphorus

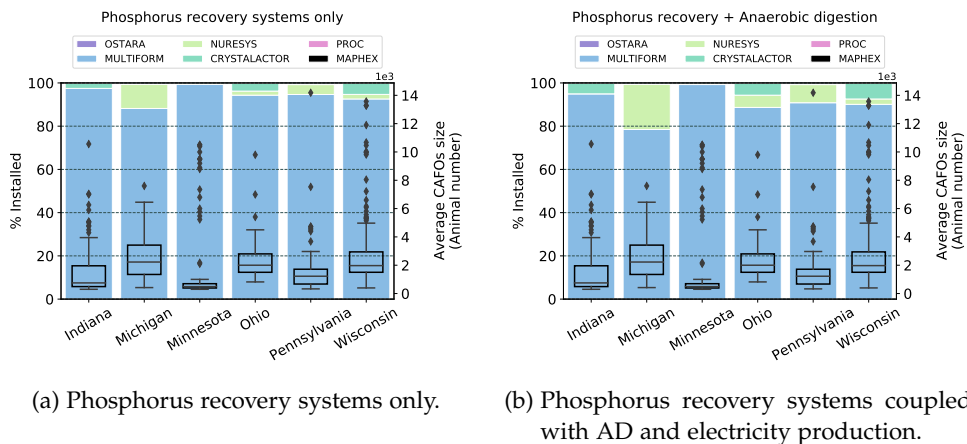


Figure 5.4: Distribution of the phosphorus recovery systems selected for the CAFOs in the Great Lakes area. The boxplots represent the distribution of CAFO sizes in each studied state.

recovery processes, Multiform is mostly selected for CAFOs up to 4,000 animal units, although it is also selected in some larger CAFOs, NuReSys are mostly selected for CAFOs between 2,000 and 6,000 animal units, while the size range for the selection of Crystalactor is similar to the previous case. The operating costs are shown in Figure 5.6. It can be observed that the operating cost of Multiform is larger than NuReSys, and in turn the operating cost of this one is larger than Crystalactor, showing an opposite pattern than capital costs.

5.3.1.2 Effect of local eutrophication risk on the selection of P recovery systems

The results obtained reveal that CAFOs scale is the main driver for the selection of phosphorus recovery technologies. However, the role of the environmental vulnerability to eutrophication can be appreciated in those CAFOs where two different systems show similar economic performance. From the results illustrated in Figure 5.7, it can be observed that Multiform and NuReSys technologies are selected for CAFOs with similar size. However, the economic performance of the second technology is better as consequence of the lower operating expenses and larger net revenues of this technology. Although both technologies have similar phosphorus recovery yield, Multiform shows better environmental performance since the eutrophication potential of its output streams is lower than NuReSys effluents. This difference in eutrophication potential between both technologies is mainly driven by the higher nitrogen recovery of Multiform. Therefore, in those locations that are highly vulnerable to nutrient pollution, the solution proposed by the COW2NUTRIENT framework is driven

more by environmental criteria than by economic criteria, resulting in the selection of the Multiform process.

Table 5.6: Economic results per state for installing phosphorus recovery systems in the studied states of the Great Lakes area.

State	CAPEX		OPEX		Net revenue	
	(MM USD)		(MM USD/year)		(MM USD/year)	
	S ₁	S ₂	S ₁	S ₂	S ₁	S ₂
Indiana	145.58	325.00	21.18	34.16	19.32	11.88
Michigan	191.09	480.19	36.74	55.92	41.00	32.15
Minnesota	1,591.40	2,866.31	140.74	251.58	39.61	-46.15
Ohio	68.30	179.29	12.95	20.32	14.46	10.80
Pennsylvania	148.16	332.03	21.46	35.03	20.82	12.95
Wisconsin	396.24	1,009.47	73.55	117.80	95.44	74.14

S₁: Phosphorus recovery systems only.

S₂: Phosphorus recovery systems coupled with AD and electricity production.

5.3.2 Economic results

The capital expenditures (CAPEX), operating expenses (OPEX), and net revenues (difference between incomes and operating expenses) associated with the deployment of the nutrient management systems are listed per state in Table 5.6. For the scenario considering the installation of only phosphorus recovery processes, the CAPEX and OPEX are 2,540.77 MM USD and 185.65 MM USD per year respectively. If the integration of biogas production and upgrading to power with phosphorus management is considered, the CAPEX and OPEX increase up to 5,192.29 MM USD and 267.51 MM USD per year respectively. It can be observed that, due to the high CAPEX of biogas production and upgrading stages, the net revenues decrease from 230.65 MM USD per year for the scenario considering only phosphorus recovery systems to 95.77 MM USD per year if the processes for phosphorus recovery and AD are combined.

Figures 5.5 and 5.6 show the evolution of CAPEX and OPEX of the P recovery technologies installed at the livestock facilities studied as a function of CAFOs scale. Figure 5.5a shows the CAPEX when the implementation of only P recovery systems is considered. We observe that CAFOs are grouped in sets selecting the same P recovery technology. This

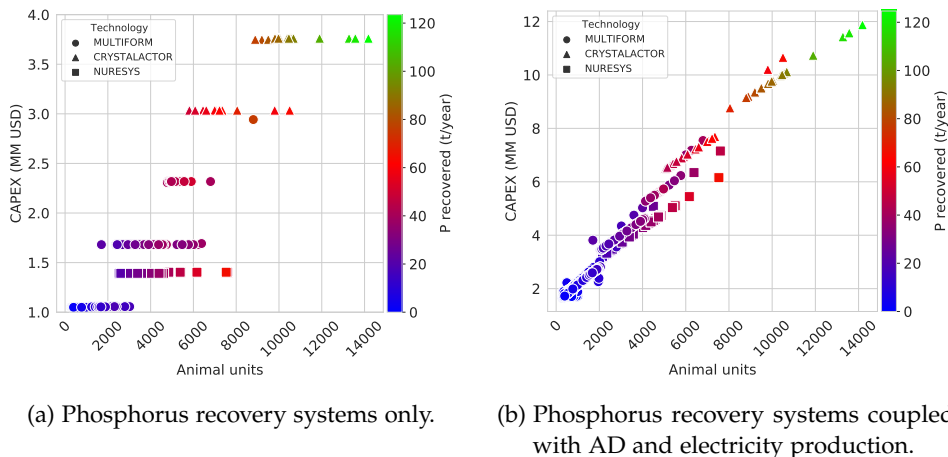


Figure 5.5: Capital expenses for deploying phosphorus recovery systems in the studied CAFOs. The dots represent the P recovery technologies installed in the studied CAFOs.

is because the manufacturers standardize the size of each P recovery technology, which in turn determines the maximum waste processing capacity of each technology (as shown in Table 6.1). This results in the use of the same P recovery equipment, and thus the same CAPEX, for all the CAFOs generating waste below the maximum processing capacity. Likewise, we note different CAPEX values for the implementation of the same P recovery technology. This is a consequence of installing of multiple in-parallel P recovery units to increase the processing capacity of such technology, since the waste generated in that CAFO exceeds its maximum processing capacity. It can also be appreciated that CAFOs with similar size might result in the installation of different technologies, or a different number of units of the same technology. This is because, although CAFOs can have a similar number of animal units, the type of the animals can be different, resulting in the generation of different amounts of manure. In the case of considering biogas production and upgrading, illustrated in Figure 5.5b, the required CAPEX increases significantly, blurring the differences in the capital investment between different P recovery processes observed in Figure 5.5a into the cost of the whole system. The integration of AD and electricity production also results in the increase of the OPEX, as shown in Figure 5.6.

The net revenue of the installed nutrient management systems according with the economic parameters described at the beginning of the section is shown in Figure 5.7. We observe a pattern characterized by the increase of the net revenues with the increase of CAFOs size. However, the implementation of P recovery technologies in CAFOs below 1,000 animal units,

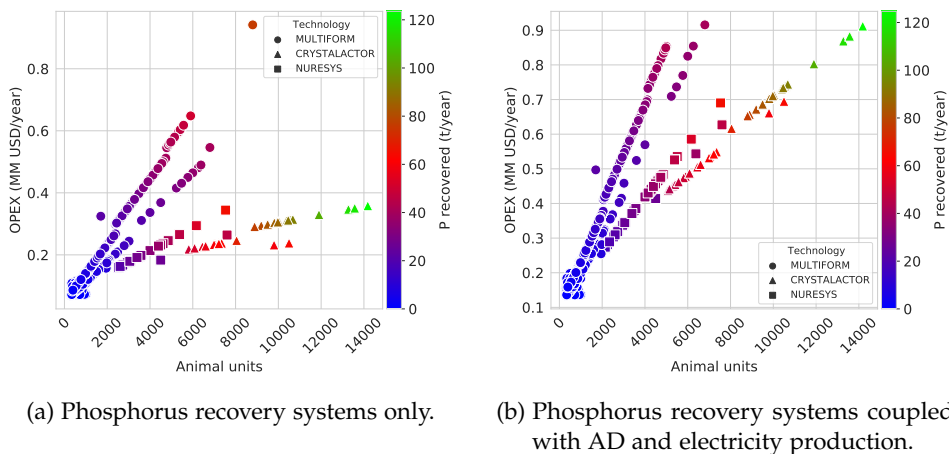


Figure 5.6: Operating expenses for deploying phosphorus recovery processes in the studied CAFOs. The dots represent the P recovery technologies installed in the studied CAFOs.

and below 2,000 animal units if biogas production and upgrading is also considered, result in economic losses. Additionally, the integration of these processes slightly decreases the net revenues of the systems installed for phosphorus recovery.

5.4 DISCUSSION

5.4.1 Economic implications

In this work, fixed incentives for P recovery and biogas-based electricity generation have been considered as starting point to explore the effect of the application of incentives in the implementation of P recovery technologies, either standalone or integrated with biogas production and upgrading processes. The results shown in Figure 5.7 reveal the effect of the economies of scale in the net revenues from the implementation of P recovery technologies in the Great Lakes area are highly dependent on the economies of scale, i.e., the larger the amount of waste to be treated, the larger the net revenues obtained. However, while for the largest CAFOs significant profits are obtained, negative revenues (i.e., economic losses) are obtained for the smallest CAFOs, even for large P credits prices such as 22 USD/kg_P recovered. This suggests that the implementation of fixed incentives is not a fair policy, since the small CAFOs are not profitable while they increase the profits of the largest CAFOs. Therefore, alternative incentive policies must be explored. A. M. Sampat et al. (2019) studied the development of a coordinated management system for the treatment of

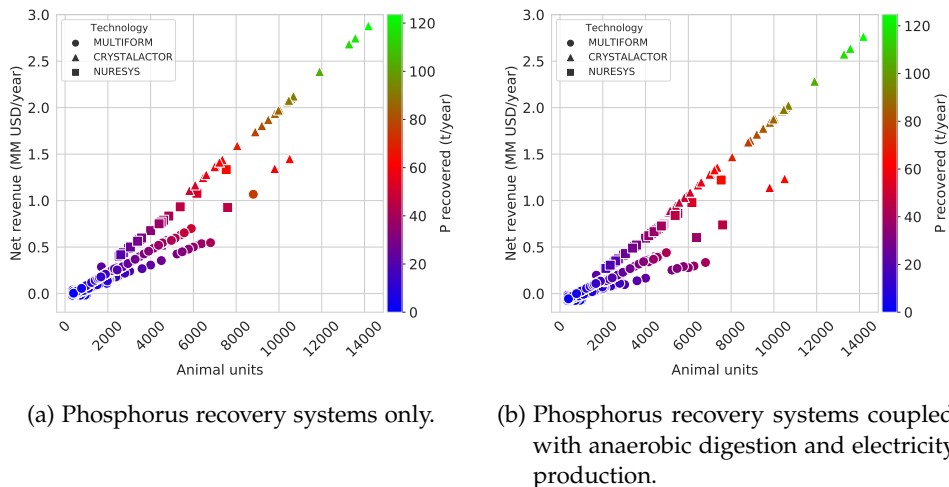


Figure 5.7: Net revenue from the phosphorus recovery processes selected in the studied CAFOs. The dots represent the P recovery technologies installed in the studied CAFOs.

cattle manure and P recovery. That framework captures the geographical phosphorus imbalance by proposing different prices for manure treatment that capture the regional remediation cost caused by P releases. They found that economic drivers are needed for a cost-effective recovery and redistribution of phosphorus, considering fixed incentives for P recovery up to 50 USD/kg_P for this purpose. Therefore, further research about the effect of implementing dynamic incentives for P recovery is needed. These incentive policies can follow different schemes, such as progressive incentives for P recovery based on the amount of manure treated, or cooperative schemes where the profits from P recovery obtained by the largest livestock facilities are redistributed to the smallest CAFOs. This is a concept that has been studied for minimizing the costs of meeting greenhouse gases emission targets (Galán-Martín et al., 2018), and could be adopted for the reduction of P releases.

Furthermore, consideration should be given to the fair allocation of incentives in those scenarios where the available incentives budget is not enough to avoid economic losses in all CAFOs. In this regard, the fairness measure considered for budget allocation must be carefully selected among the existing schemes (A. M. Sampat & Zavala, 2019).

5.4.2 Phosphorus use efficiency

Currently, manure or digestate in liquid phase is usually supplied as nutrient supplementation in croplands, or it is treated in either aerobic or

anaerobic ponds. Solid phase processing is based on composting or drying. However, the high density of manure and digestate and low concentration of nutrient prevent an efficient redistribution of the phosphorus released from CAFOs to phosphorus-deficient areas (Burns & Moody, 2002). Therefore, the implementation of phosphorus recovery processes is a desirable measure for sustainable phosphorus management. We find that implementing struvite production processes considering incentives for P recovery of 22 USD/kg_{P recovered} is economically feasible for CAFOs larger than 1,000 animal units if standalone P recovery technologies are implemented, and for CAFOs larger than 2,000 animal units if they are integrated with biogas production and upgrading processes. The requirement of large incentives to produce profit in most of the P recovery systems installed at CAFOs might raise the debate of whether it is worthwhile to implement P recovery systems; or if the economic resources should be allocated to simpler phosphorus management alternatives, such as the redistribution of either raw or pond-stored manure. In this regard, A. M. Sampat et al. (2019) studied the separation of manure in liquid and solid phases, and their further transport to demanding allocations, considering a coordinated management system in Upper Yahara watershed (Wisconsin, United States). In addition, that study considered the implementation of economic incentives from 0 to 50 USD/kg_P. However, the results showed that manure redistribution is not an economically viable technique for phosphorus recycling in this range of incentives. The main drawback of manure redistribution is the large transportation cost of both liquid and solid raw manure because of the high volume of these materials and their low phosphorus concentration. Therefore, the results reveal that on-site manure processing to generate valuable products (struvite) is more beneficial than manure redistribution.

The replacement of phosphorus from synthetic fertilizers by the recovered P, mitigating the dependency on fertilizers from non-renewable resources (phosphate rock), is an interesting alternative towards the sustainability of the agri-food sector. However, phosphorus availability for plants depends on several factors, including the P product used as fertilizer and soil pH level. Since struvite is the product recovered in all studied CAFOs, we will focus the discussion on this product. Vaneeckhaute et al. (2015) compared the bio-availability of several bio-based fertilizers, including struvite, to synthetic triple super phosphate (TSP). This study shows that P available in soil (measured as Prhizon) was a 45% higher than TSP in acidic soils (pH=5.0), but 60% lower in slightly basic soils (pH=7.9). Based on these data, one kilogram of manure processed for P recovery by struvite production can replace from $1.53 \cdot 10^{-3}$ to $3.71 \cdot 10^{-3}$ kg of TSP ($5.02 \cdot 10^{-3}$ kg of struvite are recovered per kilogram of manure processed). However, it must be noted that currently the cost of recovered P from

manure ($2.12\text{-}15.42$ USD/kg_P recovered, see Table 6.1) is considerable larger than the cost of phosphorus from synthetic TSP (1.23 USD/kg_P) (Index Mundi, 2020). As a result, from an economic perspective the complete substitution of phosphate rock is currently hindered by the large recovery costs, in addition to a limited availability of resources recovered from waste, and henceforth further exploration on resource recovery from different wastes is required to achieve P circularity reducing the recovery costs, and increasing the amount of phosphorus from organic waste, including but not limited to livestock manure.

5.5 CONCLUSION

We presented a framework for the techno-economic evaluation and selection of phosphorus recovery systems considering the local vulnerability to phosphorus pollution through a GIS environmental model. A multi-criteria decision analysis model is used for the comparison and selection of phosphorus recovery systems based on the economic performance and technological readiness level of the processes, and the eutrophication risk of the watershed where the studied CAFOs are located. Technologies for P recovery in the form of struvite are selected in all CAFOs studied. The selection of P recovery technologies is mainly driven by economic criteria, and the effect of the economies of scale is very significant. However, environmental criteria (P recovery efficiency, eutrophication potential of process effluents) are the decision criteria at some CAFOs where different technologies show similar economic performances. The results show that a preliminary screening of P recovery systems can be performed based on the size of CAFOs. Multiform can be selected for CAFOs with sizes up to 5,000 animal units, NuReSys can be selected for CAFOs with a size between 2,000 and 5,000 animal units, and Crystalactor is selected for CAFOs larger than 5,000 animal units. The implementation of these systems in the Great Lakes area involves capital expenditures of 2.5 billion USD and operating costs of 186 million USD per year if only phosphorus recovery technologies are installed, and 5.2 billion USD and 268 million USD per year respectively if biogas production and upgrading are also considered. The implementation of fixed incentives of 22 USD/kg_P recovered is considered to avoid economic losses due to P recovery costs impact in the economy of CAFOs. However, we find that the implementation of fixed incentives is not a fair policy, since the small CAFOs are not profitable while they increase the profits of the largest CAFOs. The phosphorus recovered in the form of struvite from one kilogram of manure processed can replace from $1.53 \cdot 10^{-3}$ to $3.71 \cdot 10^{-3}$ kg of synthetic triple super phosphate, but incurring in signifi-

cantly larger production costs (2.12-15.42 USD/kg_P recovered) than synthetic fertilizer (1.23 USD/kg_P).

As part of future work, customized incentive policies adapted to the particularities of each livestock facility can be proposed in order to optimize the allocation of limited monetary resources. Additionally, it would be interesting to analyze the potential of crop-livestock integration as an alternative for phosphorus recycling to the implementation of physico-chemical P recovery processes. Another interesting research line is the integration of multiple processes in order to recover additional valuable products from organic waste (such as biochar), adapting the concept of refinery to resource recovery from organic waste.

ACKNOWLEDGMENTS

This research was supported in part by an appointment for E. Martín-Hernández to the Research Participation Program for the Office of Research and Development, US EPA, administered by the Oak Ridge Institute for Science and Education through Interagency Agreement No. DW-89-92433001 between the US Department of Energy and the US Environmental Protection Agency. PSEM₃ research group acknowledge funding from the Junta de Castilla y León, Spain, under grant SA026G18 and grant EDU/556/2019.

Disclaimer: The views expressed in this article are those of the authors and do not necessarily reflect the views or policies of the US EPA. Mention of trade names, products, or services does not convey, and should not be interpreted as conveying, official US EPA approval, endorsement, or recommendation.

BIBLIOGRAPHY

- Allen, B. L., & Mallarino, A. P. (2006). Relationships between Extractable Soil Phosphorus and Phosphorus Saturation after Long-Term Fertilizer or Manure Application. *Soil Sci. Soc. Am. J.*, 70, 454-463. <https://doi.org/10.2136/sssaj2005.0031>
- American Society of Civil Engineers (ASCE). (2013). Chicago to Add Nutrient Recovery to Largest Plant [[Online; accessed 21-March-2019]].
- Ansari, A. A. (Ed.). (2010). *Eutrophication: causes, consequences and control* [OCLC: ocn646114298]. Dordrecht ; New York, Springer Science+Business Media, 2011.
- Australian Meat Processor Corporation. (2018). Struvite or Traditional Chemical Phosphorus Precipitation – What Option Rocks? [[Online; accessed 20-March-2019]].

- Bakshi, B., Ziv, G., & Lepech, M. (2015). Techno-ecological synergy: A framework for sustainable engineering. *Environ. Sci. Technol.*, 49(3), 1752–1760.
- Battistoni, P., De Angelis, A., Pavan, P., Prisciandaro, M., & Cecchi, F. (2001). Phosphorus removal from a real anaerobic supernatant by struvite crystallization. *Wat. Res.*, 35, 2167–2178.
- Beaulieu, J. J., DelSontro, T., & Downing, J. A. (2019). Eutrophication will increase methane emissions from lakes and impoundments during the 21st century. *Nat Commun*, 10(1), 1375. <https://doi.org/10.1038/s41467-019-10910-5>
- Beddoes, J. C., Bracmort, K. S., Burns, R. T., & Lazarus, W. F. (2007). *An Analysis of Energy Production Costs from Anaerobic Digestion Systems on U.S. Livestock Production Facilities* (tech. rep.). U.S. Department of Agriculture (USDA).
- Belarbi, Z., Daramola, D. A., & Trembly, J. P. (2020). Bench-Scale Demonstration and Thermodynamic Simulations of Electrochemical Nutrient Reduction in Wastewater via Recovery as Struvite. *Journal of the Electrochemical Society*, 167(15), 155524.
- Berg, U., Donnert, D., Weidler, P., Kaschka, E., Knoll, G., & Nüesch, R. (2006). Phosphorus removal and recovery from wastewater by tobermorite-seeded crystallisation of calcium phosphate. *Water Science and Technology*, 53(3), 131–138.
- Burns, R. T., & Moody, L. B. (2002). Phosphorus recovery from animal manures using optimized struvite precipitation. *Proceedings of Coagulants and Flocculants: Global Market and Technical Opportunities for Water Treatment Chemicals*.
- Carlson, R. E. (1977). A trophic state index for lakes: Trophic state index. *Limnol. Oceanogr.*, 22(2), 361–369. <https://doi.org/10.4319/lo.1977.22.2.0361>
- Church, C. D., Hristov, A. N., Bryant, R. B., Kleinman, P. J. A., & Fishel, S. K. (2016). A Novel Treatment System to Remove Phosphorus from Liquid Manure. *Appl. Eng. Agric.*, 32(1), 103–112. <https://doi.org/10.13031/aea.32.10999>
- Church, C. D., Hristov, A. N., Kleinman, P. J., Fishel, S. K., Reiner, M. R., & Bryant, R. B. (2018). Versatility of the MANURE PHosphorus EXtraction (MAPHEX) System in Removing Phosphorus, Odor, Microbes, and Alkalinity from Dairy Manures: A Four-Farm Case Study. *Applied Engineering in Agriculture*, 34(3), 567–572. <https://doi.org/10.13031/aea.12632>
- Cordell, D., Drangert, J.-O., & White, S. (2009). The story of phosphorus: Global food security and food for thought. *Global Environmental*

- Change*, 19(2), 292–305. <https://doi.org/10.1016/j.gloenvcha.2008.10.009>
- County of Napa. (2013). Phosphorus recovery [[Online; accessed 20-March-2019]].
- Dzombak, D. A. (2011). Nutrient Control in Large-Scale U.S. Watersheds. *The Bridge*, 41(4), 13–22.
- Egle, L., Rechberger, H., Krampe, J., & Zessner, M. (2016). Phosphorus recovery from municipal wastewater: An integrated comparative technological, environmental and economic assessment of P recovery technologies. *Science of The Total Environment*, 571, 522–542. <https://doi.org/10.1016/j.scitotenv.2016.07.019>
- Ehbrecht, A., Schönauer, S., Fuderer, T., & Schuhmann, R. (2011). P-Recovery from sewage by seeded crystallisation in a pilot plant in batch mode technology. *Water Science and Technology*, 63(2), 339–344. <https://doi.org/10.2166/wst.2011.061>
- Espinoza, L., Slaton, N. A., & Mozaffari, M. (2006). *Understanding the numbers on your soil test report* (tech. rep.). Cooperative Extension Service, University of Arkansas.
- Galán-Martín, A., Pozo, C., Azapagic, A., Grossmann, I., Mac Dowell, N., & Guillén-Gosálbez, G. (2018). Time for global action: an optimised cooperative approach towards effective climate change mitigation. *Energy & Environmental Science*, 11(3), 572–581.
- Gasser, P., Suter, J., Cinelli, M., Spada, M., Burgherr, P., Hirschberg, S., Kadziński, M., & Stojadinović, B. (2020). Comprehensive resilience assessment of electricity supply security for 140 countries. *Ecological Indicators*, 109. <https://doi.org/10.1016/j.ecolind.2019.105731>
- Han, H., Allan, J. D., & Bosch, N. S. (2012). Historical pattern of phosphorus loading to Lake Erie watersheds. *Journal of Great Lakes Research*, 38(2), 289–298.
- Index Mundi. (2020). Triple Superphosphate Monthly Price - US Dollars per Metric Ton [[Online; accessed 05-May-2020]].
- Indiana Department of Environmental Management. (2019). Confined Feeding Operation Facilities (20200402) [[Online; accessed 29-July-2019]].
- International Plant Nutrition Institute (IPNI). (2012). *A Nutrient Use Information System (NuGIS) for the U.S.* (tech. rep.). International Plant Nutrition Institute (IPNI).
- Kellogg, R. L., Lander, C. H., Moffitt, D. C., & Gollehon, N. (2000). *Manure Nutrients Relative to the Capacity of Cropland and Pastureland to Assimilate Nutrients: Spatial and Temporal Trends for the United States* (tech. rep.). United States Department of Agriculture (USDA).

- León, E., & Martín, M. (2016). Optimal production of power in a combined cycle from manure based biogas. *Energy Conv. Manage.*, 114, 89–99.
- Li, B., Dong, S. L., Huang, Y. F., Li, P., Yu, W., Wang, G. Q., & Young, B. (2021). Toward a decision support framework for sustainable phosphorus management: A case study of China. *Journal of Cleaner Production*, 279, 123441.
- Li, X., Shen, S., Xu, Y., Guo, T., Dai, H., & Lu, X. (2020). Application of Membrane Separation Processes in Phosphorus Recovery: A Review. *Science of The Total Environment*, 144346.
- Martín-Hernández, E., Guerras, L., & Martín, M. (2020). Optimal technology selection for the biogas upgrading into biomethane. *J. Clean Prod*, 267, 122032.
- Martín-Hernández, E., Ruiz-Mercado, G., & Martín, M. (2020). Model-Driven Spatial Evaluation of Nutrient Recovery from Livestock Leachate for Struvite Production. *J. Environ. Manage.*, 271, 110967.
- Martín-Hernández, E., Sampat, A., Zavala, V., & Martín, M. (2018). Optimal integrated facility for waste processing. *Chem. Eng. Res. Des.*, 131, 160–182.
- Michigan Department of Environment, Great Lakes, and Energy. (2019). Active NPDES Permits [[Online; accessed 29-July-2019]].
- Minnesota Center for Environmental Advocacy. (2019). Minnesota Confined Animal Feeding Operations [[Online; accessed 29-July-2019]].
- Møller, H., Lund, I., & Sommer, S. (2000). Solid-liquid separation of livestock slurry: efficiency and cost. *Bioresour. Technol.*, 74, 223–229.
- Moran, M. J., Shapiro, H. N., Boettner, D. D., & Bailey, M. B. (2010). *Fundamentals of engineering thermodynamics*. John Wiley & Sons.
- Muhmood, A., Lu, J., Dong, R., & Wu, S. (2019). Formation of struvite from agricultural wastewaters and its reuse on farmlands: Status and hindrances to closing the nutrient loop. *Journal of environmental management*, 230, 1–13.
- OECD and European Commission. (2008). *Handbook on Constructing Composite Indicators. Methodology and User Guide*. OECD.
- Ohio Department of Agriculture. (2019). Livestock Environmental Permitting.
- Pearce, B. J. (2015). Phosphorus Recovery Transition Tool (PRTT): a trans-disciplinary framework for implementing a regenerative urban phosphorus cycle. *Journal of Cleaner Production*, 109, 203–215.
- Pennsylvania Department of Environmental Protection. (2019). Concentrated Animal Feeding Operations [[Online; accessed 29-July-2019]].
- Pickard, B. R., Daniel, J., Mehaffey, M., Jackson, L. E., & Neale, A. (2015). EnviroAtlas: A new geospatial tool to foster ecosystem services science and resource management. *Ecosyst. Serv.*, 14, 45–55.

- Rahaman, M. S., Mavinic, D. S., Meikleham, A., & Ellis, N. (2014). Modeling phosphorus removal and recovery from anaerobic digester supernatant through struvite crystallization in a fluidized bed reactor. *Water Research*, 51, 1–10.
- Reijnders, L. (2014). Phosphorus resources, their depletion and conservation, a review. *Resources, Conservation and Recycling*, 93, 32–49.
- Robles, Á., Aguado, D., Barat, R., Borrás, L., Bouzas, A., Giménez, J. B., Martí, N., Ribes, J., Ruano, M. V., Serralta, J., Et al. (2020). New frontiers from removal to recycling of nitrogen and phosphorus from wastewater in the Circular Economy. *Bioresource technology*, 300, 122673.
- Sampat, A. M., Ruiz-Mercado, G., & Zavala, V. (2018). Economic and Environmental Analysis for Advancing Sustainable Management of Livestock Waste: A Wisconsin Case Study. *ACS Sustainable Chemistry & Engineering*, 6(5), 6018–6031.
- Sampat, A., Martín, E., Martín, M., & Zavala, V. (2017). Optimization formulations for multi-product supply chain networks. *Comput. Chem. Eng.*, 104, 296–310.
- Sampat, A. M., Hicks, A., Ruiz-Mercado, G. J., & Zavala, V. M. (2021). Valuing economic impact reductions of nutrient pollution from livestock waste. *Resources, Conservation and Recycling*, 164, 105199.
- Sampat, A. M., Hu, Y., Sharara, M., Aguirre-Villegas, H., Ruiz-Mercado, G., Larson, R. A., & Zavala, V. M. (2019). Coordinated management of organic waste and derived products. *Computers & chemical engineering*, 128, 352–363.
- Sampat, A. M., & Zavala, V. M. (2019). Fairness measures for decision-making and conflict resolution. *Optimization and Engineering*, 20(4), 1249–1272.
- Sayers, M. J., Grimm, A. G., Shuchman, R. A., Bosse, K. R., Fahnstiel, G. L., Ruberg, S. A., & Leshkevich, G. A. (2019). Satellite monitoring of harmful algal blooms in the Western Basin of Lake Erie: A 20-year time-series. *Journal of Great Lakes Research*, 45(3), 508–521.
- Sinnott, R. (2014). *Chemical engineering design* (Vol. 6). Elsevier.
- Smith, D. B., Cannon, W. F., Woodruff, L. G., Solano, F., Kilburn, J. E., & Fey, D. L. (2013). *Geochemical and Mineralogical Data for Soils of the Conterminous United States: U.S. Geological Survey Data Series 801* (tech. rep.). U.S. Geological Survey (USGS).
- Tao, W., Fattah, K., & Huchzermeier, M. (2016). Struvite recovery from anaerobically digested dairy manure: A review of application potential and hindrances. *J. Environ. Manage.*, 169, 46–57.

- Tervonen, T., & Lahdelma, R. (2007). Implementing stochastic multicriteria acceptability analysis. *European Journal of Operational Research*, 178(2), 500–513. <https://doi.org/10.1016/j.ejor.2005.12.037>
- United States Department of Agriculture. (2009). *Agricultural Water Management Field Handbook* (tech. rep.). United States Department of Agriculture (USDA).
- United States Department of Agriculture. (2019). *2017 Census of Agriculture. United Satates. Summary and State Data* (tech. rep.). United States Department of Agriculture.
- U.S. Department of Agriculture. (2011). Animal Feeding Operations (AFO) and Concentrated Animal Feeding Operations (CAFO) [[Online; accessed 10-August-2020]].
- U.S. Environmental Protection Agency. (2003). *AgSTAR Digest* (tech. rep.). U.S. Environmental Protection Agency.
- U.S. Environmental Protection Agency. (2004). *AgSTAR Handbook. A Manual For Developing Biogas Systems at Commercial Farms in the United States* (tech. rep.). U.S. Environmental Protection Agency.
- U.S. Environmental Protection Agency. (2007). *2007 National Lakes Assessment. A Collaborative Survey of the Nation's Lakes* (tech. rep.). U.S. EPA.
- U.S. Environmental Protection Agency. (2012a). *2012 National Lakes Assessment. Quality Assurance Version Project Plan* (tech. rep.). U.S. EPA.
- U.S. Environmental Protection Agency. (2012b). *National Lakes Assessment 2012. A Collaborative Survey of Lakes in the United States* (tech. rep.). U.S. EPA.
- U.S. Environmental Protection Agency. (2012c). *Regulatory Definitions of Large CAFOs, Medium CAFO, and Small CAFOs* (tech. rep.). U.S. EPA.
- U.S. Geological Survey. (2013). *Federal Standards and Procedures for the National Watershaed Boundary Dataset (WBD)* (tech. rep.). U.S. Geological Survey.
- Vaneeckhaute, C., Janda, J., Meers, E., & Tack, F. (2015). Efficiency of Soil and Fertilizer Phosphorus Use in Time: A Comparison Between Recovered Struvite, FePO₄-Sludge, Digestate, Animal Manure, and Synthetic Fertilizer. In *Nutrient Use Efficiency: from Basics to Advances* (pp. 73–85). Springer.
- van Rossum, G. (1995). *Python tutorial* (tech. rep. CS-R9526). Centrum voor Wiskunde en Informatica (CWI). Amsterdam.
- Wang, H., Xiao, K., Yang, J., Yu, Z., Yu, W., Xu, Q., Wu, Q., Liang, S., Hu, J., Hou, H., Et al. (2020). Phosphorus recovery from the liquid phase of anaerobic digestate using biochar derived from iron-rich sludge: A potential phosphorus fertilizer. *Water research*, 174, 115629.

- Werner, W. (2009). Fertilizers, 6. Environmental Aspects. In *Ullmann's Encyclopedia of Industrial Chemistry*. Weinheim, Germany. https://doi.org/10.1002/14356007.n10_n05
- Wisconsin Department of Natural Resources. (2019). DNR Runoff Management. CAFO Permittees [[Online; accessed 29-July-2019]].
- Yan, H., & Shih, K. (2016). Effects of calcium and ferric ions on struvite precipitation: A new assessment based on quantitative X-ray diffraction analysis. *Wat. Res.*, 95, 310–318.

6

ANALYSIS OF INCENTIVE POLICIES FOR PHOSPHORUS RECOVERY

6.1 INTRODUCTION

In the context of continuous human population growth, an efficient and sustainable food production system becomes a key factor to guarantee social welfare. Currently, intensive livestock farming produces most of the meat and dairy products worldwide, and the demand is expected to double by 2050 compared to 2007 (Stanford University, 2007). To meet this increasing demand, the development of intensive farming practices has resulted in the concentrated animal feeding operations (CAFOs) (U.S. Department of Agriculture, 2011), which allows larger and cheaper productivity than traditional systems. However, concerns in terms of food safety, animal health, and environmental impacts are associated with intensive livestock farming. Focusing on environmental impacts, livestock industry needs large amounts of water, represents 14.5% of the anthropogenic-based GHG emissions (Eisler et al., 2014), and is a source of nutrient releases which lead to high concentrations of phosphorus in soil and waterbodies (Sampat et al., 2017). Focusing on nutrient pollution, phosphorus releases by improper organic waste management from livestock facilities contribute largely to the eutrophication of fresh and marine waters, promoting harmful algal blooms (HABs) which can release toxins and cause the hypoxia of waterbodies as a result of algae biomass decomposition.

Therefore, the development of sustainable agricultural intensification techniques is not only a desirable but also a necessary measure to reduce the environmental impact of livestock industry while meeting the current and future food demand. In this regard, the implementation of integrated systems for manure management can recover valuable components contained in livestock waste, including phosphorus and biogas-based products, and the environmental footprint of CAFOs is decreased.

From a technical perspective, the adoption of nutrient management systems in CAFOs is feasible, but their practical implementation has to overcome several other logistical and economic barriers. Therefore, developing effective incentive policies to support the economic sustainability of livestock facilities plays a critical role in the successful adoption of phosphorus recovery technologies. This is especially relevant because, despite the additional capital and operating costs these processes entail for the

CAFOs, long-term remediation expense up to 74.5 USD per kg of released phosphorus (Sampat et al., 2021) can be avoided by recovering phosphorus before it reaches soil and waterbodies. Remediation costs are believed to not affect the owners of livestock facilities directly; however, environmental remediation costs are usually covered by public budgets funded by taxpayers, and may lead to the eventual application of specific taxes on livestock products for their environmental footprint. Different incentive schemes can be considered to promote the adoption of sustainable nutrient management systems, including phosphorus releases allowances in the form of P credits and renewable electricity certificates (REC) for energy recovery.

In this work, a systematic analysis of different incentive schemes is performed through a computational framework for the techno-economic analysis of nutrient and energy recovery technologies for livestock facilities. Suitable nutrient and energy recovery technologies are determined for each studied CAFO among the state-of-the-art processes for organic waste management. The effect of different incentive policies on the economic performance of nutrient management technologies is studied considering the environmental vulnerability to nutrient pollution in the Great Lakes area. Additionally, the combination of incentives for the recovery of both phosphorus and electricity has been considered to identify potential synergies between the different technologies involved in the processing of livestock waste. The results obtained allow for the identification of the optimal incentive policies for the implementation of sustainable nutrient management systems at CAFOs as a function of their size, type of animals, and the environmental vulnerability of the area where each studied CAFO is located. In addition, we study the allocation of limited monetary resources using a Nash scheme; this determines the break-even point for the allocation of monetary resources based on the availability of incentives.

6.2 INCENTIVE POLICY ASSESSMENT FRAMEWORK

A two-stage framework is proposed for the evaluation of incentive policies, as shown in Figure 6.1. In the first stage, the size and geographical location of the studied CAFOs are analyzed, selecting the most suitable P recovery process for each CAFO assessed from a pool of six P recovery technologies. We note that these technologies can be implemented either standalone, or integrated with anaerobic digestion (AD) for biogas production. In a second stage, the effect of incentives on the economic performance of the P recovery system recommended is evaluated.

The P recovery selection stage is composed of different models that are fed with data regarding the type and number of animals in the studied CAFO, as well as its geographical location (box *a*). The techno-economic assessment of the different phosphorus recovery technologies, and biogas production in those cases where this process is considered, is performed based on the characteristics of the CAFO (box *b*). Additionally, the assessment of the regional environmental vulnerability to nutrient pollution is carried out in a parallel stage (box *c*). The information returned by these models is normalized and aggregated in a multi-criteria decision analysis (MCDA) model to select the most suitable nutrient management technology for the evaluated livestock facility (box *d*). The stage analyzing the impact of incentives on the economic performance of the nutrient management systems is comprised by an economic model that estimates the profit of the P recovery systems implemented and the total cost of phosphorus recovery. Additionally, a cost-benefit analysis comparing the recovery cost and the economic losses due to nutrient pollution is performed (box *e*).

For the sake of brevity, a brief description of the processes is provided in this section. A detailed description of the framework employed for incentives assessment can be found in Martín-Hernández et al. (2021).

6.2.1 *Assessment of nutrient management systems*

Figure C.8 illustrates the processes considered for livestock waste management. These processes comprise all manure treatment stages from waste collection to phosphorus recovery, including the optional biogas production stages.

6.2.1.1 *Phosphorus recovery systems*

Six state-of-the-art technologies are assessed for phosphorus recovery at CAFOs. These technologies can be classified into three categories, i.e. struvite-based phosphorus recovery (Multiform, Crystalactor, Ostara Pearl, and NuReSys), calcium precipitates-based phosphorus recovery (P-RoC), and physical separation systems (MAPHEX). Table 6.1 summarizes the main parameters of the P recovery technologies assessed. The different processes, including solid-liquid separation, biogas production, and phosphorus recovery systems, are modeled based on first principles, which include mass and energy balances, thermodynamics, and product yield calculations. Additionally, data from manufacturers have been considered when available, particularly for the estimation of capital expenses (CAPEX) and operating expenditures (OPEX). A review and modeling details of the technologies considered can be found in Martín-Hernández et al. (2021).

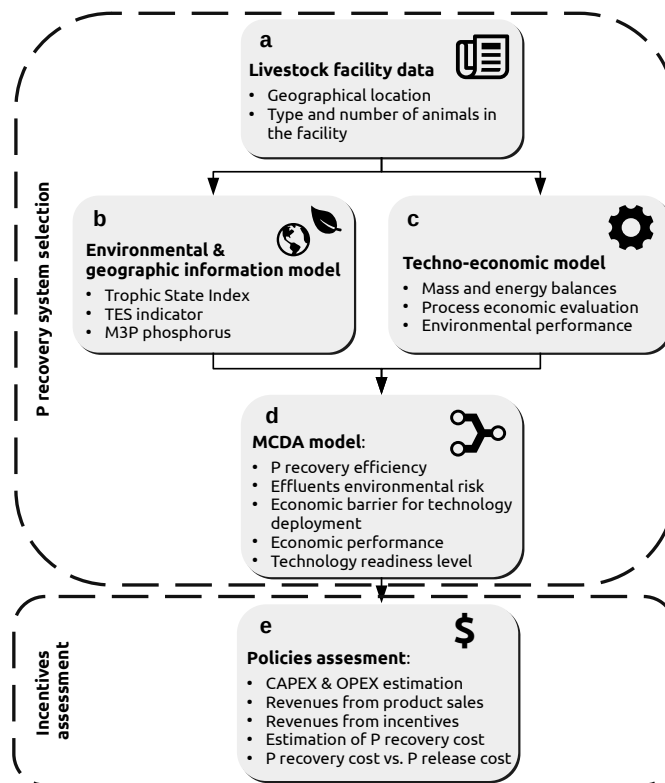


Figure 6.1: Flowchart of the models for selection, sizing, and evaluation of nutrient recovery systems at livestock facilities.

6.2.1.2 Biogas production and upgrading

Nutrient management technologies can be implemented either as standalone systems, or integrated with biogas production and upgrading processes, being both scenarios considered in this work. In scenarios in which the integrated nutrient-energy recovery processes are considered, biogas is produced through AD of cattle waste. In a second stage, biogas impurities (mainly H₂S, NH₃, and moisture) are eliminated, and carbon dioxide is removed using a pressure swing adsorption (PSA) unit. A detailed description for the modeling of AD and biogas purification processes can be found in León and Martín (2016). A comprehensive description for the PSA system and its modeling is shown in Martín-Hernández et al. (2018).

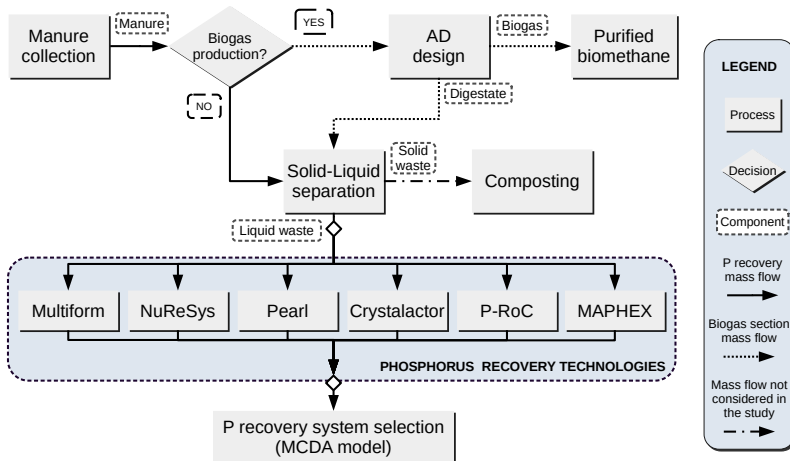


Figure 6.2: Flowchart of the processes evaluated for livestock waste management.

Table 6.1: Description of phosphorus recovery technologies considered in this work. $x_{Ca^{2+}:PO_4^{3-}}$ refers to the Ca^{2+}/PO_4^{3-} molar ratio.

P recovery process	Technology readiness level	Technology type	Phosphorus recovery efficiency (%)	Reference
Multiform	9	Struvite	$\frac{0.798-100}{1 + \left(\frac{x_{Ca^{2+}:PO_4^{3-}} - 0.576}{2.113} \right)}$	(AMPC, 2018)
Crystalactor	9	Struvite	$\frac{0.798-100}{1 + \left(\frac{x_{Ca^{2+}:PO_4^{3-}} - 0.576}{2.113} \right)}$	(Egle et al., 2016)
NuReSys	9	Struvite	$\frac{0.798-100}{1 + \left(\frac{x_{Ca^{2+}:PO_4^{3-}} - 0.576}{2.113} \right)}$	(AMPC, 2018)
Pearl	9	Struvite	$\frac{0.798-100}{1 + \left(\frac{x_{Ca^{2+}:PO_4^{3-}} - 0.576}{2.113} \right)}$	(AMPC, 2018)
P-RoC	6	Calcium precipitates	60	(Ehbrecht et al., 2011)
MAPHEX	7	Modular system based on phases separation	90	(Church et al., 2016)

6.2.2 Environmental vulnerability to nutrient pollution

A geographic information system (GIS) model is developed to estimate the environmental vulnerability to nutrient pollution of the area where each studied CAFO is located. We have considered three dimensions of phosphorus pollution to determine the eutrophication risk in each studied watershed, (i) the average Trophic State Index (TSI) of the waterbodies in the studied area (Carlson, 1977), (ii) the legacy of phosphorus in soils measured by the Mehlich 3 phosphorus (M₃P) concentration (Espinoza et al., 2006), and (iii) the balance between phosphorus releases and uptakes derived from human activities using the the techno-ecological synergy (TES) metric (Bakshi et al., 2015). These parameters have been evaluated at

a sub-basin spatial scale, which corresponds to the HUC8 level defined in the Hydrologic Unit Code (HUC) system (U.S. Geological Survey, 2013). The information retrieved by this environmental GIS-based model is used to set the priority of environmental and economic criteria, as described in the next section. A detailed description of the GIS model used to estimate the vulnerability to nutrient pollution can be found in Martín-Hernández et al. (2021).

6.2.3 *Multi-criteria decision analysis model for the assessment of nutrient management systems*

The model developed for the evaluation of on-site processes for the treatment of livestock waste is based on a multi-criteria decision analysis (MCDA) framework. This framework combines the information from the techno-economic assessment and the local environmental vulnerability to nutrient pollution. Five parameters which can be classified in three dimensions are evaluated to select the most suitable P recovery process for each CAFOs; i.e., (i) environmental dimension assessing the performance of the different technologies to mitigate phosphorus releases from CAFOs, which measured through the fraction of phosphorus recovered by each technology (criterion 1), and the eutrophication potential of its effluents (criterion 2), (ii) the economic performance of the P recovery systems, including the economic barrier for the implementation of P recovery processes measured in terms of capital cost (criterion 3), and the net present value (NPV) of each process (criterion 4), and (iii) the technical maturity of each system, measured through the technology readiness level (TRL) index (criterion 5).

We developed a flexible criteria aggregation method able that balances the operating cost of the systems and the P recovery efficiency as a function of the environmental vulnerability to eutrophication of each region through criteria prioritization. In order to promote the implementation of proven P recovery processes, the TRL index is set as the criteria with highest preference in all cases. Regarding the environmental and economic aspects, environmental criteria are prioritized in the MCDA module if high values for TSI or M₃P are reported for the area of study, which result in severe environmental risk of phosphorus pollution. As a consequence, the selection of phosphorus recovery technologies with larger recovery efficiencies is prioritized even if they incur in larger capital or operating expenses. On the other hand, economic criteria are prioritized for technology selection either of the following situations happens, (a) if the trophic state of waterbodies is oligotrophic or mesotrophic and therefore there is

no immediate eutrophication risk, but phosphorus emissions and uptakes are unbalanced, or (b) no environmental risk is reported.

For each studied CAFO, the normalized criteria are combined following the preference method described above. As a result, we obtain a composite index for each P recovery technology that collects the information of the criteria considered. Based on the value of this composite index, these processes can be compared and ranked, selecting the most suitable system for each studied CAFO. Detailed descriptions for the construction of composite indexes can be found in OECD and European Commission (2008).

In order to achieve a robust decision for the selection of the most adequate phosphorus recovery process, a sensitivity analysis considering different methods for the normalization and aggregation of economic and environmental information is performed (Gasser et al., 2020). A comprehensive description of the MCDA model for the selection of phosphorus recovery systems according to the economic and environmental parameters of each CAFO is collected in Martín-Hernández et al. (2021).

6.2.4 *Types of incentives considered*

The implementation of nutrient recovery incentives in the form of phosphorous credits (P credits) has been studied in this work. In addition, in those scenarios where biogas production is integrated, renewable electricity certificates (REC) are also considered.

P credits can provide a mechanism to promote the recovery of phosphorus that is similar to the carbon credit scheme used in the context of carbon emissions, leading to the development of a credits market around phosphorus releases. The acquisition of P credits can bring allowances for phosphorus releases. Conversely, an entity can obtain income by recovering phosphorus releases, which is the P credits definition considered in this work. Previous efforts to determine the impact of implementing phosphorus recovery incentives for livestock waste management supply chain networks have been addressed by Sampat et al. (2018). An optimal value of 22 USD per kg of phosphorus recovered is proposed to ensure the profitability of nutrient management systems implemented at CAFOs. Additionally, since the deployment of phosphorus recovery systems results in marketable nutrient-rich products in the form of struvite, incomes from the sale of these products are included in the calculation of revenues.

REC incentives for energy recovery provide a fixed remuneration for the electricity produced, which can result in a higher transaction price of electricity to cover the extra production costs and guarantee long-term

price stability. Many different REC values have been proposed by governmental organizations worldwide based on geographical factors and power production capacity (Deremince et al., 2017). Therefore, similar to the electricity market price, a value of 60 USD/MWh, has been considered as baseline price.

6.2.5 Scenarios description

A total of 36 scenarios combining incentives in the form of phosphorus credits (0, 1, 3, 5, 11, and 22 USD/kg_{P recovered}) and for the production of electricity (considering final electricity prices of 30, 60, 75, 90, and 120 USD/MWh) are evaluated for the implementation of nutrient management systems at 2,217 CAFOs in the Great Lakes area. The base value assumed for P credits is 22 USD per kg of phosphorus recovered, based on the work of Sampat et al. (2018). Although this reference value is comparatively large with respect to the price of phosphorus in commercial fertilizer, 1.23 USD/kg P (Index Mundi, 2020), we note that it is significantly lower than the economic losses due to the environmental and social impact of nutrient pollution, estimated to be 74.5 USD per kg of P released (Sampat et al., 2021). Regarding RECs, an average electricity market price of 60 USD/MWh has been selected as the base-scenario. An electricity price below this value, 30 USD/MWh, and three values above the electricity market price, 75, 90, and 120 USD/MWh have been considered. These high REC values are studied due to the need of large incentives for biogas facilities to be economically viable reported by Sampat et al. (2018).

We note that there are two special cases among the scenarios assessed. For those scenarios where P credits are 0, the only income of phosphorus recovery is from the sales of marketable nutrient-rich products in the form of struvite, in addition to the incomes from electricity generated if the corresponding technologies are selected. For those scenarios with an electricity price of 0 USD/MWh, no biogas production and upgrading process is implemented, considering only incomes associated with P credits and struvite sales are considered.

6.2.6 Study Region - The Great Lakes area

The Great Lakes area, shown in Figure 6.3, is considered to study the effect of different incentive policies on P recovery processes. This region collects several factors which make it specially vulnerable to nutrient pollution originated from livestock waste. First, it has a considerable amount of CAFOs, resulting in the generation of large amounts of organic

waste. Second, the fresh waterbodies in the region are key resources, accounting for 21% of the global freshwater supply (U.S. EPA, 2019), providing habitat to a wide range of fauna, and contributing to the local economy through recreational activities. Finally, there exists a continuous increase of cyanobacteria and HABs since the 1960s, especially in the Lake Erie, which is the shallowest lake.

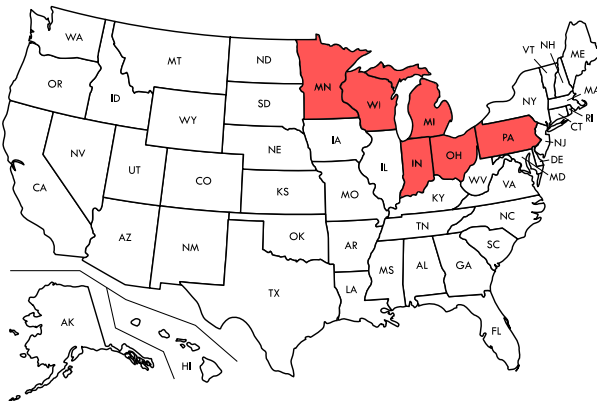


Figure 6.3: States of the Great Lakes region studied in this work.

The CAFOs considered for the deployment of livestock waste treatment processes are those livestock facilities with more than 300 animal units (U.S. Environmental Protection Agency, 2012) reported in the National Pollutant Discharge Elimination System (NPDES) by the US EPA in the Great Lakes area (i.e. Minnesota, Indiana, Ohio, Pennsylvania, Wisconsin, and Michigan). An animal unit is defined as an animal equivalent of 1,000 pounds live weight (U.S. Department of Agriculture, 2011). There are 2,217 CAFOs considered in total. The states of Illinois and New York, as well as the Ontario province in Canada, are not part of this study due to the lack of reliable data about CAFOs. The animal number, manure generated, and phosphorus releases by CAFOs in the studied states are reported in Table C.10.

6.3 RESULTS AND DISCUSSION

6.3.1 Single incentives

In this section, the effect of the implementation of single P credits or REC incentives is studied. The capital and operating costs associated with the installation of P recovery systems if no incentives are considered are reported Martín-Hernández et al. (2021).

Table 6.2: Livestock residues and phosphorus releases by CAFOs in the Great Lakes area.

	Pennsylvania	Ohio	Indiana	Michigan	Minnesota	Wisconsin
Number of CAFOs	131	53	119	144	1,487	283
Total animal units	196,617	128,008	187,355	354,460	943,094	744,015
Dairy animal units (%)	85.06	79.17	81.93	87.90	45.43	98.38
Beef animal units (%)	14.94	20.83	18.07	12.10	54.57	1.62
Manure generated (kt/year)	$2.60 \cdot 10^3$	$1.68 \cdot 10^3$	$2.48 \cdot 10^3$	$4.76 \cdot 10^3$	$1.13 \cdot 10^4$	$1.03 \cdot 10^4$
Phosphorus releases (t/year)	$2.08 \cdot 10^3$	$1.34 \cdot 10^3$	$1.98 \cdot 10^3$	$3.80 \cdot 10^3$	$9.02 \cdot 10^3$	$8.20 \cdot 10^3$
Reference	1	2	3	4	5	6

¹ (Pennsylvania Department of Environmental Protection, 2019)

² (Ohio Department of Agriculture, 2019)

³ (Indiana Department of Environmental Management, 2019)

⁴ (Michigan Department of Environment, Great Lakes, and Energy, 2019)

⁵ (Minnesota Center for Environmental Advocacy, 2019)

⁶ (Wisconsin Department of Natural Resources, 2019)

6.3.1.1 Effect of P credits

The effect of applying P credits on the economic performance of nutrient management systems has been studied. Revenues from struvite sales are also considered in those CAFOs installing struvite production technologies. Since in this first scenario only the effect of P credits is studied, incomes from electricity production are excluded; and therefore, the nutrient management systems are not integrated with biogas production. The effect of the value of P credits over the profitability of the nutrient recovery systems is shown in Fig 6.4a, where the distribution of CAFOs size is shown using boxplots. It can be observed that, for P credits values strictly below 11 USD per kg of recovered phosphorus, the proportion of profitable P recovery processes (those installed processes whose incomes are larger than the operating expenses) is small and constant. However, when the value of the incentive is set at 11 USD per kg of recovered phosphorus, the increase in the number of profitable processes is very significant for all states except Minnesota, which CAFOs median size is the smallest. For states with large CAFOs, i.e. Michigan, Ohio and Wisconsin, the percentage of profitable processes can reach around 80% under high P credits; while for Indiana and Pennsylvania, with medium-size CAFOs, around 40% are profitable. For P credits of 22 USD per kg of recovered phosphorus, there is an additional 25% increase of profitable nutrient recovery systems in those states

with large CAFOs. In the states with medium size CAFOs the increase of profitable processes is also very significant, reaching approximately 80% of the studied CAFOs. Finally, for the case of Minnesota, there is a large increase in the profitable P recovery systems installed as well, reaching near the 60% of the CAFOs studied.

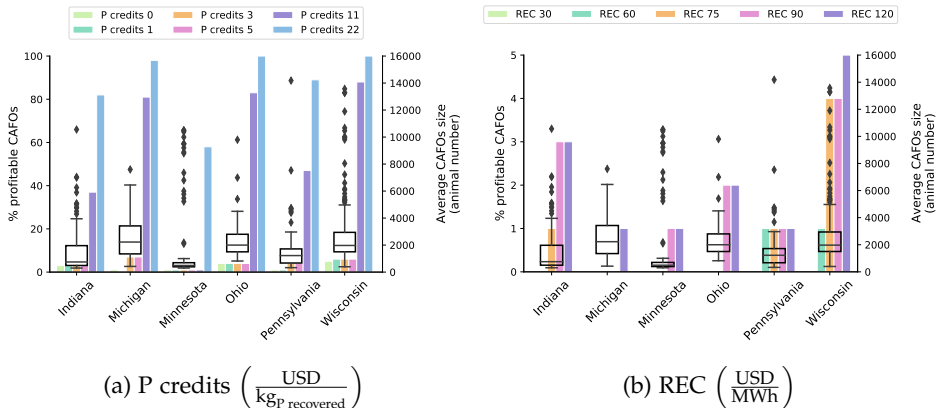


Figure 6.4: Distribution of profitable phosphorus recovery processes in the Great Lakes area for the scenarios considering phosphorus credits and renewable energy credits. The box-plots represent the distribution of CAFOs size in each state.

6.3.1.2 Effect of renewable energy certificates

The effect of REC in the implementation of P recovery systems is studied in this section. Integration of biogas production with P recovery processes is considered in all the cases studied in this scenario. In addition to revenues obtained from RECs, incomes from the sales of struvite produced by the phosphorus recovery processes have been considered as well. The effect of P credits is excluded in this scenario.

Figure 6.4b shows the percentage of profitable P recovery processes for each studied state together with the distribution of the size of CAFOs. As it can be observed, the impact of the incomes from electricity in the economic performance is much less significant than the effect of P credits given the incentive ranges considered. Only the largest CAFOs, most of which represent outliers in the distribution of CAFOs size, are profitable when prices equal to or above 75 USD/MWh are considered. The large CAPEX prevent the economic feasibility of biogas production in small and medium CAFOs. Therefore, only large-scale CAFOs can benefit from the operation of biogas processes to cover the cost of P recovery systems via biogas-based electricity production.

6.3.2 Combined effect of incentives for phosphorus and renewable electricity recovery

Synergies derived from the combination of P credits and RECs might be obtained when integrating phosphorus recovery technologies with biogas production and upgrading processes. However, since the deployment of the biogas processes involves large investments and considerable operating costs, a detailed analysis must be conducted to identify the most cost-effective incentives policy.

The results obtained from combining the incentive schemes described in previous sections are shown in Figure 6.5. The fraction of profitable processes is shown in Figure 6.5a, which are defined as those CAFOs with positive net incomes. It can be observed that, if the value of P credits and RECs are set similar to the market prices (i.e. 1 USD/kg_{P recovered} and 60-75 USD/MWh respectively), the fraction of profitable processes is very low. Wisconsin is the state with the largest share of profitable P recovery processes under this scenario, which is 4-5% of the total CAFOs.

Phosphorus credits have a larger impact on the profitability of nutrient management systems, near to 100% for P credits of 22 USD/kg_{P recovered} for states with large CAFOs (i.e. Michigan, Ohio and Wisconsin). The price of electricity has a weak influence on the profitability of the deployed systems in these scenarios. For states with medium-size CAFOs, Indiana and Pennsylvania, the share of profitable processes is around 80-85%. For Minnesota, which is the state with the smallest median CAFOs size, the share is 58%. Therefore, the installation of AD processes has a significantly negative impact in the states with small and medium size CAFOs due to the lack of economies of scale. A similar behavior is found when the value of phosphorus credits is reduced to 11 USD/kg_{P recovered}.

This pattern is reverted when P credits of 3-5 USD/kg_{P recovered} are considered. For these scenarios the share of profitable processes is considerably reduced compared to the previous scenarios. Actually, for Indiana, Minnesota, and Ohio, there is no difference between setting phosphorus credits incentives below 5 USD/kg_{P recovered} and the case considering no P credits (where the only income of phosphorus recovery is from the sales of nutrient-rich products obtained). However, in all states except Minnesota, the amount of profitable systems increases for electricity prices larger than 60 USD/MWh, reaching a share of P recovery processes with positive net incomes up to 22 % for Michigan. For the scenario considering P credits of 1 USD/kg_{P recovered}, only Ohio shows a slight improvement in the fraction of profitable facilities if the production of electricity is also considered. Therefore, there is a threshold for P credits between 1 and 3 USD/kg_{P recovered} below which no improvement in the fraction of profitable

P recovery systems is observed. For those scenarios where no incentive for phosphorus recovery is considered, the results obtained have been previously described in Section 6.3.1.2. It is interesting to note, as a consequence of the large capital and operating expenses of AD processes, the economic performance of the scenarios considering only P recovery systems is at least as profitable as the profitability of the scenarios considering biogas generation associates the largest REC incentives.

The net treatment cost per ton of manure processed captures the perspective of CAFOs owners on P recovery. It is defined as the difference between the revenues (sum of struvite sales, R_c (USD/year), and incentives, I_c (USD/year)) and the operating expenditures of livestock treatment processes, $OPEX_c$ (USD/year), as shown in Eq. 6.1. F_{manure_c} denotes the mass flow of manure processed in ton/year.

$$\text{Net treatment cost}_c \left(\frac{\text{USD}}{\text{t}_{\text{manure}}} \right) = \frac{R_c + I_c - OPEX_c}{F_{\text{manure}_c}} \quad (6.1)$$

The results obtained in terms of net treatment cost are illustrated in Figure 6.5b. These show a base cost for the recovery of phosphorus between 5.81 and 12.47 USD per ton of processed manure if no incentives or anaerobic digestion stages are considered. From this base case, it can be observed that the costs vary following the same pattern as the fraction of profitable processes described previously. The installation of biogas processes is not profitable by itself, increasing the processing costs by 1.2-1.9 times over the base case if no P credits are considered, and it is only beneficial for specific scenarios which have large size CAFOs, and moderate P credits (>3 USD/kg_{P recovered}) and electricity incentives (>60 USD/MWh). The scenarios combining states with large CAFOs and high value for P credits, and the optional production of renewable energy from biogas result in negative processing costs. This means that phosphorus recovery results in profits for the CAFO. We note that, as the analysis of the different scenarios is carried out at the state level, a negative processing cost indicate that, under certain schemes for incentives, the profitable P recovery processes are able to balance out the non-profitable ones in the state.

It is worth noting that the results reveal that in the largest CAFOs the recovery of phosphorus is more feasible, due to the economies of scale. At the same time, however, these large-scale CAFOs also represent the major environmental threats due to the release of larger amounts of phosphorus.

6.3.3 Environmental cost-benefit analysis

CAFOs are an environmental concern in terms of nutrient pollution as a consequence of the high spatial concentration of animals, resulting in large releases of phosphorus. The long-term environmental impact of phosphorus releases result in large economic losses, accounting for the remediation cost of environmental degradation and the economic impact on the local population affected by HABs. Therefore, an analysis for the cost-effectiveness of the total cost involved in phosphorus recovery, including the amortization of the investment, operating costs, and total cost of incentives, can show the economic advantages of phosphorus recovery.

$$\text{Total treatment cost}_c \left(\frac{\text{USD}}{\text{kg}_P \text{ recovered}} \right) = R_c + I_c + OPEX_c \quad (6.2)$$

Figure 6.6 shows the total cost of phosphorus recovery under different policies, defined in Eq. 6.2, compared with the economic losses due to phosphorus releases into the environment. It can be observed that all scenarios studied result in a phosphorus recovery cost lower than the economic losses due to phosphorus releases, estimated in 74.5 USD per kg of phosphorus released by Sampat et al. (2021). Phosphorus recovery is, therefore, more cost-effective than its release to the environment. The lowest total cost for phosphorus recovery is obtained in the scenario not involving any incentive (REC: o - PC: o), resulting in costs between 3 and 5 times lower than the economic cost of phosphorus release to the environment. The application of incentives increases the total monetary cost of phosphorus recovery, mainly driven by the application of phosphorus credits. However, since incentives are an income for the owners of livestock facilities, the economic cost of nutrient management systems for the owners of CAFOs is progressively reduced, increasing the number of profitable P recovery systems, and reducing the recovery cost of phosphorus, as it is shown in Fig. 6.5.

The role of the size of CAFOs in the cost of phosphorus recovery can be also observed in this study. Accordingly with the results shown in previous sections, those states with larger average size of CAFOs, such as Wisconsin, Ohio, and Michigan, have recovery costs significantly lower than the states where medium and small size CAFOs are predominant. It is worth noting that the total cost of phosphorus recovery is lower than the economic losses due to the release of phosphorus to the environment for all the evaluated states and policies.

6.3.4 Fair distribution of incentives

The effect of different incentive schemes has been previously discussed, revealing that the P recovery systems in small CAFOs require significant economic support in the form of incentives to balance the monetary losses, while in the largest CAFOs these systems can be self-profitable. This situation leads to the problem of the fair distribution of available incentives, which is particularly relevant in the case that the available budget is not sufficient to cover the operating expenses of the unprofitable P recovery processes. In this section, the minimum necessary incentives for all P recovery systems in the studied area to reach the economical neutrality (i.e., no economic profits or losses are obtained) is firstly determined. In a second stage, a fairness-guided distribution of incentives among CAFOs is studied when the available incentives are lower than the monetary amount determined, i.e., they are not sufficient to cover the operating expenses of unprofitable processes. Due to the marginal benefits obtained by installing AD processes, as described in Section 6.3.2, the implementation of only P recovery systems is assumed in both studies, and therefore only incentives for P recovery are considered.

The minimum cost of incentives necessary for covering the economic losses of unprofitable processes, estimated in 222.6 million USD, is determined through the formulation of an optimization problem. The objective function of this problem minimizes the incentives used, Eq. 6.3a, subject to achieve the economical neutrality, Eq. 6.3b. Here, \mathcal{C} denotes the set of CAFOs studied, I_c the incentives allocated, and $OPEX_c$ and R_c the operating expenses and revenues of the P recovery system installed in each CAFO c respectively.

$$\min \sum_{c \in \mathcal{C}} I_c \quad (6.3a)$$

$$\text{s.t. } I_c + R_c - OPEX_c \geq 0 \quad (6.3b)$$

The results obtained, shown in Figure 6.7, reveal the crucial role of the economies of scale in the amount of incentives that must be deployed to cover the economic losses of P recovery systems. We note that the discrepancies of incentives for CAFOs of similar size that can be observed in the figure are due to different technology installed. The selection of different P recovery processes for CAFOs of similar size is based on the eutrophication risk of each watershed, as described in Martín-Hernández et al. (2021). It can also be observed the 99.9% of CAFOs require incentives below the P releasing cost to the environment. A correlation to estimate the amount of incentives needed to cover the operating expenses as a function

of CAFOs capacities is proposed in Eq. 6.4 , where AU_c denotes the animal units of CAFO c .

$$I_c \left(\frac{\text{USD}}{\text{kg P}} \right) = \frac{3.383 \cdot 10^6}{1 + (AU_c \cdot 2.223 \cdot 10^5)^{0.647}} \quad (6.4)$$

The fair allocation of incentives when the monetary amount available is not sufficient to cover the expenses of all P recovery processes has been addressed by using the Nash allocation scheme. The Nash approach has been selected because this scheme is able to capture the scales of the different stakeholders (CAFO facilities) in order to achieve a fair distribution of a certain resource (incentives), as it was demonstrated by Sampat and Zavala (2019). This scheme is formulated in Eqs. 6.5a-6.5b, where $I_{\text{available}}$ denotes the available incentives.

$$\max \sum_{c \in \mathcal{C}} \ln (I_c + R_c - OPEX_c) \quad (6.5a)$$

$$\text{s.t. } \sum_{c \in \mathcal{C}} I_c \leq I_{\text{available}} \quad (6.5b)$$

Figure 6.8a illustrates the distribution of incentives as a function of the net revenues of the P recovery system installed in each CAFO c before any incentive is applied, Eq 6.6.

$$\text{Net revenue before incentives}_c \left(\frac{\text{USD}}{\text{year}} \right) = R_c - OPEX_c \quad (6.6)$$

The cases where the available budget are the 10%, 30%, 50%, 70%, and 100% of the incentives needed to cover the economic losses of unprofitable CAFOs are analyzed (22.3, 66.8, 111.3, 155.8 and 222.6 MM USD respectively). The last case is equivalent to the scenario studied above. It can be observed that the available incentives are allocated accordingly to the net revenues of each CAFO, promoting the allocation of larger incentives to the less profitable P recovery processes. Since the available incentives are limited, a break-even point determining the profitability level of the P recovery systems below which the incentives should be allocated is set for each scenario. As a result, the fewer incentives available, the more restrictive the break-even point is. Additionally, it can be observed that the displacement of the break-even points is progressively reduced as the available incentives increase, resulting in a marginal improvement between the scenarios considering the 50% and 70% of the economic resources needed to guarantee the economic neutrality of the nutrient management

systems. In Figure 6.8b we observe that, for each case evaluated, the allocation of limited incentives under the Nash scheme result in a uniform net revenue for those CAFOs receiving incentives. Additionally, we note that the economic losses have been mitigated in these facilities by the allocation of incentives. However, they are unable to be profitable due to the limited budget available. In addition, a correlation to estimate the fairness point as a function of available incentives has been developed based on these results, Eq. 6.7.

$$\text{Break-even point}_c \left(\frac{\text{USD}}{\text{year}} \right) = -2.482 \cdot 10^5 \cdot (0.955^{(R_c - OPEX_c)}) \quad (6.7)$$

6.4 CONCLUSIONS

The application of different incentives to promote the implementation of nutrient management systems at CAFOs is studied in this work, including the potential integration of phosphorus recovery technologies with the production of renewable electricity from biogas.

The results reveal that the recovery of phosphorus is more economically feasible in the largest CAFOs due to the economies of scale. The deployment of phosphorus recovery processes is self-profitable through struvite sales only for the largest P recovery processes, which represent less than the 5 % over the total CAFOs in all the studied states. However, the application of P credits increases the fraction of profitable processes around to 100% in the states with large-size CAFOs (Michigan, Ohio and Wisconsin), and up to 80% for the states with medium-size CAFOs (Indiana and Pennsylvania). The integration of phosphorus recovery technologies with anaerobic digestion and biogas upgrading processes does not result in any practical improvement in terms of economic performance unless incentives for phosphorus recovery are considered, since the revenues from electricity sales can not cover the investment and operating cost of these processes given current market values.

The total cost of phosphorus recovery, including the investment amortization, operating costs, and total cost of incentives is lower than the long-term economic losses due to phosphorus pollution for all the evaluated states and policies, proving that sustainable nutrient management systems are economically and environmentally beneficial. Correlations to estimate the incentives necessary for P recovery systems to achieve economic neutrality has been also proposed. Additionally, the fair distribution of limited incen-

tives has been studied, determining the break-even point for the allocation of monetary resources based on the availability of incentives.

Future work is aimed at assessing the effect of biomethane production in the economy of the waste treatment systems, and the integration within a logistics network model for the developing of nutrient pollution and ecosystem integrated responses at regional spatial resolution.

ACKNOWLEDGMENTS

This research was supported in part by an appointment for E.M.H. to the Research Participation Program for the Office of Research and Development, US EPA, administered by the Oak Ridge Institute for Science and Education through Interagency Agreement No. DW-89-92433001 between the US Department of Energy and the US Environmental Protection Agency. E.M.H. and M.M. acknowledge funding from Junta de Castilla y León, Spain, under grant SA026G18 and grant EDU/556/2019. Y.H. and V.M.Z. acknowledge funding from the U.S. Department of Agriculture, National Institute of Food and Agriculture, under grant number 2017-67003-26055.

Disclaimer: The views expressed in this article are those of the authors and do not necessarily reflect the views or policies of the U.S. EPA. Mention of trade names, products, or services does not convey, and should not be interpreted as conveying, official U.S. EPA approval, endorsement, or recommendation.

BIBLIOGRAPHY

- AMPC. (2018). Struvite or Traditional Chemical Phosphorus Precipitation – What Option Rocks? [[Online; accessed 20-March-2019]].
- Bakshi, B., Ziv, G., & Lepech, M. (2015). Techno-ecological synergy: A framework for sustainable engineering. *Environ. Sci. Technol.*, 49(3), 1752–1760.
- Carlson, R. E. (1977). A trophic state index for lakes: Trophic state index. *Limnol. Oceanogr.*, 22(2), 361–369. <https://doi.org/10.4319/lo.1977.22.2.0361>
- Church, C. D., Hristov, A. N., Bryant, R. B., Kleinman, P. J. A., & Fishel, S. K. (2016). A Novel Treatment System to Remove Phosphorus from Liquid Manure. *Appl. Eng. Agric.*, 32(1), 103–112. <https://doi.org/10.13031/aea.32.10999>
- Dereminice, B., Scheidl, S., Stambasky, J., & Wellinger, A. (2017). *Data bank with existing incentives and subsequent development of biogas plants compared to national targets* (tech. rep.). European Biogas Association).

- Egle, L., Rechberger, H., Krampe, J., & Zessner, M. (2016). Phosphorus recovery from municipal wastewater: An integrated comparative technological, environmental and economic assessment of P recovery technologies. *Science of The Total Environment*, 571, 522–542. <https://doi.org/10.1016/j.scitotenv.2016.07.019>
- Ehbrecht, A., Schönauer, S., Fuderer, T., & Schuhmann, R. (2011). P-Recovery from sewage by seeded crystallisation in a pilot plant in batch mode technology. *Water Science and Technology*, 63(2), 339–344. <https://doi.org/10.2166/wst.2011.061>
- Eisler, M. C., Lee, M. R. F., Tarlton, J. F., Martin, G. B., Beddington, J., Dungait, J. A. J., Greathead, H., Liu, J., Mathew, S., Miller, H., Misselbrook, T., Murray, P., Vinod, V. K., Van Saun, R., & Winter, M. (2014). Agriculture: Steps to sustainable livestock. *Nature News*, 507(7490), 32. <https://doi.org/10.1038/507032a>
- Espinoza, L., Slaton, N. A., & Mozaffari, M. (2006). *Understanding the numbers on your soil test report* (tech. rep.). Cooperative Extension Service, University of Arkansas.
- Gasser, P., Suter, J., Cinelli, M., Spada, M., Burgherr, P., Hirschberg, S., Kadziński, M., & Stojadinović, B. (2020). Comprehensive resilience assessment of electricity supply security for 140 countries. *Ecological Indicators*, 109. <https://doi.org/10.1016/j.ecolind.2019.105731>
- Index Mundi. (2020). Triple Superphosphate Monthly Price - US Dollars per Metric Ton [[Online; accessed 05-May-2020]].
- Indiana Department of Environmental Management. (2019). Confined Feeding Operation Facilities (20200402) [[Online; accessed 29-July-2019]].
- León, E., & Martín, M. (2016). Optimal production of power in a combined cycle from manure based biogas. *Energy Conv. Manage.*, 114, 89–99.
- Martín-Hernández, E., Martín, M., & Ruiz-Mercado, G. (2021). A geospatial environmental and techno-economic framework for sustainable phosphorus management at livestock facilities [(In Press)]. *Resources, Conservation & Recycling*.
- Martín-Hernández, E., Sampat, A., Zavala, V., & Martín, M. (2018). Optimal integrated facility for waste processing. *Chem. Eng. Res. Des.*, 131, 160–182.
- Michigan Department of Environment, Great Lakes, and Energy. (2019). Active NPDES Permits [[Online; accessed 29-July-2019]].
- Minnesota Center for Environmental Advocacy. (2019). Minnesota Confined Animal Feeding Operations [[Online; accessed 29-July-2019]].
- OECD and European Commission. (2008). *Handbook on Constructing Composite Indicators. Methodology and User Guide*. OECD.

- Ohio Department of Agriculture. (2019). Livestock Environmental Permitting.
- Pennsylvania Department of Environmental Protection. (2019). Concentrated Animal Feeding Operations [[Online; accessed 29-July-2019]].
- Sampat, A., Hicks, A., Ruiz-Mercado, G. J., & Zavala, V. M. (2021). Valuing economic impact reductions of nutrient pollution from livestock waste. *Resources, Conservation and Recycling*, 164, 105199. <https://doi.org/https://doi.org/10.1016/j.resconrec.2020.105199>
- Sampat, A., Martín, E., Martín, M., & Zavala, V. (2017). Optimization formulations for multi-product supply chain networks. *Comput. Chem. Eng.*, 104, 296–310.
- Sampat, A., Ruiz-Mercado, G., & Zavala, V. (2018). Economic and Environmental Analysis for Advancing Sustainable Management of Livestock Waste: A Wisconsin Case Study. *ACS Sustainable Chemistry & Engineering*, 6(5), 6018–6031.
- Sampat, A., & Zavala, V. (2019). Fairness measures for decision-making and conflict resolution. *Optimization and Engineering*, 20(4), 1249–1272.
- Stanford University. (2007). Harmful Environmental Effects Of Livestock Production On The Planet 'Increasingly Serious,' Says Panel [[Online; accessed 21-November-2019]].
- U.S. Department of Agriculture. (2011). Animal Feeding Operations (AFO) and Concentrated Animal Feeding Operations (CAFO) [[Online; accessed 10-August-2020]].
- U.S. Environmental Protection Agency. (2012). *Regulatory Definitions of Large CAFOs, Medium CAFO, and Small CAFOs* (tech. rep.). U.S. EPA.
- U.S. EPA. (2019). Facts and Figures about the Great Lakes [[Online; accessed 22-November-2019]].
- U.S. Geological Survey. (2013). *Federal Standards and Procedures for the National Watershed Boundary Dataset (WBD)* (tech. rep.). U.S. Geological Survey.
- Wisconsin Department of Natural Resources. (2019). DNR Runoff Management. CAFO Permittees [[Online; accessed 29-July-2019]].

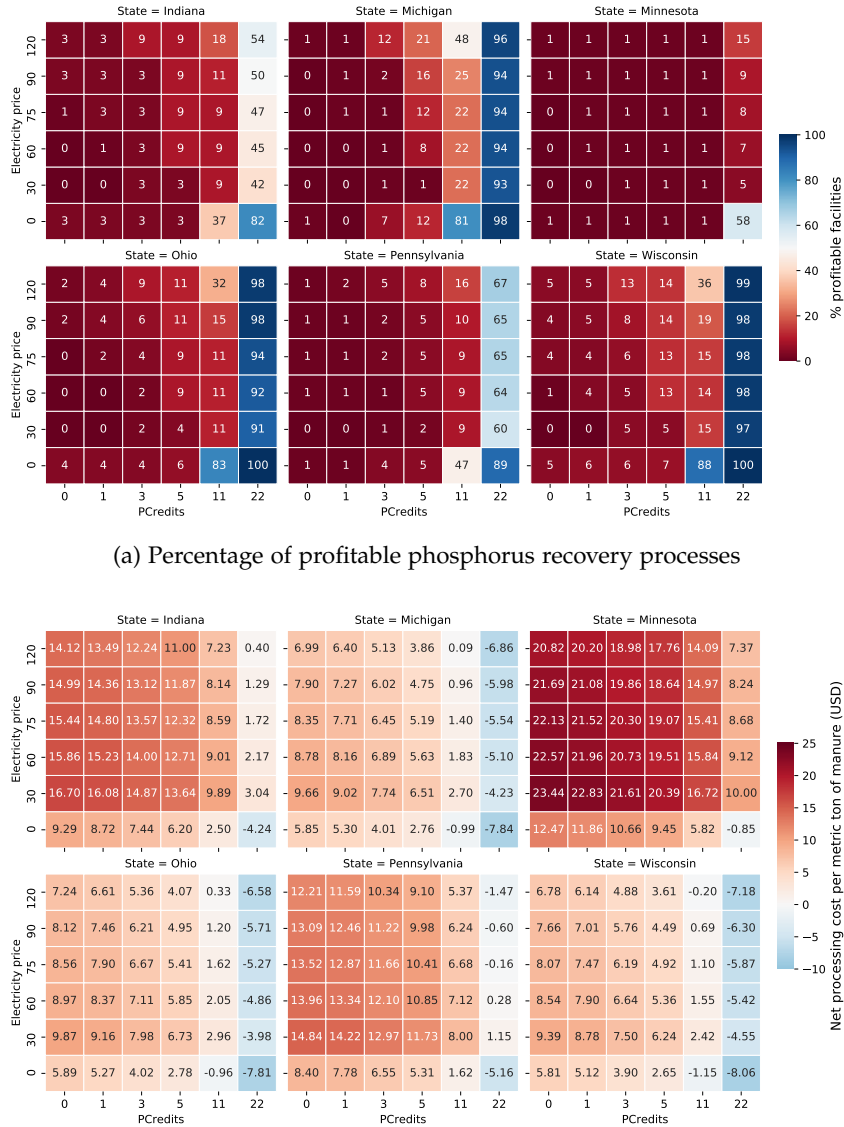


Figure 6.5: Economic evaluation of P recovery processes for the different incentives scenarios studied

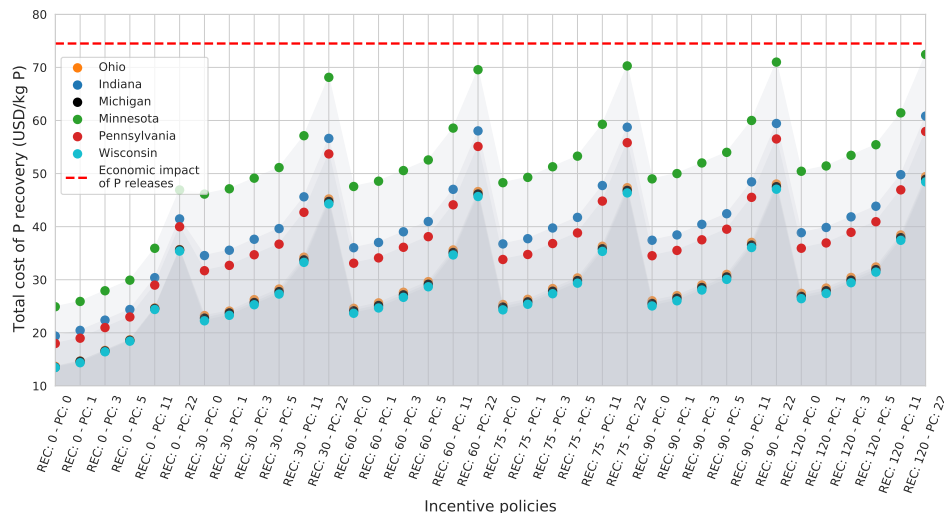


Figure 6.6: Comparison of the total cost of phosphorus recovery for each scenario assessed and the environmental remediation cost due to phosphorus releases. REC denotes the electricity incentive values considered in USD/MWh, and PC denotes the value of phosphorus credits in USD/kg_P recovered. The red dotted line represents the economic losses due to phosphorus releases to the environment.

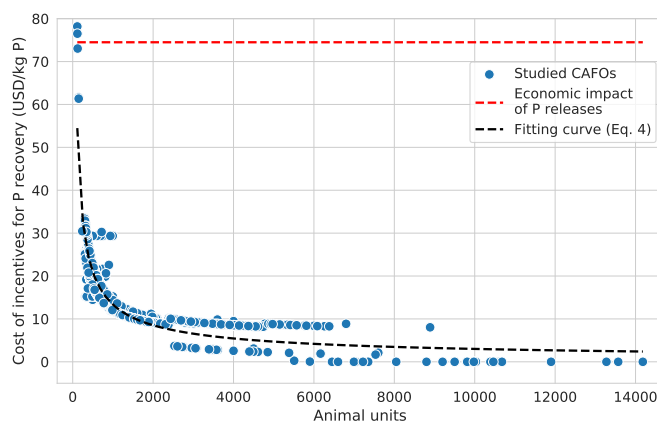


Figure 6.7: Allocation of incentives for achieving the economic neutrality of nutrient recovery systems minimizing the total cost of incentives.

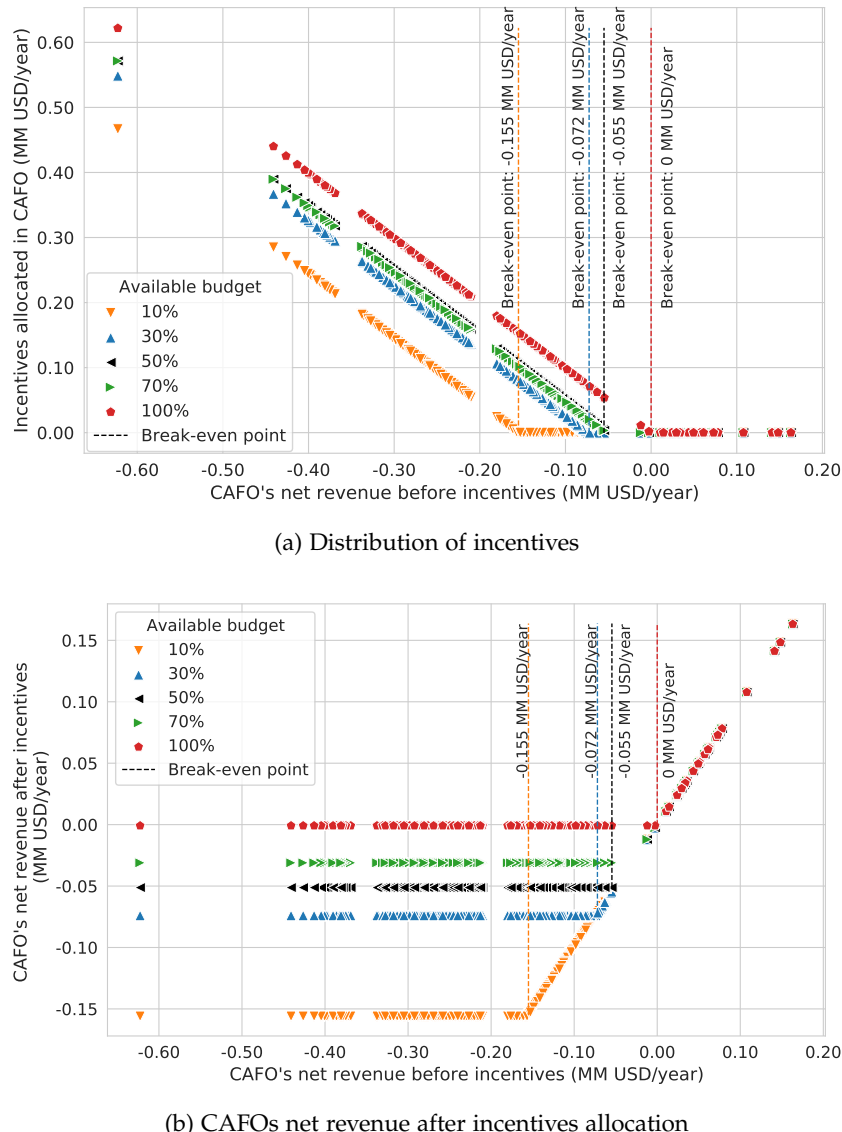


Figure 6.8: Distribution of incentives considering the Nash allocation scheme. Scenarios assuming available incentives equal to the 10%, 30%, 50%, 70%, and 100% of the incentives needed to cover the economic losses of unprofitable P recovery systems in the Great Lakes area are illustrated.

Part II

NITROGEN MANAGEMENT AND RECOVERY

Part III

INTEGRATION OF ANAEROBIC DIGESTION AND NUTRIENT MANAGEMENT SYSTEMS

OPTIMAL TECHNOLOGY SELECTION FOR THE BIOGAS UPGRADING TO BIOMETHANE

ADD NOMENCLATURE
UPDATE LETTER OF SUP MAT REFERENCES

7.1 INTRODUCTION

Modern societies are characterized by the generation of large amounts of waste, arising from the manufacturing and production of goods and services to satisfy social demands. The traditional manufacturing model is one-way linear, starting with the extraction of the raw material from the environment, the manufacturing process, the use of the manufactured goods, and the final disposal of these goods, discarding the residues generated along the linear path. In addition, each of these stages involves energy consumption. According to the World Commission on Environment and Development (WCED) (1987), the one-way linear manufacturing process is an unsustainable production model, depleting natural resources and degrading the environment. The large amount of residues generated is a challenge in terms of treatment, but at the same time, it presents an opportunity towards the production of sustainable resources and energy through the development of circular economies around them (World Energy Council, 2016). Therefore, waste-to-energy initiatives have gained support towards sustainability (Korhonen et al., 2018). Among the treatment technologies for organic waste, anaerobic digestion is deemed promising as a renewable source of CH₄ and CO₂ for the production of biogas. Several studies have evaluated the use of the biogas for different purposes, including the production of chemicals. However, since the production cost of chemicals from biogas is high, the biogas is typically used as energy source.

Biogas can be used directly in gas turbines (Somehsaraei et al., 2014), or in generators (Reddy et al., 2016). However, the large infrastructure available for the transport and use of natural gas in Europe (European network of transmission system operators for gas (Entossg), 2015) and the United States (U.S. Energy Information Administration (EIA), 2019a) suggests the purification of the biogas, also referred to as upgrading, into a composition similar to natural gas. The amount of residues available

provides the capability of substituting non-renewable natural gas with biomethane in large regions, such as in Castile and Leon (Spain), where the amount of municipal solid wastes (MSW) available can cover the regional demand for natural gas (Taifouris & Martin, 2018). There are several technologies to achieve this purpose, including hydrogenation or CO₂ removal.

On the one hand, it is possible to hydrogenate the CO₂ contained in biogas into methane (Stangeland et al., 2017). However, the main issue is the high cost of producing hydrogen from renewable energy sources, such as wind (Davis & Martín, 2014b) or solar energy (Davis & Martín, 2014a), resulting in non-competitive costs of biomethane (Curto & Martín, 2019) but in particular regions of high availability of solar or wind (de la Cruz & Martín, 2016). Alternatively, direct methanation of CO₂ within the digester has also been studied at laboratory scale (Tynjala, T., 2015).

On the other hand, several CO₂ capture technologies can be used to remove the carbon dioxide within the biogas obtaining high purity biomethane. A number of reviews have been published describing different CO₂ capture processes, including general perspectives (Adamu et al., 2020), specific reviews for pre and postcombustion gases (MacDowell et al., 2010) and biogas upgrading processes (Adnan et al., 2019; Miltner et al., 2017). Techno-economic assessments and life cycle analysis for different technologies have been performed including membranes processes (Fang et al., 2018), adsorption and its comparison with membranes (Giordano et al., 2018), chemical absorption (Morero et al., 2017), and biogas methanation (Curto & Martín, 2019), even comparing amines with ex-situ methanation (Vo et al., 2018). Furthermore, the liquefaction of biomethane has attracted the interest of researchers since, similar to liquefied conventional natural gas, it can be easily transported (Qyyum et al., 2020). However, the selection of the optimal technology for CO₂ capture has only been addressed in the context of post-combustion processes where membranes (Gassner et al., 2009), chemical absorption (Hasan et al., 2012a), or PSA (Hasan et al., 2012b) have been evaluated individually, or within a process design problem from the economic point of view (Klemeš et al., 2007). Additionally, comparisons among different materials/solvents for the same capturing technology to determine the optimal configuration are also available, such as different membrane configurations based on simulation (Makaruk et al., 2010) and optimization (Gilassi et al., 2019) approaches, or different solvents (Lee et al., 2013). Nonetheless, recently a few recent works carried out systematic comparisons of different processes, such as the work of Pellegrini et al. (2018), where a comparison of cryogenic and amine scrubbing technologies is presented. However, this work extends the comparison to all mature CO₂ capture technologies within

the context of an entire facility for production and upgrading of biogas. Therefore, there exists a gap in the literature regarding the determination of the optimal technology for biomethane production. It should be noted that, while biomethane upgrading technologies are similar to post-combustion capture processes, the CO₂ concentration in biogas is higher. Therefore, the results of the studies developed for post-combustion gases cannot be directly extrapolated to the biogas case.

This work presents a systematic framework to evaluate different technologies for biogas upgrading from a conceptual point of view, focusing on CO₂ capture processes. A hybrid heuristic-mathematical modelling approach has been developed to consider different technology configurations. In addition, an economic analysis for the production of biomethane considering four wastes (cattle manure, swine manure, municipal food waste, and sludge) has been carried out to evaluate the economic feasibility of these processes. The selection of these waste is based on the large availability and amount produced by society that constitute a challenge in waste management. The rest of the paper is organized as follows: Section 7.2 presents the methodology for technology selection. Section 7.3 describes the modelling of the alternative upgrading technologies. Section 7.4 shows the results of the analysis, including the specifications for the optimal technology selected for biogas upgrading, as well as the economic evaluation results. Additionally, carbon dioxide capture will be compared with the hydrogenation of CO₂ for further reference on the cleaner process for biomethane production. Finally, Section 7.5 draws the conclusions.

7.2 METHODOLOGY FOR PROCESS DESIGN

The entire facility for the production and upgrading of biogas is comprised of three stages: the anaerobic digestion stage, where the organic matter fraction of the waste treated is decomposed producing biogas, the initial biogas conditioning stage, where H₂S and ammonia are removed, and the purification step that removes the CO₂ to reach enough purity to be injected into the grid. Therefore, the lower limit specified for the final purity of the biomethane is a CH₄ concentration equal to 98% in order to ensure compliance with current regulations Spanish Ministry of Industry, Energy and Tourism (2013).

Anaerobic digestion transforms the organic matter into biogas and a residue, digestate. Digestate is a material rich in nutrients León and Martín (2016), particularly nitrogen and phosphorus, that can be further used as fertilizers. Biogas is a mixture of CO₂ and methane, including smaller quantities of impurities such as ammonia, nitrogen, hydrogen sulphide,

and water. These impurities are removed from the biogas using reactive beds for the H_2S , adsorption for ammonia and nitrogen and condensation for water removal. Finally, a set of technologies for the removal of carbon dioxide are evaluated using a hybrid heuristic-mathematical optimization methodology. This methodology, as shown in Fig. 7.1, starts with a screening stage based on information and data reported in literature, selecting the CO_2 capture technologies, and their technical configurations regarding different solvents, adsorbent media and membrane materials, which are more feasible to adapt to the biomethane production process. Secondly, a mathematical optimization stage determines the optimal configuration among the alternatives available for each technology. Finally, a superstructure model joining the models of biogas production, purification, and the different upgrading processes is formulated as a nonlinear programming problem (NLP) problem Trespalacios and Grossmann (2014) to select the optimal upgrading process. Once the optimal biogas upgrading is determined, a rigorous simulation should be performed for the selected process before plant design. However, the scope of this work is limited to the selection of the optimal upgrading technology for bio-methane production from biogas.

This process will be evaluated for four waste sources: cattle and swine manure, municipal food waste, and sludge. The CO_2 captured, even if it may need further purification, is to be used within the context of carbon capture and utilization for the production of chemicals or in other industries. Table 7.1 shows the average composition of the four waste types analyzed.

Table 7.1: Characteristics of the four waste types evaluated.

	Cattle manure (European Commission-Directive-General for Environment, 2011)	Swine manure (European Commission-Directive-General for Environment, 2011; Iepson, 2010)	Sludge (European Commission-Directive-General for Environment, 2011)	Urban food waste (European Commission-Directive-General for Environment, 2011)
$V_{\text{biog}} \text{ (m}^3/\text{kg})$	0.25	0.25	0.25	0.44
$w_{\text{H}_2\text{O}} \text{ (% wt)}$	0.25	0.25	0.17	0.31
$w_{\text{NH}_3} \text{ (% dry wt)}$	0.08	0.29	0.04	0.95
$w_{\text{NO}_x} \text{ (% dry wt)}$	0.004	0.000	0.17	0.003
$w_{\text{SO}_2} \text{ (% dry wt)}$	0.000	0.002	0.0005	0.031
$w_{\text{NO}_x} \text{ (% dry wt)}$	0.006	0.010	0.015	0.009
$w_{\text{NO}_x} \text{ (% dry wt)}$	0.007	0.007	0.0011	0.009
R_{CO_2}	20	15	15	15

7.3 PROCESS DESIGN

7.3.1 Technology screening

The technologies for CO_2 capture considered in the model are presented in Table 7.2. The technologies selected after the heuristic stage are chemical absorption, PSA, and membrane separation systems. Water scrubbing is a limiting case of the use of amine solutions, where amine concentration would be zero. According to the literature the use of water scrubbing

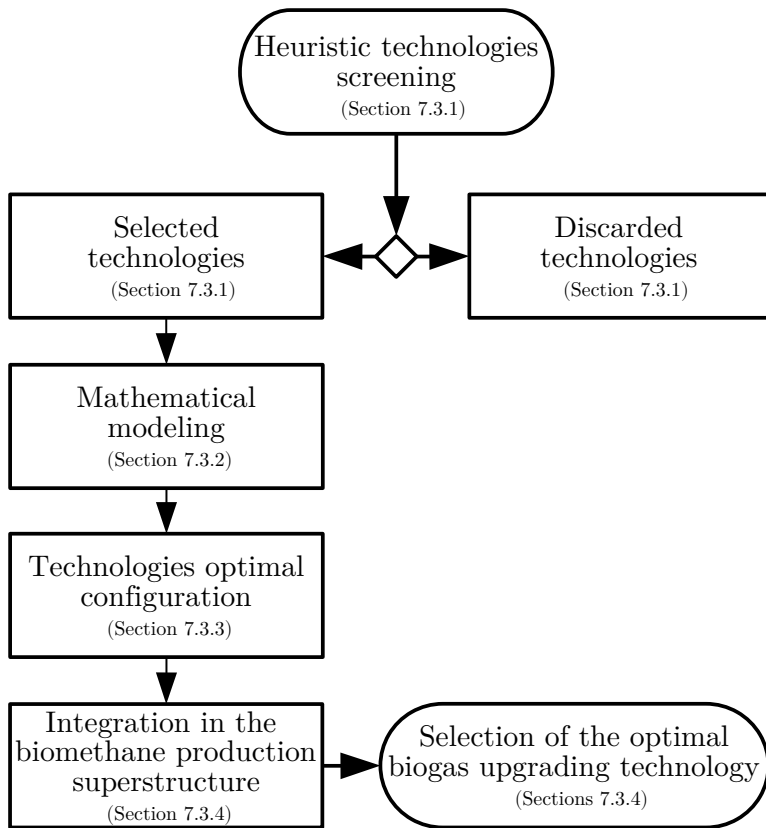


Figure 7.1: Scheme of the methodology followed to determine the optimal biogas upgrading technology.

is more energy demanding, 3:1, than the use of amines (Pellegrini et al., 2015). Therefore, among scrubbing only amines will be considered. CO₂ hydrogenation is not actually a technology based on the removal of the sour gas, but a transformation process that can be compared outside of the framework used in this work for the CO₂ capture processes (Curto & Martín, 2019). Finally, cryogenic separation is still under development and the costs are high (Adnan et al., 2019). Each of the preselected technologies shows different configurations to be selected upon:

- In the case of amine scrubbing, three different amines are considered: monoethanolamine (MEA), diethanolamine (DEA), and methyl diethanolamine (MDEA) (GPSA, 2004).
- Pressure swing adsorption (PSA) systems can use different solid beds. Activated carbon presented a capture capacity about 25% lower than zeolites 13X and 4A (Hauchhum & Mahanta, 2014). The material cost being similar, and the lower adsorption of methane in the activated

carbon (Ferella et al., 2017), results in the preselection of the zeolites beds over activated carbon.

- Regarding the membrane systems, there are two variables to be considered, the configuration of the membrane units, and the material of the membranes. Among the possible configurations for the membrane units, single-stage or multi-stage arrangements can be found. Multiple stage results in larger methane recovery and lower costs (Deng & Hägg, 2010). Among the multiple membrane stage systems, configurations with one compression stage (Makaruk et al., 2010) or multiple compression stages (Molino et al., 2013) are available. According to the literature, dual-stage membrane systems with single compression stage, considering only compression before the membrane system with no recompression stage between membrane units, have been deemed as the most economic under a wide range of feed compositions (Kim et al., 2017). Finally, the membrane materials are defined by the permeability of the gases. Lists of membrane materials for the separation of CO₂ from CH₄ can be found in several reviews (Chen et al., 2015; Vrbová & Ciahotnyý, 2017; Zhang & Chen, 2013). Among the common materials with larger permeabilities, cellulose acetate, polyimide, and polycarbonate are considered.

Table 7.2: CO₂ capture technologies considered in the study.

CO ₂ capture technology	Result after heuristic screening
Water scrubbing	Discarded
Amines scrubbing	Preselected
Pressure Swing Adsorption	Preselected
Membranes	Preselected
CO ₂ hydrogenation	Discarded
Cryogenic	Discarded

7.3.2 Mathematical modelling

In this section the mathematical optimization stage of the procedure is presented and the models for the different units involved in biogas upgrading via CO₂ capture are described. For a more detailed description of the mathematical modelling, the reader is referred to the Supplementary Material, section E.2.

7.3.2.1 Biogas production and conditioning

The modelling of the biogas production and conditioning has been developed based on first principles in previous works León and Martín (2016), and therefore no further details are provided here. Anaerobic digestion is modelled based on mass and energy balances and yield data from the literature. For economic evaluation purposes, a standard digester size of 6,000 m³ is considered (Rohstoffe eV, 2010). The biogas composition must be within the typical ratios for each of the raw materials. However, we consider it to be a variable that can be adjusted depending on its final use (León & Martín, 2016).

The compressors are modelled assuming polytropic behaviour, with a polytropic coefficient of 1.4, and an efficiency equal to 0.85 (Moran and Shapiro, 2003). Regarding the biogas conditioning stage, a bed of Fe₂O₃ is used for H₂S removal through the reaction described below. Experimental data shows almost 100% removal yield for H₂S using a fixed bed of Fe₂O₃.



Finally, ammonia and water are removed using a PSA system, considering removal yields equal to 100% (GPSA, 2004; Inc., 2006).

7.3.2.2 Absorption: amines

The amine scrubbing systems consist of an absorption column where the amine solution is put into contact with the biogas. The amine rich in CO₂ is heated up before being fed to the stripping column where the CO₂ is desorbed from the amine, which is recycled to the first column. The fresh amine used for making-up the losses of amine is mixed with the recycle stream from the regeneration column at the same temperature. The systems using amines typically operate at low temperatures, around 25-30 °C, and partial pressures of CO₂ above 0.05 bar, reaching removal yields of 90%-95% (Zhang & Chen, 2013). In contrast to post-combustion gases, which contain large amounts of nitrogen, biogas is composed mainly of methane and CO₂, resulting in higher carbon dioxide partial pressures requiring lower operating pressures. CO₂ partial pressures above 0.1 bar have been assumed to secure high removal yields (Zhang & Chen, 2013), resulting in the need to operate at total pressures around 1-1.5 bar to secure the appropriate CO₂ partial pressures (Movaghfarnejad & Akbari, 2011; Xue et al., 2017).

Each unit is modelled based on first principles using industrial data (GPSA, 2012). To compute the flow of fresh amines, the CO₂ pickup rate

and the column efficiency are used from industrial data. The energy balance to the preheater, the condenser and the reboiler of the CO₂ desorption column and the cooler are computed also using industrial rules of thumb. For the complete model see the Supplementary Material.

The model for the selection of the amine absorption is formulated as an NLP problem including the units described in sections 7.3.2.1 and E.2.1 of the Supplementary Material.

7.3.2.3 PSA

The stream of gases passes through the bed of zeolites and the carbon dioxide is captured by adsorption. The system consists of the compression train and the zeolite beds. The models for each of the units are based on the thermodynamics of gas compression and solid-gas Langmuir adsorption. The details can be seen in the Supplementary Material.

The adsorption capacity of the zeolites is directly related to the partial pressure of the CO₂. Therefore, the feed pressure is an operating variable adjusted using a system of compressors with intercooling. Each compression stage is modelled assumed polytropic behaviour and a compression efficiency of 0.85. The heat exchangers are modelled using mass and energy balances so that the gas temperature is from 25 to 60 °C entering the adsorption bed. The removal yield is assumed to be 98%, so that the exit gas contains less than 2% CO₂ (Ferella et al., 2017). The mass of zeolite depends on the adsorption capacity that is computed as a function of the operating pressure and temperature using Langmuir adsorption models for the three materials. The operating time before regeneration must be below 20 min for the product gas to contain only traces of CO₂ (Hauchhum & Mahanta, 2014). Thus, two beds operate in parallel, one in adsorption, one in desorption mode. In addition, the adsorption capacity decays cycle after cycle until it stabilizes around 65% of the initial capacity given by Langmuir adoption isotherm. Therefore, the adsorption capacity is corrected to compute the amount of zeolite used in the PSA system. Furthermore, a lifetime of the zeolites bed of 5 years has been considered based on data reported by (Xiao, G., Webley, P., Hoadley, A., Ho, M., Wiley, D., 2013).

The process is modelled as an NLP optimization problem including the models described in sections 7.3.2.1 and E.2.2 of the Supplementary Material.

7.3.2.4 Membranes

A dual-stage membrane system with single compression stage before the membrane module and no recompression stage between modules is considered since it has been deemed as the most economic arrangement under a wide range of feed compositions (Kim et al., 2017). The compressor is modelled as discussed above, assuming polytropic compression of the gas, see Supplementary Material for further details. Each membrane module is modelled using mass balances considering the permeate and retentate streams, the flux of the gases across the membrane, that is a function of the concentration gradient between both sides of the membrane (Fernandes Rodrigues, 2009). The flux is the parameter which allows computing the area of the membrane, based on the permeability of the membrane. As the driving force in the membrane separation process is the concentration gradient, the removal of CO₂ results in a change in the composition of the stream along the membrane, leading to a change in the driving force which controls the process. Therefore, an average molar fraction between the feed and the retentate composition is used to compute the separation driving force. Three different membrane materials are selected aiming at large CO₂ permeability, low methane permeability, and therefore, high selectivity; cellulose acetate, polyamide, and polycarbonate (Vrbová & Ciahotný, 2017). The solution of the optimization problem will yield intermediate conditions to assure natural gas composition of the biomethane.

The process model is formulated as an NLP problem, including the models described in sections 7.3.2.1 and E.2.3 of the Supplementary Material, where the main decision variables are the operating pressure of the membrane, their areas and the flux across the membrane.

7.3.3 Selection of optimal configurations

7.3.3.1 Absorption: amines

Eq. 7.2 and the objective function shown in Eq. 7.3 are added to the model described in section 7.3.2.2 for determining the optimal amine for biogas upgrading. The first term, BioCH₄, presents the profit from the biomethane generated using the price of the natural gas given by U.S. Energy Information Administration (EIA) (2019b), and the second term corresponds to the operation considering the amortization of the investment costs of the amines purification systems, calculated in Eq. 7.3, where the investment cost is annualized with K equal to 3 (Douglas, 1988).

$$Profit_{Amine\ system} = BioCH_4 - Cost_{Amine\ system} \quad (7.2)$$

$$Cost_{Amine\ system} =$$

$$C_{Steam} \sum_i \frac{Q_i}{\lambda} \cdot \tau_{year} + \frac{1}{K} C_{Amine} \cdot f c_{Amine} \cdot \tau_{year} \quad (7.3)$$

The cost of each amine is taken to be 1.3 USD/kg for MEA, 1.32 USD/kg for DEA, and 3.09 USD/kg for MDEA, based on Nuchitprasittichai and Cremaschi (2013). The cost of high pressure steam (42 bar) is assumed to be 0.019 USD/kg (Pérez-Uresti et al., 2019). The NLP problem consists of 288 equations and 953 variables per amine evaluated and is solved using a multistart initialization approach with CONOPT as the preferred solver where the main decision variables are the pressures temperatures and flow rates.

7.3.3.2 PSA

The main decision variables to select among the zeolite materials are the operating pressure and temperature at the PSA bed and the size of the zeolites bed. To estimate the cost of the PSA system, Eqs. 7.4 and 7.5 are included in the model described in section 7.3.2.3, assuming that the zeolite bed loses efficiency over time, resulting in a lifetime of 5 years before it needs to be replaced (Xiao, G., Webley, P., Hoadley, A., Ho, M., Wiley, D., 2013). As the plant life is considered to be 20 years, the zeolites bed must be replaced 4 times during the plant life, N Cycle. The cost of the zeolites considered is 5 USD/kg for both, zeolite 13 X and zeolite 4A (Xiao, G., Webley, P., Hoadley, A., Ho, M., Wiley, D., 2013).

$$Profit_{PSA\ system} = BioCH_4 - Cost_{PSA\ system} \quad (7.4)$$

$$Cost_{PSA\ system} = \quad (7.5)$$

$$C_{Electricity} \cdot W_{Compressor} + \frac{1}{K} M_{Zeolite} \cdot C_{Zeolite} \cdot N_{Cycle}$$

The NLP problems, consisting 283 equations and 828 variables per adsorbent material, are solved similarly as in the case of the selection of amines.

7.3.3.3 Membranes

The selection of membrane material is carried out using the model described in 7.3.2.4, and an objective function considering the cost of the gas compression and the amortization of the investment costs of the membranes, Eqs. 7.6 and 7.7.

$$\text{Profit}_{\text{Membrane system}} = \text{BioCH}_4 - \text{Cost}_{\text{Membrane system}} \quad (7.6)$$

$$\begin{aligned} \text{Cost}_{\text{Membrane system}} = & \\ C_{\text{Electricity}} \cdot W_{\text{Compressor}} + \frac{1}{K} \cdot C_{\text{Membrane}} \cdot \frac{1}{L_f} & \\ \cdot N_{\text{Membranes}} \left(\sum_{i \in \text{stages}} \text{Area}_i \right) & \end{aligned} \quad (7.7)$$

A value of 50 USD/m² will be used based on the literature (Kim et al., 2017). Considering the plant life equal to 20 years, the membranes with a typical lifetime of 4 years must be replaced 5 times during the plant life, $N_{\text{Membranes}}$ (Scholz et al., 2015). Each NLP consists of 299 equations and 869 variables and it is solved as the ones formulated for the previous cases.

7.3.4 Superstructure configuration

Once the best configuration from each technology is selected, the superstructure containing all the technologies evaluated is built considering only the best amine, membrane material and adsorbent bed, see Fig. 7.2. The superstructure includes the models presented in sections 7.3.2.1 to 7.3.2.4 and described in the Supplementary Material, section E.2. The superstructure is optimized evaluating all the processes simultaneously, for each waste raw material selecting only one technology, using as objective function Eq. 7.8.

$$\text{Profit} = \quad (7.8)$$

$$\text{BioCH}_4 - \text{Cost}_{\text{Membrane system}} - \text{Cost}_{\text{PSA system}} - \text{Cost}_{\text{Amine system}}$$

The superstructure model consists of 383 equations and 1367 variables, resulting in an NLP problem solved using a multistart optimization procedure with CONOPT as the preferred solver. The main decision variables are operating conditions including flows, temperatures, pressures, whereas

the value for the variables of the non-selected technologies is null, including the mass flow. Binary variables per technology are not needed for the selection among the technologies since the costs are related to the flow processed per each technology.

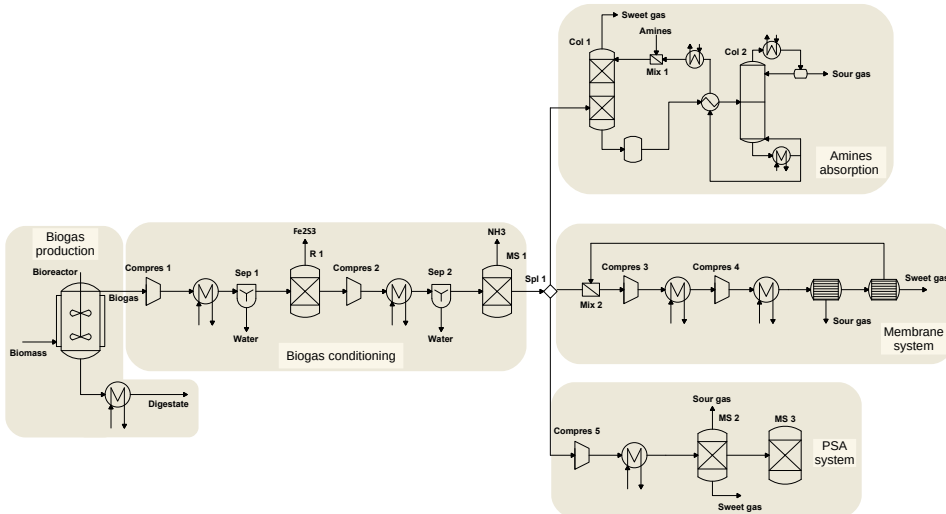


Figure 7.2: Scheme of the proposed superstructure for biogas upgrading into biomethane.

7.3.5 Economic evaluation

Finally, a detailed economic evaluation for biomethane production from different wastes is performed. The production and investment costs are estimated using the factorial method presented in Towler and Sinnott (2009). It is based on the estimation of the unit costs, using the same factors as presented in Davis and Martín (2014a, 2014b) for further comparison with other renewable based methane production processes. The details on the method and correlations used for the economic assessment can be seen in the Supplementary Material, section E.3.

7.4 RESULTS

This section draws the results for the composition of the biogas obtained, technology selection, economic evaluation, the comparison of different technologies beyond biogas upgrading for the production of biomethane, and a scale-up study.

7.4.1 Biogas composition

The amount of each component of biogas is not fixed, but limited by upper and lower bounds for each component, as a range of values provided by the literature. The model aims at the composition of biogas that optimizes the production of methane, resulting in the same composition for all wastes, shown in Table 7.3.

Table 7.3: Raw biogas composition.

	CH ₄	CO ₂	H ₄ S	NH ₃	N ₂	O ₂	H ₂ O
Biogas composition (% mol)	56.8	25.2	≤0.2	≤ 7.6 · 10 ⁻³	1.7	0.4	15.7

7.4.2 Selection of technology

This section is divided into the selection of the best configuration per preselected technology and the optimization of the operating conditions where an economic objective function has been considered.

7.4.2.1 Selection of the optimal configuration

The selection of the optimal configuration of each technology, amines, PSA and membranes is carried out in a first optimization stage. Since the composition turned out to be the same for all wastes, the selection of technologies was also the same for the four wastes. In the case of the amines, DEA is the best among the amines. Note that the prices for the different amines change, but the recycle of the amines is such that the largest share of the cost comes from the energy involved in the regeneration column. Regarding adsorbent beds, zeolite 13 X shows the largest adsorption capacity. Finally, polyimide results as the best membrane material.

7.4.2.2 Selection of the optimal technology and operating conditions

The selection of technology for biogas upgrading was performed for four different wastes: cattle and swine manure, municipal food waste and sludge. The biogas upgrading technology selected for all residues is pressure swing adsorption. The results of the optimization problem formulated returns the optimal operating conditions of the biomethanation production facility for the wastes evaluated, as shown in Table 7.4.

Regarding the wastes studied, food waste is the most promising one for biomethane production due to the larger organic matter content.

Table 7.4: Main process parameters for the selected technology, pressure swing adsorption.

	Food waste	Cattle manure	Pig manure	Sludge
Waste flow (kg/s)	9.795	9.795	9.795	9.795
kg methane/kg feed	0.0355	0.00826	0.00449	0.00929
Methane produced (10^{-6} Nm ³ /yr)	15.132	3.521	1.914	3.960
P _{PSA} (atm)	2	2	2	2
T _{PSA} (°C)	25	25	25	25
M _{Zeolite} (kg)	6835	1583	856	1781
Steam (MW)	4.2	3.7	3.3	4.9
Cooling (MW)	3.3	0.7	0.4	1.0
Power (kW)	223	51.2	28	58.0
NPK ratio	1.1/0.9/0.47	1.1/1.1/0.6	0.8/2.5/1.3	0.0/4.6/2.4
R _{CN}	13.7	21.0	7.8	14.8

7.4.3 Estimation of production and investment costs

Table 7.5 shows the summary of the results of the economic evaluation considering the best upgrading technology for the different raw materials evaluated, and Fig. 7.3 presents the break-down of the production costs. Food waste is the most competitive residue for biomethane production, resulting in a production cost of 0.36 EUR/Nm³. On the other hand, the low organic load in manure results in production costs from 3 to 5 times larger than the production cost of biomethane from food waste. In all cases, the production cost is higher than current natural gas costs (0.18 EUR/Nm³) (U.S. Energy Information Administration (EIA), 2019b) by at least a factor of 2. Therefore, the NPV or the ROI would be negative resulting in the need for additional income to balance the production costs obtaining credit from the nutrients contained within digestate, or through the application of incentive policies resulting in competitive market prices for biomethane. Considering the first alternative, food waste based biomethane, the most favourable case, becomes competitive if a credit of 0.022 EUR per kilogram of the fertilizer is obtained considering a methane market value of 5 EUR/MMBTU (0.18 EUR/Nm³), while the more expensive biomethane,

obtained from swine manure, can be competitive at the cost of 0.116 EUR/kg of fertilizer. Considering a feed-in premium (FiP) incentive scheme, where bonuses are paid above the benchmark market price to subsidize the biomethane production, a range of bonus values between the 100% and 1000% of the methane market value are needed to reach a competitive selling price.

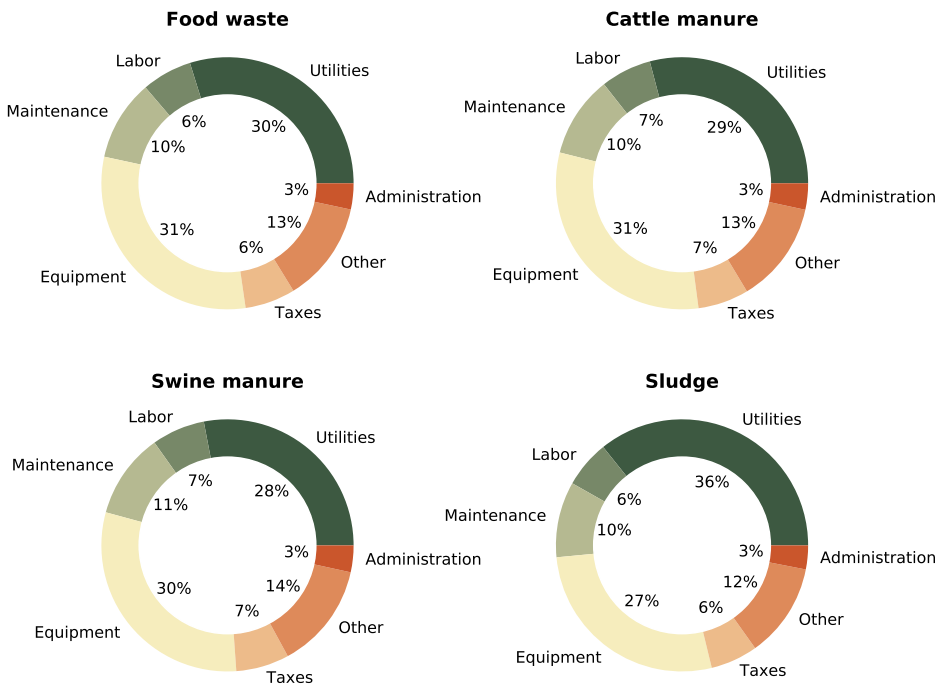


Figure 7.3: Breakdown of biomethane production costs for each residue analyzed.

Regarding investment costs, the processing of larger flows of biogas for the processing of food waste results in up to 25% larger investment costs, from 49 M EUR to 66 M EUR, although as the flows of raw waste are similar for the different residues evaluated the number of digesters required is the same.

For the most promising waste towards biomethane production, food municipal waste, the production and investment costs are computed in detail for the selected technologies, namely, PSA, membranes and amines, as shown in Table 7.6. It is possible to see that membranes and PSA show similar economic results, slightly in favour of the first technology. Membrane systems require 3 times more power than PSA units, resulting in a slightly more expensive alternative than the PSA. The optimal operating pressure of membranes is 65 bar, in the order of that presented by Kim et al. (2017), while the pressure of the PSA system is 2.05 bar, according

with the results reported in (Ferella et al., 2017) for biogas upgrading, and in the lower bound of the operating conditions reported by Santos et al. (2011). Amines scrubbing results the most expensive upgrading technology resulting in a cost 10% higher, mainly due to the larger consumption of utilities in the form of steam for the regeneration of the solvent. In all cases, with a reasonable credit from the fertilizer it would be possible to produce biomethane at a competitive cost, while the FiP bonus are between 100% and 117% of the methane market value.

Table 7.5: Summary of the cost estimation for biomethane production considering the optimal biogas upgrading technology, PSA system.

	Food Waste	Cattle Manure	Pig Manure	Sludge
Nºof digesters	6	6	6	6
Investment cost (M EUR)	66.4	54.4	48.7	51.3
Production cost (M EUR/yr)	5.1	4.0	3.6	4.2
Production cost (no credit)	0.36 $\frac{\text{EUR}}{\text{Nm}^3}$ 10.0 $\frac{\text{EUR}}{\text{MMBTU}}$	1.24 $\frac{\text{EUR}}{\text{Nm}^3}$ 33.5 $\frac{\text{EUR}}{\text{MMBTU}}$	2.00 $\frac{\text{EUR}}{\text{Nm}^3}$ 55.4 $\frac{\text{EUR}}{\text{MMBTU}}$	1.15 $\frac{\text{EUR}}{\text{Nm}^3}$ 31.8 $\frac{\text{EUR}}{\text{MMBTU}}$
EUR/kg fertilizer to achieve 5 EUR/MMBTU	0.022	0.048	0.116	0.041
EUR/Nm ³ FiP bonus to achieve 5 EUR/MMBTU	0.18	1.029	1.819	0.97

7.4.4 Comparison with renewable-based hydrogenation processes

The results presented in this work are compared with two different technologies for renewable methane production, the hydrogenation of the CO₂ contained in the biogas, reported by Curto and Martín (2019), and synthetic methane produced from CO₂ hydrogenation, as presented by Davis and Martín (2014a, 2014b). In both cases, renewable energy is used to produce hydrogen, resulting in a high dependency between the methane production cost and the local availability of the renewable energy sources, i.e. solar irradiance and wind.

For the hydrogenation of the CO₂ within the biogas, the production costs depend on the mode of operation, continuum production or variable with the availability of solar energy. Considering a facility for food waste processing, with a production capacity of 0.67 kg/s of biomethane, a range of production costs of 0.57-0.27 EUR/Nm³ for CO₂ hydrogenation under steady and varying conditions respectively is found, with investment costs of 229 M EUR and 116 M EUR for the same two operating modes in Spain (Curto & Martín, 2019).

Table 7.6: Detailed analysis for production of biomethane from food waste comparing technologies.

	Food Waste		
	PSA	Membranes	Amines
Waste flow (kg/s)	9.795	9.795	9.795
Kg Methane/kg feed	0.0355	0.0355	0.0355
Nºof digesters	6	6	6
Steam (MW)	4.2	4.2	6.1
Cooling (MW)	3.3	3.4	5.0
Power (kW)	223	665	145
Investment cost (M EUR)	66.4	65.2	67.1
Production cost (M EUR/yr)	5.1	5.3	5.7
Production cost (no credit)	0.36 $\frac{\text{EUR}}{\text{Nm}^3}$ 10.0 $\frac{\text{EUR}}{\text{MMBTU}}$	0.38 $\frac{\text{EUR}}{\text{Nm}^3}$ 10.5 $\frac{\text{EUR}}{\text{MMBTU}}$	0.39 $\frac{\text{EUR}}{\text{Nm}^3}$ 10.7 $\frac{\text{EUR}}{\text{MMBTU}}$
EUR/kg fertilizer to achieve 5 EUR/MMBTU	0.022	0.023	0.026
EUR/Nm ³ FiP bonus to achieve 5 EUR/MMBTU	0.18	0.20	0.21

Alternatively, direct hydrogenation of CO₂ also allows the production of methane. For a facility with a methane production capacity of 0.78 kg/s, considering wind-based energy located in the most favourable allocation in Spain an investment of 375 M EUR is required. The production cost of synthetic methane is 0.48 EUR/Nm³, equivalent to 13.1 EUR/MMBTU (Davis and Martín, 2014a). On the other hand, if solar is used as source of renewable energy, the investment and production costs are reduced to 240 M EUR and 0.33 EUR/m³ (9.2 EUR/MMBTU) respectively in normal climate conditions Davis and Martín (2014a).

However, the comparison is not straightforward due to two reasons: the economies of scale and the effect of the credits obtained from digestate. The comparison can be carried out based on the feed flowrate, as in all cases a flow of waste of 10 kg/s is considered. Alternatively, the facility presented in this work is scaled-up to reach a similar methane production capacity. However, the difficulty of determining the correct credit obtained from the digestate makes difficult the direct comparison of biomethane/methane production costs.

7.4.4.1 Comparison based on feed flowrate

By comparing facilities that process the same waste flowrate, see Table 7.6, to the ones reported in the previous two paragraphs, the investment costs are lower in case of biogas upgrading using carbon capture technologies. The production of biomethane via CO₂ capture can be more competitive than the processes based on hydrogenation of CO₂ within the biogas except if the production rate is allowed to follow the availability of renewable energy. In addition, CO₂ capture is more attractive than the direct hydrogenation of CO₂ using wind as energy source for the production of the hydrogen, and only slightly more expensive than using solar energy. However, the biomethane production capacity is the lowest of all three processes. Furthermore, note that allocations with favourable wind and solar based hydrogen production were selected.

7.4.4.2 Comparison based on production capacity

By scaling up the facility presented in this work, just for food residues and the best technology, the PSA, the production capacity is doubled reaching 0.72 kg/s of methane for comparison with previous work. This production capacity is between the two alternatives presented above (Curto & Martín, 2019; Davis & Martín, 2014a, 2014b). The economic results for the scale-up of the carbon capture facility processing food are shown in Table 7.7 where it can be observed that the investment cost is in between the value obtained for continuum operation and the value obtained for variable hydrogenation of the CO₂ within the biogas. The production cost of the scaled-up facility is promising, 0.30 EUR/Nm³. Comparing this value with the ones from biogas hydrogenation or direct CO₂ hydrogenation, it is possible to observe that the production costs are competitive, and can be even lower than those of both technologies if a credit from the digestate can be obtained. The one drawback of the facility that uses carbon capture technologies is the need to find a use to the captured CO₂. The advantage is that it does not require additional power to produce renewable hydrogen.

Therefore, the recommendation among biogas upgrading via CO₂ capture, via CO₂ hydrogenation or synthetic methane production, would depend on the availability of solar or wind energy. Considering the case of Spain, the use of variable production of methane with the solar energy by direct hydrogenation of the CO₂ contained in the biogas is the best alternative (Curto & Martín, 2019). However, this is only competitive in the south of the country. Renewable methane can be the alternative when the power is produced in regions of high wind velocity (de la Cruz & Martín, 2016). Otherwise, the use of CO₂ capture technologies is preferred.

Table 7.7: Operating conditions and economic parameter for the scaled-up plant from food waste.

	Food Waste
kg Methane/kg feed	0.72 / 20
N°of digesters	12
Investment cost (M EUR)	124.5
Production cost (M EUR/yr)	8.6
Credit digestate (M EUR/yr)	38.3
Production cost (no credit)	0.30 $\frac{\text{EUR}}{\text{Nm}^3}$ 8.21 $\frac{\text{EUR}}{\text{MMBTU}}$
EUR/kg fertilizer to achieve 5 EUR/MMBTU	0.014

7.4.5 Plant scale-up study

Economies of scale play an important role in the chemical industry, reducing the cost as the facilities are larger. Because of the distributed availability of the residues and the difficulty of transport, it is relevant to evaluate the effect of the scale on the process economics. Two of the four residues, food waste and cattle manure, are considered for further analysis due to the large amounts of wastes produced and the environmental concerns involved. In the first case the aim is to evaluate the cost for the biomethane for different city sizes as a function of the residues that they collect. Cities from 50 k to 5 million habitants are considered using the waste production rates of Spain, as shown in Fig. 7.4. Similar relationship between population and food waste generated can be expected for other countries or regions with a similar development level, although the results can be slightly affected by variations of some parameters, such as the amount of waste generated per person per year and the distribution of the population between urban and rural areas. The second case of study corresponds to cattle manure, assessing the biomethane production cost as a function of the size of concentrated animal feeding operations (CAFOs), considering facilities up to 16.000 cows. For a detailed description of the procedure followed in the scale-up study we refer the reader to the section S4 of the Supplementary Material. The cost of each unit is modelled as a function of the size, which is related to the mass or energy flow, as presented in the section E.4 of the Supplementary Material. The investment and production costs are estimated as described in section 7.3.5. Fig. 7.5

shows the production and investment costs as a function of the city size, and Fig. 7.6 shows the scale-up for cattle manure.

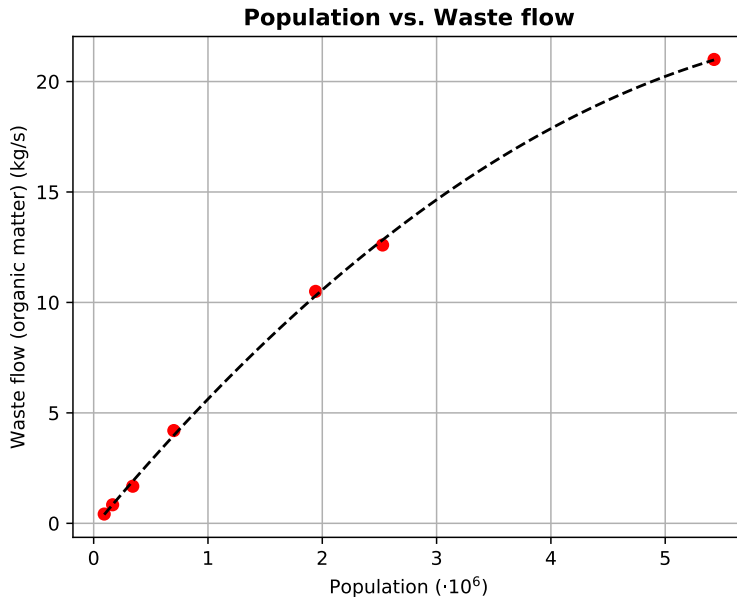


Figure 7.4: Relation between population and food waste produced in Spain.

The results show that large cities above 1 million inhabitants are able to produce biomethane at competitive prices, even more if credit is obtained from the digestate. However, the lower concentration of organic matter in cattle manure results in non-competitive prices for the biomethane produced even for the largest CAFOs considered. Therefore, manure digestion can be a way to self-produce energy, particularly in isolated places, but at larger cost. After the scale-up study we correlated the investment and production costs of biomethane as a function of the plant size. The fitting parameters for the correlations can be found in Table 7.8.

7.5 CONCLUSIONS

In this work the upgrading of the biogas produced from different waste sources is studied comparing different carbon capture technologies following a systematic framework. A hybrid heuristic-mathematical approach is developed for the systematic process design. The heuristic screening stage based on literature data is used to narrow the search. Next, a mathematical optimization approach is used to compare the most promising technologies and determine their operating conditions from an economic point of view. The framework is flexible to include more alternatives and compare novel

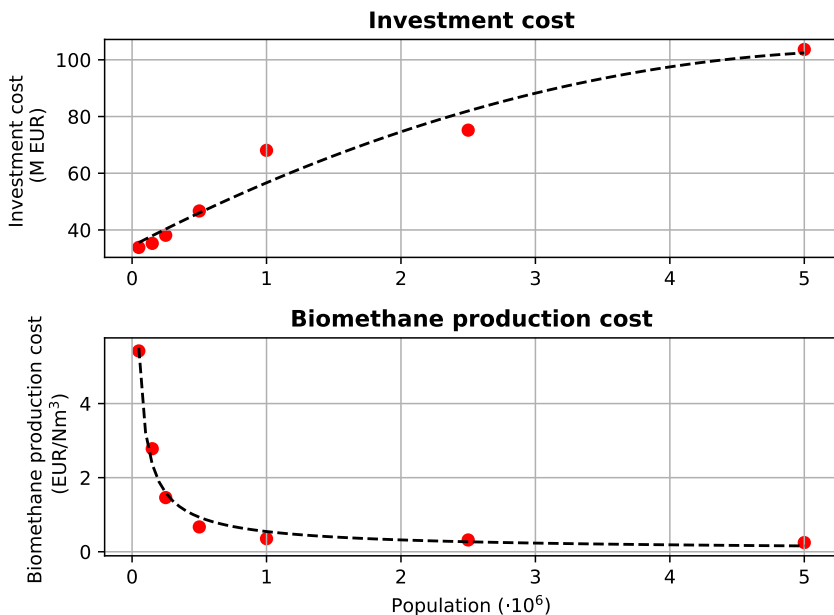


Figure 7.5: Scale-up in the investment costs for municipal food waste.

Table 7.8: Scale-up correlations for investment and production costs for food waste and cattle manure.

	Correlation	Food Waste		Cattle
		$V = \text{Population} \cdot 10^{-6}$	$V = \text{Number of animals} \cdot 10^{-6}$	
Waste flow (kg/s)	$F = a \cdot V^2 + b \cdot V + c$	$a = -0.430$ $b = 6.231$ $c = -0.175$		
Investment (MV)	$I = a \cdot V^2 + b \cdot V + c$	$a = -2.173$ $b = 24.485$ $c = 34.325$	$a = 0$ $b = 0.003$ $c = 16.769$	
Production costs (EUR/Nm ³)	$C = a \cdot V^b$	$a = 0.546$ $b = -0.771$	$a = 220.023$ $b = -0.553$	

technologies for different wastes, but relies on the prediction capacity of the models. The study evaluated swine and cattle manure, food solid waste and sludge.

The heuristic screening suggests the use of amine scrubbing, PSA adsorption, and membrane separation systems. Within each one of them, different configurations are evaluated, focusing on the study of different amines, including MEA, DEA, and MDEA, different membranes, including polycarbonate, polyimide, and cellulose acetate, and two types of zeolites for

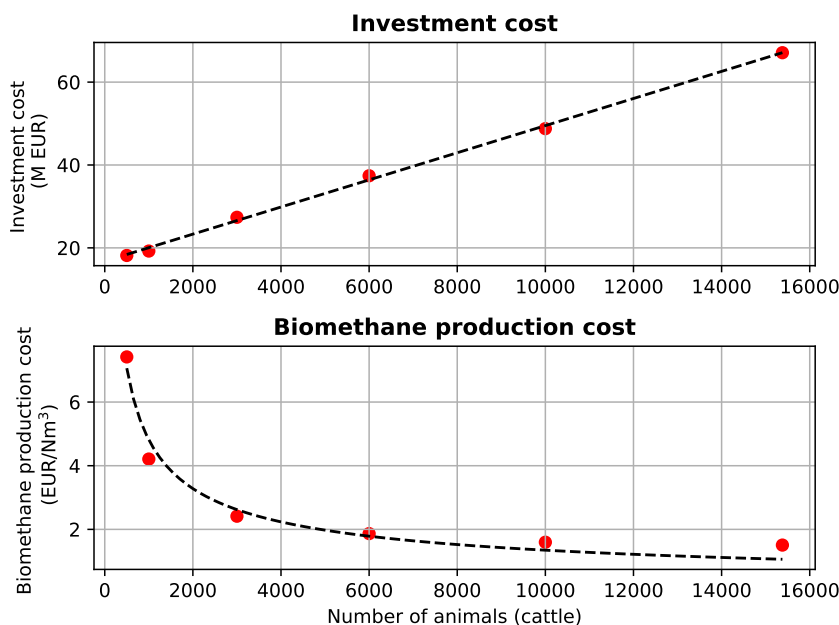


Figure 7.6: Scale-up in the investment costs for cattle manure.

PSA systems, 13X and 4A. The selection of the best configuration for each technology is carried out formulating and solving an optimization problem for each technology. DEA, zeolite 13X and polyimide are the alternative selected. Next, a superstructure is formulated as an optimization problem for the processing of food waste, cattle manure, swine manure, and sludge, assessing the upgrading technologies for the production of high purity biomethane. The optimal technology for CO₂ capture for all residues studied is PSA systems with zeolite 13X as adsorbent material, although the use of membranes is just slightly more expensive. A detailed economic evaluation is performed for the entire biomethane production plant, yielding the production and investment costs for the production of biomethane. Food waste is the most promising waste due to the largest organic matter, resulting in an investment cost of 67 M EUR and a production cost of 0.36 EUR/Nm³ for the processing of 10 kg/s of waste. Finally, the upgrading of biogas using CO₂ capture is compared to direct CO₂ hydrogenation and direct production of synthetic methane. The comparison is in favour of the direct hydrogenation of CO₂, although this result is highly dependent on the availability of solar or wind energy. For low availabilities of these resources, biomethane production through CO₂ capture is suggested.

This framework is of general use of the systematic evaluation of technologies and can be extended for comparison of newly developed materials and technologies as well as the evaluation of different wastes. Life cycle

assessment (LCA) can be added for a multiobjective kind of optimization beyond the production cost aiming at the most sustainable production of biomethane.

NOMENCLATURE

Variables

A	Antoine equation coefficient
$A_{membrane}$	Area of membrane (m^2)
B	Antoine equation coefficient
$BioCH_4$	Biomethane produced benefit (EUR/year)
C	Antoine equation coefficient
CO_{2eff}	Removal efficiency of CO_2
C_i	Cost of element i (EUR/unit or EUR/year)
D_c	Diameter of the amine contactor (in)
D_r	Diameter of the regeneration column (in)
F	Total flow (kmol/s)
F_{amine}	Flow of amine (gal/min)
F_{gas}	Flow of gas (MMscfd)
$GPSA$	Correction factor
I	Investment cost (M EUR)
J_i	Flux of component i (kmol/ m^2s)
K	Coefficient in Langmuir correlation
L_f	Membranes cycles for costing purposes
MW_i	Molecular weight of component i (kg/kmol)
NPK	Mass ratio of nitrogen, phosphorus and potassium
PC	Production costs (EUR/Nm 3)
P_i	Vapor pressure of component i (mmHg)
P_{unit}	Pressure at $unit$ (mmHg)
$Perm_i$	Permeability of component i (kmol/(kPa·m))
$Profit$	Profit (EUR/year)
Q_{unit}	Thermal energy involved in $unit$ (kW)
R	Universal gas constant, (kJ/kmol·K)
R_{CN}	Mass carbon to nitrogen ratio
T_{unit}	Operating temperature at $unit$ (K)

V_{biogas}	Biogas produced per mass unit of waste (m^3/kg)
WF	Waste flow (kg/s)
W_{unit}	Electrical energy of <i>unit</i> (kW)
Y	Specific humidity
ΔH_{reac}	Heat of reaction (kJ/kg)
δ	Membrane thickness
ϵ_i	Permeance of component i ($\text{kmol}/(\text{kPa}\cdot\text{m}^2)$)
η	CO_2 removal yield for the PSA system
η_c	Compressor efficiency
λ_i	Vaporization latent heat of specie i (kJ/kg)
τ	Cycle time at the PSA (s)
τ_{year}	Annual time operation (s)
fc_i	Flow of component i (kg/s)
$m_{zeolites}$	Amount of zeolites (kg)
q	Adsorption capacity (mol/g)
q_m	Maximum adsorption capacity (mol/g)
$q_{unit,amine}$	Experimental value of the thermal energy consumed in amine processing <i>unit</i> ((BTU/h)/(gal/min))
w_C	Carbon (% dry wt)
w_{DM}	Dry matter (% wt)
w_K	Potassium (% dry wt)
$w_{N_{org}}$	Organic nitrogen (% dry wt)
w_N	Inorganic nitrogen (% dry wt)
w_P	Phosphorous (% dry wt)
w_{VS}	Volatile matter (% dry wt)
y_i	Molar fraction of component i
z	Polytropic coefficient

Units

CD	Condensation vessel
Col	Column
Compress	Compressor
Cond	Condenser
Feed	Distillation column feed
HX	Heat exchanger

MEM	Membrane
Mix	Mixer
MS	Molecular sieve
Reb	Reboiler
Sep	Decanter
Src	Source

Subscripts

Amine	Amine adsorption system
Electricity	Electricity
Membrane	Membrane system
PSA	PSA system
Sat	Saturated

Acronyms

CAFO	Concentrated animal feeding operation
DEA	Diethanolamine
MDEA	Methyl diethanolamine
MEA	Monoethanolamine
NLP	Non-linear programming
PSA	Pressure swing adsorption

ACKNOWLEDGMENTS

Authors thank funding from Junta de Castilla y León, Spain, under grant SA026G18 and grant EDU/556/2019, and PSEM3 research group for software licenses.

BIBLIOGRAPHY

- Adamu, A., Russo-Abegão, F., & Boodhoo, K. (2020). Process intensification technologies for CO₂ capture and conversion—a review. *BMC Chemical Engineering*, 2(1), 1–18.
- Adnan, A. I., Ong, M. Y., Nomanbhay, S., Chew, K. W., & Show, P. L. (2019). Technologies for biogas upgrading to biomethane: A review. *Bioengineering*, 6(4), 92.

- Chen, X. Y., Vinh-Thang, H., Ramirez, A. A., Rodrigue, D., & Kaliaguine, S. (2015). Membrane gas separation technologies for biogas upgrading. *Rsc Advances*, 5(31), 24399–24448.
- Curto, D., & Martín, M. (2019). Renewable based biogas upgrading. *Journal of Cleaner Production*, 224, 50–59.
- Davis, W., & Martín, M. (2014a). Optimal year-round operation for methane production from CO₂ and water using wind and/or solar energy. *Journal of cleaner production*, 80, 252–261.
- Davis, W., & Martín, M. (2014b). Optimal year-round operation for methane production from CO₂ and water using wind energy. *Energy*, 69, 497–505.
- de la Cruz, V., & Martín, M. (2016). Characterization and optimal site matching of wind turbines: Effects on the economics of synthetic methane production. *Journal of Cleaner Production*, 133, 1302–1311.
- Deng, L., & Hägg, M.-B. (2010). Techno-economic evaluation of biogas upgrading process using CO₂ facilitated transport membrane. *International Journal of Greenhouse Gas Control*, 4(4), 638–646.
- Douglas, J. M. (1988). *Conceptual design of chemical processes* (Vol. 1110). McGraw-Hill New York.
- European Commission-Directorate-General for Environment. (2001). *Properties of wastes relevant to agricultural benefit and environmental impact*. Ref: CO 4953-2/11768-1 (tech. rep.). European Commission.
- European network of transmission system operators for gas (Entossg). (2015). The European natural gas network [[Online; accessed 1-May-2019]].
- Fang, J., Jin, X., & Huang, K. (2018). Life cycle analysis of a combined CO₂ capture and conversion membrane reactor. *Journal of Membrane Science*, 549, 142–150.
- Ferella, F., Puca, A., Taglieri, G., Rossi, L., & Gallucci, K. (2017). Separation of carbon dioxide for biogas upgrading to biomethane. *Journal of Cleaner Production*, 164, 1205–1218.
- Fernandes Rodrigues, D. (2009). *Model Development of a Membrane Gas Permeation Unit for the Separation of Hydrogen and Carbon Dioxide* (Master's thesis). Instituto Superior Técnico, Lisbon.
- Gassner, M., Baciocchi, R., Maréchal, F., & Mazzotti, M. (2009). Integrated design of a gas separation system for the upgrade of crude SNG with membranes. *Chemical Engineering and Processing: Process Intensification*, 48(9), 1391–1404.
- Gilassi, S., Taghavi, S. M., Rodrigue, D., & Kaliaguine, S. (2019). Optimizing membrane module for biogas separation. *International Journal of Greenhouse Gas Control*, 83, 195–207.
- Giordano, L., Roizard, D., & Favre, E. (2018). Life cycle assessment of post-combustion CO₂ capture: A comparison between membrane

- separation and chemical absorption processes. *International Journal of Greenhouse Gas Control*, 68, 146–163.
- GPSA. (2004). *GPSA engineering data book, 12th ed.* (tech. rep.). Gas Processors Suppliers Association.
- GPSA. (2012). *GPSA engineering data book, 13th ed.* (tech. rep.). Gas Processors Suppliers Association.
- Hasan, M. F., Baliban, R. C., Elia, J. A., & Floudas, C. A. (2012a). Modeling, simulation, and optimization of postcombustion CO₂ capture for variable feed concentration and flow rate. 1. Chemical absorption and membrane processes. *Industrial & Engineering Chemistry Research*, 51(48), 15642–15644.
- Hasan, M. F., Baliban, R. C., Elia, J. A., & Floudas, C. A. (2012b). Modeling, simulation, and optimization of postcombustion CO₂ capture for variable feed concentration and flow rate. 2. Pressure swing adsorption and vacuum swing adsorption processes. *Industrial & engineering chemistry research*, 51(48), 15665–15682.
- Hauchhum, L., & Mahanta, P. (2014). Carbon dioxide adsorption on zeolites and activated carbon by pressure swing adsorption in a fixed bed. *International Journal of Energy and Environmental Engineering*, 5(4), 349–356.
- Inc., N. (2006). *Equipment Design and Cost Estimation for Small Modular Biomass Systems, Synthesis Gas Cleanup, and Oxygen Separation Equipment. Task 2: Gas Cleanup Design and Cost Estimates – Black Liquor Gasification* (tech. rep.). National Renewable Energy Laboratory (NREL).
- Jepsen, S. (2018). *Co-digestion of animal manure and organic household waste - the Danish experience* (tech. rep.). Danish Environmental Protection Agency.
- Kim, M., Kim, S., & Kim, J. (2017). Optimization-based approach for design and integration of carbon dioxide separation processes using membrane technology. *Energy Procedia*, 136, 336–341.
- Klemeš, J., Bulatov, I., & Cockerill, T. (2007). Techno-economic modelling and cost functions of CO₂ capture processes. *Computers & chemical engineering*, 31(5-6), 445–455.
- Korhonen, J., Honkasalo, A., & Seppälä, J. (2018). Circular economy: the concept and its limitations. *Ecological economics*, 143, 37–46.
- Lee, A. S., Eslick, J. C., Miller, D. C., & Kitchin, J. R. (2013). Comparisons of amine solvents for post-combustion CO₂ capture: A multi-objective analysis approach. *International Journal of Greenhouse Gas Control*, 18, 68–74.

- León, E., & Martín, M. (2016). Optimal production of power in a combined cycle from manure based biogas. *Energy Conversion and Management*, 114, 89–99.
- MacDowell, N., Florin, N., Buchard, A., Hallett, J., Galindo, A., Jackson, G., Adjiman, C. S., Williams, C. K., Shah, N., & Fennell, P. (2010). An overview of CO₂ capture technologies. *Energy & Environmental Science*, 3(11), 1645–1669.
- Makaruk, A., Miltner, M., & Harasek, M. (2010). Membrane biogas upgrading processes for the production of natural gas substitute. *Separation and Purification Technology*, 74(1), 83–92.
- Miltner, M., Makaruk, A., & Harasek, M. (2017). Review on available biogas upgrading technologies and innovations towards advanced solutions. *Journal of Cleaner Production*, 161, 1329–1337.
- Molino, A., Migliori, M., Ding, Y., Bikson, B., Giordano, G., & Braccio, G. (2013). Biogas upgrading via membrane process: modelling of pilot plant scale and the end uses for the grid injection. *Fuel*, 107, 585–592.
- Morero, B., Groppelli, E. S., & Campanella, E. A. (2017). Evaluation of biogas upgrading technologies using a response surface methodology for process simulation. *Journal of cleaner production*, 141, 978–988.
- Movaghfarnejad, K., & Akbari, M. (2011). Simulation of CO₂ capture process. *International Journal of Chemical and Molecular Engineering*, 5(10), 843–847.
- Nuchitprasittichai, A., & Cremaschi, S. (2013). Optimization of CO₂ Capture Process with Aqueous Amines: A Comparison of Two Simulation–Optimization Approaches. *Industrial & Engineering Chemistry Research*, 52(30), 10236–10243.
- Pellegrini, L. A., De Guido, G., Consonni, S., Bortoluzzib, G., & Gatti, M. (2015). From biogas to biomethane: How the biogas source influences the purification costs. *Chemical Engineering Transactions*, 43, 409–414.
- Pellegrini, L. A., De Guido, G., & Langé, S. (2018). Biogas to liquefied biomethane via cryogenic upgrading technologies. *Renewable Energy*, 124, 75–83.
- Pérez-Uresti, S. I., Martín, M., & Jiménez-Gutiérrez, A. (2019). Superstructure approach for the design of renewable-based utility plants. *Computers & Chemical Engineering*, 123, 371–388.
- Qyyum, M. A., Haider, J., Qadeer, K., Valentina, V., Khan, A., Yasin, M., Aslam, M., De Guido, G., Pellegrini, L. A., & Lee, M. (2020). Biogas to liquefied biomethane: Assessment of 3P's—Production, processing, and prospects. *Renewable and Sustainable Energy Reviews*, 119, 109561.

- Reddy, K., Aravindhan, S., & Mallick, T. K. (2016). Investigation of performance and emission characteristics of a biogas fuelled electric generator integrated with solar concentrated photovoltaic system. *Renewable Energy*, 92, 233–243.
- Rohstoffe eV, F. N. (2010). *Guía sobre el biogás desde la producción hasta el uso* (tech. rep.). Ministerio Federal de Alimentación, Agricultura y Protección al Consumidor, Repúblida Federal Alemana.
- Santos, M. P., Grande, C. A., & Rodrigues, A. E. (2011). Pressure swing adsorption for biogas upgrading. Effect of recycling streams in pressure swing adsorption design. *Industrial & engineering chemistry research*, 50(2), 974–985.
- Scholz, M., Alders, M., Lohaus, T., & Wessling, M. (2015). Structural optimization of membrane-based biogas upgrading processes. *Journal of membrane science*, 474, 1–10.
- Somehsaraei, H. N., Majoumerd, M. M., Breuhaus, P., & Assadi, M. (2014). Performance analysis of a biogas-fueled micro gas turbine using a validated thermodynamic model. *Applied thermal engineering*, 66(1–2), 181–190.
- Spanish Ministry of Industry, Energy and Tourism. (2013). 21 December 2012 from the General Directorate of Mines and Energy Policy [In Spanish]. Boletín Oficial del Estado, Sec. I. Pag. 889.
- Stangeland, K., Kalai, D., Li, H., & Yu, Z. (2017). CO₂ methanation: the effect of catalysts and reaction conditions. *Energy Procedia*, 105, 2022–2027.
- Taifouris, M. R., & Martin, M. (2018). Multiscale scheme for the optimal use of residues for the production of biogas across Castile and Leon. *Journal of cleaner production*, 185, 239–251.
- Towler, G., & Sinnott, R. (2009). *Chemical engineering design* (5th ed.). Elsevier.
- Trespalacios, F., & Grossmann, I. E. (2014). Review of mixed-integer nonlinear and generalized disjunctive programming methods. *Chemie Ingenieur Technik*, 86(7), 991–1012.
- Tynjala, T. (2015). Biological Methanation of Hydrogen: a Way to Increase Methane Yield in Biogas Plants. Lappeenranta University of Technology. [[Online; accessed 23-February-2019]].
- U.S. Energy Information Administration (EIA). (2019a). Natural gas pipelines [[Online; accessed 29-April-2019]].
- U.S. Energy Information Administration (EIA). (2019b). Natural gas prices [[Online; accessed 29-April-2019]].
- Vo, T. T., Wall, D. M., Ring, D., Rajendran, K., & Murphy, J. D. (2018). Techno-economic analysis of biogas upgrading via amine scrubber,

- carbon capture and ex-situ methanation. *Applied energy*, 212, 1191–1202.
- Vrbová, V., & Ciahotnyý, K. (2017). Upgrading biogas to biomethane using membrane separation. *Energy & Fuels*, 31(9), 9393–9401.
- World Commission on Environment and Development (WCED). (1987). *Our Common Future*. Oxford University Press.
- World Energy Council. (2016). *World energy resources 2016* (tech. rep.). World Energy Council.
- Xiao, G., Webley, P., Hoadley, A., Ho, M., Wiley, D. (2013). *Low Cost Hybrid Capture Technology Development: Final Report*. Ref No: 3-0510-0046. (tech. rep.). Cooperative Research Centre for Greenhouse Gas Technologies. CO2CRC Publication, Canberra, Australia.
- Xue, B., Yu, Y., Chen, J., Luo, X., & Wang, M. (2017). A comparative study of MEA and DEA for post-combustion CO₂ capture with different process configurations. *International Journal of Coal Science & Technology*, 4(1), 15–24.
- Zhang, Y., & Chen, C.-C. (2013). Modeling CO₂ absorption and desorption by aqueous monoethanolamine solution with Aspen rate-based model. *Energy Procedia*, 37, 1584–1596.

Part IV
APPENDIX

A

APPENDIX A: SUPPLEMENTARY INFORMATION OF CHAPTER 2

All the units involved in the flowsheet are modeled using mass and energy balances, thermodynamic relationships, chemical and vapor-liquid equilibria, and product yield calculations. Therefore, the variables of the equation oriented framework comprise the total mass flows, component mass flows, component mass fractions, temperatures and pressures of the streams in the process network. The components that are tracked in our calculations belong to the following set:

{Wa, CO₂, CO, O₂, N₂, H₂S, NH₃, CH₄, SO₂, C, H, O, N, N_{org}, P, K, S, Rest, Cattle slurry, Pig slurry, Poultry slurry, P₂O₅, CaCO₃, FeCl₃, Antifoam, Fe₂(SO₄)₃, Al₂(SO₄)₃, AlCl₃, MgCl₂, NaOH, Struvite seeds, Mg, Cl, Struvite, K-Struvite, MgCl₂ CSTR, NaOH CSTR, Mg CSTR, Cl CSTR, Struvite CSTR, KStruvite CSTR, FeCl₃ Coag}

In the following subsections we briefly present the main equations used to characterize the operation of the different units. Simpler balances based on removal efficiency or stoichiometry, or the equations that connect two units are omitted and only the conversion, the chemical reactions, and the removal efficiency are presented.

The decision on the technology to use to process the digestate requires the evaluation of the cost. Its estimation uses the factorial method based on the equipment units costs Sinnott (1999). The total physical plant cost involving equipment erection, piping instrumentation, electrical, buildings, utilities, storages, site development, and ancillary buildings is 3.15 times the total equipment cost for processes which uses fluids and solids. On the other hand, the fixed cost, which includes design and engineering, contractor's fee, and contingency items is determined as 1.4 times the total physical plant cost for fluid and solid processes. In the subsequent cost estimation, these parameters are designed as f_i for the total physical plant parameter and f_j for the fixed cost parameter.

A.1 BIOGAS PRODUCTION

The anaerobic fermentation of different types of manure generates biogas, methane and carbon dioxide, through a series of reactions such as hydrolysis, acidogenesis, acetogenesis and methanogenesis (Al Seadi et al., 2008). The biogas produced shows a variable composition in methane and CO₂ depending on the composition of the manure processed and the operating conditions. The lower the temperature, the longer the retention time. We operate at 55 °C for 20 days. A part from methane and CO₂, nitrogen, H₂S, and NH₃ are produced (Kaparaju & Rintala, 2013). Thus, in order to compute the biogas composition a mass balance is performed considering the composition of the different manure sources:

$$MW_{dry\text{-}biogas} = \sum_{a'} Y_{a'/biogas-dry} \cdot MW_{a'} \quad (\text{A.1})$$

where the typical composition, Y_i , of the biogas is given by the following bounds:

$$\begin{aligned} 0.7 &\leq Y_{CH_4} \leq 0.5 \\ 0.3 &\leq Y_{CO_2} \leq 0.5 \\ 0.02 &\leq Y_{N_2} \leq 0.06 \\ 0.005 &\leq Y_{O_2} \leq 0.16 \\ Y_{H_2S} &\leq 0.002 \\ 9 \cdot 10^{-5} &\leq Y_{NH_3} \leq 1 \cdot 10^{-4} \end{aligned} \quad (\text{A.2})$$

The contact between biogas and the liquid residue results in biogas saturated with water. Gas moisture is computed using Antoine correlation as per Eq. A.3. The flow of dry biogas is determined using Eq A.4. To compute the power in the compressor, we need to determine the molar mass of the biogas as in Eq. A.5. The mass flow rate of each component is computed from its molecular weight and the total mass flow rate, Eqs. A.6-A.7.

$$y_{biogas} = \frac{MW_{H_2O}}{MW_{biogas-dry}} \frac{Pv(T)}{P - Pv(T)} \quad (\text{A.3})$$

$$F_{biogas} = \rho_{biogas} \sum_{Waste} w'_{SV/Waste} \cdot w_{MS/Waste} \cdot F_{Waste} \cdot V_{biogas/Waste} \quad (\text{A.4})$$

$$fc_{H_2O}^{biogas} = y_{biogas} \cdot \sum_{a'} fc_{a'}^{biogas} \quad (\text{A.5})$$

$$\begin{aligned} \frac{fc_{a'}^{Bioreactor, Compres1}}{MW_{a'}} &= \\ \frac{Y_{a'/biogas-dry}}{MW_{biogas-dry}} \left(F^{Bioreactor, Compres1} - fc_{H_2O}^{Bioreactor, Compres1} \right) \end{aligned} \quad (\text{A.6})$$

$$MW_{biogas} \sum_a \frac{x_{a/biogas}}{MW_a} = \sum_a x_{a/biogas} \quad (\text{A.7})$$

The lower and upper limits for the generation of biogas are given by Eq. A.8 (Al Seadi et al., 2008):

$$\begin{aligned} 0.20 \leq V_{biogas/Waste} &\leq 0.50 \\ 0.10 \leq w_{MS/Waste} &\leq 0.20 \\ 0.50 \leq w_{VS/Waste} &\leq 0.80 \end{aligned} \quad (\text{A.8})$$

The mass of waste that does not leave as biogas constitutes the digestate as follows (Al Seadi et al., 2008):

$$w'_{C/k} = R_{C-N/k} \left(w'_{Norg/k} + w'_{NH_3/k} \right) \quad (\text{A.9})$$

Each manure type has its own composition (Department for Environment Food and Rural Affairs (DEFRA), 2011).

$$\begin{aligned} 6 \leq R_{C-N/Waste} &\leq 20 \\ 0.005 \leq w_{N/Waste} &\leq 0.047 \\ 0.005 \leq w_{Norg/Waste} &\leq 0.036 \\ 0.008 \leq w_{P/Waste} &\leq 0.013 \\ 0.033 \leq w_{K/Waste} &\leq 0.1 \end{aligned} \quad (\text{A.10})$$

$$\begin{aligned} w_{C/Waste} + w_{Norg/Waste} + w_{NH_3/Waste} + w_{P/Waste} + \\ w_{K/Waste} + w_{Rest/Waste} = 1 \end{aligned} \quad (\text{A.11})$$

Atom mass balances are performed to compute the products of the reactors. We consider balances for carbon, organic nitrogen (N_{org}), inorganic nitrogen (N), phosphate and potassium. The carbon either leaves in the form of CO_2 or CH_4 with the gas or as part of the waste in the digestate, Eq. A.12. The organic nitrogen in the digestate is given by the fraction of organic nitrogen in the digestate minus the nitrogen released as gas, Eq. A.13. Similarly, the inorganic nitrogen that is not used to produce ammonia that accompanies the gas or is left as residue is computed using the values above, Eq. A.14. P and K directly leave the reactor as part of the digestate, Eqs. A.15-A.16. The rest that is not accounted for is assumed to be a residual part leaving the reactor with the digestate.

$$fc_C^{digestate} = w'_C \cdot w_{MS} \cdot F_{Waste} - fc_{CH_4} \frac{MW_C}{MW_{CH_4}} - fc_{CO_2} \frac{MW_C}{MW_{CO_2}} \quad (A.12)$$

$$fc_{N_{org}}^{digestate} = w'_{N_{org}/Waste} \cdot w_{MS/Waste} \cdot F_{Waste} - fc_{N_2} \frac{MW_N}{MW_{N_2}} \quad (A.13)$$

$$fc_N^{digestate} = w'_{N/Waste} \cdot w_{MS/Waste} \cdot F_{Waste} - fc_{NH_3} \frac{MW_N}{MW_{NH_3}} \quad (A.14)$$

$$fc_P^{digestate} = w'_{P/Waste} \cdot w_{MS/Waste} \cdot F_{Waste} \quad (A.15)$$

$$fc_K^{digestate} = w'_{K/Waste} \cdot w_{MS/Waste} \cdot F_{Waste} \quad (A.16)$$

$$fc_{Rest}^{digestate} = w'_{Rest/Waste} \cdot w_{MS/Waste} \cdot F_{Waste} + \quad (A.17)$$

$$fc_{CH_4}^{biogas} \cdot \frac{4 \cdot MW_H}{MW_{CH_4}} - fc_{CO_2}^{biogas} \cdot \frac{2 \cdot MW_O}{MW_{CO_2}} -$$

$$fc_{NH_3}^{biogas} \cdot \frac{3 \cdot MW_H}{MW_{NH_3}} - fc_{H_2S}^{biogas} - fc_{O_2}^{biogas}$$

$$fc_{H_2O}^{digestate} = (1 - w_{MS/Waste}) \cdot F_{Waste} - fc_{H_2O}^{biogas} \quad (A.18)$$

The energy balance to the digester is as follows:

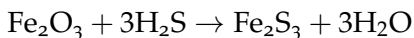
$$Q_{digester} = \Delta H_{reaction} - F \cdot c_p \cdot (T_{digester} - T_{in}) \quad (A.19)$$

$$\Delta H_{reaction} = \sum_{products} \Delta H_{comb} - \sum_{reactants} \Delta H_{comb}$$

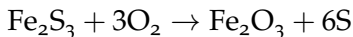
The digestate is further conditioned.

A.2 H₂S REMOVAL

Since biogas is burned for power production, any sulfur compound would potentially produce SO₂. We can avoid it by removing the H₂S. A reactive bed of Fe₂O₃ that operates at 25-50 °C is used. The actual removal is carried out following the chemical reaction below (Ryckebosch et al., 2011).



Thus, the model of this unit is based on a mass balance based on the stoichiometry of the reaction assuming 100% conversion. The bed can be regenerated using oxygen (Ryckebosch et al., 2011).



A.3 CO₂, NH₃ AND H₂O REMOVAL (PSA)

The flue gas from the gas turbine is to be used as heat source to produce steam for the steam turbine. Therefore, it is interesting that the stream has high temperature. CO₂ is removed from biogas using a packed bed of zeolite 5A operating at 25 °C and 4.5 bar. To secure continuous operation, two adsorbent beds operate in parallel so that while one is in adsorbent mode, the second one is under regeneration. We assume a recovery of 100% for NH₃ and H₂O (because of their low total quantities in the biogas, in general), 95% for CO₂ and 0% for any other gas of the mixture (Association, 2004; Inc., 2006).

A.4 BRAYTON CYCLE

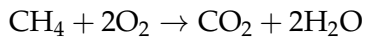
The process consists of a three stage polytropic compressor with intercooling. Each compressor is modelled assuming polytropic behavior using Eqs. A.20 - A.21 to compute the exit temperature and the power required for each stage. After each compression stage, intercooling is used to reduce the power input. The polytropic coefficient, k , is taken to be 1.4 based on an offline simulation using CHEMCAD®. The efficiency of the compressor is assumed to be 85% (Moran & Shapiro, 2003). A maximum compression ratio of 40 for air is used, based on typical achievements (Aero-engines, 1997). The intercooling stage is modeled as simple energy balance to compute the cooling required to cool down the gas to the initial temperature of the previous compressor.

$$T_{out/compressor} = T_{in/compressor} + T_{in/compressor} \left(\left(\frac{P_{out/compressor}}{P_{in/compressor}} \right)^{\frac{z-1}{z}} - 1 \right) \frac{1}{\eta_c} \quad (\text{A.20})$$

Eq21

$$W_{compressor} = (F) \cdot \frac{R \cdot z \cdot (T_{in/compressor})}{((MW) \cdot (z - 1))} \frac{1}{\eta_c} \left(\left(\frac{P_{out/compressor}}{P_{in/compressor}} \right)^{\frac{z-1}{z}} - 1 \right) \quad (\text{A.21})$$

The combustion of the biogas, see reactions below, heats up the mixture. We use an excess of 20% of air with respect to the stoichiometry and assume 100% conversion of the reaction.



The material balance is based on the stoichiometry of the chemical reaction stated above and an energy balance is used to compute temperature of the gases exiting the gas turbine as given by Eq. A.22:

$$Q_{Furnace} = \sum_h \Delta H_{f,h}^{Furnace, GasTurb}(T) - \sum_h \Delta H_{f,h}^{Compress2, Furnace}(T) - \sum_h \Delta H_{f,h}^{Compress3, Furnace}(T) \quad (\text{A.22})$$

The hot flue gas is expanded in the gas turbine to generate power. Eq. A.21 is used to model the performance of the gas turbine. The polytropic coefficient is taken to be 1.3, also based on an offline simulation using CHEMCAD ®, with an efficiency of 85% (Moran & Shapiro, 2003). Finally, the exhaust gas is cooled down and used to generate high pressure steam to be fed to the Rankine cycle.

A.5 RANKINE CYCLE

The steam is generated in a system of heat exchangers. Two alternatives are evaluated:

1. Only a fraction of the flue gas from the gas turbine is used to produce the high pressure steam fed to the steam turbine. The rest of the gas is used for the regeneration step.

2. The entire flue gas is used to heat up the saturated steam before feeding it to the high pressure turbine. Next, it is used to reheat the expanded steam before feeding it to the medium pressure turbine.

In the second body of the turbine, part of the steam is extracted at a medium pressure and it is used to heat up the condensate. The rest of the steam is finally expanded to an exhaust pressure, condensed and recycled. The flue gas is used for heating up and evaporating this stream. Due to the size of the plants and their typical location, a farm, it is expected that a lagoon is used to condensate the working fluid. Each unit is modeled using mass and energy balances as well as thermodynamic properties (Martín & Martín, 2013; Vidal & Martín, 2015).

The enthalpy and entropy of steam as a function of the temperature and pressure are correlated as in previous work (Martín & Martín, 2013; Vidal & Martín, 2015). The equations can be found in the appendix below. Therefore, the stream exiting the first body can be calculated using Eqs. A.23-A.28, assuming an isentropic efficiency, η_s , of 0.9.

$$\eta_s = \frac{H_{steam}^{Turb1,HX5} - H_{steam,HX4,Turb1}}{H_{steam,isoentropy} - H_{steam}^{HX4,Turb1}} \quad (\text{A.23})$$

where:

$$H_{steam,isoentropy} = f(p_{Turb1,HX5}, T^*_{Turb1,HX5}) \quad (\text{A.24})$$

T^* represents the isentropic temperature after the expansion computed as follows:

$$\begin{aligned} s_{steam}^{HX4,Turb1} &= \\ f(p_{HX4,Turb1}, T_{HX4,Turb1}) &= f(p_{Turb1,HX5}, T^*_{Turb1,HX5}) \end{aligned} \quad (\text{A.25})$$

We make sure that the output of the turbine is superheated steam by maintaining its temperature above the one that corresponds to saturation for the pressure of the stream.

$$p_{turb,2} \cdot 760 = e^{\left(A_{H_2O} - \frac{B_{H_2O}}{(C_{H_2O} \cdot T_{turb,1,min})} \right)} \quad (\text{A.26})$$

$$T_{Turb,1,HX5} > T_{turb,1,min} \quad (\text{A.27})$$

The energy that is obtained in the steam expansion in the first turbine is given by Eq. A.28:

$$W_{Turbine1} = fc_{H2O}^{HX4,Turb1} \cdot (H_{steam}^{HX4,Turb1} - H_{steam}^{Turb1,HX5}) \quad (\text{A.28})$$

The stream, as superheated vapor, is heated up again in HX5 using a fraction of the exhaust gas from the gas turbine, Eq. A.29, or the entire flow depending on the flowsheet configuration, Eq. A.30. Next, the superheated steam is fed to a second turbine. HX5 is modeled using Eq. A.29-A.31.

$$Q_{HX5} = fc_{H2O}^{Turb1,HX5} \cdot (H_{steam}^{HX5,Turb2} - H_{steam}^{Turb1,HX5}) \quad (\text{A.29})$$

$$Q_{HX5} = -F_{Spl1,HX5}^{Sp1,HX5} \cdot \int_{T_{Spl1,HX5}}^{T_{HX5,Mix1}} Cp_{sat} dT \quad (\text{A.30})$$

$$Q_{HX5} = -F_{HX4,HX5}^{HX4,HX5} \cdot \int_{T_{(HX4,HX5)}}^{T_{HX5,Mix1}} Cp_{salt} dT \quad (\text{A.31})$$

In the second turbine there is another expansion to a lower pressure. Part of the stream will be sent to HX7, while the rest is used in the third body of the turbine, where it is expanded to a pressure below atmosphere, see Eq. A.32; this pressure ranges from 0.05 bar to 0.31 bar in the literature (Vidal & Martín, 2015). The second and third bodies of the turbine are calculated similarly to the first one, assuming 0.9 isentropic efficiency in all stages.

$$fc_{H2O}^{HX5,Turb2} = fc_{H2O}^{Turb2,HX7} + fc_{H2O}^{Turb2,Turb3} \quad (\text{A.32})$$

The stream extracted from the medium pressure turbine is sent to HX7, where it will be used to reheat the liquid obtained after condensing the exhaust of the third body of the turbine. The exhaust of the low pressure turbine is assumed to be saturated vapor. This stream is condensed in HX6:

$$Q_{(HX6)} = fc_{H2O}^{Turb3,HX6} \cdot (H_{liq}^{HX6,HX7} - H_{steam}^{Turb3,HX6}) \quad (\text{A.33})$$

This energy must be removed in the cooling system. We assume that a lagoon is used to cool down the water used to condense the saturated steam before reuse. This part is not included in the model. When mixing the exhaust of the second turbine with the compressed liquid from HX6, we must bear in mind that the outlet should be liquid since it is going to be compressed and heated up as a liquid in HX8. Eq. A.34 ensures this fact:

$$T_{HX7,HX8} \leq T_{turb,2,min} \quad (\text{A.34})$$

BIBLIOGRAPHY

- Aero-engines, J. (1997). *Jane's Information Group*, (tech. rep.). Sentinel House.
- Al Seadi, T., Rutz, D., Prassl, H., Köttner, M., Finsterwalder, T., Volk, S., & Janssen, R. (2008). *Biogas handbook* (2008th ed.). Denmark, Syddansk Universitet.
- Association, G. P. S. (2004). *GPSA engineering data book, 12th ed.* (tech. rep.). Gas Processors Suppliers Association.
- Department for Environment Food and Rural Affairs (DEFRA). (2011). Fertiliser Manual (RB209) [[Online; accessed 29-April-2017]].
- Inc., N. (2006). *Equipment Design and Cost Estimation for Small Modular Biomass Systems, Synthesis Gas Cleanup, and Oxygen Separation Equipment. Task 2: Gas Cleanup Design and Cost Estimates – Black Liquor Gasification* (tech. rep.). National Renewable Energy Laboratory (NREL).
- Kaparaju, P., & Rintala, J. (2013). Generation of heat and power from biogas for stationary applications: boilers, gas engines and turbines, combined heat and power (CHP) plants and fuel cells. In *The biogas handbook* (pp. 404–427). Elsevier.
- Martín, L., & Martín, M. (2013). Optimal year-round operation of a concentrated solar energy plant in the south of Europe. *Applied Thermal Engineering*, 59(1-2), 627–633.
- Moran, M., & Shapiro, H. (2003). *Fundamentals of Engineering Thermodynamics* (5th ed.). Wiley.
- Ryckebosch, E., Drouillon, M., & Vervaeren, H. (2011). Techniques for transformation of biogas to biomethane. *Biomass and bioenergy*, 35(5), 1633–1645.
- Sinnott, R. (1999). Coulson and Richardson's Chemical Engineering (2nd ed.). *Chemical engineering design*.
- Vidal, M., & Martín, M. (2015). Optimal coupling of biomass and solar energy for the production of electricity and chemicals. *Comp. Chem. Eng*, 72, 273–283.

B

APPENDIX B: SUPPLEMENTARY INFORMATION OF CHAPTER 3

B.1 CATTLE ORGANIC WASTE COMPOSITION

To calculate the distribution functions of the different compounds of the cattle organic waste, 37 data sets for cattle organic waste compositions from 20 bibliographic references were evaluated. Table B.1 collects the main statistical parameters of the data, and Table B.2 shown the data obtained from literature.

B.2 DISTRIBUTION FUNCTIONS OF ELEMENTS FROM CATTLE WASTE

The kernel density estimation (KDE) method is used to fit the probability function to data distribution and to determine the probability density distributions of calcium, nitrogen, phosphorus, potassium, ammonia/total nitrogen, and phosphate/total phosphorus. As histograms, KDE is a non-parametric way to estimate the probability density function of a random variable. However, in the KDE method, kernels are functions associated with each data set. Thus, the unknown density function can be computed as the weighted sum of these functions (Duong, 2001).

The calculation procedure is divided into three steps. First, cattle organic waste composition data are collected from the literature. Second, the KDEs of all compounds are estimated, and finally, distribution functions are fitted, using the kernel density estimations to validate the chosen distribution. The probability density distributions which best fit the data distribution are normal distribution functions for the distribution of nitrogen as in Figure B.1a, ammonia/total nitrogen molar ratio as observed in Figure B.1b, and phosphorus as shown in Figure B.1c. Lognormal distribution functions are the best fit for phosphate/total phosphorus molar ratio as in Figure B.1d, calcium, as shown in Figure B.1e, and potassium as observed in Figure B.1f.

Table B.1: Statistical summary of cattle organic waste composition. Data from (Alburquerque et al., 2012; Bolzonella et al., 2018; Gell et al., 2011; Krichmann & Witter, 1992; Ledda et al., 2016; Løes et al., 2017; Martin, 2003; Möller & Müller, 2012; Möller et al., 2008; Moset et al., 2017; Normak et al., 2012; Rigby & Smith, 2011; Risberg et al., 2017; Seppälä et al., 2013; Smith et al., 2007; Sørensen et al., 2011; Tampere & Viiralt, 2014; Walsh et al., 2012; Xia et al., 2012; Zheng et al., 2016).

	DM (% mass)	C (% mass)	Ca (% mass)	K (% mass)	N (% mass)	P (% mass)	$\frac{\text{Ca}^{2+}}{\text{Total Ca}}$	$\frac{\text{K}^+}{\text{Total K}}$	$\frac{\text{N-NH}_4^+}{\text{Total N}}$	$\frac{\text{P-PO}_4^{3-}}{\text{Total P}}$
count	36	6	9	12	35	24	1	1	31	13
mean	5.858	2.478	0.117	0.253	0.384	0.059	0.154	1.000	0.590	0.541
std	1.778	0.946	0.027	0.158	0.133	0.038	NaN	NaN	0.117	0.159
min	2.624	1.200	0.080	0.084	0.114	0.005	0.154	1.000	0.348	0.216
25.00%	4.610	1.719	0.100	0.148	0.299	0.032	0.154	1.000	0.516	0.421
50.00%	5.668	2.788	0.110	0.223	0.399	0.048	0.154	1.000	0.616	0.597
75.00%	7.362	3.194	0.129	0.276	0.449	0.080	0.154	1.000	0.666	0.671
max	9.200	3.400	0.165	0.635	0.789	0.164	0.154	1.000	0.820	0.700

Table B.2: Data obtained from literature.

Dry matter (% wt)	N (% wt)	P (% wt)	K (% wt)	C (% wt)	Ca (% wt)	PO ₄ ratio	NH ₄ /N ratio	Ca ²⁺ /Ca ratio	K ⁺ /K ratio	Reference
7.35	0.52	0.15	0.64	2.98	0.17	0.35	0.63			Möller and Müller, 2012
4.90	0.79	0.04	0.16		0.13	0.33	0.68	0.15	1	Rigby and Smith, 2011
7.40	0.42	0.03	0.23				0.38			Smith et al., 2007
6.50	0.45						0.60			Smith et al., 2007
5.58	0.46						0.64			Smith et al., 2007
4.49	0.51	0.05	0.12				0.82			Smith et al., 2007
8.47	0.55	0.05				0.67	0.56			Smith et al., 2007
5.69	0.35	0.04				0.70	0.65			Smith et al., 2007
8.30	0.57	0.05				0.64	0.50			Smith et al., 2007
6.75	0.37	0.03				0.57	0.64			Smith et al., 2007
3.80	0.40	0.03				0.70	0.67			Smith et al., 2007
5.50	0.35	0.03				0.60	0.45			Smith et al., 2007
7.99	0.45	0.03				0.62	0.55			Smith et al., 2007
7.52	0.41	0.03				0.54	0.58			Smith et al., 2007
7.40	0.34			3.40			0.65			Risberg et al., 2017
6.10	0.41			2.60			0.68			Risberg et al., 2017
4.80	0.27	0.05	0.36			0.22	0.35			Seppälä et al., 2013
4.12	0.20						0.52			Alburquerque et al., 2012
7.84	0.25						0.38			Alburquerque et al., 2012
2.62	0.15						0.53			Alburquerque et al., 2012
7.00	0.34	0.16				0.42	0.52			Bolzonella et al., 2018
6.10	0.20									Gell et al., 2011
6.24	0.47						0.42			Moiset et al., 2017
7.20	0.36	0.08					0.51			Ledda et al., 2016
	0.27	0.06	0.08		0.13					Kirchmann and Witter, 1992
9.20	0.40	0.06	0.43	3.27						Möller et al., 2008
5.20	0.11	0.01	0.09	1.42	0.10					Walsh et al., 2012
4.40										Zheng et al., 2016
4.65	0.29						0.62			Sørensen et al., 2011
4.82	0.31						0.67			Sørensen et al., 2011
3.50	0.43	0.08	0.22		0.11		0.72			Tampere and Viiralt, 2014
3.80	0.44	0.08	0.22		0.08		0.73			Tampere and Viiralt, 2014
3.20	0.43	0.08	0.24		0.10		0.77			Tampere and Viiralt, 2014
3.00	0.24	0.03		1.20	0.09		0.63			Løes et al., 2017
9.11	0.55	0.09				0.67	0.56			Martin, 2003
4.70	0.40	0.08	0.25		0.15		0.72			Normak et al., 2012
5.65										Xia et al., 2012

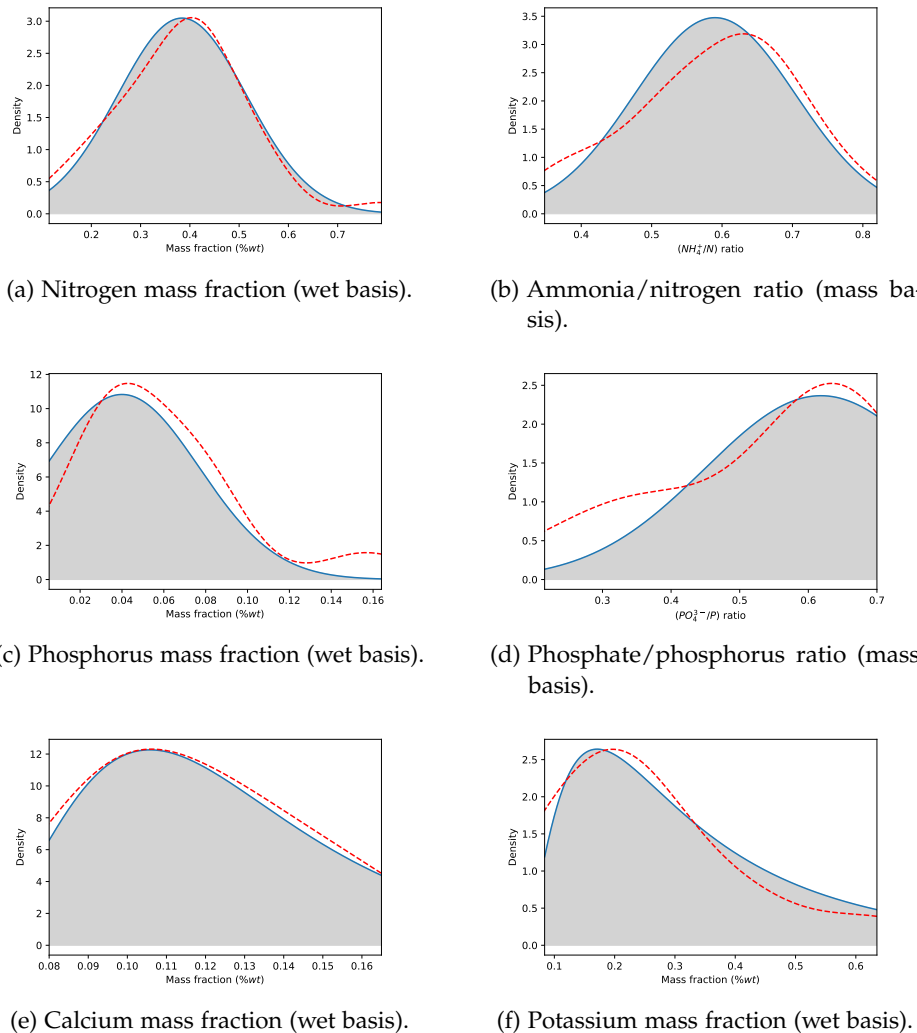


Figure B.1: Kernel density estimation (red dashed line) and probability density distribution (blue solid line) for the evaluated components in cattle organic waste.

B.3 THERMODYNAMIC MODELING OF THE CARBONATES SYSTEM

To calculate the total carbonate content, the concept of defining alkalinity will be used. The formal definition of total alkalinity is the capacity of a solution to buffer changes in pH that would make the solution more acidic. From the perspective of charge balance, total alkalinity can be considered as a measure of the number of protons that can be accepted by the proton acceptors present in the dissolution. Therefore, total alkalinity, TA , is calculated as the excess of proton acceptors over donors with respect to a chosen zero level of protons, as in Eq. B.1:

$$TA = \text{proton acceptors} - \text{proton donors} \quad (\text{B.1})$$

Note that the distribution of different species for various systems, such as carbonic acid and phosphoric acid, depend on pH, and the contribution of each species to alkalinity, is a function of its electrical charge. For our case, the chemical systems considered are water, carbonic acid, phosphoric acid, and ammonia systems

A zero level of protons is a reference system defined by choosing a certain chemical compound for each system at a certain pH selected arbitrarily. This reference chemical is the dominant species at the selected pH. The chemical species above this zero level of protons will be proton acceptors while species below this level will be proton donors in a determined chemical system. There is a standard defined by Dickson (1981), where the reference pH value is set to 4.5 and chosen as the zero level of protons. For a more detailed discussion about alkalinity, we refer to Wolf-Gladrow et al. (2007). The dominant chemical substances for each system at the reference pH of 4.5 are H_2O , H_2CO_3 , $H_2PO_4^-$ and NH_4^+ . With these considerations, the proton donors and acceptors for each system are collected in Table B.3:

Table B.3: Proton donors and acceptors for each chemical system.

Chemical system	Proton donors	Proton acceptors
Water	$\{H^+\}$	$\{OH^-\}$
Carbonic acid	$\{H^+\}$	$\{HCO_3^-\}$, $2 \cdot \{CO_3^{2-}\}$
Phosphoric acid	$\{H_3PO_4\}$, $\{H^+\}$	$\{HPO_4^{2-}\}$, $2 \cdot \{PO_4^{3-}\}$
Ammonia system	$\{H^+\}$	$\{NH_3\}$

Therefore, the alkalinity due to carbonates, called carbonate alkalinity (Alk_{carb}), as described in Eq. B.2, can be calculated from total alkalinity value minus the alkalinity contribution of the other compounds, Eq. B.4. The activities of the chemical species from water, phosphoric acid, and ammonia systems are obtained by solving the equilibrium and mass balance equations described previously.

The formulation of the alkalinity problem is described next. First, the alkalinity given in milligrams of CaCO_3 per liter is transformed into equivalents per liter by Eq. B.3 and the carbonate alkalinity is calculated through Eq. B.4.

$$Alk_{carb} = \{\text{HCO}_3^-\} + 2\{\text{CO}_3^{2-}\} \quad (\text{B.2})$$

$$Alk \left(\frac{Eq}{L} \right) = \frac{mg_{\text{CaCO}_3}}{L} \cdot \frac{1\text{ g}}{1000\text{ mg}} \cdot \frac{1Eq}{50\text{ g}} \quad (\text{B.3})$$

$$Alk_{carb} = Alk - \{\text{OH}^-\} - \{\text{HPO}_4^{2-}\} - 2\{\text{PO}_4^{3-}\} \\ - \{\text{NH}_3\} + \{\text{H}_3\text{PO}_4\} + \{\text{H}^+\} \quad (\text{B.4})$$

To compute the distribution of carbonate species, the fractions of each compound (α_{CO_2} , $\alpha_{\text{HCO}_3^-}$ and $\alpha_{\text{CO}_3^{2-}}$), which only depend on the pH, are calculated by employing Eqs. B.5 - B.7 (Wolf-Gladrow et al., 2007). As only HCO_3^- , and CO_3^{2-} contribute to alkalinity, the first one with one equivalent and the second one with two equivalents, as shown in Eq. B.2, it is necessary to add Eq. B.8. Because cattle waste has basic pH and the major species are HCO_3^- and CO_3^{2-} , it has been considered that total

carbonates calculated in Eq. B.8, are equal to the sum of all carbonate species in the organic waste.

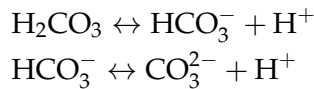
$$\alpha_{CO_2} = \frac{\{H^+\}^2}{\{H^+\}^2 + \{H^+\} K_{sp_{H_2CO_3}} + K_{sp_{H_2CO_3}} K_{sp_{HCO_3^-}}} \quad (B.5)$$

$$\alpha_{HCO_3^-} = \frac{\{H^+\} K_{sp_{H_2CO_3}}}{\{H^+\}^2 + \{H^+\} K_{sp_{H_2CO_3}} + K_{sp_{H_2CO_3}} K_{sp_{HCO_3^-}}} \quad (B.6)$$

$$\alpha_{CO_3^{2-}} = \frac{K_{sp_{H_2CO_3}} K_{sp_{HCO_3^-}}}{\{H^+\}^2 + \{H^+\} K_{sp_{H_2CO_3}} + K_{sp_{H_2CO_3}} K_{sp_{HCO_3^-}}} \quad (B.7)$$

$$\text{Total carbonates} = \frac{Alk_{carb}}{\alpha_{HCO_3^-} + 2\alpha_{CO_3^{2-}}} \quad (B.8)$$

Once the total carbonates concentration is known, the thermodynamic models for carbonate species existing in aqueous phase can be defined for the following species



Two elements are necessary to define the thermodynamic models for carbante species, the therodynamic equilibria defined by the Eq. B.9, computed using activity coefficients, and mass balance defined by Eq. B.11. Finally, solving the equations 2 to 11 the concentrations of the different carbonate species are determined. pK_{sp} values for all systems evaluated in this work are collected in Table B.4.

$$K_{sp} = \frac{\prod \{Products\}}{\prod \{Reactants\}} \quad (B.9)$$

$$[i]_{initial} = \sum_{products} [i]_{products} \quad (B.10)$$

$$i \in \{CO_3^{2-}\}$$

$$\text{Total carbonates} = [H_2CO_3] + [HCO_3^-] + [CO_3^{2-}] \quad (B.11)$$

Table B.4: pK_{sp} values for the considered aqueous phase chemical systems.

Name	Chemical system	pK_{sp}	Source
Ammonia	$\text{NH}_4^+ \leftrightarrow \text{NH}_3 + \text{H}^+$	9.2	Bates and Pinching, 1949
Water	$\text{H}_2\text{O} \leftrightarrow \text{OH}^- + \text{H}^+$	14	Skoog et al., 2014
Phosphoric acid	$\text{H}_3\text{PO}_4 \leftrightarrow \text{H}_2\text{PO}_4^- + \text{H}^+$	2.1	Ohlinger et al., 1998
	$\text{H}_2\text{PO}_4^- \leftrightarrow \text{HPO}_4^{2-} + \text{H}^+$	7.2	Ohlinger et al., 1998
Carbonic acid	$\text{HPO}_4^{2-} \leftrightarrow \text{PO}_4^{3-} + \text{H}^+$	12.35	Ohlinger et al., 1998
	$\text{H}_2\text{CO}_3 \leftrightarrow \text{HCO}_3^- + \text{H}^+$	6.35	Skoog et al., 2014
	$\text{HCO}_3^- \leftrightarrow \text{CO}_3^{2-} + \text{H}^+$	10.33	Skoog et al., 2014

B.4 SURROGATE MODELS TO ESTIMATE PRECIPITATES FORMATION FROM LIVESTOCK WASTE

B.4.1 Influence of magnesium

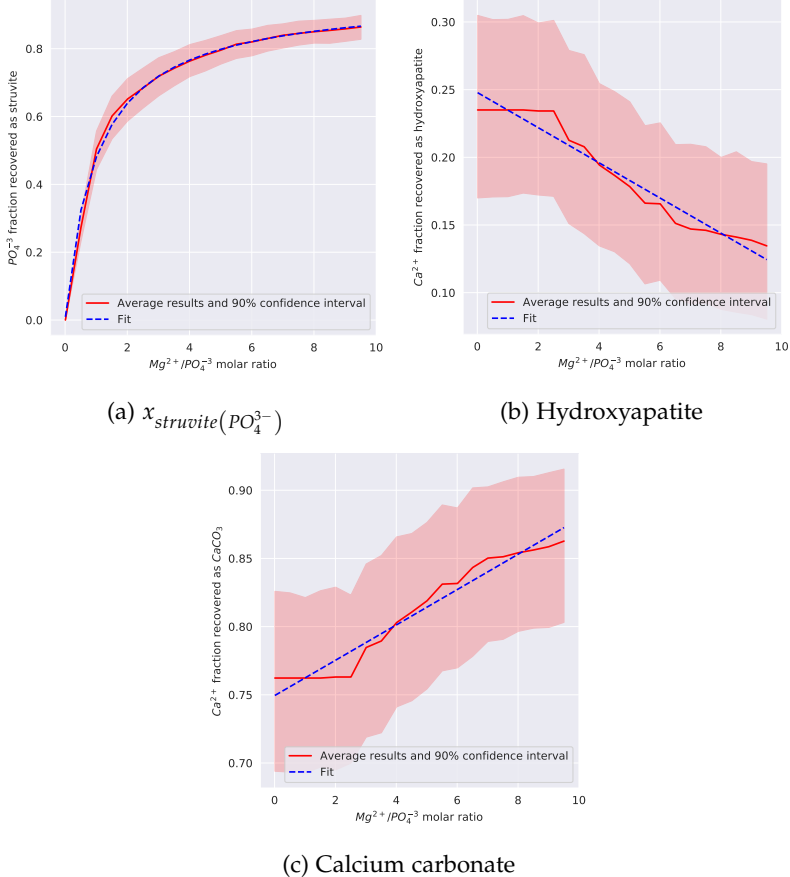


Figure B.2: Evolution phosphorus as phosphate fraction recovered as struvite and calcium fraction recovered as precipitates along Mg^{2+}/PO_4^{3-} molar ratio values considering 50 different composition data sets.

B.4.1.1 Influence of calcium

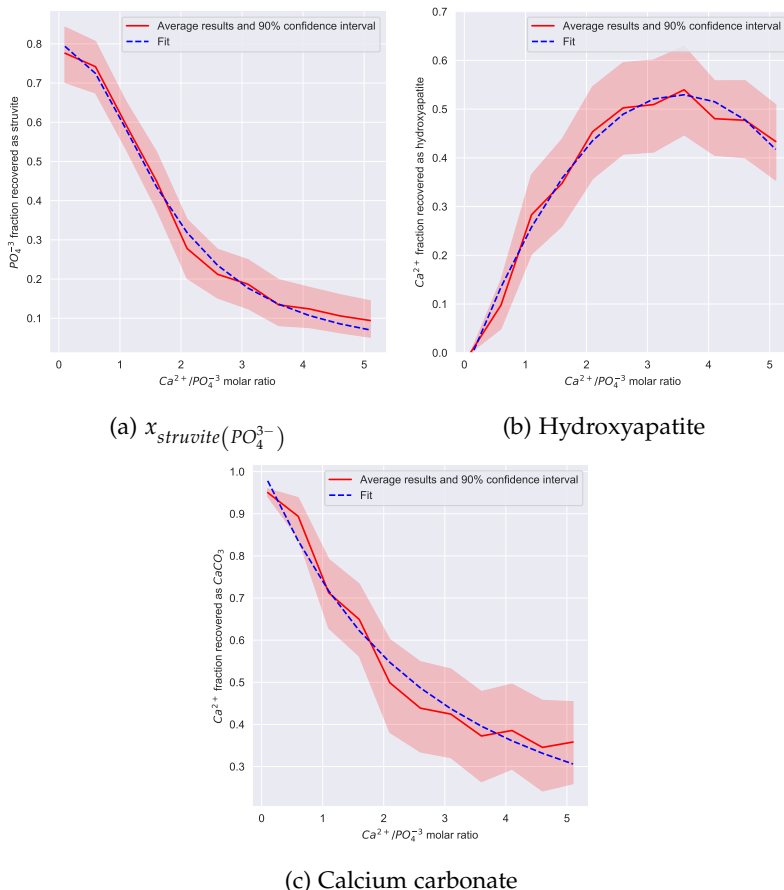


Figure B.3: Evolution of phosphorus as phosphate fraction recovered as struvite and calcium fraction recovered as precipitates along $\text{Ca}^{2+}/\text{PO}_4^{3-}$ molar ratio values considering 50 different composition data sets.

B.4.1.2 Influence of alkalinity

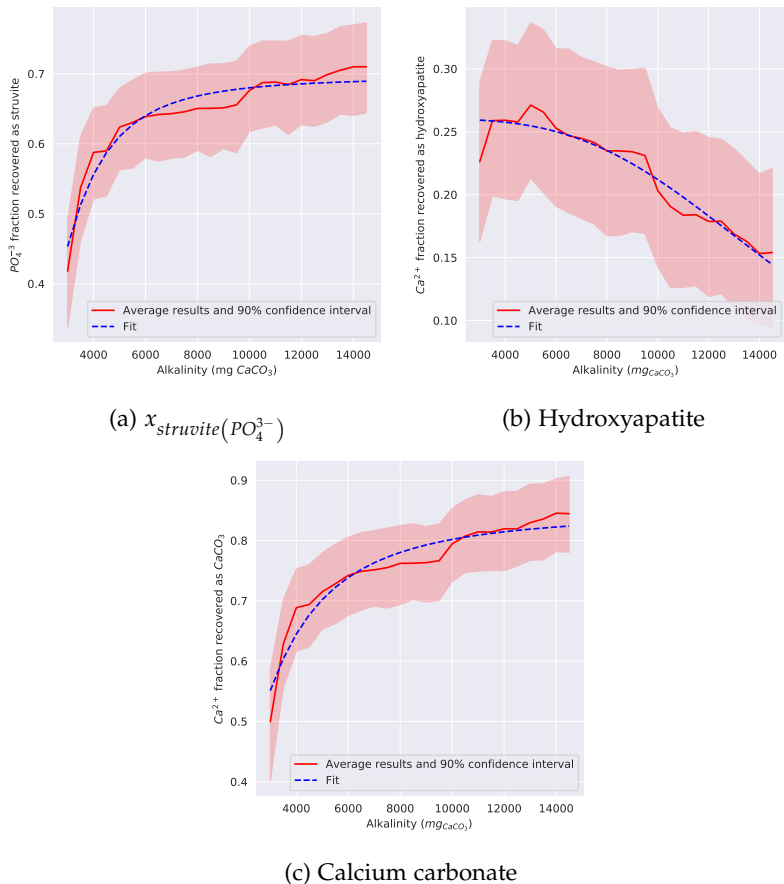


Figure B.4: Evolution of phosphorus as phosphate fraction recovered as struvite and calcium fraction recovered as precipitates among alkalinity values considering 50 different composition data sets.

BIBLIOGRAPHY

- Alburquerque, J., de la Fuente, C., & Bernal, M. (2012). Chemical properties of anaerobic digestates affecting C and N dynamics in amended soils. *Agric. Ecosyst. Environ.*, 160, 15–22.
- Bates, R. G., & Pinching, G. (1949). Acid dissociation constant of ammonium ion at 0–50 °C, and the base strength of ammonia. *Journal of Research of the National Bureau of Standards*, 42, 419–430.
- Bolzonella, D., Fatone, F., Gottardo, M., & Frison, N. (2018). Nutrients recovery from anaerobic digestate of agro-waste: Techno-economic assessment of full scale applications. *J. Environ. Manage.*, 216, 111–119.
- Dickson, A. (1981). An exact definition of total alkalinity and a procedure for the estimation of alkalinity and total inorganic carbon from titration data. *Deep-Sea Res.*, 28(6), 609–623.
- Duong, T. (2001). An introduction to kernel density estimation. *University of Western Australia*.
- Gell, K., van Groenigen, J., & Cayuela, M. (2011). Residues of bioenergy production chains as soil amendments: Immediate and temporal phytotoxicity. *J. Hazard. Mater.*, 186, 2017–2025.
- Kirchmann, H., & Witter, E. (1992). Composition of fresh, aerobic and anaerobic farm animal dungs. *Bioresour. Technol.*, 40(2), 137–142.
- Ledda, C., Schievano, A., Scaglia, B., Rossoni, M., G., A. F. F., & Adani, F. (2016). Integration of microalgae production with anaerobic digestion of dairy cattle manure: an overall mass and energy balance of the process. *J. Clean. Prod.*, 112, 103–112.
- Løes, A., Pommeresche, R., & Khalil, R. (2017). *Effects of marble application to manure and anaerobic digestates* (tech. rep.). NORSØK.
- Martin, J. (2003). *A Comparison of Dairy Cattle Manure Management with and without Anaerobic Digestion and Biogas Utilization* (tech. rep.). AgSTAR Program, U.S. Environmental Protection Agency.
- Möller, K., & Müller, T. (2012). Effects of anaerobic digestion on digestate nutrient availability and crop growth: A review. *Eng. Life Sci.*, 12(3), 242–257.
- Möller, K., Stinner, W., Deuker, A., & Leithold, G. (2008). Effects of different manuring systems with and without biogas digestion on nitrogen cycle and crop yield in mixed organic dairy farming. *Nutr. Cycl. Agroecosyst.*, 82(3), 209–232.
- Moset, V., Fontaine, D., & Møller, H. (2017). Co-digestion of cattle manure and grass harvested with different technologies. Effect on methane yield, digestate composition and energy balance. *Energy*, 141, 451–460.

- Normak, A., Suurpere, J., Orupõld, K., Jõgi, E., & Kokin, E. (2012). Simulation of anaerobic digestion of cattle manure. *Agronomy Research Biosystem Engineering Special Issue*, 1, 167–174.
- Ohlinger, K. N., Young, T., & Schroeder, E. (1998). Predicting struvite formation in digestion. *Wat. Res.*, 32(12), 3607–3614.
- Rigby, H., & Smith, S. (2011). *New Markets for Digestate from Anaerobic Digestion* (tech. rep.). WRAP (Waste and Resources Action Programme).
- Risberg, K., Cederlund, H., Pell, M., Arthurson, V., & Schnürer, A. (2017). Comparative characterization of digestate versus pig slurry and cow manure - Chemical composition and effects on soil microbial activity. *Waste Manag.*, 61, 529–538.
- Seppälä, M., Pyykkönen, V., Väisänen, A., & Rintala, J. (2013). Biomethane production from maize and liquid cow manure - Effect of share of maize, post-methanation potential and digestate characteristics. *Fuel*, 107, 209–216.
- Skoog, D., West, D., Holler, F., & Crouch, S. (2014). *Fundamentals of analytical chemistry*. Cengage Learning.
- Smith, K., Grylls, J., Metcalfe, P., Jeffrey, B., & Sinclair, A. (2007). *Nutrient Value of Digestate from Farm-Based Biogas Plants in Scotland* (tech. rep.). Scottish Executive Environment and Rural Affairs Department.
- Sørensen, P., Mejnertsen, P., & Møller, H. (2011). Nitrogen fertilizer value of digestates from anaerobic digestion of animal manures and crops. *NJF Report*, 7(8), 42–44.
- Tampere, M., & Viiralt, R. (2014). The efficiency of biogas digestate on grassland compared to mineral fertilizer and cattle slurry. *Research for Rural Development*, 1, 89–94.
- Walsh, J., Jones, D., Edwards-Jones, G., & Williams, A. (2012). Replacing inorganic fertilizer with anaerobic digestate may maintain agricultural productivity at less environmental cost. *J. Plant. Nutr. Soil Sci.*, 175(6), 840–845.
- Wolf-Gladrow, D., Zeebe, R., Klaas, C., Kötzinger, A., & Dickson, A. (2007). Total alkalinity: The explicit conservative expression and its application to biogeochemical processes. *Mar. Chem.*, 106, 287–300.
- Xia, M., Tao, W., Wang, Z., & Pei, Y. (2012). Treatment of anaerobically digested dairy manure in a two-stage biofiltration system. *Water Sci. Technol.*, 65(11), 1975–1981.
- Zheng, Y., Ke, L., Xia, D., Zheng, Y., Wang, Y., Li, H., & Li, Q. (2016). Enhancement of digestates dewaterability by CTAB combined with CFA pretreatment. *Sep. Purif. Technol.*, 163, 282–289.

C

APPENDIX C: SUPPLEMENTARY INFORMATION OF CHAPTER 4

C.1 ENVIRONMENTAL GEOGRAPHIC INFORMATION MODEL

C.1.1 *Trophic State Index*

Carlson (1977) proposed the Trophic State Index (TSI) as a metric to determine the trophic status of waterbodies. This is used by the U.S. Environmental Protection Agency (US EPA) (U.S. Environmental Protection Agency, 2012a). This index can be calculated using three parameters: concentration of chlorophyll- α (chl- α), concentration of total phosphorus, and water turbidity measured through the Secchi depth. Only the two first methods has been used in this work since they are less affected to exogenous phenomena (such as atmospheric conditions, or variations in the flow of water streams). Correlations to compute the TSI from these parameters are shown in Eq. C.1 and C.2 , where Chl denotes the concentration of chlorophyll- α , and TP denotes the concentration of total phosphorus in mg/m^3 (Carlson, 1977).

The TSI of a waterbody is scored in a range from zero to one hundred, which can be correlated with the oligotrophic, mesotrophic, eutrophic and hypereutrophic classes as shown in Table C.1. Oligotrophic and mesotrophic denote low and intermediate biomass productivities, while eutrophic and hypereutrophic are referred to waterbodies with high biological productivity and frequent algal blooms. Combined data for chl- α and total phosphorus concentrations retrieved from the National Lakes Assessments (NLA) carried out by the US EPA in the years 2007 and 2012 (U.S. Environmental Protection Agency, 2007, 2012b) is used to determine the Trophic State Index of lentic waters in the contiguous U.S, as shown in Fig. C.1. No TSI values are assigned to the watersheds without reported data.

$$TSI_{chl-\alpha} = 10 \cdot \left(6 - \frac{2.04 - 0.68 \cdot \ln (Chl)}{(2)} \right) \quad (C.1)$$

$$TSI_{TP} = 10 \cdot \left(6 - \frac{\ln (\frac{48}{TP})}{(2)} \right) \quad (C.2)$$

Table C.1: Relation between TSI value and trophic class.

TSI	<40	40-50	50-70	>70
Trophic Class	Oligotrophic	Mesotrophic	Eutrophic	Hypereutrophic

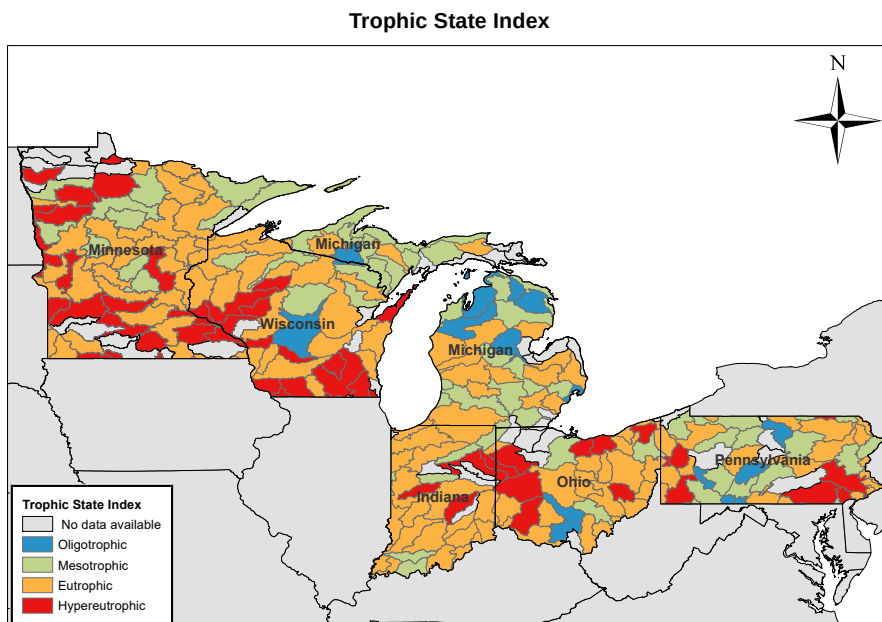


Figure C.1: Trophic State Index in the contiguous US HUC8 watersheds

C.1.2 Balance of anthropogenic phosphorus releases

Agricultural releases are a main source of human-based phosphorus releases due to the excessive use of synthetic fertilizers and livestock waste for nutrient supplementation in croplands (Dzombak, 2011). Since this work is limited to the assessment of agricultural phosphorus releases, other possible sources of phosphorus releases are not considered. Agricultural phosphorus releases have been estimated from data reported by the Nutrient Use Geographic Information System (NuGIS) project. Further information about the methodology used for the estimation of human-based phosphorus releases can be found in International Plant Nutrition Institute (IPNI) (2012).

The anthropogenic phosphorus uptakes considered are those due to the crops grown in each watershed. In addition, phosphorus retained by wetlands is considered. Data from **USDAWaste** is used to estimate the phosphorus uptakes of different crops, attending to their different

phosphorus requirements and yield rates. To determine the crops grown in each watershed, the land cover uses are first determined using data from the US EPA EnviroAtlas database for the most recent year available (2011), differentiating between croplands, pasturelands, wetlands, and developed areas (urban areas) (Pickard et al., 2015). To estimate the distribution of crops in croplands, including corn, soybeans, small grains, cotton, rice, vegetables, orchards, greenhouse and other crops (i.e., fruits, sugar crops, and oil crops) (United States Department of Agriculture, 2019), data from the 2017 U.S. Census of Agriculture is used. In case of two or more crops were harvested from the same land during the year (double cropping), the area was counted for each crop. Since the data from the 2017 U.S. Census of Agriculture are published at HUC6 resolution, they have been reconciled to HUC8 level by the fraction of occupied area by each HUC8 watershed in the corresponding HUC6 watershed. The wetlands phosphorus uptake value assessed is $0.77 \text{ gP m}^{-2} \text{ year}^{-1}$, based on data reported by Kadlec (2016).

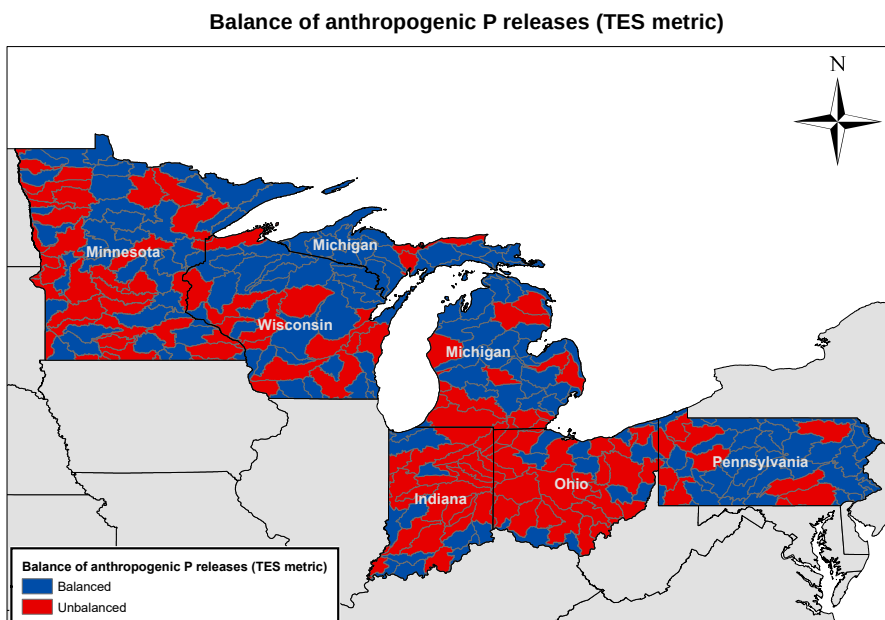


Figure C.2: Balance of anthropogenic phosphorus releases in the contiguous US at a HUC8 spatial resolution

C.1.3 Phosphorus in soils

Phosphorus concentration in soils is considered to evaluate the legacy phosphorous continuously builds-up in soils. However, only a fraction of

phosphorus is available for plants. To measure this phosphorus fraction available for plants, several standardized phosphorus soil tests have been proposed, including Olsen, Bray 1 and Mehlich 3 tests. Among them, Mehlich 3 (M₃P) has been selected as a measure of the concentration of P in soils since it is a widely used metric, and it is the P soil test least affected by changes in soil pH. To estimate the fraction of phosphorus available for plants from total phosphorus concentration data, a correlation developed by Allen and Mallarino (2006) has been used, Eq. C.3. However, this correlation has been developed for agricultural soils in Iowa. Due to the lack of wider studies in this regard, the M₃P estimations calculated for the contiguous U.S. must be considered as an exploratory effort to determine the phosphorus saturation in soils across the the contiguous U.S. in an attempt to select the most suitable nutrients management technology according to the geographic environmental indicators. Datasets for samples from the soil A horizon published by the U.S. Geological Survey (USGS) in the "Geochemical and Mineralogical Data for Soils of the Conterminous United States" report were used to evaluate the concentration of total phosphorus along the contiguous U.S. (D. B. Smith et al., 2013).

$$M_3P \text{ (% over TP)} = \frac{4.698 \cdot 10^{-1}}{1 + (\text{TotalP (mg/kg)} \cdot 1.336 \cdot 10^{-3})^{-2.148}} \quad (C.3)$$

The relationship between M₃P test value and the quality of soil is shown in Table C.2. Soil fertility levels below optimum indicate that nutrient supplementation is needed to enhance the yield of crops, optimum values indicates that no nutrient supplementation is needed, and excessive soil fertility level indicate over-saturation of phosphorus in soil that can reach waterbodies by runoff (Espinoza et al., 2006).

Table C.2: Relation between Mehlich 3 phosphorus and soil fertility level (Espinoza et al., 2006).

Soil Fertility Level	M ₃ P soil phosphorus concentration (ppm)
Very Low	<16
Low	16-25
Medium	26-35
Optimum	36-50
Excessive	>50

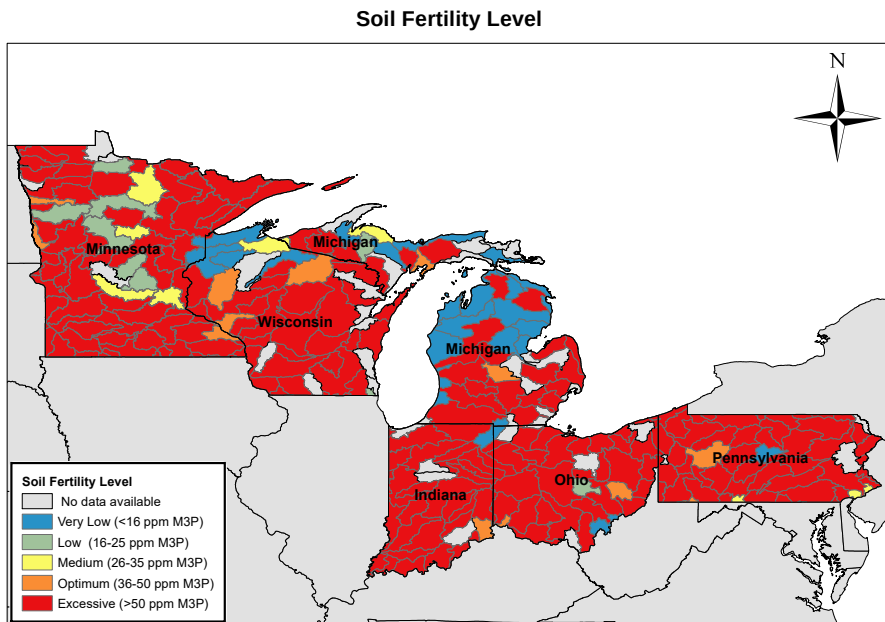


Figure C.3: Soil Fertility Level in the contiguous US at a HUC8 spatial resolution

C.2 FRAMEWORK DEVELOPMENT

C.2.1 Data entry

Table C.3: Livestock waste composition and generation rates for different types of animals (Kellogg et al., 2000; United States Department of Agriculture, 2009).

Livestock type	Water (%wt)	Organic matter (%wt)	Total N (%wt)	Total P (%wt)	Total Ca (%wt)	Total K (%wt)	Generation rate (kg/day)	Animal unit equivalence
Dairy cow	87	10,98	0,59	0,08	0,12	0,20	37,88	0,74
Dairy heifer	83	13,04	0,48	0,09	0,12	0,21	29,95	0,94
Dairy calf	83	9,28	0,51	0,06	0,12	0,13	29,95	4,00
Beef cow	88	10,58	0,34	0,08	0,12	0,24	28,58	1,00
Beef calf	88	10,00	0,58	0,10	0,12	0,38	28,14	4,00

C.2.2 Techno-economic model

C.2.2.1 Manure conditioning model

U.S. EPA determines that the content of total solids in manure should be less than 15%, as shown in Fig. C.4 (U.S. Environmental Protection

Table C.4: Predefined economic parameters.

Parameter	Value
Discount rate (%)	7
Phosphorus credits (USD / kg P recovered)	22
Electricity price (Renewable Energy Certificates) (USD/MWh)	60
Bio-methane price (Renewable Identification Number) (USD/kg)	1.25
Capital cost incentive (% over total capital cost)	0

Agency, 2004). Therefore, additional water may be added to reduce the solids content in manure before the anaerobic digestion stage.

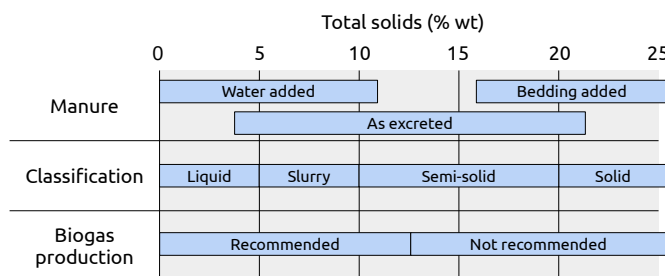


Figure C.4: Adequate manure properties for anaerobic digestion. Adapted from U.S. Environmental Protection Agency (2004).

C.2.2.2 Anaerobic digestion model

Correlations to estimate the capital cost, Eq. C.4, and operating and management costs (O&M), Eq. C.5, as a function of the animal population of CAFOs were developed using data from the US EPA AgSTAR program

Table C.5: Statistical summary of nutrients composition for cattle manure before and after anaerobic digestion (AD). All concentrations are reported in mg/L. TKN is referred to total Kjeldahl nitrogen, and TP to total phosphorus. Data from Alburquerque et al. (2012), Martin (2003), K. Smith et al. (2007), Sørensen et al. (2011).

	TKN before AD	TKN after AD	NH ₄ before AD	NH ₄ after AD	TP before AD	NH ₄ after AD	P-PO ₄ before AD	P-PO ₄ after AD
count	10.00	10.0	10.00	10.00	5.00	5.00	5.00	5.00
mean	3856.10	3967.1	1845.90	2340.10	1442.60	1449.60	811.40	946.40
std	847.41	942.9	354.59	387.34	467.14	485.29	277.67	331.88
min	2920.00	2800.0	1300.00	1810.00	813.00	838.00	457.00	562.00
25%	3050.00	3152.5	1607.50	2047.50	1170.00	1170.00	590.00	670.00
50%	3660.00	3855.0	1825.00	2340.00	1450.00	1360.00	880.00	950.00
75%	4630.75	4882.5	2159.75	2590.00	1860.00	1920.00	1050.00	1260.00
max	4960.00	5290.0	2300.00	2881.00	1920.00	1960.00	1080.00	1290.00

(U.S. Environmental Protection Agency, 2003) and the USDA (Beddoes et al., 2007) respectively, as shown in Figure C.5. It should be noted that O&M cost does not include the capital cost amortization. Therefore, to estimate the total production cost, the annualized equipment cost has been added to the O&M costs, Eq. C.6. The assumed equipment lifetime is 20 years.

$$\text{Installation cost (MM USD (2019))} = \left(4.271 \cdot 10^{-4} \cdot N_{\text{animals}} + 0.127 \right) \cdot 1.511 \quad (\text{C.4})$$

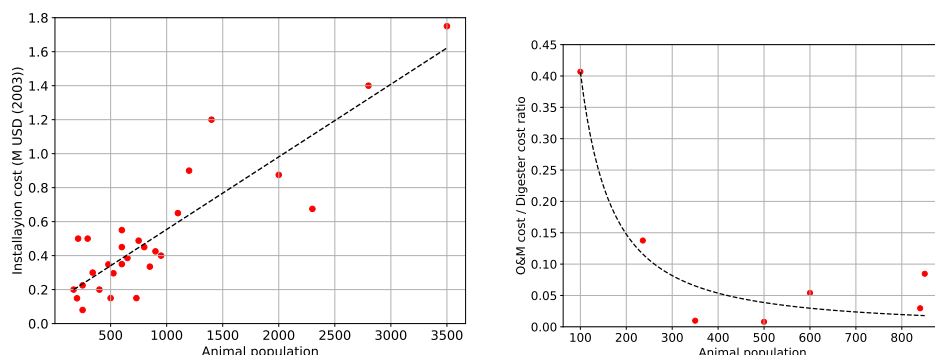
$$\frac{\text{O&M}}{\text{Installation cost}} \text{ ratio} = \frac{15.858 \cdot 10^3}{(1 + (N_{\text{animals}} \cdot 13.917)^{1.461})} \quad (\text{C.5})$$

$$\text{Operating cost} = \text{O&M costs} + \frac{\text{Investment cost}}{\text{Plant lifetime}} \quad (\text{C.6})$$

C.2.2.3 Solid-liquid separation model

Based on the evaluation reported by Møller et al. (2000), a screw press is the technology selected to carry out the solid-liquid separation stage since it is the most cost efficient liquid-solid equipment. The partition coefficients for the different components are shown in Table C.6.

To determine the commercial sizes and number of units necessary as a function of the flow to be treated, data from commercial manufacturers is



(a) Cost of AD units as a function of the number of animals (cattle). Data from U.S. Environmental Protection Agency (2003).

(b) O&M costs as a function of the number of animals (cattle). Data from Beddoes et al. (2007)

Figure C.5: Correlations between AD capital and O&M costs, and the number of cattle in the livestock facility.

Table C.6: Partition coefficients for solid-liquid manure separation using a screw press unit (Møller et al., 2000)

Element	Solid fraction	Liquid fraction
Total mass	0.08	0.92
Dry matter	0.31	0.69
Org. N	0.09	0.91
Org. P	0.22	0.78

considered (PWTEch Process Wastewater Technologies LLC., 2018). The feasible configurations in terms of screw press diameter and number of units as a function of the waste flow treated are shown in Table C.7. Data reported by Matches (2014) for this type of equipment is used to relate the unit diameter and cost, while the operating costs are calculated assuming power consumption reported by the manufacturer for each model, as shown in Fig. C.6 and Table C.8.

C.2.2.4 Nutrient recovery model

Specific correlations for livestock waste to estimate the molar fraction of PO_4^{3-} and Ca^{2+} recovered as struvite as a function of the amount of calcium contained in the waste were developed in a previous work (Martín-Hernández et al., 2020), Eqs. C.7 to C.9, where $x_{\text{Ca}^{2+}:\text{PO}_4^{3-}}$ refers to the $\text{Ca}^{2+}/\text{PO}_4^{3-}$ molar ratio, $x_{\text{struvite}(\text{PO}_4^{3-})}$ is the fraction of phosphorus as phosphate recovered as struvite, and $x_{\text{HAP}(\text{Ca}^{2+})}$ and $x_{\text{CaCO}_3(\text{Ca}^{2+})}$ are the

Table C.7: Sizing estimated for screw press units based commercial on data (PWTech Process Wastewater Technologies LLC., 2018)

Load capacity $(\frac{m^3}{day})$	Number of units			
	$\phi(m) 0.23$	$\phi(m) 0.35$	$\phi(m) 0.42$	$\phi(m) 0.56$
< 43	1	-	-	-
43 - 81	-	1	-	-
81 - 190	-	-	1	-
190 - 381	-	-	2	-
381 - 572	-	-	3	-
572 - 708	-	-	-	2
708 - 1090	-	-	-	3
1090 - 1444	-	-	-	4
> 1444	-	-	-	$\left[\frac{\text{Flow } (m^3/day)}{\text{Load Capacity } \phi 0.56 \text{ m unit}} \right]$

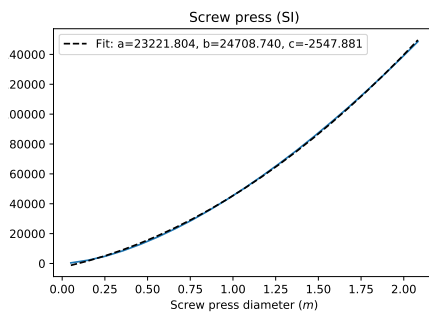
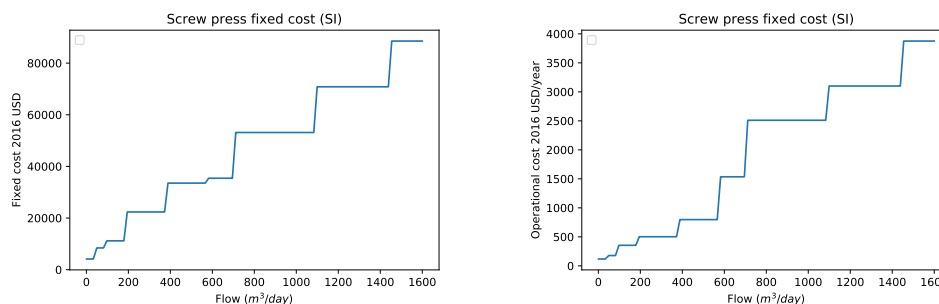


Figure C.6: Estimated screw press investment costs (USD) as a function of the size.

fraction of calcium recovered as hydroxyapatite and calcium carbonate respectively.

Table C.8: Electrical power of screw press units (PWTech Process Wastewater Technologies LLC., 2018)

Number of units	Electrical power (kW)			
	$\varnothing(m) 0.23$	$\varnothing(m) 0.35$	$\varnothing(m) 0.42$	$\varnothing(m) 0.56$
1	0.3	0.45	0.9	-
2	-	-	1.27	3.88
3	-	-	2.01	6.34
4	-	-	-	7.83



(a) Estimated investment costs for screw press units.

(b) Estimated operation costs for screw press units.

Figure C.7: Estimated capital and operating costs for screw press units.

$$x_{Struvite} = \frac{0.798}{1 + (x_{Ca^{2+}:PO_4^{3-}} \cdot 0.576)^{2.113}} \cdot 100 \quad (C.7)$$

$$x_{HAP} = (-4.321 \cdot 10^{-2} \cdot x_{Ca^{2+}:PO_4^{3-}}^2 + 0.313 \cdot x_{Ca^{2+}:PO_4^{3-}} - 3.619 \cdot 10^{-2}) \cdot 100 \quad (C.8)$$

$$x_{CaCO_3} = \frac{1.020}{1 + (x_{Ca^{2+}:PO_4^{3-}} \cdot 0.410)^{1.029}} \cdot 100 \quad (C.9)$$

PHOSPHORUS RECOVERY AS STRUVITE IN SINGLE PASS FBR REACTOR: MULTIFORM HARVEST AND CRYSTALACTOR. Phosphorus can be recovered in the form of struvite using single pass fluidized bed reactors

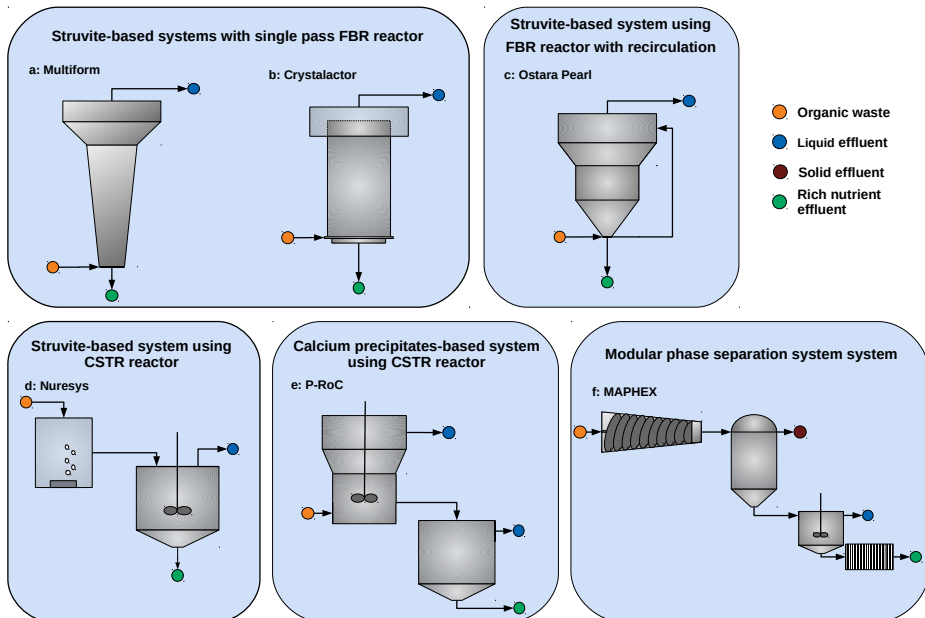


Figure C.8: Flowsheets of the nutrient recovery systems considered in the proposed framework. a: Multiform, b: Crystalactor, c: Ostara Pearl, d: Nuresys, e: P-RoC, f: MAPHEX.

(FBR). Multiform Harvest and Crystalactor are commercial technologies using this configuration, based on single pass fluidized bed reactors, with no recirculation and conical or cylindrical design respectively, where the organic waste is pumped, carrying out the struvite formation. The struvite particles grow, increasing their size, until their mass overcome the drag force of the uplift stream.

Multiform, Fig. C.8a, is a nutrient recovery system developed by the U.S. based company Multiform Harvest. It is a struvite-based process designed to be simple, robust, and fully automatized. Large struvite particles settle towards the reactor base, from where they are removed to be dried before obtaining the final product. MgCl₂ is supplied to the reactor for increasing struvite supersaturation, enhancing its precipitation. pH is adjusted using sodium hydroxide. The conical design of the reactor keeps the small and lighter particles on the large diameter section at the top of the reactor, where the superficial velocity is slower. As the particles increase their mass, they settle gradually to lower levels of the reactor, where the diameter is smaller and the superficial velocity and drag force larger, until they are finally settled on the bottom of the reactor. The liquid phase exits the reactor from the top, where the cross-section is the widest, to ensure the retention of struvite fines (Australian Meat Processor Corporation, 2018).

The techno-economic model for the Multiform process considers a unique size able to process up to 38.5 kg of phosphorus (P-PO_4) per day, with an associated capital cost of 625,000 USD per each Multiform unit, plus 420,000 USD for the struvite dryer that serves all Multiform units. The operating cost for the Multiform system unit is 15.419 USD per kg of P-PO_4 processed (Australian Meat Processor Corporation, 2018).

Crystalactor is a nutrient recovery system created by the Dutch company Royal HaskoningDHV, Fig. C.8b. It is based on a fluidized bed reactor where phosphorus is recovered as precipitates. It can be configured to recover phosphate in the form of calcium phosphates or struvite, depending on the reactant supplied. The model included in the framework considers that the system is configured for struvite production since struvite has a more consolidated market than calcium precipitates to sell the final product recovered. Under this configuration, the reactor is filled with small struvite particles playing the role of seeds to promote the precipitation process, and MgCl_2 is supplied to increase struvite supersaturation (Egle et al., 2016). It is considered that each unit is able to process up to 137.7 kg of P-PO_4 per day. The economy of scale for Crystalactor costs can be captured through the previous work developed by Egle et al. (2016) using Eq. C.10, where $n_{\text{Crystalactor}}$ represents the number of Crystalactor units installed. Crystalactor operating cost assumed is 2.12 USD per kg of P-PO_4 processed (Egle et al., 2016).

$$\text{Capital cost}_{\text{Crystalactor}} = 2.3 \cdot 10^6 + 714,285.71 \cdot n_{\text{Crystalactor}} \quad (\text{C.10})$$

PHOSPHORUS RECOVERY AS STRUVITE IN A FBR REACTOR WITH RECIRCULATION: OSTARA PEARL. Pearl is a struvite-based nutrient recovery system developed by the Canadian company Ostara, Fig. C.8c. The system is based on a continuous operated fluidized bed reactor (FBR) reactor where the waste stream is in contact with struvite particles, which promotes the precipitation of struvite. To increase the supersaturation of struvite and enhance its precipitation, MgCl_2 is supplied to the reactor in a molar ratio of 2 mol of Mg per mol of phosphate. pH is adjusted using sodium hydroxide. In the reactor, the struvite particles grow until they reach a critical mass enough to overcome the drag force of the uplift liquid. To achieve different superficial velocities along the reactor, the diameter of the reactor increases with the height, providing sufficient superficial velocity in the bottom of the vessel to fluidize the struvite seeds, while the larger diameter in the top of the reactor reduces the liquid uplift velocity, allowing retention of fine crystal seed particles in the reactor. Large struvite particles sink towards the base of the reactor, from where they are periodically withdrawn. To

increase the liquid flow in the reactor and achieve larger superficial velocities, an internal recirculation loop is used to recirculate liquid to the bottom of the reactor. A drying step is performed to remove the excess of moisture contained in the struvite particles obtained from the reactor. The liquid stream leaves the reactor at the top, where the cross-section has the largest diameter to ensure the retention of struvite fines.

Based on the information reported by Ostara (Australian Meat Processor Corporation, 2018), standard equipment sizes for the Pearl system are divided in three different capacities, Pearl 500, Pearl 2K, and Pearl 10K, with a load capacities range from 65 to 1250 kg PO₄ per day, as shown in Table C.9. Investment and operation costs for the Ostara Pearl process, including the cost of the conveyor dryer included in the process, can be found in Table C.9 (American Society of Civil Engineers (ASCE), 2013; Australian Meat Processor Corporation, 2018; County of Napa, 2013; Ohio Water Environment Association, 2011). A investment cost-equipment cost ratio of 1.9 has been considered (Australian Meat Processor Corporation, 2018).

Table C.9: Sizing and equipment cost estimated for Ostara Pearl process

	Pearl 500	Pearl 2K	Pearl 10K
Load capacity $\left(\frac{\text{kg}_{\text{P-PO}_4}}{\text{day}} \right)$	65	250	1250
Capital cost (USD) $\frac{\text{Investment}}{\text{kg}_{\text{PO}_4}} \left(\frac{\text{USD}}{\text{kg}} \right)$	$2.3 \cdot 10^6$	$3.1 \cdot 10^6$	$10.0 \cdot 10^6$
	35,385	12,252	8,000

PHOSPHORUS RECOVERY AS STRUVITE IN A CSTR REACTOR:

NURESYS. NuReSys, Fig. C.8d is a nutrient recovery technology developed in Belgium by Nutrients Recovery Systems. Struvite formation is carried out in a continuous stirred tank reactor (CSTR), equipped with a special impeller to minimize the breakage of struvite crystals. NuReSys process uses a stripper as pretreatment where air is injected in the organic waste, decomposing organic carbon and increasing the pH. If pH adjustment is needed, sodium hydroxide is added to the CSTR vessel. The liquid stream is fed into the CSTR reactor for struvite precipitation. Similar to other struvite-based processes, MgCl₂ is supplied to the reactor to increase struvite supersaturation. After struvite precipitation, both solid and liquid phases are extracted from the reactor in the same stream and it is injected in a settler where the separation of phases is carried out. Struvite fines are separated from the largest struvite particles through a hydrocyclone and

they are recirculate to the process. The struvite particles are dried before their final collection (Australian Meat Processor Corporation, 2018).

Considering the data available, it has been assumed that each NuReSys system unit is able to process up to 204 kg of P-PO₄ per day, with an associated capital cost of 1,380,655 USD. NuReSys operating cost is 6.22 USD per kg of P-PO₄ processed (Australian Meat Processor Corporation, 2018).

PHOSPHORUS RECOVERY AS CALCIUM PRECIPITATES IN CSTR A REACTOR: P-ROC. P-RoC is a patented system by the Karlsruhe Institute of Technology (Germany) for phosphorus recovering as calcium precipitates, Fig. C.8e. P-RoC is based on a reactive substrate, calcium-silicate hydrate (CSH), which is the support on which phosphorus is deposited forming a calcium precipitate. The process is carried out in a CSTR reactor, where the precipitates are formed. Liquid and solid phases are separated by sedimentation in a settler, and the obtained particles are finally dried in two consecutive steps composed by a belt filter and a conveyor dryer (Ehbrecht et al., 2011).

As P-RoC is not yet a fully commercial technology, the capital cost is estimated through a preliminary design of each equipment: CSTR reactor, settler, and belt dryer. The estimation of the investment of the CSTR reactor unit is the result of the sum of the vessel and the agitator costs. For design purposes, a maximum CSTR volume of 45 m³ is considered (Turton, 2010). For larger volumes, multiple units installed in parallel are considered, Eq. C.11. The vessel cost is based on data reported by CAPCOST (Turton, 2010), from which the correlation shown in Fig. C.9 has been developed.

$$\text{Number of CSTR} = \left\lceil \frac{\text{Total volume}}{\text{Max. size}} \right\rceil \quad (\text{C.11})$$

The clarifier cost has been estimated as a vessel, using the correlation shown in Fig. C.9. The residence time assumed is 1 hour (Ehbrecht et al., 2011). A vacuum conveyor filter has been selected for struvite recovery from the outlet reactor stream since previous studies report the use of this equipment (Matynia et al., 2013). For design purposes, a filter rate of 0.011 kg/(m²·s) and a maximum area of 1,200 ft² are considered (Couper et al., 2012). The unit cost is based on the correlations reported in Couper et al. (2012). This correlation is based on the area of the filter. Vacuum conveyor filter area and cost are collected in Eqs. C.12 and C.13. The final drying of struvite is achieved with a conveyor dryer. For design purposes, a drying time of 2,100 s and a dryer capacity of 20.85 kg/m² are assumed based on

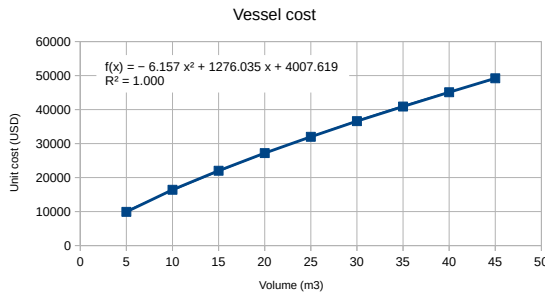


Figure C.9: Estimated investment costs for a non-jacketed vessel, based on data from CAPCOST (Turton, 2010).

data reported on Table 12-21 of Perry and Green (2007). The dryer loading and dryer area are estimated using Eqs. C.14 and C.15, respectively.

$$\text{Area}_{\text{filter}} \left(\text{m}^2 \right) = \frac{\text{Flow} \left(\frac{\text{kg}}{\text{s}} \right)}{\text{Rate}_{\text{filtration}} \left(\frac{\text{kg}}{\text{m}^2 \cdot \text{s}} \right)} \quad (\text{C.12})$$

$$\text{Filter cost (2009 USD)} = \frac{45506}{\text{Area}_{\text{filter}}^{0.5} \left(\text{ft}^2 \right)} \cdot \text{Area}_{\text{filter}} \left(\text{ft}^2 \right) \quad (\text{C.13})$$

$$\text{Loading}_{\text{dryer}} \left(\text{kg} \right) = \text{Flow} \left(\frac{\text{kg}}{\text{s}} \right) \cdot \text{time}_{\text{drying}} \left(\text{s} \right) \quad (\text{C.14})$$

$$\text{Area}_{\text{dryer}} \left(\text{m}^2 \right) = \frac{\text{Loading}_{\text{dryer}} \left(\text{kg} \right)}{\text{Capacity}_{\text{dryer}} \left(\frac{\text{kg}}{\text{m}^2} \right)} \quad (\text{C.15})$$

The cost estimation for a conveyor unit is based on data reported in Table 12-23 of Perry and Green (2007). The correlation developed, relating the unit cost and its area can be found in Fig. C.10. Additionally, based on these data, a maximum conveyor dryer size of 90 m² is assumed.

Based on data reported by Egle et al. (2016), it has been considered that operation costs are variable as a function of the processed amount of

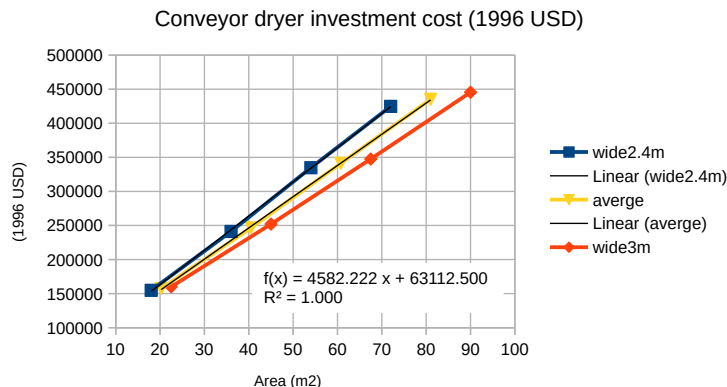


Figure C.10: Estimated investment costs for conveyor dryer unit.

P-PO₄. as it is shown in Eq. C.16, where x_{P-PO_4} represents the kg of P-PO₄ processed per day

$$\text{Operation Cost}_{\text{P-RoC}} \left(\frac{\text{USD}}{kg_{P-PO_4}} \right) = \begin{cases} 115.5, & \text{if } x_{P-PO_4} < 135 \\ -0.09 \cdot x_{P-PO_4} + 127.19, & \text{if } 135 \geq x_{P-PO_4} \geq 662 \\ 67.9, & \text{if } x_{P-PO_4} > 662 \end{cases} \quad (\text{C.16})$$

PHOSPHORUS RECOVERY THROUGH A MODULAR PHASES SEPARATION SYSTEM: MAPHEX. MAPHEX is a nutrient recovery system based on physico-chemical separations developed by Penn State University and the USDA, Fig. C.8f. It involves three stages: liquid-solid separation with an screw press and a centrifuge, addition of iron sulfate to improve nutrients retention, and filtration with diatomaceous earth as filter media. It is conceived as a mobile modular system which can be set in two interconnected truck trailers (Church et al., 2016; Church et al., 2018). Each MAPHEX unit is able to process up to 18.54 kg of P-PO₄ fed per day, with an associated operation cost of 110.8 USD per kg of P-PO₄ processed. Capital cost of a MAPHEX unit is 291,000 USD (Church et al., 2016; Church et al., 2018).

C.3 MULTI-CRITERIA DECISION MODEL

In the SMAA method, the feasible space of each weight is explored through the Monte Carlo method (Tervonen & Lahdelma, 2007), retrieving

a set of weights for all criteria according to the assigned order. Fig. C.11 shows the feasible weight space for a problem with three criteria.

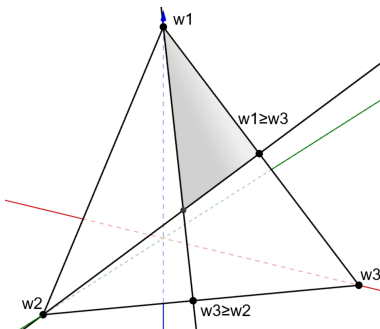


Figure C.11: Example of feasible weights space for a three criteria problem considering ranking of criteria. Figure adapted from Tervonen and Lahdelma (2007)

C.4 DESCRIPTION OF THE GREAT LAKES AREA

BIBLIOGRAPHY

- Alburquerque, J., de la Fuente, C., & Bernal, M. (2012). Chemical properties of anaerobic digestates affecting C and N dynamics in amended soils. *Agric. Ecosyst. Environ.*, 160, 15–22.
- Allen, B. L., & Mallarino, A. P. (2006). Relationships between Extractable Soil Phosphorus and Phosphorus Saturation after Long-Term Fertilizer or Manure Application. *Soil Sci. Soc. Am. J.*, 70, 454–463. <https://doi.org/10.2136/sssaj2005.0031>
- American Society of Civil Engineers (ASCE). (2013). Chicago to Add Nutrient Recovery to Largest Plant [[Online; accessed 21-March-2019]].
- Australian Meat Processor Corporation. (2018). Struvite or Traditional Chemical Phosphorus Precipitation – What Option Rocks? [[Online; accessed 20-March-2019]].
- Beddoes, J. C., Bracmort, K. S., Burns, R. T., & Lazarus, W. F. (2007). *An Analysis of Energy Production Costs from Anaerobic Digestion Systems on U.S. Livestock Production Facilities* (tech. rep.). U.S. Department of Agriculture (USDA).
- Carlson, R. E. (1977). A trophic state index for lakes: Trophic state index. *Limnol. Oceanogr.*, 22(2), 361–369. <https://doi.org/10.4319/lo.1977.22.2.0361>
- Church, C. D., Hristov, A. N., Bryant, R. B., Kleinman, P. J. A., & Fishel, S. K. (2016). A Novel Treatment System to Remove Phosphorus

Table C.10: Livestock residues and phosphorus releases by concentrated animal operation in the Great Lakes area, year 2019. (Indiana Department of Environmental Management, 2019; Michigan Department of Environment, Great Lakes, and Energy, 2019; Minnesota Center for Environmental Advocacy, 2019; Ohio Department of Agriculture, 2019; Pennsylvania Department of Environmental Protection, 2019; Wisconsin Department of Natural Resources, 2019)

	Pennsylvania	Ohio	Indiana	Michigan	Minnesota	Wisconsin
Total animal units	195,967	128,008	187,355	354,460	943,094	743,777
Manure generated (kg/year)	$2.60 \cdot 10^9$	$1.68 \cdot 10^9$	$2.48 \cdot 10^9$	$4.76 \cdot 10^9$	$1.13 \cdot 10^{10}$	$1.03 \cdot 10^{10}$
Phosphorus releases (kg/year)	$2.07 \cdot 10^6$	$1.34 \cdot 10^6$	$1.98 \cdot 10^6$	$3.80 \cdot 10^6$	$9.02 \cdot 10^6$	$8.20 \cdot 10^6$
Dairy Animal units	167,247	101,341	153,495	311,553	428,459	731,927
Manure generated from dairy cows (kg/year)	$2.29 \cdot 10^9$	$1.40 \cdot 10^9$	$2.12 \cdot 10^9$	$4.31 \cdot 10^9$	$5.95 \cdot 10^9$	$1.01 \cdot 10^{10}$
Phosphorus released from dairy cows(kg/year)	$1.83 \cdot 10^6$	$1.12 \cdot 10^6$	$1.70 \cdot 10^6$	$3.45 \cdot 10^6$	$4.76 \cdot 10^6$	$8.10 \cdot 10^6$
Beef animal units	29,370	26,667	33,860	42,907	51,4635	12,088
Manure generated from beef cows (kg/year)	$3.02 \cdot 10^8$	$2.78 \cdot 10^8$	$3.53 \cdot 10^8$	$4.48 \cdot 10^8$	$5.33 \cdot 10^9$	$1.26 \cdot 10^8$
Phosphorus released from beef cows(kg/year)	$2.42 \cdot 10^5$	$2.23 \cdot 10^5$	$2.83 \cdot 10^5$	$3.58 \cdot 10^5$	$4.26 \cdot 10^6$	$1.01 \cdot 10^5$

from Liquid Manure. *Appl. Eng. Agric.*, 32(1), 103–112. <https://doi.org/10.13031/aea.32.10999>

Church, C. D., Hristov, A. N., Kleinman, P. J., Fishel, S. K., Reiner, M. R., & Bryant, R. B. (2018). Versatility of the Manure Phosphorus Extraction (MAPHEX) System in Removing Phosphorus, Odor, Microbes, and Alkalinity from Dairy Manures: A Four-Farm Case Study. *Applied Engineering in Agriculture*, 34(3), 567–572. <https://doi.org/10.13031/aea.12632>

County of Napa. (2013). Phosphorus recovery [[Online; accessed 20-March-2019]].

Couper, J. R., Penney, W. R., Fair, J. R., & Walas, S. M. (2012). *Chemical Process Equipment (Third Edition)* (Third Edition). Boston, Butterworth-

- Heinemann. <https://doi.org/https://doi.org/10.1016/B978-0-12-396959-0.00032-X>
- Dzombak, D. A. (2011). Nutrient Control in Large-Scale U.S. Watersheds. *The Bridge*, 41(4), 13–22.
- Egle, L., Rechberger, H., Krampe, J., & Zessner, M. (2016). Phosphorus recovery from municipal wastewater: An integrated comparative technological, environmental and economic assessment of P recovery technologies. *Science of The Total Environment*, 571, 522–542. <https://doi.org/10.1016/j.scitotenv.2016.07.019>
- Ehbrecht, A., Schönauer, S., Fuderer, T., & Schuhmann, R. (2011). P-Recovery from sewage by seeded crystallisation in a pilot plant in batch mode technology. *Water Science and Technology*, 63(2), 339–344. <https://doi.org/10.2166/wst.2011.061>
- Espinoza, L., Slaton, N. A., & Mozaffari, M. (2006). *Understanding the numbers on your soil test report* (tech. rep.). Cooperative Extension Service, University of Arkansas.
- Indiana Department of Environmental Management. (2019). Confined Feeding Operation Facilities (20200402) [[Online; accessed 29-July-2019]].
- International Plant Nutrition Institute (IPNI). (2012). *A Nutrient Use Information System (NuGIS) for the U.S.* (tech. rep.). International Plant Nutrition Institute (IPNI).
- Kadlec, R. (2016). Large Constructed Wetlands for Phosphorus Control: A Review. *Water*, 8, 243.
- Kellogg, R. L., Lander, C. H., Moffitt, D. C., & Gollehon, N. (2000). *Manure Nutrients Relative to the Capacity of Cropland and Pastureland to Assimilate Nutrients: Spatial and Temporal Trends for the United States* (tech. rep.). United States Department of Agriculture (USDA).
- Martin, J. (2003). *A Comparison of Dairy Cattle Manure Management with and without Anaerobic Digestion and Biogas Utilization* (tech. rep.). AgSTAR Program, U.S. Environmental Protection Agency.
- Martín-Hernández, E., Ruiz-Mercado, G., & Martín, M. (2020). Model-Driven Spatial Evaluation of Nutrient Recovery from Livestock Leachate for Struvite Production. *J. Environ. Manage.*, 271, 110967.
- Matches. (2014). Matches' Process Equipment Cost Estimates [[Online; accessed 29-March-2018]].
- Matynia, A., Wierzbowska, B., Hutnik, N., Mazienczuk, A., Kozik, A., & Piotrowski, K. (2013). Separation of struvite from mineral fertilizer industry wastewater. *Procedia. Environ. Sci.*, 18, 766–775.
- Michigan Department of Environment, Great Lakes, and Energy. (2019). Active NPDES Permits [[Online; accessed 29-July-2019]].

- Minnesota Center for Environmental Advocacy. (2019). Minnesota Confined Animal Feeding Operations [[Online; accessed 29-July-2019]].
- Møller, H., Lund, I., & Sommer, S. (2000). Solid-liquid separation of livestock slurry: efficiency and cost. *Bioresour. Technol.*, 74, 223–229.
- Ohio Department of Agriculture. (2019). Livestock Environmental Permitting.
- Ohio Water Environment Association. (2011). A Green Alternative for Dissolved Nutrient Recovery in Wastewater Side Streams [[Online; accessed 20-March-2019]].
- Pennsylvania Department of Environmental Protection. (2019). Concentrated Animal Feeding Operations [[Online; accessed 29-July-2019]].
- Perry, R., & Green, D. (2007). *Perry's Chemical Engineers' Handbook*. McGraw-Hill.
- Pickard, B. R., Daniel, J., Mehaffey, M., Jackson, L. E., & Neale, A. (2015). EnviroAtlas: A new geospatial tool to foster ecosystem services science and resource management. *Ecosyst. Serv.*, 14, 45–55.
- PWTech Process Wastewater Technologies LLC. (2018). *Volute Dewatering Press* (tech. rep.). PWTech Process Wastewater Technologies LLC.
- Smith, D. B., Cannon, W. F., Woodruff, L. G., Solano, F., Kilburn, J. E., & Fey, D. L. (2013). *Geochemical and Mineralogical Data for Soils of the Conterminous United States: U.S. Geological Survey Data Series 801* (tech. rep.). U.S. Geological Survey (USGS).
- Smith, K., Grylls, J., Metcalfe, P., Jeffrey, B., & Sinclair, A. (2007). *Nutrient Value of Digestate from Farm-Based Biogas Plants in Scotland* (tech. rep.). Scottish Executive Environment and Rural Affairs Department.
- Sørensen, P., Mejnertsen, P., & Møller, H. (2011). Nitrogen fertilizer value of digestates from anaerobic digestion of animal manures and crops. *NJF Report*, 7(8), 42–44.
- Tervonen, T., & Lahdelma, R. (2007). Implementing stochastic multicriteria acceptability analysis. *European Journal of Operational Research*, 178(2), 500–513. <https://doi.org/10.1016/j.ejor.2005.12.037>
- Turton, R. (2010). *CAPCOST software to accompany: Analysis, synthesis, and design of chemical processes* (tech. rep.). Upper Saddle River, N.J.: Prentice Hall PTR.
- United States Department of Agriculture. (2009). *Agricultural Waste Management Field Handbook* (tech. rep.). United States Department of Agriculture (USDA).
- United States Department of Agriculture. (2019). *2017 Census of Agriculture. United States. Summary and State Data* (tech. rep.). United States Department of Agriculture.
- U.S. Environmental Protection Agency. (2003). *AgSTAR Digest* (tech. rep.). U.S. Environmental Protection Agency.

- U.S. Environmental Protection Agency. (2004). *AgSTAR Handbook. A Manual For Developing Biogas Systems at Commercial Farms in the United States* (tech. rep.). U.S. Environmental Protection Agency.
- U.S. Environmental Protection Agency. (2007). *2007 National Lakes Assessment. A Collaborative Survey of the Nation's Lakes* (tech. rep.). U.S. EPA.
- U.S. Environmental Protection Agency. (2012a). *2012 National Lakes Assessment. Quality Assurance Version Project Plan* (tech. rep.). U.S. EPA.
- U.S. Environmental Protection Agency. (2012b). *National Lakes Assessment 2012. A Collaborative Survey of Lakes in the United States* (tech. rep.). U.S. EPA.
- Wisconsin Department of Natural Resources. (2019). DNR Runoff Management. CAFO Permittees [[Online; accessed 29-July-2019]].

D

APPENDIX D: SUPPLEMENTARY INFORMATION OF CHAPTER 6

D.1 BIOGAS PRODUCTION

E

APPENDIX E: SUPPLEMENTARY INFORMATION OF CHAPTER 7

E.1 LITERATURE REVIEW

The literature available referred to CO₂ capture is extensive, not only for combustion processes also for the particular case of biogas upgrading, there exists a lack of literature regarding the selection of the most appropriate biogas upgrading technology. It should be noted that the goal of this work it is not limited to the optimization the biogas production and upgrading processes, which it is implicitly done in the work, but the aim pursued is to determine the optimal biogas upgrading technology among the different feasible processes.

This lack in the literature was detected after a literature review, carried out with special emphasis in specific studies about biogas upgrading. On one hand, as a result of the literature review made, it could be concluded that the literature about reviews of biogas upgrading processes is extensive, even when only recent works are considered, as it is shown in Table E.1. On the other hand, just a few recent works are approaching to carry out a systematic comparison of the processes, such as the work of Collet et al. (2017), where a comparison of several CO₂ capture technologies using experimental data from other studies is presented, but without integrating and optimizing the biogas production and upgrading processes, or the study of Vo et al. (2018), where simulations of biogas upgrading processes limited to amine scrubbing and biological methanation are carried out, not including some essential upgrading technologies such as membranes or PSA. Other works, including but not limited to Capra et al. (2018), Curto and Martín (2019), Gilassi et al. (2019), determine the optimal biogas upgrading process but analyzing only one technology in each case (amines scrubbing, biogas methanation, and membrane separation). In the work presented, 5 technologies have been evaluated considering both heuristic and mathematical modelling stages (biogas methanation, water scrubbing, pressure swing adsorption systems, amines scrubbing, and membranes separation systems).

Table E.1: Relevant literature for biogas upgrading.

Author	Study performed
Angelidaki et al. (2018)	Review of biogas upgrading technologies
Awe et al. (2017)	Review of biogas upgrading technologies
Bauer et al. (2013)	Review of biogas upgrading technologies
Khan et al. (2017)	Review of biogas upgrading technologies
Miltner et al. (2017)	Review of biogas upgrading technologies
Sun et al. (2015)	Review of biogas upgrading technologies
Zhou et al. (2017)	Review of biogas upgrading technologies
Collet et al. (2017)	Techno-economic and life cycle assessment of biogas upgrading
Ferella et al. (2019)	Techno-economic assessment of strategic plans for biogas upgrading plants
Toledo-Cervantes et al. (2017)	Comparison of photosynthetic and physico-chemical biogas upgrading processes
Vo et al. (2018)	Simulation of amine scrubbing and biological methanation
Capra et al. (2018)	Optimal selection of amine scrubbing process for biogas upgrading
Curto and Martín (2019)	Optimal selection of renewable biogas methanation processes
Filipetto et al. (2019)	Optimal selection of membrane separation process for biogas upgrading
Gilassi et al. (2019)	Optimal selection of membrane separation process for biogas upgrading
Morero et al. (2017)	Optimal selection of amine scrubbing process for biogas upgrading

E.2 MODELLING APPROACH

E.2.1 Amines

The CO₂ absorption systems using amines typically operate at low temperatures, around 25-30 °C, and partial pressures above 0.05 bar, reaching removal yields of 90%-95% (Zhang & Chen, 2013). In contrast to postcombustion gases, which contains large amounts of nitrogen from air, biogas is composed mainly by methane and CO₂, resulting in higher carbon dioxide partial pressures and in the need for lower operating pressures. CO₂ partial pressures above 0.1 bar have been assumed to secure high removal yields (Zhang & Chen, 2013), resulting in the need to operate at total pressures around 1-1.5 bar to secure the appropriate CO₂ partial pressures (Movagharnejad & Akbari, 2011; Xue et al., 2017).

The total amount of solution of amines needed to absorb the CO₂ from the gas stream is calculated as a function of the amount of sour gases eliminated, Eq. E.1. According to GPSA (2012), the concentration of solution and the correction factor (GPSA) depend on the amine used, as is shown in Table E.2. The flow of the amine solutions depends on their solubility. Thus, for a fixed removal ratio, the amines solution flow required changes from one to another. It is considered there is no methane absorption in the amines flow, therefore all biomethane entering in the unit leaves the column and it is sent to storage.

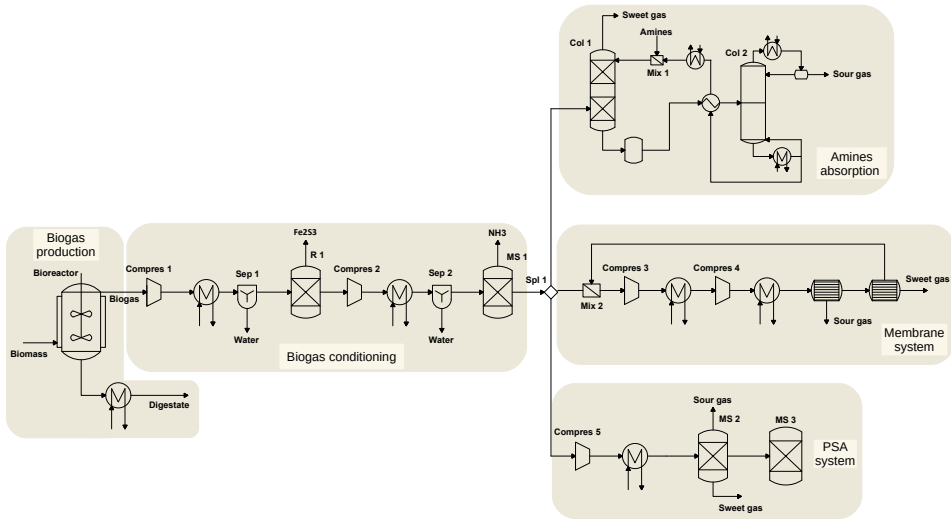


Figure E.1: Scheme of the proposed superstructure for biogas upgrading into biomethane.

$$fc_{amine} = \frac{MW_{amine}}{[amine]} \cdot \left(\frac{CO_{2eff} \cdot fc_{CO_2}}{MW_{CO_2}} \right) \cdot \left(\frac{1}{GPSA} \right) \quad (\text{E.1})$$

The solution of amine used in column 1 comes from two sources, as it shown in Eq. E.2, i.e., the amines from the regeneration column (column 2 in Figure 1), and some make-up solution to replace the amine losses with the gas outlet stream in the regeneration column. Additionally, to mix the two streams of amines at the same temperature, a heat exchanger is used to adjust the temperature of the amine flow stream which leaves the regeneration column to 25 °C.

$$fc_{amine} = fc_{recycled\ amine} + fc_{fresh\ amine} \quad (\text{E.2})$$

The mixing of the two amines streams is assumed to be adiabatic. The energy balance to the heat exchanger is as follows, Eq. E.3.

$$Q = F_{amine} \cdot q_{heat,amine} \quad (\text{E.3})$$

Where F_{amine} is referred to the total mass flow of the amines stream, and $q_{heat,amine}$ the heat flow ratio based on the rules of thumb reported by GPSA (2012). The values are collected in Table E.2.

The assumed CO₂ removal efficiency in the absorption column is 0.95, based on literature data (Zhang & Chen, 2013). The sour gas is absorbed

by the amines in the absorption column, being withdrawn from the gas phase. The absorption is an exothermic process. Therefore, this energy is to be refrigerated, and the operation of the column is isothermal, Eq. E.4. The heats of reaction are shown in Table E.3.

$$Q_{Col1} = \Delta H_{react,amine} \cdot CO_{2_{eff}} \cdot f c_{CO_2} \quad (\text{E.4})$$

The biomethane leaves the column and it is sent to storage. On the other hand, the amine with the CO₂ absorbed is sent to the regeneration column (column 2). The solution is heated up before being fed to column 2 through the heat transfer from the amines stream leaving the reboiler of the regeneration column with the aim of improving the desorption process. Rules of thumb reported in the literature are used to compute the energy involved in the heat exchanger using Eq. E.6, considering the corresponding values of qamine collected in Table E.3.

The operation of column 2 is also based on rules of thumb (GPSA, 2004, 2012) including the estimation of the energy consumption in the reboiler and the cooler refrigeration requirements. According to the literature, the inlet temperature to column 2, T_{Col2} , is equal to 93 °C, whereas the temperature of the outlet amines stream, T_{bottom} , is equal to 125 °C, while at the condenser, the temperature, T_{top} , is equal to 54 °C. Thus, the energy balances of the stream entering column 2 are described in Eq. E.5.

$$\begin{aligned} Q_{Cond} &= F_{Cond} \cdot q_{Cond,amine} \\ Q_{Reb} &= F_{Reb} \cdot q_{Reb,amine} \end{aligned} \quad (\text{E.5})$$

From the reboiler, the regenerated amine is cooled down heating up the feed to the column, Eq. E.6.

$$Q_{Cooling} = F_{Cooling} \cdot q_{Cooling,amine} \quad (\text{E.6})$$

The gas leaving the regeneration column is saturated with the amines aqueous solution, producing the losses of amines which have to be replaced before be recirculated to the absorption column. In order to calculate these losses, humidification models are used. First, the saturation pressure of the amine solution is calculated, Eq. E.7. Then, the specific humidity of the gaseous stream is computed to determine the amount of amines solution accompanying the CO₂ gaseous stream which leaves the regeneration column, Eq. E.8, where the operating pressure of the regeneration column, P_{Col2} , is equal to 1.7 bar (GPSA, 2004). As an approximation, it is assumed

that the amine solution behaves as water. The amount of amine lost with the sour gases is the one to be fed as fresh amine.

$$P_{\text{amines solution}} = \text{Exp} \left(A - \frac{B}{(C + T_{\text{top}})} \right) \quad (\text{E.7})$$

$$Y = \frac{MW_{Wa}}{MW_{\text{outlet gas}}} \cdot \frac{P_{\text{amines solution}}}{(P_{\text{Col2}} - P_{\text{amines solution}})} \quad (\text{E.8})$$

Three different amines are selected aiming a high selectivity, MEA, DEA, and MDEA. Table E.2 shows the parameters used in the amines absorption modelling for each amine considered (GPSA, 2004, 2012).

Table E.2: Amine properties for CO₂ capture GPSA (2004, 2012).

	MEA	DEA	MDEA
Gas pickup (mol/mol _{amine})	0.35	0.35-0.65	0.2-0.55
Solution concentration (wt %)	20	35	45
Heat of reaction (BTU/lb CO ₂)	620-700	580-650	570-600
GPSA	0.35	0.50	0.38
Density	1.01	1.05	1.05
Cost (EUR/kg)	1.30	1.32	3.09
Molecular weight	61	105	119

Table E.3: Amine regeneration heat loads GPSA (2004).

	Duty (BTU/hr)
Reboiler	72000 GPM
Condenser	30000 GPM
Amine feed to distillation	45000 GPM
Amine cooler	15000 GPM

The biomethane production model through amines scrubbing includes the units described in sections 7.3.2.1 and E.2.1. The NLP problem consists of 288 equations and 953 variables per amine evaluated and is solved using a multistart initialization approach with CONOPT as the preferred solver where the main decision variable are the pressures temperatures and flow rates.

E.2.2 PSA

The stream of gases passes through the bed of zeolites and the carbon dioxide is captured by adsorption. The system consists of the compression train and the zeolite beds.

The adsorption capacity of the zeolites is directly related to the partial pressure of the CO₂. Therefore, a system of compressors with intermediate cooling is implemented to determine the optimal operating pressure. As it is described previously, the compressors are modelled assuming polytropic behavior, with a polytropic coefficient z of 1.4 and an efficiency of the compression stages of 0.85, Eq. E.9.

$$T_{out/compressor} = T_{in/compressor} + T_{in/compressor} \left(\left(\frac{P_{out/compressor}}{P_{in/compressor}} \right)^{\frac{z-1}{z}} - 1 \right) \frac{1}{\eta_c}$$

$$W_{(Compressor)} = (F) \cdot \frac{R \cdot z \cdot (T_{in/compressor})}{((Mw) \cdot (z-1))} \frac{1}{\eta_c} \left(\left(\frac{P_{out/compressor}}{P_{in/compressor}} \right)^{\frac{z-1}{z}} - 1 \right)$$
(E.9)

The removal ratio is given by the breakthrough curve of the adsorbent bed. Based on experimental data (Hauchhum & Mahanta, 2014) for adsorption stages below 20 min, the CO₂ removal yield of the PSA system is assumed to be 98%, containing below 2% CO₂ at the outlet stream, (Ferella et al., 2017). The mass balance at the bed is as shown in Eq. E.10.

CO₂ stream:

$$fc_{CO_2}|_{out} = \eta fc_{CO_2}|_{in}$$

$$fc_{CH_4}|_{out} = 0.02 \cdot fc_{CH_4}|_{in}$$
(E.10)

CH₄ stream:

$$fc_{CO_2}|_{out} = (1 - \eta) fc_{CO_2}|_{in}$$

$$fc_{CH_4}|_{out} = 0.98 \cdot fc_{CH_4}|_{in}$$

To compute the mass of bed the adsorption capacity of the bed is evaluated. Based on experimental data, the Langmuir isotherm is the adsorption model considered for this process, Eq. E.11, since this is the one that best fits the performance of the zeolite 13X - CO₂ system (Hauchhum & Mahanta, 2014).

$$q = \frac{q_m \cdot K \cdot P_{CO_2}}{1 + K \cdot P_{CO_2}}$$
(E.11)

Where the parameters q_m and K depend on the adsorbent material. Considering zeolite 13X, the effect of the operating temperature, within the range of 25 °C-60 °C, for both parameters can be correlated using data available in the literature, Eq. E.12a (Hauchhum & Mahanta, 2014).

$$\begin{aligned} q_m &= -3.15551 \cdot 10^{-2} T(\text{°C}) + 5.02915 \\ K &= (1.63070 \cdot 10^{-3} T(\text{°C}))^2 - 3.68662 \cdot 10^{-1} T(\text{°C}) + 27.3737 \end{aligned} \quad (\text{E.12a})$$

$$\begin{aligned} q_m &= -1.8235510^{-2} T(\text{°C}) + 3.72021 \\ K &= 1.6307010^{-3} T(\text{°C})^2 - 3.6866210^{-1} T(\text{°C}) + 27.3737 \end{aligned} \quad (\text{E.12b})$$

As result of the breakthrough curve for the zeolite 13X – carbon dioxide system, the operating time must be below 20 min so that the exit gas (methane) contains only traces of CO₂. Similarly, correlations are developed for zeolite 4A, Eq. E.12b. The operating time of zeolite 4A must be below 20 min (Hauchhum & Mahanta, 2014). Note that the expression for the computing of the constant K in the Langmuir correlation is the same for both adsorbents evaluated.

However, the adsorption capacity decays cycle after cycle until it stabilizes around 65% of the initial capacity computed by Eq. E.13 (Hauchhum & Mahanta, 2014). Therefore, a corrected value for q is applied to compute the amount of zeolite used in the PSA system, as it can be shown in Eq. 14, where the CO₂ removal yield of the PSA system, is assumed to be 98%, containing below 2% CO₂ at the outlet stream (Ferella et al., 2017), and τ is equal to 20 min, based on the results of (Hauchhum & Mahanta, 2014). Furthermore, a lifetime of the zeolites bed of 5 years has been considered based on data reported by Xiao, G., Webley, P., Hoadley, A., Ho, M., Wiley, D. (2013). Thus for the cost, we considered that over the 20 years life time of the plant, 5 beds will be used.

$$m_{\text{Zeolite}} = \frac{1}{q \cdot 0.65} \frac{f_{\text{CO}_2} \cdot 1000}{\text{MW}(\text{CO}_2)} \eta \cdot \tau \quad (\text{E.13})$$

In the case of the PSA system, the objective function is shown in Eq. E.14. To estimate the cost of the PSA system, Eq. E.15, it is assumed that the zeolite bed loses efficiency over time, resulting in a lifetime of 5 years before it needs to be replaced (Xiao, G., Webley, P., Hoadley, A., Ho, M., Wiley, D., 2013). As the plant life is considered 20 years, the zeolites bed must be replaced 4 times during the plant life, N_{Cycle} .

$$\text{Profit} = \text{BioCH}_4 - \text{Cost}_{\text{Zeolite system}} \quad (\text{E.14})$$

$$Cost_{\text{Zeolite system}} = C_{\text{Electricity}} \cdot W_{\text{Compressor}} + \frac{1}{K} M_{\text{Zeolite}} \cdot C_{\text{Zeolite}} \cdot N_{\text{Cycle}} \quad (\text{E.15})$$

The cost of the zeolites considered is 5 USD/kg for both zeolite 13 X and zeolite 4A (Xiao, G., Webley, P., Hoadley, A., Ho, M., Wiley, D., 2013).

The production of biomethane through pressure swing adsorption includes the units described in sections 7.3.2.1 and E.2.2 consisting of an NLP problem of 283 equations and 828 variables that is solved similarly as in the case of the selection of amines where the main decision variables are the operating pressure of the adsorption tower and the size of the bed.

E.2.3 Membranes

The membrane system considered is dual-stage membrane systems with single compression stage before the membrane system and no recompression stage between membrane units, have been deemed as the most economic under a wide range of feed compositions (Kim et al., 2017). The compressor is modelled as presented above, assuming polytropic compression of the gas, Eq. E.9. Each membrane module is modelled using mass balances, considering the permeate and retentate streams, Eqs. E.16 and E.17, and the flux of the gases through the membrane, that is a function of the concentration gradient between both sides of the membrane, Eq. E.19 (Fernandes Rodrigues, 2009). The flux is the parameter which allows computing the area of the membrane, as it is shown in Eq. E.18, based on the permeability of the membrane, Eq. E.21. As the driving force in the membrane separation process is the concentration gradient, the removal of CO₂ results in a change in the composition of the stream along the membrane, leading to a change in the driving force which controls the process. Therefore, an average molar fraction between the feed and the retentate composition is used to compute the separation driving force, Eq. E.20.

$$F_{\text{feed}} = F_{\text{permeate}} + F_{\text{retentate}} \quad (\text{E.16})$$

$$F_{\text{feed}} \cdot y_{i,\text{feed}} = F_{\text{permeate}} \cdot y_{i,\text{permeate}} + F_{\text{retentate}} \cdot y_{i,\text{retentate}}; i \in (CO_2, CH_4) \quad (\text{E.17})$$

$$J_i = \frac{F_{\text{permeate}} \cdot y_{i,\text{permeate}}}{A_{\text{membrane}}}; i \in (CO_2, CH_4) \quad (\text{E.18})$$

$$J_i = \varepsilon_i [y_{feedside} \cdot P_{feed} - y_{i,permeate} \cdot P_{Permeate}] ; i \in (CO_2, CH_4) \quad (E.19)$$

$$y_{feedside} = \frac{y_{i,feed} - y_{i,retentate}}{\ln \left(\frac{y_{i,feed}}{y_{i,retentate}} \right)} ; i \in (CO_2, CH_4) \quad (E.20)$$

$$\varepsilon_i = \frac{Perm_i}{\delta} ; i \in (CO_2, CH_4) \quad (E.21)$$

Where δ is the membrane thickness, and $Perm_i$ the permeability of the component i . The usual membrane thickness for industrial units is equal to 30 nm. Three different membrane materials are selected aiming a large CO_2 permeability, low methane permeability, and therefore, high selectivity; cellulose acetate, polyamide, and polycarbonate. Table E.4 shows the permeabilities for each membrane material considered in the model at 25 °C (Vrbová & Ciahotnyý, 2017). The solution of the optimization problem will yield intermediate conditions to assure natural gas composition of the biomethane.

Table E.4: Gases permeability Vrbová and Ciahotnyý (2017).

Permeability (Barrer)		
Polymer	CH ₄	CO ₂
Cellulose acetate	0.21	6.30
Polycarbonate	0.13	4.23
Polyimide	0.25	10.7

Finally, the simplified profit objective function for the membrane separation system, Eq. E.22, considers cost of the gas compression and the amortization of the investment costs of the membranes, Eq. E.23.

$$Profit = BioCH_4 - Cost_{Membrane\ system} \quad (E.22)$$

Eq21

$$Cost_{Membrane\ system} = C_{Electricity} \cdot W_{Compressor} + \frac{1}{K} \cdot C_{Membrane} \cdot \frac{1}{L_f} \cdot N_{Membranes} \left(\sum_{i \in stages} Area_i \right) \quad (E.23)$$

A value of 50 USD/m² will be used based on the literature (Kim et al., 2017). Considering the plant life equal to 20 years, the membranes with a typical lifetime of 4 years must be replaced 5 times during the plant life, $N_{Membranes}$ (Scholz et al., 2015).

The biogas production and upgrading considering a membranes separation system is formulated as an NLP problem considering the units described in sections 7.3.2.1 and E.2.3 consisting of 299 equations and 869 variables for each material evaluated where the major decision variables are the flows, operating pressures, temperatures and the area required by the membrane units.

E.3 ECONOMIC EVALUATION

The evaluation of the cost for biomethane production is also estimated from different wastes. The production and investment costs are estimated. The CAPEX, or investment cost, is estimated based on Towler and Sinnott (2009) that presents a factorial method. This method estimates the CAPEX usinf as reference the cost of all the major units of the flowsheet.

The sizing of all the units involved in the flowsheet, see Figure 2, is carried out following the method presented in Martín and Grossmann (2011), and updated by Almena and Martín (2016). However, the following considerations for some specific units have been assumed:

- For the digester cost, assumed to be 365 EUR/m³ (Taifouris & Martin, 2018).
- The cost estimation of the columns for the amines is carried out using the rules reported in GPSA (2012). The diameter for the amine contactor can be estimated as given in Eq. E.24.

$$D_C = 44 \sqrt{\frac{F_{gas}(\text{MMscfd})}{P(\text{psia})}} \quad (\text{E.24})$$

While the diameter of the regenerator column can be estimated as given in Eq. E.25.

$$D_R = 3.0 \sqrt{F_{amine}(\text{gal/min})} \quad (\text{E.25})$$

We use the same factors as presented in Davis and Martín (2014) to estimate the investment, CAPEX, of the facility for further comparison with other renewable based methane production processes. The costs for

piping, isolation, instrumentation, and utilities infrastructure are estimated with respect to the equipment cost as 20%, 15%, 20% and 10% of its value respectively. Land and buildings costs are estimated to be 8 M EUR. These items add up to the fixed cost. The fees represent 1% of the fixed cost, other administrative expenses and overheads, and the plant layout represent 10% of the direct costs (fees plus fixed capital) and 5% of the fixed cost, respectively. Finally, the plant start-up cost represents 5% of the investment.

Furthermore, the production costs of biomethane are estimated using also the factorial method with the coefficients presented and validated in Davis and Martín (2014). For the average annual cost, the labour costs (0.5% of investment), equipment maintenance and raw materials (1% of fix costs), amortization (linear with time in 20 years), taxes (0.5% of investment), overheads (1% of investment), and administration (5% of labour, equipment maintenance, amortization, taxes and overheads) are considered. The utilities, particularly cooling water, power, and steam, are taken from the mass and energy balances performed in the superstructure model. Heat integration is carried out to reduce the utilities consumption. The cost of electricity is 0.06 EUR/kWh. The hot compressed gas is used to evaporate the water and ammonia to prepare the digestate to be sold as fertilizer. However, the credit for the digestate to be used as fertilizer is difficult to be estimated. It depends on the market that typically is saturated. Although the cost is around 0.48 EUR/kg, only a fraction is typically obtained. To be conservative, a value of one third of this one is assumed to calculate the benefits received by the sold of the digestate produced (León & Martín, 2016). In addition, the cost of the digestate for the methane to be competitive with other resources, targeting 5 EUR/MMBTU (0.17 EUR/Nm³), is computed.

E.4 SCALING-UP STUDY

The scaling-up study, based on the previous work of Sánchez and Martín (2018), is performed in the following stages. Firstly, the capital cost of the different units is correlated as a function of a design variable, such as the membrane area for membranes systems or the column sizes in function of the flow processed. This variable will be denoted as scaling variable. The scaling variable of each equipment is directly related to the processing capacity of the facility studied through the mass or energy flows involved in that particular unit. The limitations in the size of equipment are considered in the scaling-up study. When an equipment excess the size defined by the rules of thumb, that unit is duplicated, affecting to the cost estimation. In a second stage, after defined the scaling variables for all

units and the relation between these units, the mass and energy flows and the processing capacity of the facility, different capacities are evaluated, calculating the mas and energy balances, and estimating the sizes of the equipment, and the number of units in case some equipment needs to be duplicated. In a third stage, the capital and operating costs are estimated considering the equipment sizes and number of unit of each equipment using the factorial method presented in Towler and Sinnott (2009) and the estimation of the unit costs presented in Almena and Martín (2016).

BIBLIOGRAPHY

- Almena, A., & Martín, M. (2016). Technoeconomic analysis of the production of epichlorohydrin from glycerol. *Industrial & Engineering Chemistry Research*, 55(12), 3226–3238.
- Angelidaki, I., Treu, L., Tsapekos, P., Luo, G., Campanaro, S., Wenzel, H., & Kougiás, P. G. (2018). Biogas upgrading and utilization: Current status and perspectives. *Biotechnology advances*, 36(2), 452–466.
- Awe, O. W., Zhao, Y., Nzihou, A., Minh, D. P., & Lyczko, N. (2017). A review of biogas utilisation, purification and upgrading technologies. *Waste and Biomass Valorization*, 8(2), 267–283.
- Bauer, F., Hulteberg, C., Persson, T., & Tamm, D. (2013). *Biogas upgrading—Review of commercial technologies* (tech. rep.). Svenskt Gastekniskt Center AB.
- Capra, F., Fettarappa, F., Magli, F., Gatti, M., & Martelli, E. (2018). Biogas upgrading by amine scrubbing: solvent comparison between MDEA and MDEA/MEA blend. *Energy Procedia*, 148, 970–977.
- Collet, P., Flottes, E., Favre, A., Raynal, L., Pierre, H., Capela, S., & Peregrina, C. (2017). Techno-economic and Life Cycle Assessment of methane production via biogas upgrading and power to gas technology. *Applied energy*, 192, 282–295.
- Curto, D., & Martín, M. (2019). Renewable based biogas upgrading. *Journal of Cleaner Production*, 224, 50–59.
- Davis, W., & Martín, M. (2014). Optimal year-round operation for methane production from CO₂ and water using wind energy. *Energy*, 69, 497–505.
- Ferella, F., Cucchiella, F., D'Adamo, I., & Gallucci, K. (2019). A techno-economic assessment of biogas upgrading in a developed market. *Journal of Cleaner Production*, 210, 945–957.
- Ferella, F., Puca, A., Taglieri, G., Rossi, L., & Gallucci, K. (2017). Separation of carbon dioxide for biogas upgrading to biomethane. *Journal of Cleaner Production*, 164, 1205–1218.

- Fernandes Rodrigues, D. (2009). *Model Development of a Membrane Gas Permeation Unit for the Separation of Hydrogen and Carbon Dioxide* (Master's thesis). Instituto Superior Tecnico, Lisbon.
- Filipetto, D., Capra, F., Magli, F., Gatti, M., & Martelli, E. (2019). Optimization of semi-permeable membrane systems for biogas upgrading. In *Computer Aided Chemical Engineering* (pp. 1693–1698). Elsevier.
- Gilassi, S., Taghavi, S. M., Rodrigue, D., & Kaliaguine, S. (2019). Optimizing membrane module for biogas separation. *International Journal of Greenhouse Gas Control*, 83, 195–207.
- GPSA. (2004). *GPSA engineering data book, 12th ed.* (tech. rep.). Gas Processors Suppliers Association.
- GPSA. (2012). *GPSA engineering data book, 13th ed.* (tech. rep.). Gas Processors Suppliers Association.
- Hauchhum, L., & Mahanta, P. (2014). Carbon dioxide adsorption on zeolites and activated carbon by pressure swing adsorption in a fixed bed. *International Journal of Energy and Environmental Engineering*, 5(4), 349–356.
- Khan, I. U., Othman, M. H. D., Hashim, H., Matsuura, T., Ismail, A., Rezaei-DashtArzhandi, M., & Azelee, I. W. (2017). Biogas as a renewable energy fuel—A review of biogas upgrading, utilisation and storage. *Energy Conversion and Management*, 150, 277–294.
- Kim, M., Kim, S., & Kim, J. (2017). Optimization-based approach for design and integration of carbon dioxide separation processes using membrane technology. *Energy Procedia*, 136, 336–341.
- León, E., & Martín, M. (2016). Optimal production of power in a combined cycle from manure based biogas. *Energy Conversion and Management*, 114, 89–99.
- Martín, M., & Grossmann, I. E. (2011). Energy optimization of hydrogen production from lignocellulosic biomass. *Computers & chemical engineering*, 35(9), 1798–1806.
- Miltner, M., Makaruk, A., & Harasek, M. (2017). Review on available biogas upgrading technologies and innovations towards advanced solutions. *Journal of Cleaner Production*, 161, 1329–1337.
- Morero, B., GropPELLI, E. S., & Campanella, E. A. (2017). Evaluation of biogas upgrading technologies using a response surface methodology for process simulation. *Journal of cleaner production*, 141, 978–988.
- Movaghfarnejad, K., & Akbari, M. (2011). Simulation of CO₂ capture process. *International Journal of Chemical and Molecular Engineering*, 5(10), 843–847.
- Sánchez, A., & Martín, M. (2018). Scale up and scale down issues of renewable ammonia plants: Towards modular design. *Sustainable Production and Consumption*, 16, 176–192.

- Scholz, M., Alders, M., Lohaus, T., & Wessling, M. (2015). Structural optimization of membrane-based biogas upgrading processes. *Journal of membrane science*, 474, 1–10.
- Sun, Q., Li, H., Yan, J., Liu, L., Yu, Z., & Yu, X. (2015). Selection of appropriate biogas upgrading technology-a review of biogas cleaning, upgrading and utilisation. *Renewable and Sustainable Energy Reviews*, 51, 521–532.
- Taifouris, M. R., & Martin, M. (2018). Multiscale scheme for the optimal use of residues for the production of biogas across Castile and Leon. *Journal of cleaner production*, 185, 239–251.
- Toledo-Cervantes, A., Estrada, J. M., Lebrero, R., & Muñoz, R. (2017). A comparative analysis of biogas upgrading technologies: Photosynthetic vs physical/chemical processes. *Algal research*, 25, 237–243.
- Towler, G., & Sinnott, R. (2009). *Chemical engineering design* (5th ed.). Elsevier.
- Vo, T. T., Wall, D. M., Ring, D., Rajendran, K., & Murphy, J. D. (2018). Techno-economic analysis of biogas upgrading via amine scrubber, carbon capture and ex-situ methanation. *Applied energy*, 212, 1191–1202.
- Vrbová, V., & Ciahotnyý, K. (2017). Upgrading biogas to biomethane using membrane separation. *Energy & Fuels*, 31(9), 9393–9401.
- Xiao, G., Webley, P., Hoadley, A., Ho, M., Wiley, D. (2013). *Low Cost Hybrid Capture Technology Development: Final Report*. Ref No: 3-0510-0046. (tech. rep.). Cooperative Research Centre for Greenhouse Gas Technologies. CO2CRC Publication, Canberra, Australia.
- Xue, B., Yu, Y., Chen, J., Luo, X., & Wang, M. (2017). A comparative study of MEA and DEA for post-combustion CO₂ capture with different process configurations. *International Journal of Coal Science & Technology*, 4(1), 15–24.
- Zhang, Y., & Chen, C.-C. (2013). Modeling CO₂ absorption and desorption by aqueous monoethanolamine solution with Aspen rate-based model. *Energy Procedia*, 37, 1584–1596.
- Zhou, K., Chaemchuen, S., & Verpoort, F. (2017). Alternative materials in technologies for Biogas upgrading via CO₂ capture. *Renewable and sustainable energy reviews*, 79, 1414–1441.